# Abstracts Booklet

# Inaugural Quantum Information Science Principal Investigators' Meeting



# **Basic Energy Sciences, Office of Science**

June 30, July 1, 2025

Organizer: Dr. Athena Sefat

Location: Hilton Washington DC/Rockville Hotel & Executive Meeting Center

#### **FOREWORD**

This is the first Principal Investigators' (PI) meeting for the Quantum Information Science (QIS) program at Office of Basic Energy Sciences (BES) at U.S. Department of Energy (DOE). This PI meeting was sponsored by the Division of Materials Sciences and Engineering (MSE) within BES and held on June 30 and July 1, 2025. This booklet is a collection of abstracts submitted to this PI meeting.

The QIS program focuses on materials sciences and engineering, investigating the fundamental properties of materials critical for developing advanced QIS technologies. Within the BES, this program crosscuts the three MSE Division research areas, namely, Materials Discovery, Design, and Synthesis, Condensed Matter and Materials Physics, and Scattering and Instrumentation Sciences. The research within this QIS program encompasses topics described in BES Roundtable reports: BES Roundtable: Opportunities for Basic Research for Next-Generation Quantum Systems and BES Roundtable on Opportunities for Quantum Computing in Chemical and Materials Sciences. The focus is on advanced materials – both strongly interacting (correlated) and non-interacting (non-correlated) material systems – that support the foundational components for quantum state stability and control. This program aims to create and control entanglement in multi-level quantum systems to enable precise measurement of individual quantum bits while mitigating decoherence – a significant obstacle to reliable quantum computing, quantum networking, and quantum sensing.

This PI meeting brought together close to 100 program-supported researchers, to present their latest scientific breakthroughs, exchange ideas, and foster new collaborations. For BES Program Managers and the participating researchers, the meeting also provided an overview of this program. The meeting format included talks and poster sessions and was organized to include 40 regular presentations and 25 poster presentations.

BES appreciates the contributions of all QIS PIs for presenting their latest research. BES is also grateful for the outstanding support of the Oak Ridge Institute for Science and Education including that of Ms. Stephanie Fox.

Athena S. Sefat, Ph.D.
Program Manager, QIS Program
MSE Dr. Athena Sefat | U.S. DOE Office of Science (SC)

# **Table of Contents**

Agendax
Poster Listingxiv
Abstracts
<b>Hybrid Quantum Magnonics for Transduction and Sensing</b> Gregory Fuchs, Michael Flatté, and Ezekiel Johnston-Halperin
Strongly interacting spin systems in diamond for quantum sensing Ania Bleszynski Jayich, Kunal Mukherjee, David Weld, Norman Yao, Lillian Hughes, Simon Meynell, Weijie Wu, Shreyas Parthasarathy, Eveline Postelnicu, and Emily Davis
Molecular color centers for quantum sensing  Danna Freedman, James Rondinelli, David Awschalom, Mark Hersam, Jeffrey Long, and  Michael Wasielewski
Phonon Control for Next-Generation Superconducting Systems and Sensors  Alp Sipahigil, Haoxin Zhou, Kangdi Yu, Zi-Huai Zhang, Yashwanth Balaji, Mythili  Surendran, Shaul Aloni, Sinéad Griffin, and Adam Schwartzberg
High quality quantum photonic interface for tin-vacancy color centers in thin-film diamond
Jelena Vuckovic, Hope Lee, Abigail Stein, Hannah Kleidermacher, and Michael Titze, Shei Su, Luca Basso, Ania Jayich, Lillian Hughes, Hyunseok Oh, and Kyuhyun Kim
Creating and Controlling Atomic Scale Quantum Systems Stephen Jesse, Ondrej Dyck, Chris Nelson, Mina Yoon, and Andy Lupini
Scalable parallel quantum sensing with individual nitrogen-vacancy centers in diamond
Victor Brar, Matthew Cambria, Saroj Chand, Jennifer Choy, Ádam Gali, Shimon Kolkowitz, Alex Levchenko, Vincenzo Lordi, Jeronimo Maze, Robert McDermott, Keith Ray, and Caitlin Reiter
Novel Probes of Topological Superconductivity for Next-Generation Quantum
<b>Systems</b> Leon Balents, Stephen Wilson, Ganesh Pokharel, Stephen J. Gomez Alvarado, Eric Cui, Taka Park, Arman Rashidi, Jiashu Wang, Andrea Young, and Susanne Stemmer

Imaging Emergent Phenomena in Two-Dimensional Magnets Using Single-Spin Quantum Microscope	
Brian Zhou, Yu-Xuan Wang, Thomas Graham, Xin-Yue Zhang, Zhong Lin, Claire Besson,	
Md Islam, Rafael Gontijo, Ganesh Tiwari, Author, Tibendra Adhikari, Elton Santos,	
Ricardo Rama-Eiroa, Mohammad Badarneh, Kenji Watanabe, and Takashi Taniguchi	18
Probing Two-Dimensional Quantum Materials with Flying Electron Qubits  Dafei Jin	20
Magnetoelastic Coupling to Magnons	
Axel Hoffmann, Zhixin Zhang, Jinho Lim, Haoyang Ni, Author, Yi Li, Valentine Novosad,	22
Molecular Interactions Towards Light-Induced Quantum Entanglement Generation	
Vladimir Chernyak, Luca Candalori, John Klein, Oleg Poluetkov, Shaul Mukamel, Wei Xiong, Nikolai Sinitsyn, and Aaron Rury	24
Superconductor-semiconductor hybrid quantum devices	
Vlad Pribiag, Chris Palmstrøm, Sergey Frolov, Noa Marom, Kunal Mukherjee, Erik	26
Engineering diamond surfaces for efficient NV emission  Victor Brar, Jennifer T. Choy, Robert J. Hamers, Mikhail A. Kats, Minjeong Kim, Shimon Kolkowitz, Roman Kuzmin, Alex Levchenko, Vincenzo Lordi, Zhenqiang Ma, Robert McDermott, Keith G. Ray, Yuhan Tong, Ricardo Vidrio, Wenxin Wu, and Maryam Zahedian	28
Material growth and fabrication of asymmetric tunnel junctions for phonon and	
quasiparticle transport suppression	
Adam Schwartzberg, Shaul Aloni, Alp Sipahigil, Sinéad Griffin, Yashwanth Balaji, Mythili Surendran, Aidar Kemelbay, and Arian Gashi	30
Coherent Control of Magnons	
Yi Li, Moojune Song, Tomas Polakovic, Jinho Lim, Xingzhi Wang, Pratap Kumar Pal, Thomas W. Cecil, John Pearson, Ralu Divan, Wai-Kwong Kwok, Ulrich Welp, Wei Zhang, Dmytro A. Bozhko, Kab-Jin Kim, Jian Min Zuo, Axel Hoffmann, and Valentine Novosad	32
Optoelectronic Properties of Artificially Tailored Quantum Materials	
Komalavalli Thirunavukkuarasu and Wei Pan	34
THz Control of Magnetization and Polarization Through Magnon and Phonon Coherences  Keith A. Nelson, Mariano Trigo, David A. Reis, Riccardo Comin, Zhuquan Zhang, Frank  Y. Gao, Jonathan B. Curtis, Zi-Jie Liu, Yu-Che Chien, Alexander von Hoegen, Takayuki	

Kurihara, Tohru Suemoto, Prineha Narang, Edoardo Baldin, Eric Sung, Xiaoxuan Ma, Wei Ren, Shixun Cao, Gal Orenstein, Viktor Krapivin, Yijing Huang, Gilberto de la Pena Munoz, Ryan A. Duncan, Quynh Nguyen, Jade Stanton, Samuel Teitelbaum, Hasan Yavas, Takahiro Sato, Matthias C. Hoffmann, P. Kramer, Jiahao Zhang, Andrea Cavalleri, Mark P. M. Dean, Ankit S. Disa, Michael Forst, Steven L. Johnson, Matteo Mitrano, Andrew M. Rappe, Man Tou Wong, David Rohrbach, Nadia Berndt, Xi Zhang, Haoyuan Li, Nan Wang, Leon Zhang, Sanghoon Song, Yanwen Sun, May-Ling Ng, Takahiro Sato, Dillon Hanlon, Sajal Dahal, Mario D. Balcazar, Vincent Esposito, Selene She, Chance Caleb Ornelas-Skarin, Joan Vila-Comamala, Christian David, Peter Richard Miedaner, Matthias Ihme, Jerome B. Hastings, Alexei A. Maznev, Laura Foglia, and Diling Zhu	36
Quantum Entangled X-ray Beams	
Stephen M. Durbin, and Liam T. Powers	38
<b>Understanding the Many-body Properties of Rare Earth-Based Materials Relevant</b> to Next Generation QIS Applications	
R. Konik, A. Weichselbaum, T.C. Wei, and Rajesh Malla	40
Fault-Tolerant Majorana-Based Quantum Algorithms  Jasmin Bedow, Max Buss, Prashant Gupta, and Dirk K. Morr	42
High-throughput computational discovery of new quantum defects in silicon G. Hautier, Y. Xiong, Y. Zhu, H. Song, S. McBride, X. Zhang, J. Zheng, J. Liu, A. Sipahigil, and S. Griffin	44
Tunable Josephson Diode Effect for Qubit Noise Shielding  Enrico Rossi, Wei Pan, and Javad Shabani	46
<b>Topological Superconducting Heterostructures for Quantum Sensing</b> H.C. Travaglinia, J.J. Cuozzo, K.R. Sapkota, I.A. Leahy, A.D. Rice, K. Alberi, and W. Pan	48
Quantum entanglement between a semiconductor donor and a trapped ion  Kai-Mei Fu and Boris Blinov	50
Synthesis of improved mobility InAs and InGaAs-quantum wells and of PbSe SAG nanowires	
Vlad Pribiag, Chris Palmstrøm, Sergey Frolov, Noa Marom, Kunal Mukherjee, Yilmaz Gul, Stuart N. Holmes, and Michael Pepper	52
Parametric interactions in superconducting multi-qubit+cavity architectures Raymond W. Simmonds, Jose Aumentado, Archana Kamal, Zhihao Xiao, Emery Doucet, Taewan Noh, Sudhir Sahu, Leonardo Ranzani, and Luke Govia	54

Towards non-blinking and photostable perovskite quantum dots	
Chenjia Mi, Gavin C. Gee, Chance W. Lander, Donghoon Shin, Matthew L. Atteberry,	
Novruz G. Akhmedov, Lamia Hidayatova, Sohom Chandra, Jesse D. DiCenso, Michael P.	
LaSala, Wai Tak Yip, Bin Chen, Yihan Shao, and Yitong Dong,	56
Color centers in noise-free hosts for quantum sensing and communication	
applications	
Kusal Abeywickrama, Pralay Paul, Melissa Artola, Sreehari Purayil, Sumit Gaswami,	
Dhiman Biswas, Casey Kerr, Mritunjaya Parashar, Mohin Sharma, Darshpreet Kaur	
Saini, Bibhudutta Rout, Thirumalai Venkatesan, and Alisa Javad	58
Towards Hybrid Quantum Repeaters with Quantum Dots and alkali vapors	
Joanna M Zajac , Tobias Huber, Sven Höfling, Monika Dziubelski, and Sofia Pereira	61
Multiparticle Quantum Information Processing in Robust Plasmonic Lattices	
Mingyuan Hong, Fatemeh Mostafavi, Jannatul Ferdous, Riley B. Dawkins, Roberto	
Leon-Montiel, Rui-Bo Jin, Benjamin Bertoni, Ian Baum, Chenglong You, and Omar S.	
Magana-Loaiza	63
Advanced in-situ analysis and ex-situ studies of 2D Hexagonal Boron Nitride and 2D	
Ferromegnets via Aberration-Corrected Scanning Transmission Electron	
Microscopy	
Marija Drndic, Rachael Keneipp, Pia Bhatia, Jordan Gusdorff, and Lee Bassett	66
Multiscale Quantum and Classical Microscopy for Superconducting Quantum Systems	
Benjamin Lawrie, Gábor Halász, Chengyun Hua, Petro Maksymovych, Matt Brahlek, Josh Damron, Sang Yong Song , Yueh-Chun Wu , and Nirjhar Sarkar	69
Diagnostics to deduce effects of impurities and electron correlations on quantum	
material systems	
Victor Brar, Jennifer Choy, Susan Coppersmith, Mark Eriksson, Mark Friesen, Emily	
Joseph, Shimon Kolkowitz, Zach Krebs, Roman Kuzmin, Alex Levchenko, Vincenzo Lordi,	
Robert McDermott, Keith Ray, Leah Tom, and Joel Varley	71
Molecular Devices to Create Entangled Exciton States and Molecular Dye Polymers	
for Quantum Entanglement and Quantum Circuits	
W. B. Knowlton, B. Yurke, A. Supc, R. Elliot, J. Lee, L. Li, M. Ketteridge, K. Duncan, G.	
Barcenas, O. A. Mass, D. Watt, T. Azaz, K. Shaw, T. Payne, G. Pascual, S. Roy, L.	
Patten, D. B. Turner, and R. D. Pensack	74
Direct Observation of Fractional Quantum Hall Quasiparticle Braiding Statistics	
via Interferometry	
Michael J. Manfra	77

Stark shift effects from first principles in quantum defects	
S. Griffin, L. Alaerts, Y. Xiong, and G. Hautier	79
Next-Generation Parametrically-Induced Quantum Engineering (PIQUE 2.0)  Archana Kamal, Leonardo Ranzani, Guilhem Ribeill, Luke Govia, Raymond Simmonds,  Jose Aumentado, Zhihao Xiao, Taewan Noh, Emery Doucet, Tristan Brown, and Tarush  Tiwari	81
Planar Systems for Quantum Information  Kaifei Kang, Bowen Shen, Yichen Qiu, Yihang Zeng, Zhengchao Xia, Kenji Watanabe,  Takashi Taniguchi, Allan H. MacDonald, Jie Shan, and Kin Fai Mak	83
<b>Disorder-enabled control of superconducting devices</b> Gábor Halász, Nirjhar Sarkar (pd), Chengyun Hua, and Benjamin Lawrie	85
Project Title: Optical Information Processing Through Jointly-Optimized Diffractive Surfaces and Electronic Neural Networks Md Sadman Sakib Rahman, Tianyi Gan, Emir Arda Deger, Çağatay İşil, Mona Jarrahi, and Aydogan Ozcan	87
Enhanced and twisted nonlinear optical responses in quantum nanomaterials Prashant Padmanabhan, Tenzin Norden, Luis M. Martinez, Nehan Tarefder, Kevin W. C. Kwock, Luke M. McClintock, Nicholas Olsen, Luke N. Holtzman, June Ho Yeo, Liuyan Zhao, Xiaoyang Zhu, James C. Hone, Jinkyoung Yoo, Jian-Xin Zhu, P. James Schuck, Antoinette J. Taylor, Rohit P. Prasankumar, Wilton J. M. Kort-Kamp, Thomas P. Darlington, Kaiyuan Yao, Kai Du, Ana-Marija Nedić, Thaís V. Trevisan, Peter P. Orth, and Sang-Wook Cheong	90
Poster Session I	92
Quantum Computing Approaches for Correlated Multi-Orbital Materials Simulations Yongxin Yao, Thomas Iadecola, Cai-Zhuang Wang, Anirban Mukherjee, Joao C. Getelina, Martin Mootz, Feng Zhang, Noah Berthusen, Prachi Sharma, and Peter P. Orth	93
Scalable quantum photonic materials based on precision doped diamond nanostructures  Michael Titze, Shei Su, and Jelena Vuckovic	95
Holographic quantum simulation of strongly correlated electron systems	

Shyam Shankar, Andrew Potter, Joseph Sullivan, Josiah Cochran, Ameya Riswadkar, Iian Jun Liu, Aikaterini Kargioti, Theodore Shaw, Yuxuan Zhang, Travis Hosack, Daoheng Niu, Shahin Jahabani, Alice Xiong, and Noah Mugan	97
Integrated Materials Platforms for Topological Quantum Computing Devices Vlad Pribiag, Sergey Frolov, Chris Palmstrøm, Noa Marom, Kunal Mukherjee, Shixiong Zhang, Tomasz Story, Moïra Hocevar, and Vladimir Strocov	
L <b>ight-matter interaction with quantum light</b> Chengyun Hua, Benjamin Lawrie, and Yueh-Chun Wu	101
Elucidation of Quantum Spin Defect Interactions with Quantum Materials Ioshua T. Damron, Benjamin Lawrie, Gábor Halász, Chengyun Hua, and Yueh-Chun Wu	103
Understanding the Many-body Properties of Rare Earth-Based Materials Relevant to Next Generation QIS Applications  Igor A. Zaliznyak, Andreas Weichselbaum, Robert Konik, Lazar Kish, Daniel M.  Pajerowski, Andrei T. Savici, Andrey Podlesnyak, Leonid Vasylechko, and Alexei Tsvelik	105
Witnessing Quantum Entanglement Using Resonant Inelastic X-ray Scattering Mark P. M. Dean, Jonathan Pelliciari, Robert M. Konik, Igor Zaliznyak, Wei He, Lazar Kish, Yao Shen, Sophia TenHuisen, Mary H. Upton, Diego Casa, Petra Becker, Matteo Mitrano, and Jennifer Sears	107
DNA-Controlled Dye Aggregation – A Path to Create Quantum Entanglement P. H. Davis, J. E. Anthony, J. C. Dean, R. J. Stanley, J. Lee, L. Li, O. A. Mass, B. Yurke, W. B. Knowlton, E. W. Martin, P. C. Arpin, D. B. Turner, and R. D. Pensacka	109
Robust Quantum Computing for Condensed Matter Physics  Alexander Kemper and James Freericks	111
Trade off-free entanglement stabilization in superconducting circuits Leonardo Ranzani, Archana Kamal, Guilhem Ribeill, Luke Govia, Raymond Simmonds, Jose Aumentado, Daniel Campbell, Tristan Brown, Zhihao Xiao, Emery Doucet, and Tarush Tiwari	113
Quantum Sensing of Magnons Using a Qubit Wolfgang Pfaff , Sonia Rani , Xi Cao , Alejandro E. Baptista, Philip Kim, Pratap Kumar Pal, Yi Li, Valentine Novosad, and Axel Hoffmann	115
Modeling, probing, and controlling defects in materials for superconducting qubits and spin qubits  Alex Abelson, Loren D Alegria, Victor Brar, Kevin R Chaves, Yujin Cho, Jennifer Choy,  Soohyun Im, Shimon Kolkowitz, Alex Leychenko, Vincenzo Lordi, Sean R O'Kelley	

Eunjeong Kim, Luis A Martinez, Robert McDermott, Keith G. Ray, Yaniv Rosen, Paul M Voyles, and Christopher D Wilen	117
Engineering low energy modes in 1D and 2D quantum materials Felix R. Fischer, Michael F. Crommie, and Steven G. Louie	119
Van der Waals Reprogrammable Quantum Simulator Benjamin Hunt, Dengyu Yang, Qingrui Cao, Junwon Choi, Erin Akyuz, Jeremy Levy, Patrick Irvin, Ranjani Ramachandran, Muqing Yu, Jon-Paul Maria, John Hayden, Josh Nordlander, Ian Mercer, Di Xiao, Nishchay Suri, and Chong Wang	122
Poster Session II	124
Atomic Engineering and Characterization of Targeted Quantum Emitters in 2D Transition Metal Dichalcogenides through Scanning Tunneling Microscopy and First Principles computations  A. Weber Bargioni, S. Griffin, A. Raja, G. Hautier, M.M. Noack, E. Rotenberg, DF. Ogletree, D. Strubbe, G.M. Rignanese, A. Schwartzberg, M. Terrones, J. Robinson, S. Kumari, D. Zhou, Z. Yu, N. Kelly, W. Chen, J. Zhou, B. Barker, Y. Xiong, W. Chen, J.C. Thomas, P. Jacobse, B. Iliyas, and F. Wang	125
Long-lived entanglement of a spin-qubit register in silicon photonics  Hanbin Song, Xueyue Zhang, Lukasz Komza, Niccolo Fiaschi, Yihuang Xiong, Yiyang Zhi, Scott Dhuey, Adam Schwartzberg, Thomas Schenkel, Geoffroy Hautier, Zi-Huai Zhang, and Alp Sipahigil	127
Sharp emission and fine structure splitting from localized excitons in Vanadium-doped monolayer WSe2  A. Raja, G. Hautier, E. Barré, W. Chen, D. Blach, G. Gupta, Y. Xiong, L. Leyi, C. Yuan, G. Eda, S. Y. Quek, K. Watanabe, and T. Taniguchi	128
Seeking quasiparticles in perturbed matter from low-energy spin dynamics  Arnab Banerjee, Catherine Pappas, and Roger Pynn	129
Author Index	131

## Agenda

## U.S. Department of Energy (DOE), Office of Science, Basic Energy Science, Quantum Information Science (QIS) Program in Materials Sciences and Engineering (MSE) Division

## 2025 Quantum Information Sciences Principal Investigators' Meeting

Organizer: Dr. Athena Sefat, Athena.sefat@science.doe.gov
Location: Hilton Washington DC/Rockville Hotel & Executive Meeting Center
Date: June 30 & July 1, 2025

## **Monday, June 30, 2025**

7:30 – 8:25 AM	Registration & *** Breakfast***
8:25 – 8:30 AM	Welcome to Day 1: Athena Sefat
8:30 – 9:00 AM	Division & Program Updates  Andrew Schwartz, Director, DOE MSE Division  Athena Sefat, Program Manager, QIS Program in MSE

Session 1	Chair: Susan Stemmer (Univ. of California)
9:00 – 9:20 AM	Gregory Fuchs (Cornell Univ.), "Hybrid quantum magnonics for transduction
	and sensing"
9:20 – 9:40 AM	Ania Bleszynski Jayich (Univ. of California), "Strongly interacting spin
	systems in diamond for quantum sensing"
9:40 – 10:00 AM	Danna Freedman (MIT), "Molecular color centers for quantum sensing"
10:00 – 10:20 AM	Alp Sipahigil (LBNL), "Phonon control for next-generation superconducting
	systems and sensors"
10:20 – 10:40 AM	*** Break ***

Session 2	Chair: Robert Konik (BNL)
10:40 – 11:00 AM	Jelena Vuckovic (Stanford Univ.), "High quality quantum photonic interface
	for tin-vacancy color centers in thin-film diamond"
11:00 – 11:20 AM	Stephen Jesse (ORNL), "Creating and controlling atomic scale quantum
	systems"
11:20 – 11:40 AM	Shimon Kolkowitz (Univ. of California Berkeley), "Scalable parallel quantum
	sensing with individual nitrogen-vacancy centers in diamond"
11:40 – 12:00 PM	Susanne Stemmer (Univ. of California), "Novel probes of topological
	superconductivity for next-generation quantum systems"

Session 3	Working ***Lunch*** with ECRP Awards I
12:00 – 1:30 PM	Chair: Jelena Vuckovic (Stanford Univ.)
12:15 – 12:35 PM	Brian Zhou (Boston College), "Imaging emergent phenomena in two-
	dimensional magnets using single-spin quantum microscope"
12:35 – 12:55 PM	Dafei Jin (Univ. of Notre Dame), "Probing two-dimensional quantum materials
	with flying electron qubits"

Session 4	Chair: Danna Freedman (MIT)
1:30 – 1:50 PM	Axel Hoffmann (Univ. of Illinois Urbana-Champaign), "Magnetoelastic
	coupling to magnons"
1:50 – 2:10 PM	Aaron Rury (Wayne State Univ.), "Molecular Interactions Towards Light-
	Induced Quantum Entanglement Generation"
2:10 – 2:30 PM	Vlad Pribiag (Univ. of Minnesota), "Superconductor-semiconductor hybrid
	quantum devices"
2:30 – 2:50 PM	Jennifer Choy (Univ. of Wisconsin), "Engineering diamond surfaces for
	efficient NV emission"
2:50 – 3:00 PM	*** Break ***

Session 5	Chair: Ania Jayich (Univ. of California)
3:00 – 3:20 PM	Adam Schwartzberg (LBNL), "Material growth and fabrication of asymmetric
	tunnel junctions for phonon and quasiparticle transport suppression"
3:20 – 3:40 PM	Yi Li (ANL), "Coherent Control of Magnons"
3:40 – 4:00 PM	Komalavalli Thirunavukkuarasu (Florida A&M Univ.), "Optoelectronic
	properties of artificially tailored quantum materials"
4:00 – 4:20 PM	Jennifer Dionne (Stanford Univ.), "Room-temperature valley-selective emission
	in Si-MoSe2 heterostructures enabled by high quality-factor chiroptical
	cavities"
4:20 – 4:30 PM	*** Break ***

Session 6	Chair: Athena Sefat
4:30 – 5:30 PM	Introductions to Poster Session I

Session 7	Working ***Dinner*** with X-rays
5:30 – 6:30 PM	Chair: Brian Zhou (Boston College)
5:45 – 6:00 PM	Keith Nelson (MIT), "THz control of magnetization and polarization through
6:00 – 6:15 PM	magnon and phonon coherences"  Stephen Durbin (Purdue Univ.), "Quantum Entangled X-ray Beams"
0.00 0.131111	Stephen Darom (1 that only.), Quantum Entanglea A-ray Deams

Session 8	Poster Session I
6:30 – 8:30 PM	

Tuesday, July 1, 2025

8:25 – 8:30 AM	Welcome to Day 2: Athena Sefat
Session 9	Chair: Michael Manfra (Purdue University)
8:30 – 8:50 AM	Robert Konik (BNL), "Understanding the many-body properties of rare earth-based materials relevant to next generation QIS applications"
8:50 – 9:10 AM	Dirk Morr (Univ. of Illinois), "Fault-tolerant majorana-based quantum algorithms in topological superconductors"
9:10 - 9:30 AM	Geoffroy Hautier (Dartmouth College), "High-throughput computational discovery of new quantum defects in silicon"
9:30 - 9:50 AM	Enrico Rossi (College of William and Mary), "Tunable Josephson diode effect for qubit noise shielding"
9:50 – 10:10 AM	*** Break ***

Session 10	Chair: Alp Sipahigil (LBNL)
10:10 – 10:30 AM	Wei Pan (SNL), "Topological superconducting heterostructures for quantum
	sensing"
10:30 – 10:50 AM	Kai-Mei Fu (Univ. of Washington), "Quantum entanglement between a
	semiconductor donor and a trapped ion"
10:50 – 11:10 AM	Andrew Mannix (ANL), "Advancing exciton confinement and nonlinear light-
	matter interactions in non-centrosymmetric layered semiconductors"
11:10 – 11:30 AM	Chris Palmstrom (Univ. of California Santa Barbara), "Synthesis of improved
	mobility InAs and InGaAs-quantum wells and of PbSe SAG nanowires"
11:30 – 11:50 AM	Raymond Simmonds (NIST), "Parametric interactions in superconducting
	multi-qubit+cavity architectures"

Session 11	Working ***Lunch*** with ECRP Awards II
11:50 – 1:30 PM	Chair: Bill Knowlton (Boise State Univ.)
12:15 – 12:35 PM	Yitong Dong (University of Oklahoma), "Towards non-blinking and
	photostable perovskite quantum dots"
12:35 – 12:55 PM	Alisa Javadi (University of Oklahoma), "Color centers in noise-free hosts for
	quantum sensing and communication applications"
12:55 – 1:15 PM	Joanna Zajac (BNL), "Towards hybrid quantum repeaters with quantum dots
	and alkali vapors"

Session 12	Chair: Alex Weber Bargioni (LBNL)
1:30 – 1:50 PM	Omar Magana-Loaiza (Louisiana State Univ.), "Multiparticle quantum
	information processing in robust plasmonic lattices"
1:50 – 2:10 PM	Marija Drndic (Univ. of Pennsylvania), "Advanced in-situ analysis and ex-situ
	studies of 2D hexagonal BN and 2D ferromagnets via STEMS"
2:10 – 2:30 PM	Benjamin Lawrie (ORNL), "Multiscale quantum and classical microscopy
	for superconducting quantum systems"
2:30 – 2:50 PM	Victor Brar (Univ. of Wisconsin), "Diagnostics to deduce effects of impurities
	and electron correlations on quantum material systems"
2:50 – 3:00 PM	*** Break ***

Session 13	Chair: Enrico Rossi (College of William and Mary)
3:00 – 3:20 PM	Bill Knowlton (Boise State Univ.), "Molecular devices to create entangled
	exciton states and molecular dye polymers for quantum entanglement"
3:20 – 3:40 PM	Michael Manfra (Purdue University), "Direct observation of fractional
	quantum Hall quasiparticle braiding statistics via interferometry"
3:40 – 4:00 PM	Sinead Griffin (LBNL), "Stark shift effects from first principles in quantum
	defects"
4:00 – 4:20 PM	Archana Kamal (Northwestern University), "Next-generation parametrically-
	induced quantum engineering"
4:20 – 4:40 PM	Jie Shan (Cornell University), Allan MacDonald (University of Texas, Austin),
	"Planar systems for quantum information"
4:40 –5:00 PM	*** Break ***

Session 14	Chair: Athena Sefat
5:00 –5:30 PM	PI Meeting Concluding Remarks; Introductions to Poster Session II

Session 15		Working ***Dinner***
5:30 – 6:30 P	M	Chair: Axel Hoffmann (Univ. of Illinois)
Discussion To	pic:	Defects in materials for QIS - How to control & characterize, need for tools

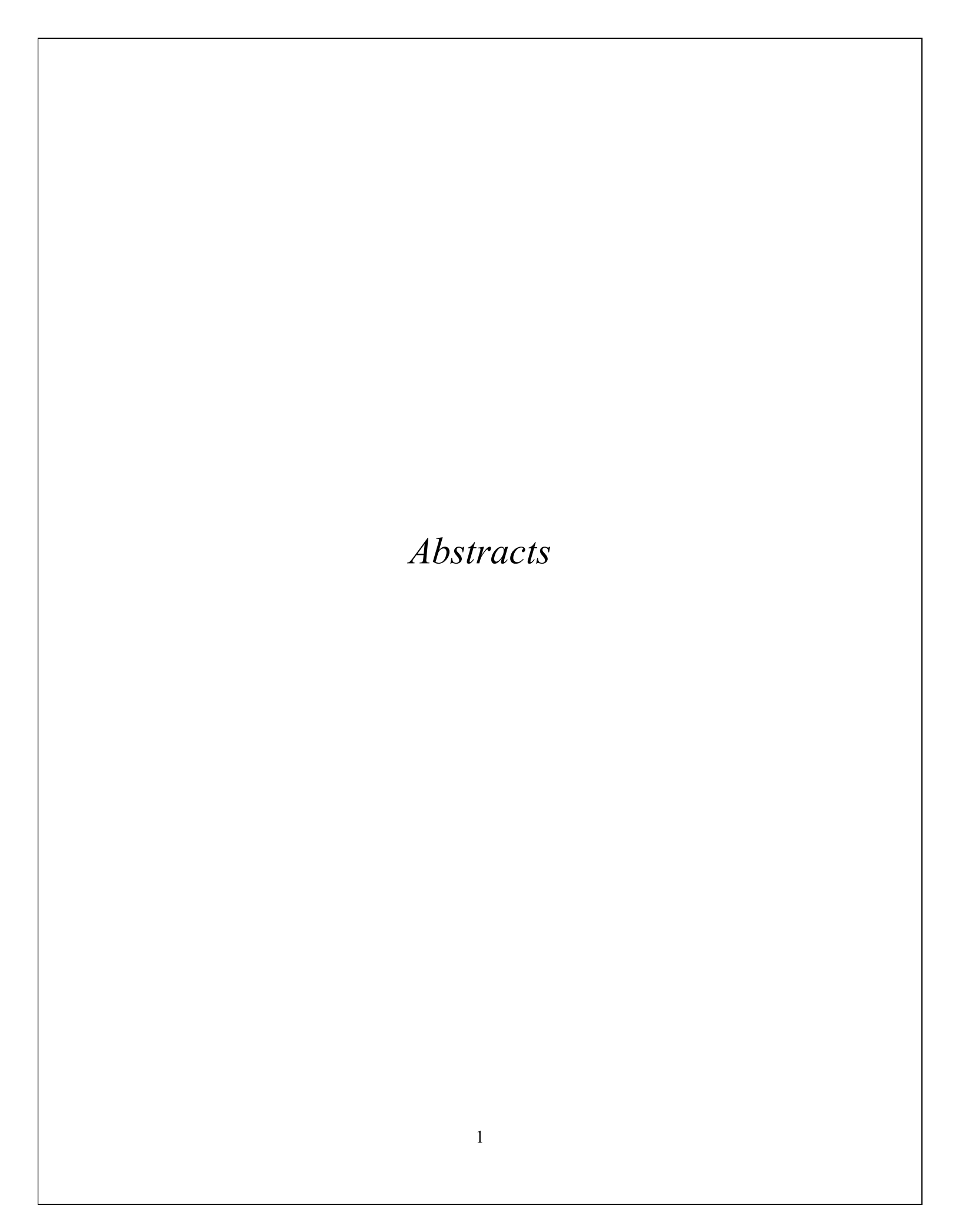
Session 16	Poster Session II
6:30 – 7:30 pm	

### Poster session I Monday, June 30, 2025

- 1. Yongxin Yao (Ames National Lab.), "Quantum computing approaches for correlated multi-orbital materials simulations"
- 2. Michael Titze (Sandia National Lab.), "Scalable quantum photonic materials based on precision doped diamond nanostructures"
- 3. Shyam Shankar (University of Texas at Austin), "Holographic quantum simulation of strongly correlated electron systems"
- 4. Sergey Frolov (University of Pittsburgh), "Integrated materials platforms for topological quantum computing devices"
- 5. Chengyun Hua (ORNL), "Light-matter interaction with quantum light"
- 6. Joshua Damron (ORNL), "Elucidation of quantum spin defect interactions with quantum materials"
- 7. Igor Zaliznyak (BNL), "Neutron scattering studies of quantum coherence in Yb spin chains"
- 8. Mark Dean (BNL), "Witnessing quantum entanglement using resonant inelastic X-ray scattering"
- 9. Ryan Pensack (Boise State Univ.), "DNA-controlled dye aggregation A path to create quantum entanglement"
- 10. Alexander Kemper (North Carolina State University), "Robust quantum computing for condensed matter physics"
- 11. Leonardo Ranzani (RTX BBN Technologies), "Trade off-free entanglement stabilization in superconducting circuits"
- 12. Ondrej Dyck (ORNL), "Creating and controlling atomic scale quantum systems"
- 13. Wolfgang Pfaff (Univ. of Illinois Urbana-Champaign), "Quantum sensing of magnons using a qubit"
- 14. Keith Ray (LLNL), "Modeling, probing, and controlling defects in materials for superconducting qubits and spin qubits"
- 15. Felix Fischer (Univ. of California Berkeley), "Engineering low energy modes in 1D and 2D quantum materials"
- 16. Benjamin Hunt (Carnegie Mellon Univ.), "Van der Waals reprogrammable quantum simulator"

## Poster session II Tuesday, July 1, 2025

- 17. Alex Weber Bargioni (LBNL), "Atomic engineering and characterization of targeted quantum emitters in 2D transition metal dichalcogenides through scanning tunneling microscopy and First Principles computations"
- 18. Alp Sipahigil (LBNL), "Long-lived entanglement of a spin-qubit register in silicon photonics"
- 19. Archana Raja (LBNL), "Sharp emission and fine structure splitting from localized excitons in Vanadium-doped monolayer WSe2"
- 20. Ezekiel Johnston-Halperin (Ohio State Univ.), "Materials development for quantum magnonics"
- 21. Michael Flatté (University of Iowa), "Entanglement gates enabled by hybrid quantum magnonics"
- 22. Allan MacDonald (University of Texas, Austin), "Theory of interacting trapped excitons on a TMD formed by a twisted hBN moiré"
- 23. Felipe da Jornada (Stanford University), "Giant exchange-mediated exciton splitting in trapped MoS2 by ferroelectric substrates"
- 24. Tony Heinz (SLAC), "Exciton trapping and wavefunction control by electric fields in 2D semiconductors"
- 25. Arnab Banerjee (Purdue University), "Seeking quasiparticles in perturbed matter from low-energy spin dynamics"



#### **Hybrid Quantum Magnonics for Transduction and Sensing**

Award Number: DE-SC0019250

Names of PI, co-PI(s): Gregory Fuchs<sup>1</sup> (PI), Michael Flatté<sup>2</sup> (co-PI), Ezekiel Johnston-Halperin<sup>3</sup> (co-PI)

**Affiliations**: 1. Cornell University, 2. University of Iowa, 3. Ohio State University

Abstract Title: Entanglement gates enabled by hybrid quantum magnonics

Abstract:Our project focuses on the hybrid quantum magnonics for quantum science and technologies based on the ultra-low loss molecular ferrimagnet vanadium tetracyanoethylene (V[TCNE]<sub>x</sub>). This molecule-based material has exhibited exceptionally narrow linewidth and magnetic damping coefficient down to  $\alpha \approx 4 \times 10^{-5}$  in thin films at room temperature, which is competitive with any other magnetic material, including the yttrium iron garnet (YIG), the conventional choice. Moreover, V[TCNE]<sub>x</sub> can be templated and grown at moderate growth temperatures ( $\sim 60^{\circ}$ C) without changing its loss properties, which is attractive for integration with superconducting quantum technologies. Recent results have demonstrated the integration of patterned magnetic structures into superconducting resonators, yielding strong photon-magnon coupling in the microwave regime in an integrated circuit architecture [1], and the creation of a double disk structure that can be quantitatively read out using nitrogen vacancy (NV) centers in diamond [2]. In this project we have focused on solving the materials, measurement, and theory problems necessary to realize these visions for hybrid quantum magnonic systems.

Here we discuss demonstrations of magnon-qubit coupling following an initial proposal [3] to realize two-qubit entangling gates mediated by virtual excitations of magnons. This was a complementary proposal to a previous qubit-magnon transduction proposal [4]. By studying the self-interaction of a single qubit with magnonic modes of a bar [5] we have validated the theoretical calculations of coupling via fringe fields. Based on the previous proposals this clearly indicates that the coupling strength can be sufficient for realistic configurations and enables qubit entangling gates wherein the qubits are separated by  $>1~\mu m$ .

Shown in Fig. 1 is the surface magnon induced longitudinal relaxation of an NV center. The dramatic increase in the relaxation when the transition is resonant with the surface wave modes provides strong evidence of the effect. The red line is the theoretical calculation, which does not include any adjustments or scaling. Thus we can confidently describe the NV-magnon coupling in a physically realizable geometry. The coupling strongly depends on the characteristics of the spin wave modes and the geometry of the magnetic material. As a result the ability to pattern and template V[TCNE]<sub>x</sub> will be essential to realizing highly efficient two-qubit entangling gates using this approach.

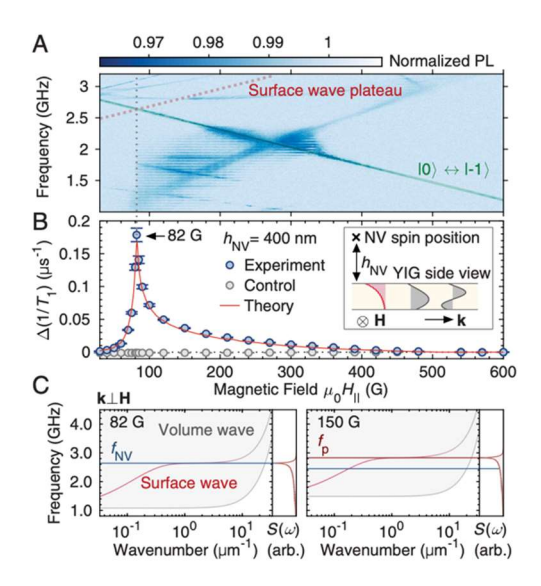


Figure 1. Surface-magnon induced longitudinal relaxation. (A) ODMR of NV centers on magnetic bar. The NV transition and the calculated surface magnon plateau are highlighted by the solid green and the dotted red lines, respectively. Vertical gray line indicates the field where the surface wave plateau is resonant with the NV transition. (B) Longitudinal relaxation rate of NV centers for the 0 to -1 transition. Blue and gray markers represent experiment with and (as control) without magnetic material, red curve is the theoretical calculation. On the vertical axis the  $\Delta$  indicates a reference of  $1/T_1$  to its value at 600 Gauss. NV-magnet distance is 400 nm. Inset shows cross section of the magnet with surface (red) and volume (gray) magnon mode profiles. k is the magnon wave vector. (C) Magnon dispersion for k perpendicular to H and noise spectra S(\omega) at 82 Gauss (left) and 150 Gauss (right). Surface magnon dispersion is shown with a pink curve with the gray gradient at large k indicating suppression of the surface-wave feature, whereas the gray area shows region of volume modes (see inset of (B)). Sharp peak in  $S(\omega)$  corresponds to the surface-wave plateau frequency  $f_p$  as indicated by horizontal red line. Blue horizontal line indicates NV frequency  $f_{NV}$ .

We will also discuss ongoing efforts to calculate the fringe fields, magnon dynamics, nonlinear features, and other properties of patterned  $V[TCNE]_x$ , as well as configurations that will enhance magnon-qubit couplings. Studies of the response of  $V[TCNE]_x$  to gating are underway and the progress will be outlined.

#### **Project supported References:**

- [1] Q. Xu et al., Advanced Science 11, 2310032 (2024). DOI: 10.1002/advs.202310032
- [2] B. A. McCullian, M. Chilcote, H. Yusuf, E. Johnston-Halperin, and G. D. Fuchs, In prep. (2025).
- [3] M. Fukami, D. R. Candido, D. D. Awschalom, and M. E. Flatté, PRX Quantum **2**, 040314 (2021). DOI: 10.1103/PRXQuantum.2.040314
- [4] D. R. Candido, G. D. Fuchs, E. Johnston-Halperin, and M. E. Flatté, Materials for Quantum Technology 1, 011001 (2020). DOI: 10.1088/2633-4356/ab9a55
- [5] M. Fukami *et al.*, Proceedings of the National Academy of Sciences 121, e2313754120 (2024). DOI: doi:10.1073/pnas.2313754120

#### Strongly interacting spin systems in diamond for quantum sensing

Ania Bleszynski Jayich<sup>1</sup> (PI), Kunal Mukherjee<sup>2</sup> (co-PI), David Weld<sup>1</sup> (co-PI), Norman Yao<sup>3</sup> (co-PI), Lillian Hughes<sup>1</sup>, Simon Meynell<sup>1</sup>, Weijie Wu<sup>3</sup>, Shreyas Parthasarathy<sup>1</sup>, Eveline Postelnicu<sup>2</sup>, Emily Davis<sup>4</sup>

<sup>1</sup>Department of Physics, University of California Santa Barbara, <sup>2</sup>Department of Materials Science and Engineering, Stanford University, <sup>3</sup>Department of Physics, Harvard University, <sup>4</sup>Department of Physics, New York University

**Abstract:** Solid-state quantum sensors are already impacting many arenas, including materials science and biology. With improvements in quantum control and materials engineering, they are poised to make significant leaps forward in their sensitivity, spatial resolution, and applicability in real-world applications in the coming years. Here we use the diamond nitrogen vacancy (NV), one of the most advanced solid-state quantum sensors to date, and demonstrate novel quantum control and materials engineering techniques in spin ensembles with strong dipolar interactions and controlled dimensionality, and we show how these systems can be uniquely leveraged for advances in quantum sensing and simulation.

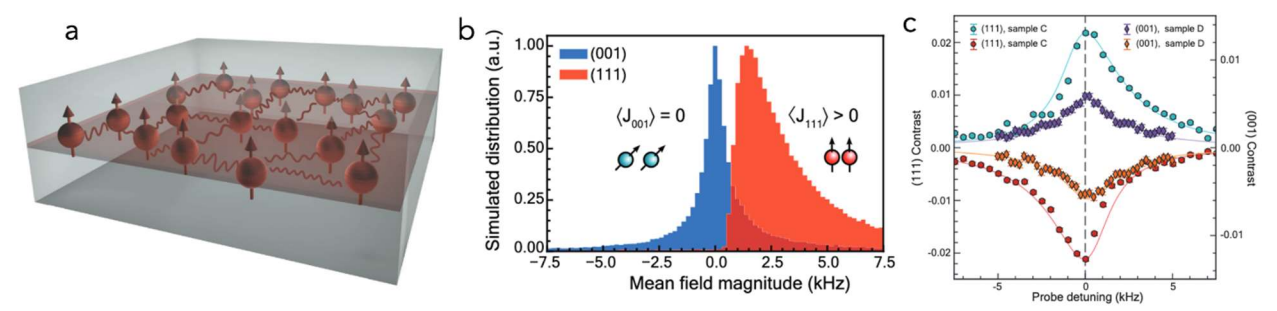


Figure 1: a) schematic of a strongly interacted 2D spin ensemble with spin quantization axis normal to the 2D plane. b) Simulated dipolar interaction-induced mean field distribution for (001) (blue) and (111) (red) NV ensembles, illustrating an asymmetric distribution for (111) due to the uniformly positive dipolar interaction energy. C) ODMR spectra for NV ensembles in (111)-oriented and (001)-oriented sample, where the asymmetric distribution of mean fields is reflected in the asymmetry of the 111-data (and not in the 100-data).

We first show the creation of strong dipolar interactions in a two-dimensional ensemble of nitrogen-vacancy (NV) centers generated via PECVD on (111)-oriented diamond substrates [1]. We find that diamond growth on the (111) plane yields high incorporation of spins, both nitrogen and NV centers, where the density of the latter is tunable via the miscut of the diamond substrate. Our process allows us to form dense, preferentially aligned, 2D NV ensembles with volume-normalized ac sensitivity down to  $\eta_{AC}$  =810 pT  $\mu m^{3/2}$   $Hz^{-1/2}$ . Importantly, we show that (111) affords maximally positive dipolar interactions among a 2D NV ensemble, which is crucial for leveraging dipolar-driven entanglement schemes and exploring new interacting spin physics. With these ensembles, we next demonstrate the ability to generate and characterize metrologically useful many-body entangled states (spin-squeezed states) [2].

Looking forward, we aim to fruitfully integrate these entanglement-enhanced sensors into close proximity with sensing targets. To that end, we discuss the challenges of bringing these sensors near a surface (such as increased decoherence) and our progress in attacking these challenges [3].

- [1] "A strongly interacting, two-dimensional, dipolar spin ensemble in (111)-oriented diamond", L. B. Hughes, S. A. Meynell, W. Wu, S. Parthasarathy, L. Chen, Z. Zhang, Z. Wang, E. J. Davis, K. Mukherjee, N. Y. Yao, A. C. B. Jayich, *Physical Review X* **15**, 021035 (2025). https://doi.org/10.1103/PhysRevX.15.021035
- [2] "Spin squeezing in an ensemble of nitrogen-vacancy centers in diamond", W. Wu, E. J. Davis, L. B. Hughes, B. Ye, Z. Wang, D. Kufel, T. Ono, S. A. Meynell, M. Block, C. Liu, H. Yang, A. C. B. Jayich, N. Y. Yao, *arXiv:2503.14585* (2025). https://doi.org/10.48550/arXiv.2503.14585
- [3] "Role of Oxygen in Laser Induced Contamination at Diamond-Vacuum Interfaces", S. Parthasarathy, M. Joos, L. B. Hughes, S. A. Meynell, T. A. Morrison, J. D. Risner-Jamtgaard, D. M. Weld, K. Mukherjee, A. C. B. Jayich, *Phys. Rev. Appl.* **22**, 024067 (2024). https://doi.org/10.1103/PhysRevApplied.22.024067

# Creating and Interfacing Designer Chemical Qubits DE-SC0025176

#### Molecular color centers for quantum sensing

PI: <u>Danna Freedman</u> | Massachusetts Institute of Technology Co-PIs James Rondinelli | Northwestern University; **David Awschalom** | University of Chicago; **Mark Hersam** | Northwestern University; **Jeffrey Long** | University of California Berkeley; **Michael Wasielewski** | Northwestern University Participants and collaborators: Mike Park, Alessandro Pereyra, Dane Johnson, Grant Smith, Dr. Noah Mendelson, Dr. Leah Weiss, Dr. Ryan Murphy, Dr. Bahman Golesorkhi, Priya Patel, José Méndez, Dr. Jens Niklas, Dr. Oleg Poluektov

**Abstract**:A bottom-up molecular approach enables the design and synthesis of tailored materials for quantum information science (QIS). As articulated in the Report of the Basic Energy Sciences Roundtable on *Opportunities for Basic Research for Next-Generation Quantum Systems*, creating and understanding new materials for QIS is crucial to realize quantum computing and quantum sensing.<sup>3–5</sup> The impact of an integrated chemical approach to the creation of designer systems was further reinforced in the recent National Academy of Sciences report on *Advancing Chemistry and Quantum Information Science*, which highlighted the essential role of chemistry in the creation of next generation quantum systems. Towards that end, our team is harnessing molecular our toolkit to *execute quantum sensing experiments to measure quantum materials*. Our approach uniquely situates molecular quantum sensors with atomic precision in van der Waals contact or covalent linkage with an analyte, thereby providing unparalleled sensitivity and enabling distance-dependent studies at unprecedentedly short length scales.<sup>9</sup>

Here, we will describe two recent accomplishments (1) the development of thin films for quantum material sensing and (2) the first molecular Er qubit. To integrate molecular qubits with 2D materials, **Hersam** deposited films onto monolayer graphene. Electron paramagnetic resonance (EPR) (**Freedman**) and magneto-photoluminescence (magneto-PL) (**Awschalom**) measurements confirm that  $Cr(o\text{-tolyl})_4$  remains microwave addressable and optically active in the thin film environment (**Figure 1**). **Hersam**, **Freedman**, and **Awschalom** have shown that the spin-state can be initialized and read-out optically for thin films grown on sapphire. Ongoing work is focused on

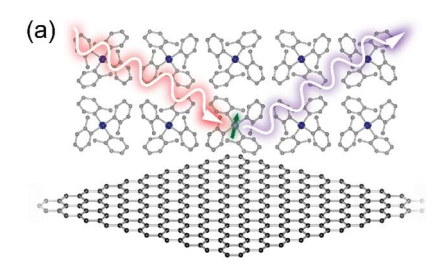


**Figure 1** | (a) Schematic illustration of a CrSn(*o*-tolyl)<sub>4</sub> molecular qubit thin film on monolayer graphene.

characterizing the spin-optical interface for thin films grown on 2D materials. In parallel, **Hersam** has been expanding the thin-film library with additional combinations of molecular qubits and host matrices. For instance, films of Cr(o-tolyl)<sub>4</sub>/Sn(4-fluoro-2-methylphenyl)<sub>4</sub> and Cr(2,3-dimethylphenyl)<sub>4</sub>/Sn(2,3-dimethylphenyl)<sub>4</sub> have been grown on monolayer graphene. This growing list of thin film compositions is expanding the quantum sensing options for optically addressable molecular qubits.

In a second area Awschalom and Long have demonstrated proof-of-principle a optically addressable molecular qubit, Cs[Er(hfac)<sub>4</sub>] (hfac = hexafluoroacetylacetone), highlighting the benefits of Kramer's ion molecules as a complementary platform for quantum sensing. As highlighted in Figure 2, the qubit features the requisite level structure and optical cycling (Figure 2) that has now enabled demonstration of optical initialization and readout (Figure 2c,d) as well as coherent ground state qubit control. We have further demonstrated optical spin-spectroscopy making use of the narrow homogeneous  $(\sim MHz)$ and inhomogeneous linewidths (~GHz), key features for the performance of this platform in future sensing applications at 1.53 μm (within the NIR-III transparency for biological materials). Note, this collaborative work leverages Long's orthogonal BES-funded efforts to synthesize lanthanide-based molecular qubits, supported at Lawrence Berkeley National Laboratory under contract no. DE-AC02-05CH11231.

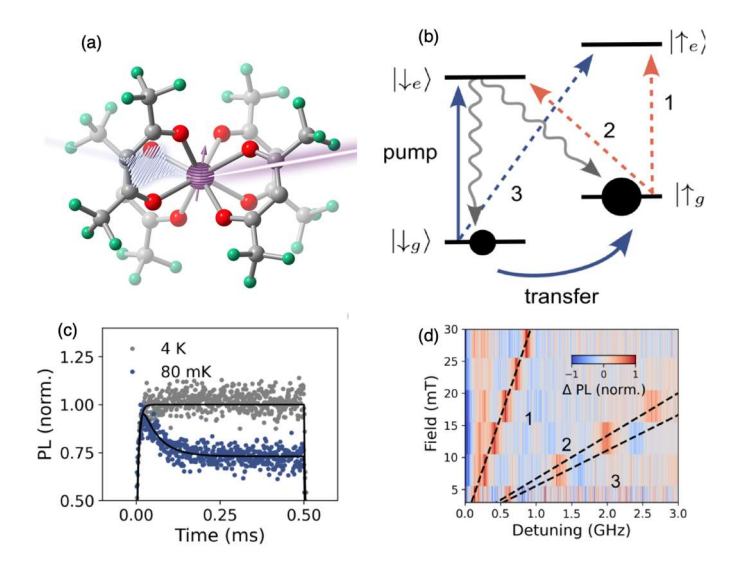


**Figure 2** | Optically addressable lanthanide molecular qubits. (a) Depiction of Cs[Er(hfac)<sub>4</sub>]. Red, grey, green, and purple correspond to oxygen, carbon, fluorine, and erbium, respectively. Cs and H atoms omitted for clarity. (b) Level diagram and spin-dependent optical transitions of Cs[Er(hfac)<sub>4</sub>]. (c) Temperature-dependent depletion of population due to optical spin pumping at millikelvin temperatures. (d) Differential photoluminescence as a function of applied magnetic field and optical detuning (via electro-optic modulation) which features enhanced photoluminescence along transitions 1,2 as labeled in (b) and diminished photoluminescence at zero detuning and 3 as labeled in (b) consistent with optical spin pumping into the electronic spin sublevel.

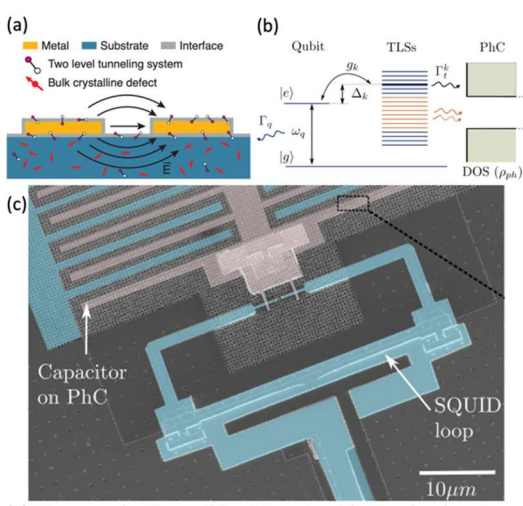
#### **Phonon Control for Next-Generation Superconducting Systems and Sensors**

#### KCAS23

<u>Alp Sipahigil</u>, Haoxin Zhou, Kangdi Yu, Zi-Huai Zhang, Yashwanth Balaji, Mythili Surendran, **Shaul Aloni**, Sinéad Griffin, Adam Schwartzberg

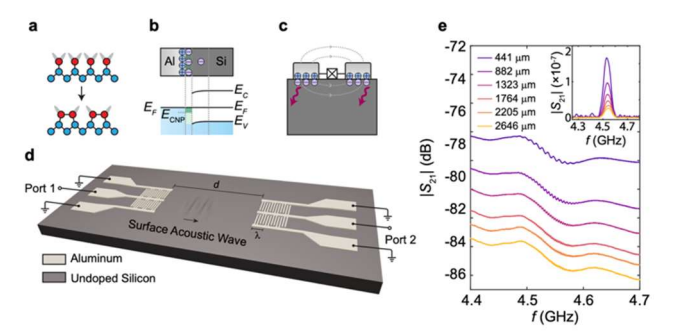
Lawrence Berkeley National Laboratory, 1 Cyclotron Road, Berkeley, California 94720, USA

Abstract:Our project aims to advance superconducting qubits and quantum sensors by understanding and their interactions with phonons. controlling Piezoelectricity results decoherence superconducting qubits by converting electrical energy of the qubit into phonons in the substrate. Traditional qubit substrates, such as sapphire and silicon, centrosymmetric crystals that lack piezoelectricity. However, in real-world quantum devices, symmetry is broken by defects and interfaces that can lead to a weak piezoelectric response and qubit decoherence by phonon radiation. In this presentation, I will discuss three recent results by our team on (i) identifying microscopic origins of superconducting qubit decoherence due to defectinduced piezoelectricity in silicon [1], (ii) suppressing phonon radiation in superconducting qubits via artificial materials with phononic bandgaps [2], and (iii) the first observation of interface piezoelectricity at the aluminumsilicon interface as a decoherence mechanism for superconducting qubits [3].



(a) Superconducting qubits interact with two-level system defects at interfaces and bulk crystalline substrates [1]. (b) Qubit-TLS interactions lead to decoherence by phonon radiation, which can be suppressed using a phononic bandgap crystal (PhC). (c) Image of a superconducting qubit embedded in an artificial, phononic bandgap material. The qubit showed slowed relaxation to the environment [2].

I will begin by presenting the first microscopic identification of two-level system defects (TLSs) in crystalline substrates (Figure 1, [1]). In this work, we used the electronic structure of acceptor defects in silicon to predict their behavior as TLSs for superconducting qubits. Our findings show that even ultralow concentrations of boron in silicon at  $10^{12}/\mathrm{cm}^{-3}$  are sufficient to limit superconducting qubit performance, pointing to the need for higher-purity silicon substrates to enable next-generation superconducting qubits. Next, I will discuss a complementary approach that suppresses TLS-induced phonon radiation



(a,b) Surface reconstruction or work function mismatch can lead to a (c) polar interface with piezoelectric response. (d) Device geometry to probe interface piezoelectricity using surface acoustic waves (SAWs). (e) Observation interface piezoelectricity using microwave transmission measurements

from superconducting qubits by utilizing artificial phononic bandgap materials. I will discuss the emergence of non-Markovian qubit dynamics inside the phononic bandgap [2] and discuss ongoing work to extend qubit lifetimes using this approach. Finally, I will present our discovery of interface piezoelectricity occurring at aluminum-silicon junctions at cryogenic temperatures (Figure 2, [3]). Breaking of centrosymmetry at material interfaces leads to a dipole density and an effective piezoelectric response. While interface piezoelectricity has been predicted as a loss mechanism for superconducting qubits two-decades ago, it has not been experimentally observed. I will present our observation of this effect using

surface acoustic wave transducers from room temperature down to 10 mK. I will discuss temperature, material processing, and bias dependence of this effect and discuss possible origins. I will conclude by discussing the consequences of interface piezoelectricity on superconducting qubits, and present ongoing work where we are directly probing this effect with a superconducting qubit.

#### References:

- [1] Z. H. Zhang\*, K. Godeneli\*, J. He, M. Odeh, H. Zhou, S. Meesala, A. Sipahigil Physical Review X 14, 041022(2024); DOI: 10.1103/PhysRevX.14.041022 (Partially supported by this program: materials characterization)
- [2] M. Odeh, K. Godeneli, E. Li, R. Tangirala, H. Zhou, X. Zhang, Z. Zhang, A. Sipahigil, "Non-Markovian dynamics of a superconducting qubit in a phononic bandgap", Nature Physics 21, 406–411 (2025); DOI: 10.1038/s41567-024-02740-5 (funded by this program)
- [3] H. Zhou, E. Li, K. Godeneli, Z. H. Zhang, S. Jahanbani, K. Yu, M. Odeh, S. Aloni, S. Griffin, A. Sipahigil, "Observation of interface piezoelectricity in superconducting devices on silicon" arXiv:2409.10626 (2024); DOI: 10.48550/arXiv.2409.10626 (funded by this program)

# Scalable quantum photonic materials based on precision doped diamond nanostructures Award Number: DE-SC0025295

#### High quality quantum photonic interface for tin-vacancy color centers in thin-film diamond

<u>Jelena Vuckovic<sup>1</sup></u> (PI), Hope Lee<sup>1</sup>, Abigail Stein<sup>1</sup>, Hannah Kleidermacher<sup>1</sup>, **Michael Titze<sup>2</sup>** (co-PI), Shei Su<sup>2</sup>, Luca Basso<sup>2</sup>, Ania Jayich <sup>3</sup> (collaborator), Lillian Hughes<sup>3</sup>, Hyunseok Oh<sup>3</sup>, Kyuhyun Kim<sup>3</sup>

<sup>1</sup>Stanford University, Stanford, CA 94305; <sup>2</sup>Sandia National Laboratories, Albuquerque, NM 87123; <sup>3</sup>University of California Santa Barbara, CA 93106

Abstract: The tin-vacancy (SnV) in diamond has been identified as one of the most promising color centers for implementation of quantum networks, facilitating their scaling beyond the present record of 3 quantum nodes. As opposed to the silicon vacancy (SiV) in diamond, the SnV provides the same properties (long coherence, robustness to interfaces), but in naturally strained diamond and at elevated temperatures of 1.7K (as opposed to mK). Our team demonstrated single shot readout for the SnV-'s electron spin with record fidelity of 87.4% [1], but this must be improved for use in quantum technologies. The fidelity is limited by low photon collection efficiency from diamond (total efficiency of ~0.1% in the mesa type structure employed in this work). For this reason, in this project we have been focusing on development of high quality quantum photonic interface for SnV in diamond, and specifically in diamond thin films which are more suitable for high quality cavity fabrication.

Diamond thin films were fabricated in collaboration with Prof. Ania Jayich's group at UC Santa Barbara via smart cut methods. We then characterized the optical properties of SnV- centers implanted in these samples via photoluminescence (PL) and photoluminescence excitation (PLE) spectroscopy. From the PL confocal scans, bright color centers, with a density suitable for photonic crystal fabrication, were identified. From PLE spectroscopy, we probed the temporal stability of implanted color centers and determined an average linewidth of ~500 MHz for emitters.

We subsequently fabricated arrays of high quality photonic crystal nanobeam cavities together with microwave delivery electrodes and wire bonding pads surrounding the thin film diamond membrane (see Figure 1).

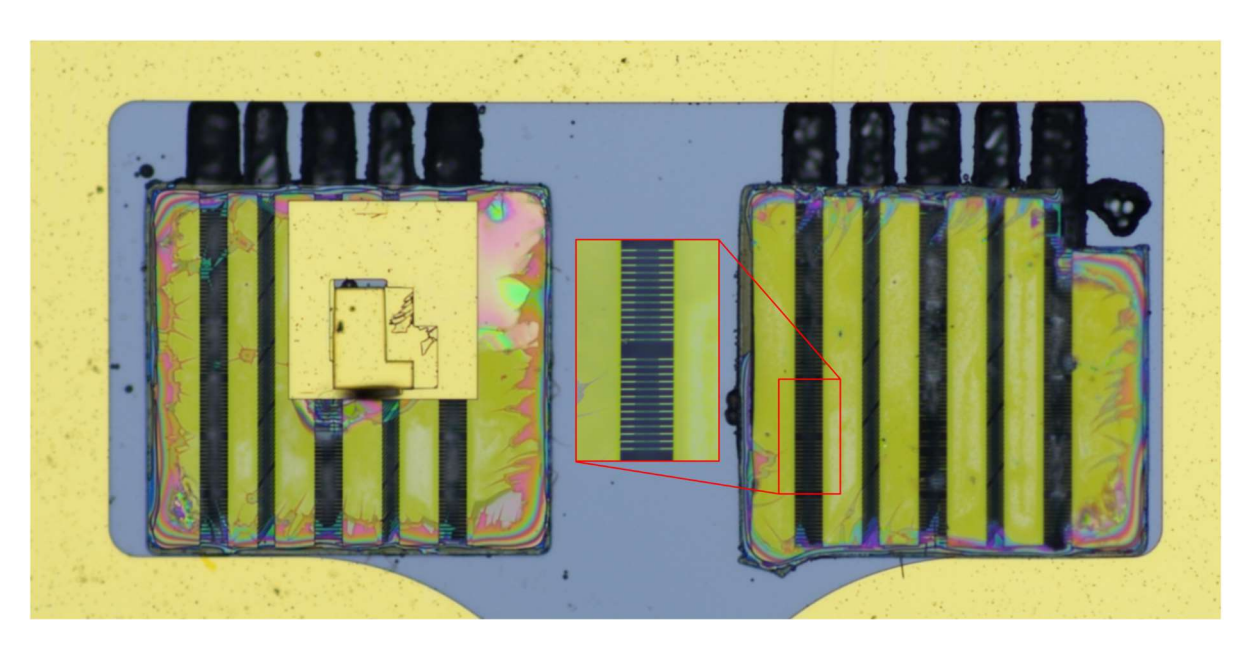


**Figure 1.** Optical microscope image of completed photonic crystal devices in diamond thin films. The films are surrounded by Au microwave delivery electrodes. A small extra Au patch is used to anchor the left side film that has a hole from the bonding process. The inset shows details of the photonic crystal nanobeams, with the darker region in the center indicating the presence of periodic etched holes.

We characterized these cavities via cross-polarized reflectance. For this configuration, the sample is mounted with cavity mode aligned to the horizontal polarization (H). A vertically polarized (V) broadband light source serves as the input, and the reflected spectrum is collected in H; the two paths are mixed with a polarizing beamsplitter. A half-wave plate oriented at  $\sim$ 22 degrees allows for partial excitation and collection of the cavity mode. From fitting spectrum peaks, we observe quality factors up to  $\sim$ 6000 at wavelengths as low as 612 nm, limited by spectrometer resolution. These resonances can then be red shifted via controlled Ar gas condensation to interact with coupled SnV- color centers, with preliminary demonstrations showing a factor of 12 PL enhancement when the cavity is on resonance with the SnV- zero phonon line.

We are currently working on measuring spontaneous emission rate enhancement (Purcell enhancement) of individual SnV's in these cavities, and will then perform spin control and single shot readout on SnV's embedded in cavities. We expect that single shot readout fidelity of an electron spin should be significantly approved, approaching 100%.

#### References:

- 1. "Single-Shot Readout and Weak Measurement of the Tin-Vacancy Qubit in Diamond," Eric I. Rosenthal, Souvik Biswas, Giovanni Scuri, Hope Lee, Abigail J. Stein, Hannah C. Kleidermacher, Jakob Grzesik, Alison E. Rugar, Shahriar Aghaeimeibodi, Daniel Riedel, Michael Titze, Edward S. Bielejec, Joonhee Choi, Christopher P. Anderson, and Jelena Vuckovic, *Physical Review X*, vol. 14, 041008 (2024) DOI: https://doi-
- 2. org.stanford.idm.oclc.org/10.1103/PhysRevX.14.041008

#### **Creating and Controlling Atomic Scale Quantum Systems**

**Award Number: ERKCK47** 

Abstract Title: Atom-by-Atom Fabrication for Quantum Information Sciences

Names of PI, coPI(s): Stephen Jesse, Ondrej Dyck, Chris Nelson, Mina Yoon, Andy Lupini

**Affiliation:** Oak Ridge National Laboratory

Abstract: Atomic-scale fabrication is pivotal for advancing quantum information sciences (QIS),

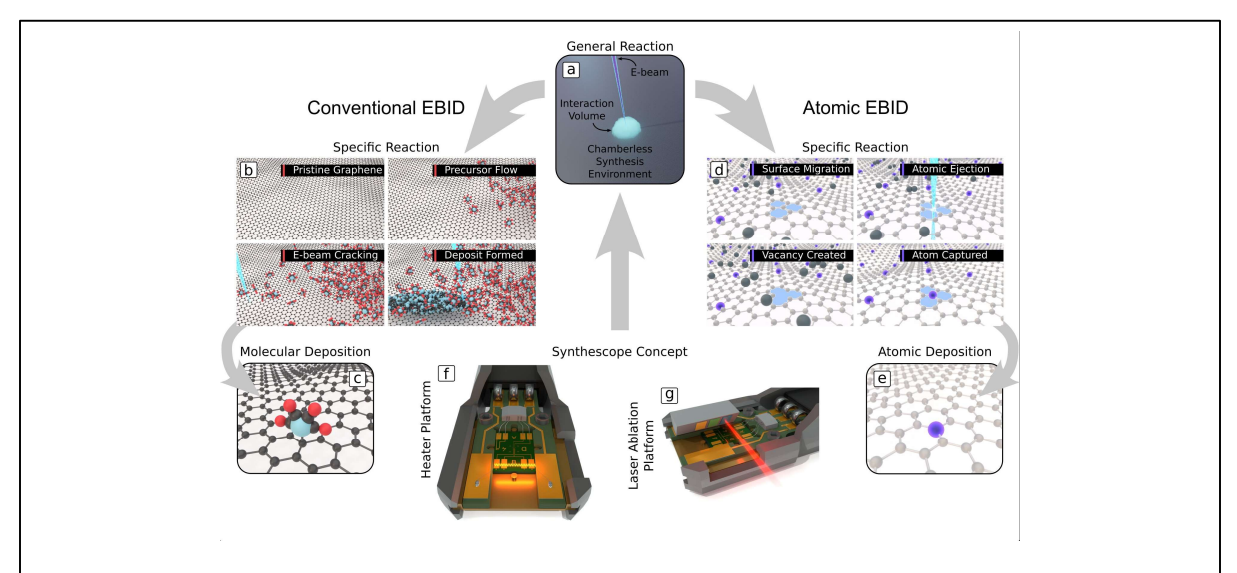


Figure 1: Synthescope concept. (a) Depiction of a general reaction. (b) Illustration of the conventional EBID process. (c) Fundamental limit of conventional EBID. (d) Illustration of an atomic EBIC process. (e) Fundamental limit of atomic EBID. (f) Schematic of heater deposition platform. (g) Schematic of laser deposition platform.

enabling the creation of tailored quantum devices such as qubits and emitters. We have developed scanning transmission electron microscopy (STEM)-based techniques to achieve atomic manipulation, directly addressing QIS needs. This abstract outlines technical advancements in electron beam-induced fabrication, focusing on "the synthescope", and applications to quantum technologies. Our approach builds on the deterministic placement of single atoms, initially demonstrated with silicon impurities in graphene. By creating chemically reactive defect sites and leveraging electron beams to position atoms, we achieved precise doping with elements like tin, chromium, and platinum. A key innovation is the synthescope, which transforms the STEM into a synthesis platform—the beam-sample interaction

volume conceived of as a chamberless synthesis environment (CSE) (Fig. 1a). Unlike traditional electron beam-induced deposition (EBID) (Fig. 1b-c), which is limited to molecular deposition, atomic EBID creates vacancies that capture single atoms, achieving the ultimate in precision at the single atom atom level (Fig. 1d-e). The abstraction of these two approaches is one where a general reaction is sought within the CSE without specifying what that reaction should be. To discover and control these reactions

we must furnish the STEM with additional capabilities aimed at environmental control. The first target is the supply of atoms. The platforms illustrated in Fig. 1f-g illustrate a heater and laser strategy. By heating the substrate to stimulate thermal migration, we enabled long-range patterning of atomic clusters, as demonstrated with copper on twisted bilayer graphene.<sup>2</sup> The filament-based heater (Fig. 2a-c) builds on this idea to evaporate source materials like tin in situ, growing nanoflakes on graphene (Fig. 2d).<sup>3</sup> An alternative laser ablation approach will further expand versatility and control (Fig. 2e-f).<sup>4</sup>

To enhance device fabrication, we are developing a quantum lab-on-a-chip in collaboration with MIT and KAUST, integrating e.g. electrical biasing, gating, magnetic fields, amplifiers, heaters, and photon detectors into a MEMS chip at the synthescope's core (black chip in Fig.2a). These added capabilities will further enhance control over the sample environment and provide access to new information channels for experiments (transport,

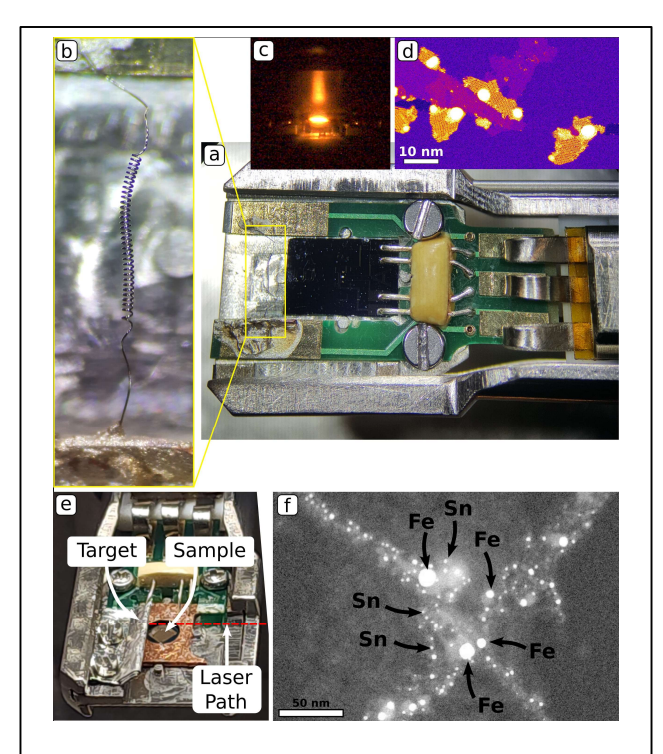


Figure 2. (a) Heater deposition platform. (b) Magnified view of W heater filament. (c) Heater operating in microscope stage. (d) Sn nanoflakes grown in situ. (e) Laser deposition platform. (f) Example Sn nanoparticles deposited in situ.

photon detection, electron density measurements). Our atomic fabrication techniques offer a promising approach to QIS. By enabling precise control over atomic structures, we pave the way for prototype quantum devices and the implementation of experiments thought to be impossible to perform due to fabrication limitations.

- (1) Dyck, O.; Lupini, A. R.; Jesse, S. Advanced Materials 2023, 35 (45), 2301560. https://doi.org/10.1002/adma.202301560.
- (2) Dyck, O.; Yeom, S.; Lupini, A. R.; Swett, J. L.; Hensley, D.; Yoon, M.; Jesse, S. Advanced Materials 2023, 35 (32), 2302906.
- (3) Dyck, O.; Lupini, A. R.; Jesse, S. Small Methods 2023, 7 (10), 2300401.
- (4) Dyck, O.; Olunloyo, O.; Xiao, K.; Wolf, B.; Moore, T. M.; Lupini, A. R.; Jesse, S. Advanced Materials Technologies 2025, 10 (5), 2401208.

#### Modeling, probing, and controlling quantum coherence in materials

**DE-SC0020313**, FWP: SCW1797 (LLNL)

#### Scalable parallel quantum sensing with individual nitrogen-vacancy centers in diamond

Victor Brar<sup>1</sup>, Matthew Cambria<sup>2</sup>, Saroj Chand<sup>2</sup>, Jennifer Choy<sup>1</sup>, Ádam Gali<sup>3</sup>, <u>Shimon Kolkowitz</u><sup>2</sup>, Alex Levchenko<sup>1</sup>, Vincenzo Lordi<sup>4</sup>, Jeronimo Maze<sup>5</sup>, Robert McDermott<sup>1</sup>, Keith Ray<sup>4</sup>, Caitlin Reiter <sup>2</sup>

<sup>1</sup>University of Wisconsin, Madison, WI, USA. <sup>2</sup>University of California, Berkeley, CA, USA. <sup>3</sup>Wigner Research Centre for Physics, Budapest, Hungary. <sup>4</sup>Lawrence Livermore National Laboratory, Livermore, CA, USA. <sup>5</sup>Pontificia Universidad Católica de Chile, Santiago, Chile.

Abstract: In this collaborative QIS project our central aim is to apply a detailed understanding of decoherence to develop next-generation quantum sensors and high-fidelity qubits that are amenable to scaling. Our team of theorists and experimentalists are working closely together to achieve the following aims: (i) Refine quantum probes and theoretical models to determine the microscopic origins of noise from surfaces, interfaces, and the bulk across a range of quantum platforms. (ii) Integrate the quantum probes and theoretical models we have developed to cross-validate experimental and theoretical results and conclusions, and to gain deeper insights into coherence in materials. (iii) Harness our newfound knowledge and understanding to inform system-level design of quantum devices in order to mitigate and eliminate materials-induced decoherence. The improvements in materials properties and quantum device design enabled by our efforts will open a wider range of parameters and geometries for viable qubits and quantum sensors, improving the prospects for scaling solid-state qubits toward fully error-corrected fault-tolerant arrays, and enhancing the spatial resolution and sensitivity of quantum sensors.

One focus of our efforts has been on understanding the microscopic origins of decoherence in nitrogen vacancy (NV) centers in diamond. Most applications of NV centers take advantage of their long electronic spin coherence times. Spin-phonon relaxation places an ultimate limit on the achievable coherence times, but surprisingly the limits as a function of temperature had not previously been fully characterized. In addition, the microscopic origins of spin-phonon coupling were not fully understood. We characterized the phonon-limited three-level relaxation rates in multiple samples with differing defect concentrations over a broad range of experimentally relevant temperatures. We developed a self-consistent microscopic model that fully explains the observed relaxation rates, and that clarifies and corrects prior longstanding misunderstandings in the field. These results were published in Physical Review Letters [1]. In the process, we also discovered a physically motivated analytical expression for the temperature dependence of the zero-field splitting of the NV center electronic spin, which is widely used for nanoscale thermometry [2].

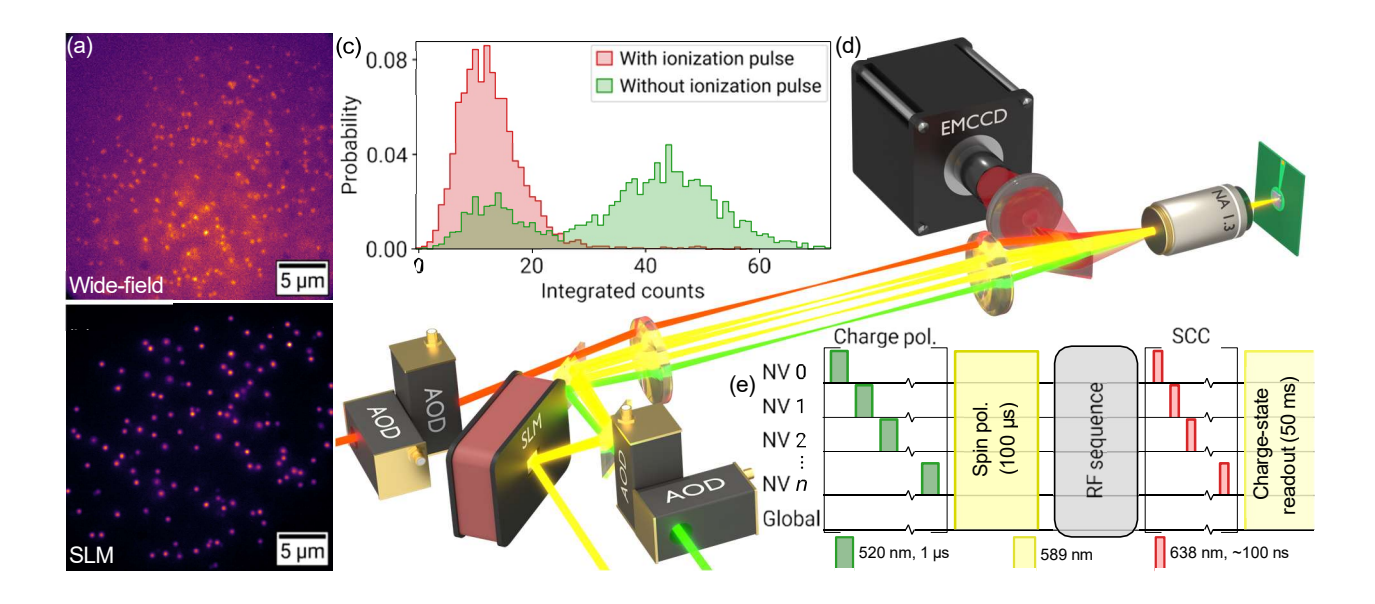


**Figure 1:** (a) Image of NV centers in diamond under wide-field 520-nm illumination. (b) Same region under 589-nm illumination patterned with a spatial light modulator (SLM). 108 charge-stable single NV centers are targeted, exhibiting consistent ODMR signals. (c) NV center charge-state manipulation and readout. (d) Experimental apparatus for multi-NV center quantum sensing. (e) Experimental sequence for parallel spin measurements. Figure adapted from Ref. [3]

Another focus of our efforts has been on leveraging our improved understanding of the physics of the NV center to scale up nanoscale quantum sensing. Typically, quantum sensing experiments using NV centers are performed either with a single isolated NV center or with an unresolved ensemble of many NV centers, resulting in a trade-off between measurement speed and spatial resolution or control over individual defects. We developed a new experimental platform with the capability to coherently manipulate and measure over 100 NV centers in parallel. These results have been accepted for publication in *Physical Review X* [3]. We are currently in the process of integrating our novel multiplexed quantum sensing technique with a cryostat in order to study the origins of flux noise at superconductor interfaces.

- [1] MC Cambria, A Norambuena, HT Dinani, G Thiering, A Gardill, I Kemeny, Y Li, V Lordi, Á Gali, JR Maze, et al. Temperature-dependent spin-lattice relaxation of the nitrogen-vacancy spin triplet in diamond. *Physical Review Letters*, 130(25):256903, 2023. DOI:10.1103/PhysRevLett.130.256903.
- [2] MC Cambria, G Thiering, A Norambuena, HT Dinani, A Gardill, I Kemeny, V Lordi, Á Gali, JR Maze, and S Kolkowitz. Physically motivated analytical expression for the temperature dependence of the zero-field splitting of the nitrogen-vacancy center in diamond. *Physical Review B*, 108(18):L180102, 2023. DOI:10.1103/PhysRevB.108.L180102.
- [3] MC Cambria, S Chand, C Reiter, and S Kolkowitz. Scalable parallel measurement of individual nitrogen-vacancy centers. *accepted for publication at Physical Review X, preprint available at arXiv:2408.11715*, 2025. DOI:10.48550/arXiv.2408.11715.

Partially prepared by LLNL under Contract DE-AC52-07NA27344.

# Novel Probes of Topological Superconductivity for Next-Generation Quantum Systems DE-SC0020305

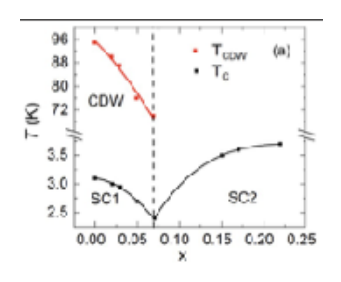
Leon Balents (co-PI), Stephen Wilson (co-PI), Ganesh Pokharel, Stephen J. Gomez Alvarado, Eric Cui, Taka Park, Arman Rashidi, Jiashu Wang, Andrea Young (co-PI), Susanne Stemmer (PI) University of California, Santa Barbara

Abstract: Topological superconductors host quasiparticles that are of great interest for generating quantum entangled states that are inherently and robustly protected against decoherence. Although several promising candidates have been identified, experimental techniques that unequivocally diagnose topological superconductivity are currently lacking. In this collaborative project between three experimental groups (Wilson, Young, Stemmer) and one theory group (Balents), we utilize topological superconductor candidates developed by our team to advance, test, and refine new techniques for probing the physics of topological superconductors. We aim at advancing local detection of signatures of their unique quasiparticles via their influence on observables like vortices, currents, or temperature, as well as more global measurements, such as x-ray scattering and transport, including thermoelectric and thermal signatures. To this end, the project is currently focusing on two main materials platforms: (i) kagome superconductors and (ii) synthetic structures that interface a superconductor with a topological material.

The kagome family offers a tunable platform for identifying signatures of topological superconductivity through phenomena, such as composite pairing, and through the interplay with charge correlations, such as charge density waves (CDWs), short-range charge correlations [1], and nematicity [2]. For example, theoretical studies of electronic instabilities in kagome metals in this project found superconductors, charge, orbital moment, and spin density waves when the Fermi energy was close to saddle points [3]. Experimentally, it was found that the addition of holes lifts the Van Hove points above the Fermi level and rapidly suppresses the CDW instability, resulting in "double-dome" superconductivity (Fig. 1). Recent experiments focused on gaining a better understanding of the interplay between charge correlations and superconductivity. To this end, the Wilson and Young groups imaged vortex lattices via nano-SQUID ona-tip (nSOT) measurements and determined charge correlations via synchrotron x-ray diffraction. An example is shown in Fig. 1. The nSOT measurements show the vortex lattice in the kagome superconductor CsV<sub>3</sub>Sb<sub>5</sub>. This vortex lattice persists across the entirety of the electronic phase diagram—across both superconducting domes, signifying 2e pairing both in the presence and absence of CDW order. Complementary x-ray measurements showed that the charge correlations abruptly vanish in the second superconducting dome. This is distinct from prior measurements of hole-doped CsV<sub>3</sub>Sb<sub>5</sub>. We are currently preparing a manuscript reporting on these studies.

In parallel with the experimental work, we are developing theoretical models of the mechanisms that can lead to unconventional superconductivity in these materials. In the limit of a perfectly flat band, the behavior is dictated by quantum geometry. In this project, we aim at understanding how quantum geometry influences the selection of emergent orders, such as intrinsic topological superconductivity. To this end, the Balents group has developed a formalism to determine the maximum susceptibility within flat bands, for both charge/spin density and superconducting orders. For repulsive interactions we found dominant antiferromagnetic order, while for attractive interactions we predicted unconventional superconducting states. We performed numerically exact determinantal Monte Carlo simulations, which confirmed the theoretical predictions [4].

The second major platform in this project are synthetic topological superconducting candidates, consisting of hybrid interfaces, either within a single materials platform [5] or by combining superconductors with topological or Chern insulators. To this end, we have focused on developing junctions that are compatible



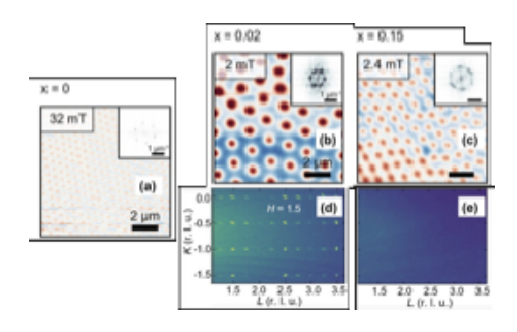


Fig. 1: (Left) CDW order and super-conductivity in CsV<sub>3-x</sub>Ti<sub>x</sub>Sb<sub>5</sub> as a function of hole-doping x. (Right) Evolution of the vortex lattice and charge correlations in CsV<sub>3-x</sub>Ti<sub>x</sub>Sb<sub>5:</sub> (a-c) vortex lattice (d) CDW order (e) Vanishing charge correlations in the second SC dome.

with nSOT imaging and that allow for new types of transport probes, including thermoelectric measurements. We found phenomena, such as diode effects, in the hybrid junctions. A model that incorporates the self-field induced by the superconducting current in the junctions describes some of the observations. A manuscript has been submitted. We have also fabricated superconductor/quantum Hall hybrid junctions and are currently analyzing the data.

#### References (\* indicates this project is acknowledged):

- [1]\* Frustrated Ising charge correlations in the kagome metal ScV<sub>6</sub>Sn<sub>6</sub>, S. J. Gomez Alvarado, G. Pokharel, B. R. Ortiz, Joseph A. M. Paddison, S. Sarker, J. P. C. Ruff, and S. D. Wilson, Phys. Rev. B 110, L140304 (2024). DOI: 10.1103/PhysRevB.110.L140304
- [2]\* Electronic nematicity without charge density waves in titanium-based kagome metal, H. Li, S. Cheng, B. R. Ortiz, H. Tan, D. Werhahn, K. Zeng, D. Johrendt, B. Yan, Z. Wang, S. D. Wilson & I. Zeljkovic, Nat. Phys. 19, 1591 (2023). DOI: 10.1038/s41567-023-02176-3
- [3]\* Electronic instabilities of kagome metals: Saddle points and Landau theory, T. Park, Mengxing Ye, Leon Balents, Phys. Rev. B 104, 035142 (2021). DOI: 10.1103/PhysRevB.104.035142
- [4]\* Identifying Instabilities with Quantum Geometry in Flat Band Systems, J.-X. Zhang, W. O. Wang, L. Balents, and L. Savary, submitted, arXiv: 2504.03882 (2025). DOI: 10.48550/arXiv.2504.03882.
- [5]\* Imaging inter-valley coherent order in magic-angle twisted trilayer graphene, H. Kim et al., Nature 623, 942 (2023). DOI: 10.1038/s41586-023-06663-8

# Imaging Emergent Phenomena in Two-Dimensional Magnets Using Single-Spin Quantum Microscope

#### **DE-SC0024177**

<u>Brian Zhou</u><sup>1</sup>, Yu-Xuan Wang<sup>1</sup>, Thomas Graham<sup>1</sup>, Xin-Yue Zhang<sup>1</sup>, Zhong Lin<sup>2</sup>, Claire Besson<sup>2</sup>, Md Islam<sup>2</sup>, Rafael Gontijo<sup>2</sup>, Ganesh Tiwari<sup>2</sup>, Tibendra Adhikari<sup>2</sup>, Elton Santos<sup>3</sup>, Ricardo Rama-Eiroa<sup>3</sup>, Mohammad Badarneh<sup>3</sup>, Kenji Watanabe<sup>4</sup>, Takashi Taniguchi<sup>4</sup>

- 1) Boston College, Chestnut Hill, MA
- <sup>2)</sup> Binghamton University, Binghamton, NY
- 3) University of Edinburgh, Edinburgh, United Kingdom
- <sup>4)</sup> National Institute for Materials Science, Namiki, Tsukuba, Japan

#### **Abstract:**

This project aims to leverage and enhance the exceptional capabilities of quantum sensors based on the single electron spin of the nitrogen-vacancy (NV) center in diamond to deepen our understanding and drive the device integration of two-dimensional magnetic materials. A key focus is to transcend basic static characterizations by investigating dynamical phenomena and novel control mechanisms that may emerge under optical, electrical or magnetic perturbations, as well as via interfaces between heterogeneous systems. Our efforts, which rely on precise quantum control to isolate weak target signals from the noise, have the potential to unlock next-generation magnetic memories that overcome the energy efficiency bottleneck in current high-performance quantum-classical computing systems.

As a recent breakthrough, we have visualized for the first time the antiphase states in even-layer regions of an A-type antiferromagnet (AFM) with scanning NV magnetometry. Previously, it was believed that even-layer A-type AFMs have perfectly compensated magnetizations; however, by improving the stray field sensitivity of the quantum sensor, we were able to resolve a minute, uncompensated surface magnetization. This surface magnetization allowed us to visualize the nominally degenerate antiphase states (e.g.,  $\uparrow\downarrow$  vs  $\downarrow\uparrow$  in bilayer; see Fig. 1a) and crucially the domain walls between them [1]. Moreover, by directly configuring the antiphase states of even-layer regions surrounding an odd-layer region, we revealed a strong *lateral* exchange bias (Fig. 1b) and elucidated its microscopic domain wall origin [1]. This lateral exchange bias, stemming from the intrinsic intralayer exchange interaction within a pristine single material, offers superior robustness and predictability compared to conventional exchange biases realized in vertical ferromagnet-AFM bilayers, where the buried vertical interfaces are prone to disorder.

Our upcoming efforts will target the integration of these 2D AFMs into deployable devices, such as in magnetic tunnel junctions, where our novel exchange bias can perform an essential role in stabilizing the magnetization of the reference layer. Moreover, we will pursue customized dynamical sensing schemes with scanning NV magnetometry, requiring more advanced experimental synchronization, to broaden the range of dynamics, signals and samples that can be studied.

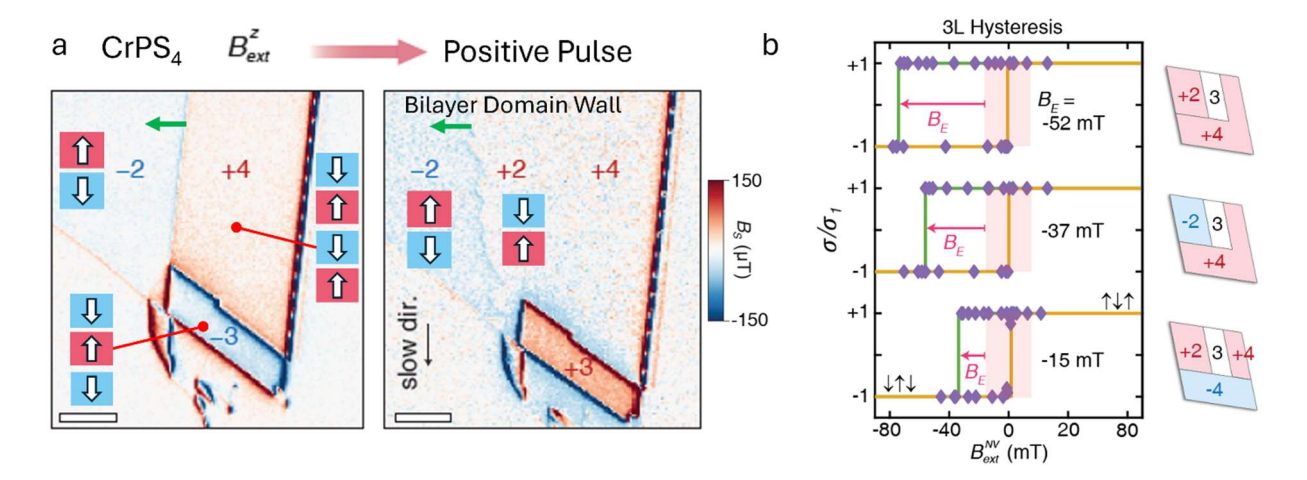


**Figure 1** Antiferromagnet domains and lateral exchange bias in atomically thin CrPS<sub>4</sub> visualized by single spin quantum sensing.

[1] Y.-X. Wang, T. K. M. Graham, R. Rama-Eiroa, A. Islam, M. H. Badarneh, R. N. Gontijo, G. P. Tiwari, T. Adhikari, X. Zhang, K. Watanabe, C. Besson, E. J. G. Santos, Z. Lin, and B. B. Zhou, Configurable antiferromagnetic domains and lateral exchange bias in atomically thin CrPS<sub>4</sub>, to appear in *Nature Materials* at <a href="https://doi.org/10.1038/s41563-025-02259-x">https://doi.org/10.1038/s41563-025-02259-x</a> (2025).

#### Probing Two-Dimensional Quantum Materials with Flying Electron Qubits

Award Number: DE-SC0025542

#### **Dafei Jin**

University of Notre Dame

#### **Abstract:**

We utilize our prior accomplishment in QIS – the long-coherence high-fidelity electron-on-solid-neon (eNe) qubit platform <sup>1,2</sup> – to develop a quantum-enabled SPM. The eNe-SPM is ideally suited to probe the electronic structures and phase transitions in two-dimensional (2D) quantum materials, i.e., exfoliated few-layer van der Waals (vdW) materials, at near-zero (~10mK) temperatures. (See **Fig. 1.**) With this

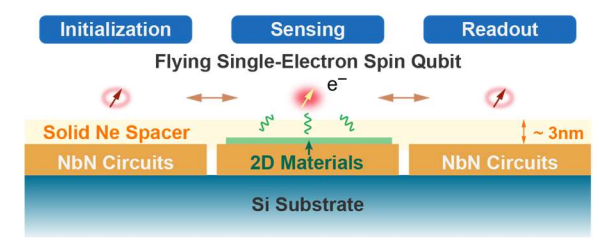


**Fig. 1**: Schematic of the electron-on-solid-neon (eNe) qubit enabled scanning probe microscopy (SPM).

technique, 2D quantum materials under investigation are transferred onto a superconducting quantum circuit and coated with a ~3nm thick noninvasive spacer – solid Ne. A single-electron qubit flying above the solid Ne at a ~1nm distance is transported, trapped, controlled, and read out by the quantum circuit. The spin states of the qubit (sensor) electron strongly interact with the spin or current states of the material (target) electrons and shed light on the local properties (e.g., spin texture and supercurrent) of the materials. Position scanning can be achieved by continuously sweeping the sensor electron above the materials with electric fields free of mechanical vibration or heat generation. The spatial resolution can reach ~1nm, which is limited only by the sharpness of the electron wavefunction and the precision of control electronics. The ultralong spin coherence time (~1s) <sup>3</sup> and charge coherence time (~0.1ms) <sup>2</sup> versus the ultrashort transport time (~10ns) and spin-to-charge conversion time (~5ns) in this system guarantee ultrahigh sensing fidelity. In the end, we intend to implement this new technique to study magnetic and topological materials, unconventional superconductors, quantum spin liquids, etc.

Last year, we made several crucial breakthroughs for this project. This award critically supported the growth and characterization of solid neon, as the key to all subsequent developments.

- We measured the charge noise spectrum of eNe qubits and confirmed their order-of-magnitude quietness compared to semiconducting quantum-dot qubits. 4 (See Fig. 2.)
- We promoted the operation temperature of eNe qubits to above 100mK and observed their much slower performance downgrade compared to superconducting transmon qubits.
- We achieved the first set of entangled two-qubit gates in the eNe system, which paves the way toward multi-qubit distributed quantum sensing in the longer term. <sup>5</sup>
- We built a new experimental setup to accurately measure the electron mobility on solid neon, which will calibrate the electron spin shuttling in the proposed scanning probe technique.

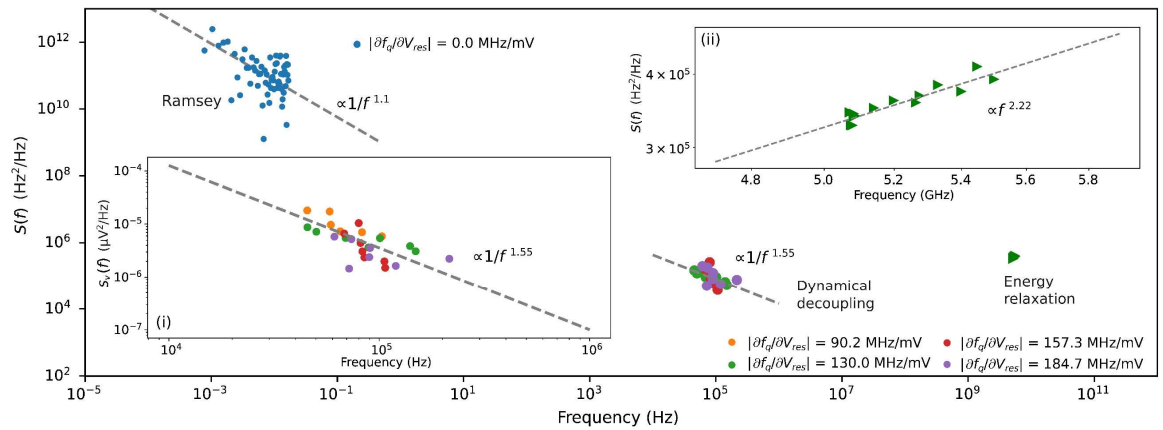


**Fig. 2**: Noise spectrum of an eNe qubit. Color dots in the main plot for 0.01–1MHz: total noise density derived from dynamical decoupling data at different qubit bias points. Blue dots in the main plot for  $10^{-3}$ – $10^{-1}$ Hz: calculated total noise density from long-term Ramsey measurements when biased at charge sweet-spot. Green triangles in the main plot near 5GHz: transverse noise of the eNe qubit. Inset (i): equivalent charge (voltage) noise on the resonator electrode. Inset (ii): zoom-in of transverse noise. Gray dashed lines: power-law fits of frequency-dependent noise. <sup>4</sup>

Next year, we have several tasks to complete. This award is the primary support for all these efforts.

- We will use a 4K cryogenic atomic force microscope (AFM) to *in situ* study the surface morphology of solid neon grown on a 2D material, specifically graphene and hexagonal boron nitride (hBN).
- We will attempt to trap a layer of 2D electrons atop a solid-Ne-coated 2D material and move the electrons around by surrounding electrodes.
- We will fabricate a prototype spin-charge conversion device containing a superconducting resonator and a micromagnet.

#### References

- X. Zhou, G. Koolstra, X. Zhang, G. Yang, X. Han, B. Dizdar, X. Li, R. Divan, W. Guo, K. W. Murch, D. I. Schuster, and D. Jin, "Single electrons on solid neon as a new solid-state qubit platform", Nature 605, 46–50 (2022). DOI: 10.1038/s41586-022-04539-x
- X. Zhou, X. Li, Q. Chen, G. Koolstra, G. Yang, B. Dizdar, Y. Huang, C. S. Wang, X. Han, X. Zhang, D. I. Schuster, and D. Jin, "Electron charge qubits with 0.1 millisecond coherence time", Nat. Phys. 20, 116–122 (2024). DOI: 10.1038/s41567-023-02247-5
- 3. Q. Chen, I. Martin, L. Jiang, and D. Jin, "Electron spin coherence on a solid neon surface", **Quantum Sci. Technol.** 7, 045016 (2022). DOI: 10.1088/2058-9565/ac82c3
- 4. X. Li, C. S. Wang, B. Dizdar, Y. Huang, Y. Wen, W. Guo, X. Zhang, X. Han, X. Zhou, and D. Jin, "Noise-resilient solid host for electron qubits above 100 mK", arXiv:2502.01005 (2025), under review in Nature Electronics. DOI: 10.21203/rs.3.rs-5988860/v1 (Award acknowledged.)
- 5. X. Li, Y. Huang, X. Han, X. Zhou, and D. Jin, "Coherent manipulation of interacting electron qubits on solid neon", arXiv:2503.23738 (2025). DOI: 10.48550/arXiv.2503.23738 (Award acknowledged.)

# Hybrid Magnon Systems DE-SC0022060

## **Magnetoelastic Coupling to Magnons**

<u>Axel Hoffmann<sup>1,2,3</sup></u>, Zhixin Zhang<sup>1</sup>, Jinho Lim<sup>1</sup>, Haoyang Ni<sup>1</sup>, Yi Li<sup>4</sup>, Valentine Novosad<sup>4</sup>, Mijin Lim<sup>1</sup>, André Schleife<sup>1,2,10</sup>, and Jian-Min Zuo<sup>4</sup>

- 1. Department of Materials Science and Engineering, University of Illinois Urbana-Champaign, Urbana, IL 61801, USA.
- 2. Materials Research Laboratory, University of Illinois Urbana-Champaign, Urbana, IL 61801, USA.
- 3. Department of Physics, University of Illinois Urbana-Champaign, Urbana, IL 61801, USA.
- 4. Materials Science Division, Argonne National Laboratory, Lemont, IL 60439, USA.
- 5. National Center for Supercomputing Applications, University of Illinois Urbana-Champaign, Urbana, IL 61801, USA.

#### **Abstract**

The inherent time-reversal breaking of magnetic materials makes them ideally suited for non-reciprocal phenomena. Indeed, non-reciprocal microwave propagation, such as in isolators and circulators, are often engineered by careful mode matching with magnetic excitations. However, the direct conversion of microwave photons to magnons suffers often from inefficiencies that are hard to overcome. Therefore, our goal is to boost magnon non-reciprocity and magnon-photon coupling via magnetoelastic interactions by combining surface acoustic wave devices with magnetoelastic materials.

Towards the goal of utilizing magnetoelastic coupling, we have systematically studied the magnetostriction and temperature dependent magnetic damping in B-doped Fe<sub>80</sub>Ga<sub>20</sub> thin films grown by magnetron sputtering [1]. We observed that the incorporation of boron induced a phase transition from poly-crystalline to amorphous, confirmed by X-ray diffraction and high-resolution transmission electron microscopy. We identified that 10% boron doping, which was in the mixed phase regime, was optimal for simultaneously realizing large magnetostriction of 50 ppm and low magnetic damping of 6×10<sup>-3</sup>, see Fig. 1. Furthermore, we have conducted temperature dependent magnetic damping studies and observed a peak in

magnetic damping at around 40 K, which we attributed to magnetoelastic coupling. We found the magnetic damping at 5 K was lower than room temperature damping, indicating potentially further suppressed damping in quantum regimes at mK. Subsequently, (Fe<sub>80</sub>Ga<sub>20</sub>)<sub>90</sub>B<sub>10</sub> films were integrated into surface acoustic wave (SAW) devices prepared on both LiNbO<sub>3</sub> and AlN to study magnon phonon coupling, including acoustic wave driven ferromagnetic resonance.

Furthermore, we are working with bulk acoustic wave (BAW) based coherent magnon-phonon coupling in a single-crystal YIG substrate. We have successfully deposited high-quality piezoelectric AlN thin film on the YIG substrate, and fabricated top and bottom electrodes with a Pt/AlN/Pt vertical structure. The sample will allow us to excite perpendicular BAW across the YIG thickness, which will couple to perpendicular standing spin waves with matching frequency and wavelength to provide coherent magnon-phonon coupling.

Building on these results we will use SAW devices to study magnon-phonon coupling as a function of  $(Fe_{80}Ga_{20})_{1-x}B_x$  composition. Furthermore, we will use these devices to study the temperature dependence of magnetostriction, which will allow us to determine whether magnetoelastic SAW devices can be used for non-reciprocal coupling at cryogenic temperatures for quantum operations. In addition, we will

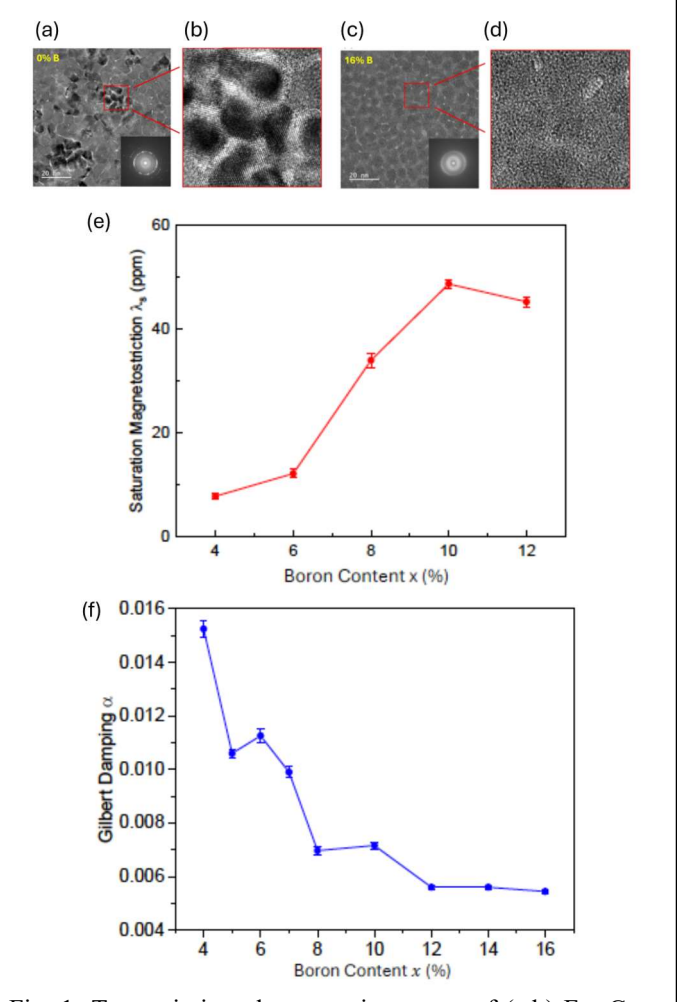


Fig. 1: Transmission electron microscopy of (a,b)  $Fe_{80}Ga_{20}$  and (c,d)  $(Fe_{80}Ga_{20})_{84}B_{16}$ . Boron-doping dependence of (e) magnetostriction and (f) magnetic damping in  $(Fe_{80}Ga_{20})_{1x}B_x$ .

compare to first-principles total energy simulations to gain detailed understanding of magnetostriction in these compounds and to distinguish energy changes induced by composition and strain. In parallel we will also explore magnon-phonon coupling in high quality YIG. We will explore both SAW coupling with YIG thin films and perpendicular acoustic wave coupled to standing spin wave in bulk YIG disks. Due to the strict substrate requirements for high-quality YIG growth, we plan to fabricate piezoelectric AlN layers on top of YIG for SAW propagation. We will also tune the lateral profile of the AlN layer and compare the coupling efficiency between AlN layer with uniform thickness and AlN layer with a thickness gradient right on top of YIG.

### References

1. Z. Zhang, J. Lim, H. Ni, J.-M. Zuo, and A. Hoffmann, *Magnetostriction and Temperature Dependent Gilbert Damping in Boron Doped Fe<sub>80</sub>Ga<sub>20</sub> Thin Films, Phys. Rev. Mater., submitted; doi: 0.48550/arXiv.2505.11472.* 

# Project Title: Multi-component Cavity Polaritons for Tunable Intermolecular Entanglement and Controlled Photon-to-Electron Quantum Transduction

Award: DE-SC0022134

## Abstract Title: Molecular Interactions Towards Light-Induced Quantum Entanglement Generation

Vladimir Chernyak<sup>1</sup>, Luca Candalori<sup>1</sup>, John Klein<sup>1</sup>, Oleg Poluetkov<sup>2</sup>, Shaul Mukamel<sup>3</sup>, Wei Xiong<sup>4</sup>, Nikolai Sinitsyn<sup>5</sup>, and **Aaron Rury**<sup>1</sup>

**Affiliation(s)**: <sup>1</sup>Wayne State University, <sup>2</sup>Argonne National Laboratory, <sup>3</sup>University of California-Irvine, <sup>4</sup>University of California-San Diego, <sup>5</sup>Los Alamos National Laboratory

**Abstract:** Given their ability to be modified structurally, molecules present unique opportunities as components in quantum information science and technology (QIST). By modifying the identities or positions of specific functional groups, synthetic chemists can change the energies of light molecules absorb, control their physical dispersion into different media, and modulate the lifetimes of excited states driven by photoexcitation. Despite this promise, it remains unclear how these amenable changes to their structure affect the ability of molecules to produce quantum information such as intermolecular quantum entanglement. Moreover, there remains few methods through which decoherence mechanisms that destroy quantum entanglement can be minimized to enhance the applicability of molecular systems in QIST. We have undertaken a combined theoretical and experimental approach to assess these types of issues.

Our theoretical efforts have been broadly made along three separate thrusts. I will highlight the accomplishments our group members have made establishing the mechanisms of quantum entanglement generation via the driving of model material systems in simple cavities by incident classical light fields. Our group has defined methods to compute a naïve estimate of the quantum concurrence, which estimates the maximum level of entanglement between two systems [1]. These calculations indicate that one can generate quantum correlations between an incident, classical light field and a material system embedded within an electromagnetic (EM) resonator. These calculations predict how the naïve concurrence will evolve in time as a function of different light-matter coupling conditions. These results indicate the ability to generate quantum correlations related to entanglement through the strong coupling of light and matter within an EM resonator.

The experimental efforts have been divided into two general thrusts. First, we have designed, fabricated, and characterized different types of hybrid states known as cavity polaritons through strong light-matter coupling within EM resonators. The efforts in this thrust were then distributed into separate areas based on the types of materials resonances used to couple strongly to cavity photons. In one area, group members utilized the electronic transitions of porphyrin-based molecules to form cavity polaritons in nano-scale EM resonators to assess how cavity polariton formation affects molecular dynamics central to maintain quantum entanglement. Precision spectroscopic studies on these systems enabled determination of the coupling conditions needed to suppress energetic disorder in molecular light absorbers due to vibrational dynamics. which represents a fundamental impediment to entanglement maintenance [2]. Additional studies leveraged a newly developed spectroscopic method, angle-resolved photoluminescence excitation spectroscopy, to determine the cavity polariton constituent that limits the hybrid light-matter state lifetime. These studies indicate that the coherence time between light and matter can be extended by over an order of magnitude when compared to the bare molecular state, which improves this performance metric for maintaining quantum entanglement in molecular systems [3].

In the second area of the first experimental thrust, group members have used vibrational resonances of molecular systems to form cavity polaritons in micro-scale, mid-infrared EM resonators. Using 2-dimensional infrared (2DIR) spectroscopy, these studies have enabled our group to assess how coherence can be controlled with resonator design. By creating trenches lithographically in Fabry-Perot micro-resonators, we demonstrate cavity polariton formation in 3-dimensionally confined spatial regions whose energies do not disperse with incidence angle conventionally [4]. Additionally, group members have

designed and applied a 2DIR hyperspectral imaging apparatus to assess how coherences induced by incident laser pulses propagate in these resonator systems spatially.

In the second experimental thrust area, group members have been assessing electron spins in porphyrin-based molecular materials towards light-mediated entanglement generation in these systems. Combined time-resolved electron paramagnetic resonance (EPR) and optical spectroscopic studies have shown that singlet and triplet molecular states do not delocalize their respective densities in correlated ways [5]. While no spin delocalization was found for photo-excited Zn-porphyrins, time-resolved EPR spectra at low temperatures suggest that adjacent electron spins in H-aggregates of paramagnetic Cu-porphyrin molecules can delocalize.

## References

- [1] "Qubit Entanglement Generated by Classical Light Driving an Optical Cavity", Ahn, S.; Moskalenko, A.S.; Chernyak, V.Y.; Mukamel, S., *Physical Review Research*, **5**, 043195 (2023). https://doi.org/10.1103/PhysRevResearch.5.043195
- [2] "Motional Narrowing through Photonic Exchange: Rational Suppression of Excitonic Disorder from Molecular Cavity Polariton Formation", Sachithra T. Wanasinghe, Adelina Gjoni, Wade Burson, Caris Majeski, Bradley Zaslona, and **Aaron S. Rury**, *The Journal of Physical Chemistry Letters*, **2024**, 15 (21), 5705-5713 https://doi.org/10.1021/acs.jpclett.3c03217
- [3] "Assessing the Determinants of Cavity Polariton Relaxation using Angle-Resolved Photoluminescence Excitation Spectroscopy", Elizabeth Odewale, Sachithra T. Wanasinghe, and **Aaron S. Rury**, *The Journal of Physical Chemistry Letters*, **2024**, 15, 5705-5713 https://doi.org/10.1021/acs.jpclett.4c01120
- [4] "Enabling multiple intercavity polariton coherences by adding quantum confinement to cavity molecular polaritons.", Z. Yang, H. H. Bhakta, and W. Xiong, *Proceedings of the National Academy of Sciences, USA*, (2022), 120 (1) e2206062120 https://doi.org/10.1073/pnas.2206062120
- [5] "Decorrelated singlet and triplet exciton delocalization in acetylene-bridged Zn-porphyrin dimers", Hasini Medagedara, Mandefro Y. Teferi, Sachithra T. Wanasinghe, Wade Burson, Shahad Kizi, Bradly Zaslona, Kristy L. Mardis, Jens Niklas, Oleg G. Poluektov, and **Aaron S. Rury**, *Chemical Science*, 2024, **15**, 1736-1751 https://doi.org/10.1039/D3SC03327A

# Integrated Materials Platforms for Topological Quantum Computing Devices DE-SC0019274

## Abstract Title: Superconductor-semiconductor hybrid quantum devices

<u>Vlad Pribiag<sup>1</sup></u>, Chris Palmstrøm<sup>2</sup>, Sergey Frolov<sup>3</sup>, Noa Marom<sup>4</sup>, Kunal Mukherjee<sup>5</sup>, Erik Bakkers<sup>6</sup>, Régis Melin<sup>7</sup>

1. U. Minnesota, 2. U. C. Santa Barbara, 3. U. Pittsburgh, 4. Carnegie Mellon University, 5. Stanford University, 6. T. U. Eindhoven, 7. CNRS Grenoble

**Abstract:** A significant challenge towards developing robust quantum computing systems with large numbers of logical qubits is rapid decoherence. A promising approach to addressing this challenge is based on the concept of fault-tolerant quantum computing architectures that leverage topological quantum states such as Majorana zero-modes (MZM). Substantial progress toward realizing and detecting topological states has been enabled by quantum devices which combine semiconductors with superconductors due to the combination of processing-friendly materials that offer high spin-orbit coupling, large g-factors, ballistic transport, and the ability to create transparent interfaces with various superconductors. However, further breakthroughs leading to topological quantum computation require next-generation quantum nanostructures that offer substantial improvement in the electronic purity together with optimal coupling across the superconductor-semiconductor interface. *Here we discuss our recent results under this project, focusing on superconductor-semiconductor quantum devices*. This work is a subset of our larger effort supported by this grant, which combines quantum device fabrication and characterization with materials synthesis and data interpretation informed by ab initio simulations and machine learning to develop robust, tunable and scalable platforms for the manipulation of quantum states.

(i) Few-mode quantum transport, Josephson junctions and  $\pi$ -shifted quartets using PbTe nanowires-toward topological states: We have used MBE-grown PbTe selective-area grown (SAG) nanowires to create quantum devices and study their normal and superconducting transport properties. In our recently-published work [1] we have seen very encouraging initial results in these nanowires, including well-defined conductance quantization plateaus (Fig. 1). This is superior to typical results reported to date in InSb or InAs nanowires, on which the community has previously focused. It could be indicative of low disorder effects in transport, which could have a major impact on developing MZM experimental platforms. We have also shown that these PbTe nanowires can be used to make superconducting devices, such as Josephson junctions, using Al contacts (Fig 1). A second major breakthrough from this work has been the observation of full

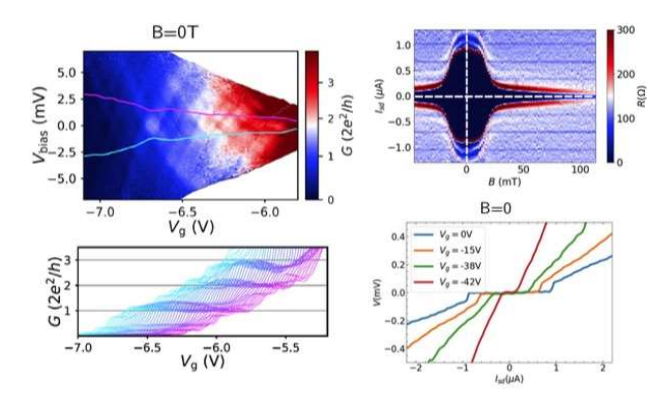


Fig. 1: Quantum transport results on PbTe SAG nanowire quantum devices. (top-left) Conductance in the few-quantum-modes regime, showing plateaus and phase-coherent transport. (bottom-left) Line cuts showing conductance plateaus. A slight modulation with bias is also seen, possibly attributable to a nearby quantum dot. (top-right) and (bottom-right) Transport in the superconducting regime (adapted from our Ref. [1]).

multi-terminal superconducting correlations ( $\pi$ -shifted Cooper quartets) using nanowires with three branches, each connected to a superconductor. These results establish PbTe SAG nanowires as a promising

platform for pursuing MZMs and advancing the emerging field of multi-terminal superconducting devices. We are currently exploring ways to improve the superconductor-semiconductor interface and further reduce disorder. We are also exploring super-semi devices with PbSe, for which our preliminary first-principles calculations have identified promising interfaces with several superconductors.

- (ii) Reproducible Quantum Devices: A significant goal for the project is to put materials discovery for quantum computing on firm footing. Here we are navigating a landscape where not all claims of advancement in topological effects have historically been backed by solid data. To this end, we have fabricated InAs/Sn and InSb/Al superconductor-semiconductor devices and explored tunneling zero-bias peaks previously reported as evidence of MZM (hysteretic supercurrents and subgap bound state spectra, and zero-bias peaks at zero external magnetic field) [2–4]. However, in this case the team has determined that they originate from Andreev bound states and are not of topological origin. The results also show the possibility to control superconductivity in a thin shell of Sn or Al superconductor, as well as induced superconductivity in an InAs or InSb nanowire using remote but nearby micromagnets.
- (iii) Gate-tunable three-terminal superconducting diode: We have demonstrated a gate-tunable three-terminal superconducting diode that can rectify superconducting signals, with the polarity and efficiency of rectification being tunable by electrostatic gating, and operating in ambient magnetic field [5]. The multi-terminal nature of our diode device allows for integration and simultaneous rectification of multiple signals. The devices display a high degree of reproducibility. These results are very timely due to the rapidly-growing interest in superconducting diodes. Such devices could be relevant as a basis for cryogenic on-chip control circuits for superconducting qubits. Among of the most intriguing implications of this work are the potential to use such devices for topologically-stabilized superconducting circuits and for hybrid neuromorphic circuits for AI.

### **References:**

- [1]M. Gupta et al., Evidence for π-shifted Cooper quartets in PbTe nanowire three-terminal Josephson junctions, Nano Lett. **24**, 13903 (2024) DOI: 10.1021/acs.nanolett.4c02414.
- [2]S. M. Frolov et al., "Smoking gun" signatures of topological milestones in trivial materials by measurement fine-tuning and data postselection, ArXiv:2309.09368 (2023) DOI: 10.48550/arXiv.2309.09368.
- [3]Y. Jiang et al., Zero-bias conductance peaks at zero applied magnetic field due to stray fields from integrated micromagnets in hybrid nanowire quantum dots, ArXiv:2305.19970 (2023) DOI: 10.48550/arXiv.2305.19970.
- [4]C. Riggert et al., Matters Arising from S. Vaitiekenas et al., "Zero-bias peaks at zero magnetic field in ferromagnetic hybrid nanowires" Nature Physics 2021, ArXiv:2501.03986 (2025) DOI: 10.48550/arXiv.2501.03986.
- [5]M. Gupta et al., *Gate-tunable superconducting diode effect in a three-terminal Josephson device*, Nat. Commun. **14**, 3078 (2023) DOI: 10.1038/s41467-023-38856-0.

# Modeling, probing, and controlling quantum coherence in materials DE-SC0020313, FWP: SCW1674

## Engineering diamond surfaces for efficient NV emission

Victor Brar<sup>1</sup>, <u>Jennifer T. Choy</u><sup>1</sup>, Robert J. Hamers<sup>1</sup>, Mikhail A. Kats<sup>1</sup>, Minjeong Kim<sup>1</sup>, **Shimon** Kolkowitz<sup>2</sup>, Roman Kuzmin<sup>1</sup>, **Alex Levchenko**<sup>1</sup>, Vincenzo Lordi<sup>3</sup>, Zhenqiang Ma<sup>1</sup>, **Robert** McDermott<sup>1</sup>, Keith G. Ray<sup>3</sup>, Yuhan Tong<sup>1</sup>, Ricardo Vidrio<sup>1</sup>, Wenxin Wu<sup>1</sup>, Maryam Zahedian<sup>1</sup>

<sup>1</sup>University of Wisconsin – Madison, <sup>2</sup>University of California, Berkeley, <sup>3</sup>Lawrence Livermore National Laboratory

**Abstract:** Spin defects in diamond, such as the negatively charged nitrogen-vacancy (NV) centers, can be highly sensitive to local (nanoscale) changes in magnetic field, temperature, and strain, which make them useful quantum sensors to measure spatially varying magnetic and electric fields in nearby materials, including superconductors and 2D materials. However, near-surface quantum defects within 10 nm from the surface tend to exhibit spin decoherence. Additionally, in a high-refractive-index environment such as diamond, most of the nonclassical light emitted is trapped within the bulk crystal due total internal reflection at the interface.

In this collaboration, we strive to better-understand and control interfaces in diamond, towards generating brighter and more-coherent near-surface emitters. One theme of this work is to use materials analysis tools, such as X-ray Photoelectron Spectroscopy (XPS), to provide molecular and atomistic insights on diamond surfaces. We conducted detailed investigations of diamond surfaces with various terminations and ligands to optimize the performance of near-surface NV centers. Using angle-resolved XPS, our work has revealed the presence of sub-nanometer-thick native sp2 carbon on oxidized diamond surfaces (Figure 1) [1], which has implications for the stability and coherence of near-surface NV centers used in quantum sensing. We also studied the effects of molecular contamination and sp<sup>2</sup> carbon on the oxidation of diamond surfaces [2], from which we gained insights into the layered heterogeneity of diamond surfaces, allowing us to optimize surface treatments. Our experimental efforts are performed alongside density functional theory calculations of surface energies and electron affinity for different types of carbonoxygen bonding and surface coverage. By analyzing the electron affinity for partial coverage and mixed binding cases, we can model the complex surfaces present after realistic experimental conditions, as well as inform treatment methods for positive electron affinity surfaces with low charge noise.

In parallel, we address the issue of NV emission extraction by developing a framework for analyzing the room-temperature emission rates of near-surface NV centers of various orientations and diamond crystal cuts [3], which is helpful for understanding the depth-dependent radiative behavior of near-surface NV centers. This analysis is crucial for any sensing measurements relying on radiative lifetime determination (such as FRET) and for designing photonic devices that modify color center emission. We then designed and implemented crystalline silicon antennas to enhance light extraction from near-surface NV centers [4], demonstrating an order-of-magnitude improvement in single-photon emission in comparison to a bare diamond surface. Notably, the silicon antennas are formed by membrane transfer of crystalline silicon from a silicon-on-insulator wafer and avoids etching of the diamond surface to prevent degradation emitter's

quantum properties. In our collaboration, we will apply the aforementioned techniques to prepare bright and coherent NV centers to probe charge noise at interfaces of superconductors and dielectrics.

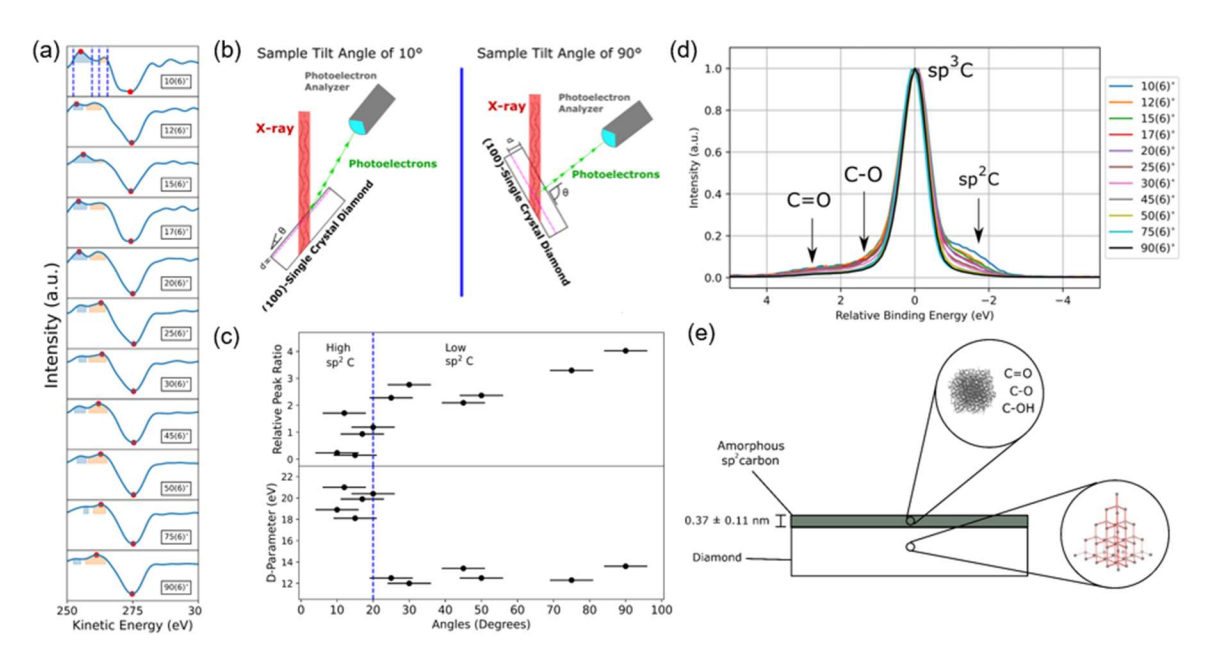


Figure 1: (a) Angle-resolved auger spectra for oxygen-terminated diamond. (b) Experimental configuration. (c) (Top) Relative peak ratio and (Bottom) Calculated D-parameter values plotted as a function of sample tilt angles, along with the regimes of high sp<sup>2</sup> C and low sp<sup>2</sup> C. (d) Angle-dependent C1s spectra. (e) Model of oxidized diamond surfaces, based on ARXPS data.



Figure 2: (a)-(c) Schematic, simulation, and fabrication of silicon nanoscale light extractor for near-surface NVs in diamond. (d) (Left) NV fluorescence from bare diamond and (Right) fluorescence enhanced by silicon antennas.

- [1] Vidrio, R et al. arXiv preprint arXiv:2409.06934 (2024). https://doi.org/10.48550/arXiv.2409.06934
- [2] Vidrio, R et al. *Materials for Quantum Technology* 4.2 (2024): 025201. https://doi.org/10.1088/2633-4356/ad4e8a
- [3] Zahedian, M et al. *Laser & Photonics Reviews* 17.4 (2023): 2200529. https://doi.org/10.1002/lpor.202200529
- [4] Kim, M et al. Nano Letters 25.12 (2025): 4659-4666. https://doi.org/10.1021/acs.nanolett.4c04299

# Phonon Control for Next-Generation Superconducting Systems and Sensors KCAS23

# Material growth and fabrication of asymmetric tunnel junctions for phonon and quasiparticle transport suppression

<u>Adam Schwartzberg</u>, Shaul Aloni, Alp Sipahigil, Sinéad Griffin, Yashwanth Balaji, Mythili Surendran, Aidar Kemelbay, Arian Gashi

Lawrence Berkeley National Laboratory, 1 Cyclotron Road, Berkeley, California 94720, USA

**Abstract:** One of the main goals of the PhononNext project is the suppression of quasiparticle interactions in superconducting quantum devices. In superconducting qubits, suppressing effects due to phonon interactions is critical for improving coherence times and reducing error rates, particularly during energetic impact events. In this project, we are developing materials and fabrication techniques to fabricate asymmetric Josephson junctions (JJs) composed of two superconducting materials with different superconducting gap energies. This approach with a large gap asymmetry will reduce quasiparticle tunneling across the junction which produces correlated errors and decreases qubit coherence time. A recent

work has demonstrated the effectiveness of this technique, controlling the superconducting gap by changing JJ layer thicknesses using a single material. However, the amount of gap engineering that can be achieved with a single material is limited. Here, we combine aluminum with the superconducting transition metal nitride niobium nitride (NbN), which has a comparatively large superconducting gap energy, to demonstrate a significantly asymmetric JJ and the potential available when other materials can be used.

In the first part of the work we studied how NbN growth affects crystallinity and superconducting gap.<sup>2</sup> Films are grown with reactive sputtering which

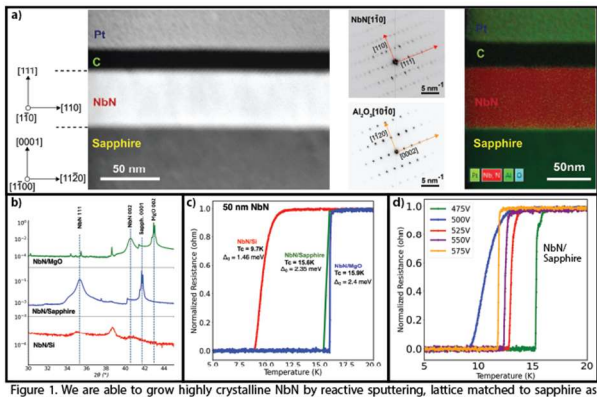


Figure 1. We are able to grow highly crystalline NbN by reactive sputtering, lattice matched to sappshies as shown in TEM cross section, electron diffraction and EDS (a). As the lattice match of the substate decreases odoes the crystalline phase purity and the critical temperature/superconducting gap of the deposited material, as shown by x-ray diffraction (b) and low temperature transport (c). We also find that we can tune the superconducting gap by changing growth parameters, in this case substrate bias, enableing another route for superconducting gap control (d).

enables epitaxial growth on sapphire (fig 1a). The NbN film crystal morphology and transition temperature/superconducting gap are sensitive to the lattice of the substrate onto which it is grown, resulting in reduced order when growing on silicon, and increased order on MgO, which has a superior lattice match to NbN (fig 1b and 1c respectively). Because growth conditions are somewhat limited for fabrication processes, this is critical information to understand how the superconducting gap will be affected. It also enables some degree of superconducting gap tunability. However, we found that by carefully controlling growth parameters we were able to more precisely tune the superconducting gap, which will be useful for more precise gap engineering in our devices (fig 1d).

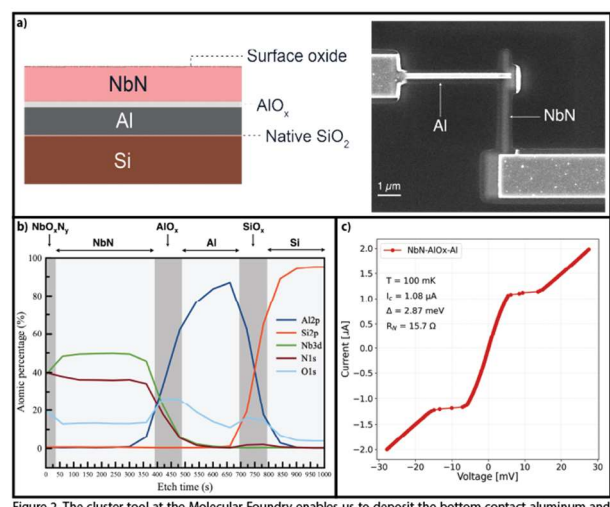


Figure 2. The cluster tool at the Molecular Foundry enables us to deposit the bottom contact aluminum and aluminum via conventional e-beam evaporation and oxidation, followed by reactive sputtering of NbN in a separate chamber without breaking vacuum (a). XPS depth profiling shows excellent elemental control ove NbN, alumina, and aluminum (b). Ic measurements of these devices show non-ideal supercurrent behavior that is likely due to the NbN layer being toot thin (c).

In the second part of our work we have focused on fabrication and testing of the asymmetric JJs.<sup>3</sup> Taking advantage of the high degree of control available through the quantum fabrication cluster tool at the Molecular Foundry, we were able to fabricate asymmetric Al/AlOx/NbN junctions. After the first evaporation and oxidation step, we transfer the wafer through vacuum to the reactive sputtering chamber and carry out a specialized, long distance sputtering process that enables better growth directionality (fig 2a). We tested the composition of each layer of this film to confirm that there was limited or no intermixing using XPS depth profiling (fig 2b). Finally, we carried out transport measurements at operational temperatures (100 mK) to observe the junction behavior. While we do find supercurrent, as

expected, the slope is not as steep as it should be (fig 2c). Additionally, we find that the room temperature resistance of these asymmetric junctions to be two times higher than expected. We believe that both effects may be due to the NbN film being too thin, approximately 10 nm, which is currently set somewhat by fabrication limits. We are now developing improved fabrication methods to reach our targeted thickness of 30-50 nm, enabling us to determine the nature of the anomalous tunnel current shape and leading to improved device performance.

## References

[1] McEwen, M., Miao, K. C., Atalaya, J., Bilmes, A., Crook, A., Bovaird, J., Kreikebaum, J. M., Zobrist, N., Jeffrey, E., Ying, B., Bengtsson, A., Chang, H.-S., Dunsworth, A., Kelly, J., Zhang, Y., Forati, E., Acharya, R., Iveland, J., Liu, W., Kim, S., Burkett, B., Megrant, A., Chen, Y., Neill, C., Sank, D., Devoret, M. & Opremcak, A. Resisting high-energy impact events through gap engineering in superconducting qubit arrays. *Phys. Rev. Lett.* **133**, 240601 (2024).

[2] Surendran, M., Balaji, Y., Kemelbay, A., Gashi, A., Zhang, Z., Zhou, H., Sipahigil, A., Schwartzberg, A., & Aloni, S. Understanding and controlling growth of transition metal nitrides for next-generation superconducting quantum devices. *APS Global Summit Presentation* MAR-T18 (2025).

[3] Balaji, Y., Surendran, M., Kemelbay, A., Gashi, A., Zhou, H., Yu, K., Sipahigil, A., Aloni, S. & Schwartzberg, A. Fabrication of Josephson Junctions with alternative materials using hybrid deposition techniques. *APS Global Summit Presentation* MAR-F33 (2025).

Partially prepared by LLNL under Contract DE-AC52-07NA27344

# Hybrid Magnon Systems DE-SC0022060

## **Coherent Control of Magnons**

<u>Yi Li<sup>1</sup></u>, Moojune Song<sup>1,2</sup>, Tomas Polakovic<sup>3</sup>, **Jinho Lim<sup>4,5</sup>**, **Xingzhi Wang<sup>4,5</sup>**, **Pratap Kumar Pal<sup>1,4,5</sup>**, Thomas W. Cecil<sup>6</sup>, John Pearson<sup>1,7</sup>, Ralu Divan<sup>7</sup>, Wai-Kwong Kwok<sup>1</sup>, Ulrich Welp<sup>1</sup>, Wei Zhang<sup>8</sup>, Dmytro A. Bozhko<sup>9</sup>, Kab-Jin Kim<sup>2</sup>, **Jian-Min Zuo<sup>4,5</sup>**, **Axel Hoffmann<sup>4,5,10</sup>**, and **Valentine Novosad<sup>1</sup>** 

- 1. Materials Science Division, Argonne National Laboratory, Lemont, IL 60439, USA.
- 2. Department of Physics, Korea Advanced Institute of Science and Technology, Daejon 34141, Republic of Korea.
- 3. Physics Division, Argonne National Laboratory, Lemont, IL 60439, USA.
- 4. Materials Science and Engineering, University of Illinois Urbana-Champaign, Urbana, IL 61801, USA.
- 5. Materials Research Laboratory, University of Illinois Urbana-Champaign, Urbana, IL 61801, USA.
- 6. High Energy Physics Division, Argonne National Laboratory, Lemont, IL 60439, USA.
- 7. Center for Nanoscale Materials, Argonne National Laboratory, Lemont, IL 60439, USA.
- 8. Department of Physics and Astronomy, University of North Carolina, Chapel Hill, NC, 27599, USA.
- 9. Department of Physics and Energy Science, University of Colorado Colardo Springs, CO 80918, USA.
- 10. Department of Physics, University of Illinois Urbana-Champaign, Urbana, IL 61801, USA

## Abstract

Magnons, the quanta of collective spin excitations in magnetically ordered media, exhibit unique features for microwave quantum engineering, with examples of non-reciprocity in the form of propagating spin wave, highly desired for noise-isolated qubit operations with on-chip integration, and magneto-optical coupling for microwave-to-optic transduction, highly desired for implementing quantum transduction and building quantum interconnects. For either purpose, the capability of coherent magnon control in the time domain is crucial for designing coherent magnon gate operations and extend the dynamic control into the quantum regime.

Towards the objective of coherent control of propagating magnons, we demonstrate single-shot magnon pulse interference between two remotely coupled Y<sub>3</sub>Fe<sub>5</sub>O<sub>12</sub> (YIG) spheres embedded in a superconducting resonator [1] (see Fig. 1). Using a pair of vertical antennas to selectively couple to the two YIG spheres with minimal cross-talk to the in-plane superconducting resonator, we realize real-time constructive and destructive magnon interference by precisely controlling the frequency and time delay of two consecutive microwave pulses applied to one YIG sphere. In addition, we show a diffraction-grating-like interference pattern using up to four consecutive magnon pulses, where the interference peak becomes increasingly enhanced and sharpened with the number of pulses. Our results reveal that magnons can preserve full coherence, while being transferred between distant magnetic resonators. This is a

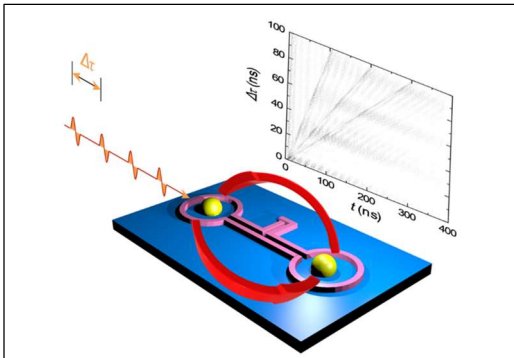


Fig. 1: Magnon interference: Real-time magnon interference is demonstrated between two remotely coupled yttrium iron garnet (YIG) spheres on a compact magnon-superconducting-resonator hybrid circuit [1].

critical requirement for implementing coherent magnon gate operations in real time. Moreover, the experiments were conducted on a chip-integrated cryogenic superconducting circuit platform along with high-fidelity interference performance. This work establishes a robust foundation for integrating magnonics with cQED and developing magnon-based quantum information processing and quantum sensing.

For future development of coherent control of propagating magnons, we are developing on-chip magnon-superconducting resonator hybrid system that couples to spatially nonuniform spin wave modes in a YIG thin film. We have fabricated quarter-wavelength NbN superconducting resonators directly on top of epitaxial YIG films grown on Y<sub>3</sub>Sc<sub>2</sub>Ga<sub>3</sub>O<sub>12</sub> (YSGG) substrates. High Q-factor up to 100,000 is measured for NbN resonators fabricated directly on YSGG, and a high Q-factor of 3,000 is measured for NbN resonators fabricated on the YIG/YSGG film at 1.3 K. Strong coupling and mode anticrossing are observed between the superconducting resonator mode and the Damon-Eshbach (DE) spin wave mode of the YIG film. Our results introduce the first all-on-chip superconducting hybrid magnonic circuit base on low-damping YIG thin films, which will become the next-generation circuit platform for exploring propagating-magnon-based quantum information science. We will further use our recently developed single-shot electrical detection technique of propagating spin waves [2] to explore time-domain propagating magnon control.

#### Reference

- M. Song, T. Polakovic, J. Lim, T. W. Cecil, J. Pearson, R. Divan, W.-K. Kwok, U. Welp, A. Hoffmann, K.-J. Kim, V. Novosad, Y. Li, Single-shot magnon interference in a magnon-superconducting-resonator hybrid circuit, Nat. Commun. 16, 3649 (2025). DOI: 10.1038/s41467-025-58482-2
- 3. M. Song, J. Lim, W. Zhang, D. A. Bozhko, R. Divan, A. Hoffmann, K.-J. Kim, V. Novosad, Y. Li, Single-shot electrical detection of short-wavelength magnon pulse transmission in a magnonic thin-film waveguide, npj Spintronics 3, 12 (2025). DOI: 10.1038/s44306-025-00072-5

## **Optoelectronic Properties of Artificially Tailored Quantum Materials**

#### **DE-SC0024486**

# Komalavalli Thirunavukkuarasu (PI) and Wei Pan (Co-PI)

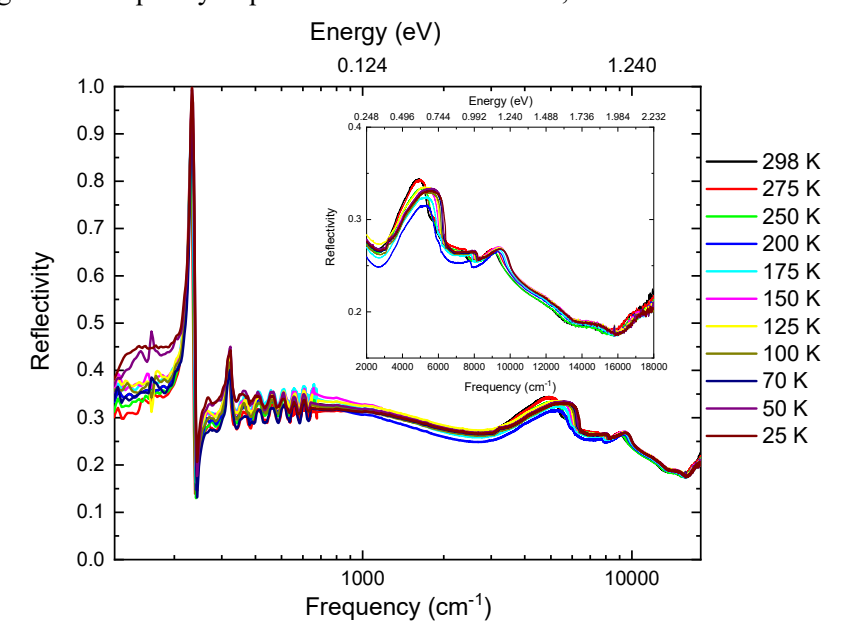
### Florida A&M University and Sandia National Laboratories

#### **Abstract:**

We present our recent results from broadband optical spectroscopic investigations on Moiré superlattices (MSL) based on 2D electron gas quantum wells. To create MSLs using IL, two separate, rotated AG patterns are created in the photoresist prior to development. By carefully controlling the angles between the four exposures defining the AG patterns, the twist angle between the two AG lattices can be defined without requiring post-processing alignment. The first set of parallel lines for AG1 is formed in the resist followed by a second set of parallel lines for AG2 with a twist angle of 5 degree. This is followed by the third set of lines at a twist angle of 60 degrees with respective to the first set. Finally, a fourth set of parallel lines is defined at a twist angle of 60 degree with respective to the second set. The laser intensity and expose time for each set of parallel lines are the same as in AG pattern. The first and third sets of lines create the first AG1 pattern. The second and forth sets of lines create the second AG2 pattern with a twist angle of 5 degrees. After post-exposure bake, photoresist development and RIE, holes are etched through the 2DEG, and MSLs are generated [1].

To study the electronic structure of the MSL devices over a broad energy range, we employed broadband optical spectroscopic techniques of Fourier transform infrared (FTIR) spectroscopy and ellipsometry. The infrared measurements were performed using the FTIR spectrometer Bruker IFS80v coupled to a Hyperion 2000 microscope. The FTIR microscope can cover a broad frequency range from 100 to 18000 cm<sup>-1</sup> i.e., far-infrared (FIR) to visible frequencies. It employs three different light sources for the different ranges in the infrared frequencies. Depending on the frequency required for the measurement, different combinations

of source, beamsplitter and the detector are chosen. The siliconbased bolometer used in the FIR frequency range is a cryogenic detector operated at liquid helium temperature, while mercury cadmium telluride (MCT) and InSb detectors used at midinfrared (MIR) and near-infrared (NIR) frequencies, respectively, are operated at liquid nitrogen temperature. A silicon diode detector used was measurements in the visible range. The variable temperature



environment was achieved using an optical cold finger cryostat coupled to the Hyperion microscope.

Broadband reflectivity measurements were performed for four samples: MSL 300/300/5, MSL 300/250/5, AG 300 and the substrate sample in the temperature range from 25 K to 300 K. Furthermore, higher frequency data from 18000 cm<sup>-1</sup> to 47000 cm<sup>-1</sup> was also obtained for the four studied samples using room temperature ellipsometry. The results obtained for MSL 300/300/5 are shown in Figure as an example. All four samples exhibit minimum change in the overall reflectivity with decreasing temperature. However, the phonons at FIR frequency range and the electronic transitions in the NIR frequency show temperature-dependent red shift (inset of Figure). These changes in the reflectivity spectra correspond to the evolution of band structure of this MSL device close to Fermi level [2]. Therefore, by comparing data from the MSL devices with the optical response of the substrate and single AG layer, we will be able to reveal the mechanism of the band structure evolution.

Our plan is to perform Kramers-Kronig transformation of the temperature dependent reflectivity of the samples to obtain optical conductivity. The optical conductivity being an additive optical constant will allow for deconvolution of contributions to the optical response from various components of the MSL device. In addition, we will continue to obtain more information using Raman scattering and photoluminescence on these samples to obtain comprehensive understanding of the quantum phenomena in these artificially tailored materials.

#### References:

- [1] Lithography defined semiconductor moirés with anomalous in-gap quantum Hall states, W. Pan1, D.B. Burckel, C.D. Spataru, K.S. Sapkota, A.J. Muhowski, S.D. Hawkins, J.F. Klem, L.S. Smith, D.A. Temple, Z. Enderson, Z. Jiang, K. Thirunavukkuarasu, L. Xiang, M. Ozerov, D. Smirnov, C. Niu, P.D. Ye, P. Pai, and F. Zhang, submitted to Nano Letters (2025).
- [2] Recent Advances in Moiré Superlattice Structures of Twisted Bilayer and Multilayer Graphene, Xiao-Feng Li, Ruo-Xuan Sun, Su-Yun Wang, Xiao Li, Zhi-Bo Liu, and Jian-Guo Tian, Chinese Physics Letters, **39**, 037301 (2022).

# Multimodal Quantum Material Control Monitored with Ultrafast Coherent X-Rays Award Number DE-SC0019126

## THz Control of Magnetization and Polarization Through Magnon and Phonon Coherences

Keith A. Nelson¹, Mariano Trigo², David A. Reis², Riccardo Comin¹, Zhuquan Zhang¹, Frank Y. Gao³, Jonathan B. Curtis¹³, Zi-Jie Liu¹, Yu-Che Chien¹, Alexander von Hoegen¹, Takayuki Kurihara¹⁴, Tohru Suemoto¹⁴, Prineha Narang¹³, Edoardo Baldini³, Eric Sung¹, Xiaoxuan Ma⁴, Wei Ren⁴, Shixun Cao⁴, Gal Orenstein², Viktor Krapivin², Yijing Huang⁵, Gilberto de la Pena Munoz², Ryan A. Duncan², Quynh Nguyen², Jade Stanton², Samuel Teitelbaum⁶, Hasan Yavas², Takahiro Sato², Matthias C. Hoffmann², P. Kramer², Jiahao Zhang⁵, Andrea Cavalleri¹⁰, Mark P. M. Dean⁶, Ankit S. Disa⁶, Michael Forst¹⁰, Steven L. Johnson¹¹, Matteo Mitrano¹², Andrew M. Rappe⁵, Man Tou Wong¹, David Rohrbach¹, Nadia Berndt¹, Xi Zhang¹, Haoyuan Li², Nan Wang², Leon Zhang², Sanghoon Song², Yanwen Sun², May-Ling Ng³, Takahiro Sato³, Dillon Hanlon⁴, Sajal Dahal², Mario D. Balcazar², Vincent Esposito², Selene She², Chance Caleb Ornelas-Skarin², Joan Vila-Comamala¹¹, Christian David¹¹, Peter Richard Miedaner¹, Matthias Ihme², Jerome B. Hastings², Alexei A. Maznev¹, Laura Foglia¹¹, Diling Zhu²

<sup>1</sup>Massachusetts Institute of Technology, <sup>2</sup>SLAC/Stanford University, <sup>3</sup>University of Texas, Austin, <sup>4</sup>Shanghai University, <sup>5</sup>University of Illinois at Urbana-Champaign, <sup>6</sup>Arizona State University, <sup>7</sup>University of Pennsylvania, <sup>8</sup>Brookhaven National Lab, <sup>9</sup>Cornell University, <sup>10</sup>Max Planck Institute, Hamburg, <sup>11</sup>SwissFEL/Paul Scherrer Institute, <sup>12</sup>Harvard University, <sup>13</sup>UCLA, <sup>14</sup>University of Tokyo

Abstract: The primary project goals are advances in our ability to control, monitor, and theoretically model novel quantum phases of matter. We use multiple dynamic stimuli to control multiple coupled modes including optical and acoustic phonons, magnons, and low-frequency electronic excitations. THz and long-wavelength IR excitation fields are used to drive optical phonons, magnons, and electronic responses; optical pulses to excite selected acoustic/shock waves that deliver specified inplane or through-plane uniaxial strains; and crossed X-ray pulses to drive material responses with specified nanoscale spatial modulations that may reach length scales comparable to those that form spontaneously in many quantum phases. We probe the dynamic material responses with ultrashort coherent X-ray probe pulses at XFELs, and in THz through visible spectral regions using tabletop ultrafast laser systems. In some cases, we induce transformations of matter into new states with altered structural, electronic, and/or magnetic characteristics. X-ray diffraction and diffuse scattering, X-ray absorption, and resonant X-ray scattering measurements may be conducted to monitor the formation and duration of these states including their nanoscale textures.

Two recent experimental efforts will be reviewed. First, nonlinear THz excitation of magnon coherences in YFeO<sub>3</sub> and ErFeO<sub>3</sub> canted antiferromagnetic crystals will be illustrated. 2D THz EPR spectroscopy of the induced magnon responses has revealed nonlinear coupling of two orthogonally polarized magnon modes [1-3]. The spectra reveal sum and difference frequency generation; upconversion through which excitation of one magnon mode generates a coherence of the other; and parametric amplification of the lower-frequency mode by the higher-frequency one. These nonlinear interactions could provide the fundamental underpinnings for nonlinear magnonic signal processing with ultrahigh bandwidths and extremely low power consumption. The measurements were conducted by focusing free-space THz fields onto the samples. However, we have very recently conducted 2D THz spectroscopy of magnons using an integrated solid-state platform in which the THz fields are generated optically and interacted with a sample to produce new nonlinear THz signals that are measured optically, all with no free-space THz field propagation. The system is compatible with samples in a magnet bore or an XFEL facility. Finally, we have recently used enhanced THz field

amplitudes to generate large-amplitude magnon responses, revealed through multiple-quantum (up to 7-quantum) coherences observed in 2D THz spectra. We are hopeful that versatile switching of macroscopic magnetization will be possible.

We have used THz fields to induce a transient ferroelectric (FE) configuration in SrTiO<sub>3</sub>, starting in its low-temperature quantum paraelectric phase [4]. Since we used a spatially uniform THz driving field, we initially believed that the induced FE ordering, monitored using optical SHG and birefringence measurements, was also spatially uniform. But in more recent XFEL diffuse scattering measurements, the FE dynamics were observed not at a Bragg diffraction peak but off-Bragg by a wavevector magnitude that indicated FE regions of ~ 10 nm dimensions [5]. The results strongly suggested that pre-existing, randomly oriented polar nanoregions were driven into a highly oriented collective configuration. The soft optical phonon and transverse acoustic phonon dynamics are consistent with theoretical predictions that a spatially modulated polarization-density wave configuration can be formed, stabilized by flexoelectric effects. We hope to combine x-ray transient grating and THz excitation to induce a potentially metastable configuration with long-range spatially periodic ordering.

#### **References:**

- 1. "Terahertz field-induced nonlinear coupling of two magnon modes in an antiferromagnet," Z. Zhang, F. Y. Gao, J. B. Curtis, Z.-J. Liu, Y.-C. Chien, A. von Hoegen, T. Kurihara, T. Suemoto, P. Narang, E. Baldini, and K. A. Nelson, *Nature Physics* **20**, 801-806 (2024). <a href="https://doi.org/10.1038/s41567-024-02386-3">https://doi.org/10.1038/s41567-024-02386-3</a>
- 2. "Terahertz-field-driven magnon upconversion in an antiferromagnet," Z. Zhang, F. Y. Gao, Y.-C. Chien, Z.-J. Liu, J. B. Curtis, E. Sung, X. Ma, W. Ren, S. Cao, P. Narang, A. von Hoegen, E. Baldini, and K. A. Nelson, *Nature Physics* **20**, 788–793 (2024). https://doi.org/10.1038/s41567-023-02350-7
- 3. "Terahertz stimulated parametric downconversion of a magnon mode in an antiferromagnet," Z. Zhang, Y.-C. Chien, M. T. Wong, F. Y. Gao, Z.-J. Liu, X. Ma, S. Cao, E. Baldini, and K. A. Nelson, *Science Advances* 11, <a href="https://www.science.org/doi/10.1126/sciadv.adv3757">https://www.science.org/doi/10.1126/sciadv.adv3757</a>.
- 4. "Terahertz field-induced ferroelectricity in quantum paraelectric SrTiO<sub>3</sub>," X. Li, T. Qiu, J. Zhang, E. Baldini, J. Lu, A. M. Rappe, and K. A. Nelson, *Science* **364**, 1079-1082 (2019). https://doi.org/10.1126/science.aaw4913
- 5. "Observation of polarization density waves in SrTiO<sub>3</sub>," G. Orenstein, et al., *Nature Physics* (2025) <a href="https://doi.org/10.1038/s41567-025-02874-0">https://doi.org/10.1038/s41567-025-02874-0</a>.

## **Quantum Entangled X-ray Beams**

#### **DE-SC0023176**

## Stephen M. Durbin, and Liam T. Powers

Department of Physics & Astronomy, Purdue University, West Lafayette IN 47907

**Abstract:** Photons play key roles in many aspects of Quantum Information Science (QIS), especially as entangled pairs. The Hong-Ou-Mandel (HOM) effect is the most famous example, where pairs of indistinguishable photons are combined into maximally entangled N00N states with N=2 (biphotons). Although x-ray synchrotrons are now among the brightest sources of photons in existence, efforts to apply quantum optics to x-rays have been quite limited. This QIS project aims to bring quantum optics to x-ray synchrotrons by using HOM interference to generate pairs of entangled x-rays. Preliminary results from recent beam time at the APS-U x-ray synchrotron (Argonne) show the defining property of HOM for a pair of indistinguishable photons entering the two input ports of a beam splitter: instead of one photon exiting from each of the two exit ports, some of these pairs bunch together into one or the other exit port. Quantum mechanics forbids such photons from the classically allowed choice of exiting on separate paths. Boson statistics requires them to bunch together. The result is an entangled two-photon state.

Reproducing the HOM effect with a synchrotron source requires first splitting the beam so that the two beams can be recombined at a second (HOM) beamsplitter. This required the development of a new Mach-Zehnder interferometer (Figure 1). Obtaining two indistinguishable photons from the same x-ray bunch requires a very high brightness source to increase the photon degeneracy factor. To utilize the enhanced brightness of the APS-U it was essential to preserve brightness throughout, so we developed a new silicon Bragg beam splitter to minimize losses. Furthermore, a synchrotron HOM measurement needs to record and analyze the exit photons from each synchrotron pulse, which in the APS-U brightness mode has a rate of 13 MHz. For this we developed a novel scheme involving two APD detectors and an FPGA-based signal analysis system.<sup>2</sup>

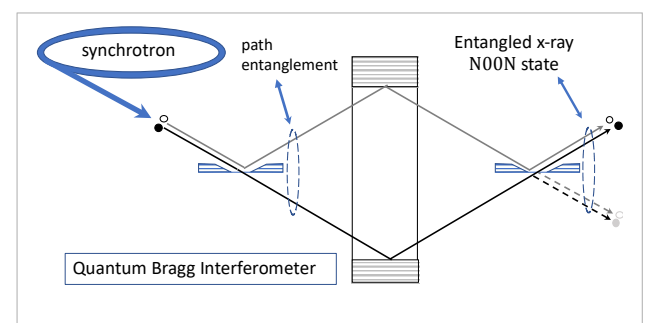


Figure 1: Overview the interferometer that splits the synchrotron beam and recombines them at the HOM beamsplitter, creating a two-photon maximally entangled N00N state.

Data from over 10<sup>8</sup> individual measurements using 8 keV x-rays at the APS-U synchrotron (Argonne) were recorded as the HOM beamsplitter was translated through the intersection point where the incident photons can be indistinguishable. As shown in Figure 2, the rate of coincident pairs (1-1) dropped while the rate of two photons together (2-0 and 0-2) increased by a similar amount. The difference shown corresponds to well over 10<sup>4</sup> entangled x-ray pairs per second. Further experimental improvements and

beamline optimization should increase this rate substantially over these preliminary results.

The goal of creating quantum entangled x-ray beams appears to be in reach. The overall mission is to use these beams as probes for detecting entanglement in quantum materials. Such an effort would begin with resonance enhanced x-ray scattering (REXS) in the 7-12 keV energy range. A number of interesting quantum magnets are available containing elements with  $L_{III}$  absorption edges in this range, including Ho, Er, Yb, Hf, Os, and Ir.

#### REFERENCES

- (1) Powers, L. T.; Kwasniewski, M. Z.; Durbin, S. M. Variable Bragg x-ray beam splitters. *AIP Adv* **2025**, *15* (4). DOI: 10.1063/5.0257347.
- (2) Powers, L. T.; Jacobsen, A. M.; Durbin, S. M. Counting multiple X-rays per pulse with an avalanche photodiode

a  $\begin{array}{c} 2 \\ 0 \\ 0 \\ 2 \\ 1.01 \\ \end{array}$ 1.05  $\begin{array}{c} 2-0, \\ 0-2 \\ \end{array}$ 2  $\begin{array}{c} 0 \\ 0-2 \\ \end{array}$ 1.01  $\begin{array}{c} 0 \\ 0-2 \\ \end{array}$ 2  $\begin{array}{c} 0 \\ 0-2 \\ \end{array}$ 1.01  $\begin{array}{c} 0 \\ 0-2 \\ \end{array}$ 1.02  $\begin{array}{c} 0 \\ 0-2 \\ \end{array}$ 1.01  $\begin{array}{c} 0 \\ 0-2 \\ \end{array}$ 1.02  $\begin{array}{c} 0 \\ 0-2 \\ \end{array}$ 1.03  $\begin{array}{c} 0 \\ 0-2 \\ \end{array}$ 1.01  $\begin{array}{c} 0 \\ 0-2 \\ \end{array}$ 1.02  $\begin{array}{c} 0 \\ 0-2 \\ \end{array}$ 1.03  $\begin{array}{c} 0 \\ 0-2 \\ \end{array}$ 1.01  $\begin{array}{c} 0 \\ 0-2 \\ \end{array}$ 1.02  $\begin{array}{c} 0 \\ 0-2 \\ \end{array}$ 1.03  $\begin{array}{c} 0 \\ 0-2 \\ \end{array}$ 1.01  $\begin{array}{c} 0 \\ 0-2 \\ \end{array}$ 1.02  $\begin{array}{c} 0 \\ 0-2 \\ \end{array}$ 1.03  $\begin{array}{c} 0 \\ 0-2 \\ \end{array}$ 1.01  $\begin{array}{c} 0 \\ 0-2 \\ \end{array}$ 1.02  $\begin{array}{c} 0 \\ 0-2 \\ \end{array}$ 1.03  $\begin{array}{c} 0 \\ 0-2 \\ \end{array}$ 1.04  $\begin{array}{c} 0 \\ 0-2 \\ \end{array}$ 1.05  $\begin{array}{c} 0 \\ 0-2 \\ \end{array}$ 1.01  $\begin{array}{c} 0 \\ 0-2 \\ \end{array}$ 1.02  $\begin{array}{c} 0 \\ 0-2 \\ \end{array}$ 1.03  $\begin{array}{c} 0 \\ 0-2 \\ \end{array}$ 1.03  $\begin{array}{c} 0 \\ 0-2 \\ \end{array}$ 1.01  $\begin{array}{c} 0 \\ 0-2 \\ \end{array}$ 

Figure 2: a) and b) show the bosonic bunching of exit photons that combine to form a N00N state; c) the two photons taking separate exit paths (classically allowed but quantum forbidden); d) data with 8 keV x-rays (APS-U) showing the HOM dip in coincident pairs and corresponding increase in biphoton bunching.

detector. J Synchrotron Radiat 2025, 32 (Pt 3), 629-633. DOI: 10.1107/s1600577525002462.

# Project Title: Understanding the Many-body Properties of Rare Earth-Based Materials Relevant to Next Generation QIS Applications

**Award Number: PM-062** 

**Abstract Title: Detecting Multipartite Entanglement in Real Materials** 

Names of PI, (co-PI): R. Konik<sup>1</sup> (PI), A. Weichselbaum<sup>1</sup>(co-PI), T.C. Wei<sup>2</sup> (co-PI), Rajesh Malla (Postdoc)

Affiliation(s): <sup>1</sup>CMPMSD, BNL, Upton, NY 11973, USA, <sup>2</sup>Physics Dept., Stony Brook University

**Abstract:** We have developed a new means to quantify multipartite entanglement in a quantum material. Multipartite entanglement is relevant to a range of quantum technologies including quantum communication, enhanced quantum metrology, quantum sensing, quantum machine learning, quantum imaging, and quantum computation. In our work we have shown how to turn the spectroscopic information measured in single electron probe techniques such as scanning tunneling microscopy (STM) and angle resolved photoemission (ARPES) into a lower bound on a material's multipartite entanglement. We have done this in the framework of the quantum Fisher information (QFI).

The quantum Fisher information (QFI), a concept from quantum metrology, provides a way to connect bounds on the multipartite entanglement with integrated spectral information that is obtained in a spectroscopic experiment. This connection had been established previously in

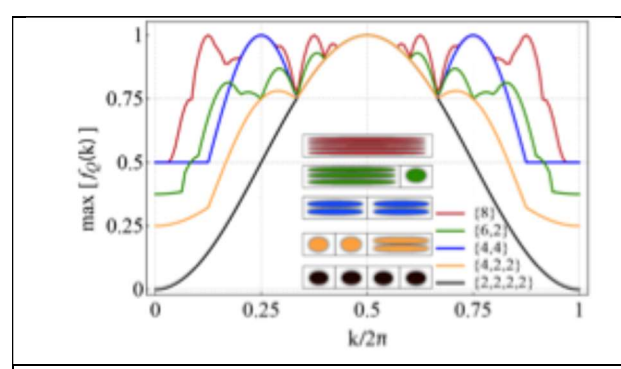


Fig. 1: The maximal QFI for various entanglement patterns is plotted as a function of k for an eight-site spinless fermionic system at half-filling. The entanglement patterns are shown schematically in the inset. The system is split up into independent blocks where electrons are confined within a block as visualized by the colored clouds. The smallest block size here contains two sites and the bars separating individual sites have been omitted within a block.

neutron scattering experiments measuring the dynamical spin response of materials [1]. We have shown in this work how to use the spectroscopies measured in an ARPES or STM experiment to infer a value of the quantum Fisher information (OFI) and then use this value to place a bound on the multipartite entanglement in the material [2]. We have done so considering the symmetries of the material, in particular particle number conservation. The bounds that the QFI must exceed in order to infer a certain level of entanglement when symmetries are present requires a non-trivial computation. These bounds are described in Fig. 1 when particle number conservation is present. While computing these bounds does require additional work, in doing so we are able to extract more fine-grained information about the entanglement in a system. We are not only able to tell whether a block of entangled n-sites is present in the material's wavefunction, but we also obtain information on the presence of patterns of entangled blocks.

As future work in this space, we intend to use symmetries to refine the QFI bounds that are employed in neutron scattering spectroscopy to show that magnetic materials are entangled. In preliminary

work, we have shown that neutron spectroscopy can infer more entanglement in a spin chain with SU(2) invariance than previously thought.

We also plan to investigate the role that degrees of freedom not directly probed by a spectroscopy affect the level of entanglement that can be detected. As an important example, phonons are typically present in quantum materials. However, in Ref. [2], our investigation supposed that only itinerant charge degrees of freedom were present. We thus plan to investigate how phonons alter the QFI bounds that must be exceeded for entanglement to be detected. More generally we will investigate the performance of the QFI as a means to detect entanglement using spectroscopies when there are multiple degrees of freedom present in a material.

[1] "Witnessing entanglement in quantum magnets using neutron scattering", A. Scheie, P. Laurell, A. M. Samarakoon, B. Lake, S. E. Nagler, G. E. Granroth, S. Okamoto, G. Alvarez, and D. A. Tennant, Phys. Rev. B 103, 224434 (2021).

[2] (funded by this project) "Detecting Multipartite Entanglement Patterns Using Single-Particle Green's Functions", R. Malla, A. Weichselbaum, T.C. Wei, R. Konik, Physical Review Letter 133 260202 (2024), DOI: 10.1103/PhysRevLett.133.260202.

# Non-Equilibrium Physics at the Nanoscale DE-FG02-05ER46225

## Fault-Tolerant Majorana-Based Quantum Algorithms in Topological Superconductors

Jasmin Bedow, Max Buss, Prashant Gupta, and Dirk K. Morr

## **University of Illinois Chicago**

#### **Abstract**

Advances in the quantum engineering of complex systems at the atomic level, in combination with the ability to probe and manipulate them at nanoscopic length and time scales, have not only paved the way for next generation quantum materials, but have also opened unprecedented opportunities for advancing quantum information science and the realization of quantum computing. The PI's research program has therefore identified a critical need to develop a theoretical framework to investigate and visualize nonequilibrium processes over varying time and length scales that are key to the implementation of quantum algorithms. To this end, the PI's program has focused on two-dimensional (2D) topological superconductors that host Majorana zero modes (MZMs) and Majorana edge modes (MEMs) whose non-Abelian braiding statistics and robustness against disorder and decoherence has provided a new framework for the realization of fault-tolerant quantum computing. The PI's research program has made significant advances toward these goals by developing novel theoretical methods to (i) simulate the full many-body dynamics of faulttolerant quantum algorithms for unprecedented system sizes up to 2500 sites and on time scales ranging from a few femtoseconds to nanoseconds [1,2], and (ii) visualize quantum process such as MZM braiding in space and time via the non-equilibrium local density of states,  $N_{neq}$ , which is proportional to the differential conductance measured in scanning tunneling spectroscopy [1]. In particular, the PI's group demonstrated the first, successful simulation of a Majorana-based, fault-tolerant quantum algorithm to solve the Bernstein-Vazirani problem in 2D magnet-superconductor hybrid (MSH) structures from initialization to read-out of the final many-body state [3]. Using the Majorana zero modes' topological properties, we introduced an optimized braiding protocol and a scalable architecture for the implementation of the algorithm with an arbitrary number of qubits. We visualized the algorithm's execution in real time and space by computing the zero-energy non-equilibrium local density of states  $N_{neq}$  [see Fig.1(a)], allowing us to represent the quantum code via Majorana world lines [see Fig.1(b)]. We showed that the algorithm's final qubit state can be read out using capacitive charge measurements, allowing us to even identify faulty implementations of the algorithm.

We subsequently demonstrated that a crucial component of quantum algorithms -- the quantum memory - can be realized using Majorana edge modes [4]. To this end, we proposed a novel material platform in which trivial domains are embedded in a 2D topological superconductor (see Fig. 2). We showed that while MEMs can store qubit states, MZMs located in vortex cores [5] can be employed to execute quantum gates. This execution is achieved by moving vortices in real time through the edges of topological phases, converting delocalized MEMs into localized vortex core MZMs (see Fig. 2). Computing the full many-body dynamics of quantum gate processes, we demonstrated that all Clifford gates can be successfully realized in this novel material platform, opening the path for the future implementation of complex, scalable quantum algorithms.

### References

- J. Bedow, E. Mascot, T. Hodge, S. Rachel and D. K. Morr, Simulation of Topological Quantum Gates in Magnet- Superconductor Hybrid Structures, npj Quant. Mat. 9, 99 (2024); DOI:10.1038/s41535-024-00703-w
- E. Mascot, T. Hodge, D. Crawford, J. Bedow, D. K. Morr, and S. Rachel, *Many-Body Majorana Braiding without an Exponential Hilbert Space*, Phys. Rev. Lett. 131, 176601 (2023); DOI:10.1103/PhysRevLett.131.176601.
- 3. J. Bedow and D.K. Morr, Solving the Bernstein-Vazirani Problem using Majorana-based Topological Quantum Algorithms, under review in npj Quant. Inf.; arXiv:2503.10770;
- 4. J. Bedow and D.K. Morr, *Majorana Edge Modes as Quantum Memory for Topological Quantum Computing*, under review in Phys. Rev. Lett.; arXiv:2505.08888.
- 5. M. Buss, J. Bedow, P. Gupta, and D. K. Morr, *Braiding of Majorana Zero Modes in Vortex Cores*, under review in Phys. Rev. B. Letters; arXiv:2504.16841

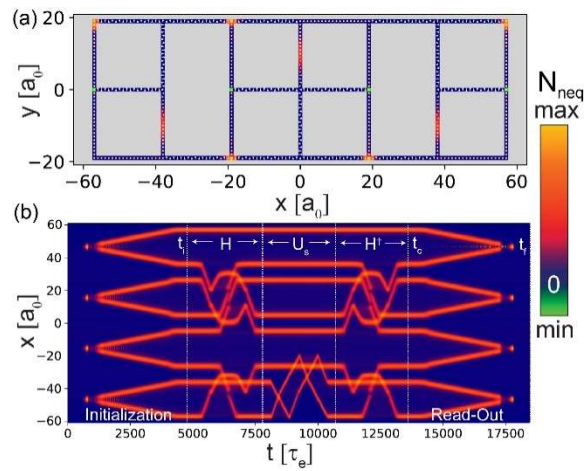


Figure 2 (a)  $N_{neq}$  during a Hadamard gate. (b) MZM world lines of the BV algorithm – the quantum code.

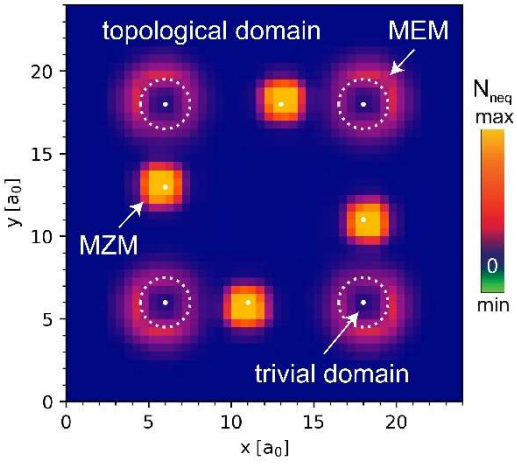


Figure 3:  $N_{neq}$  during a Hadamard gate with MEMs and vortex core MZMs.

# Mapping the genome of coherent quantum defects for Quantum Information Science DE-SC0022289

## High-throughput computational discovery of new quantum defects in silicon

<u>G. Hautier</u><sup>1,2</sup>, Y. Xiong<sup>1</sup>, Y. Zhu<sup>1</sup>, H. Song<sup>3</sup>, S. McBride<sup>1</sup>, X. Zhang<sup>3</sup>, J. Zheng<sup>1</sup>, J. Liu<sup>1</sup>, A. Sipahigil<sup>3,4</sup>, S. Griffin<sup>4</sup>

<sup>1</sup>Dartmouth College, <sup>2</sup>Rice University, <sup>3</sup>UCBerkeley, <sup>4</sup>Lawrence Berkeley National Laboratory

**Abstract:** Color centers in semiconductors are important building blocks of quantum networks and sensors. A series of well-established quantum defects exist especially in diamond (e.g., the NV center and the silicon divacancy) and have shown promises in demonstrating entanglement at long distance or quantum sensing. However, these defects have all limitations coming from their host (e.g., diamond is difficult to process) or from the defect in itself (e.g., the NV shows low optical coherence). Ultimately the performances of quantum networks and quantum sensing device will depend on the properties of these defects and there is a growing need to discover and develop new quantum defects sometimes in emerging hosts and/or understand their properties.

We will present our approach to systematically search for new quantum defects with attractive properties using first principles high-throughput computational screening and focusing on silicon. Silicon is an emerging host for quantum defects with tremendous advantages in terms of ease of process and nanofabrication. Color centers in silicon have recently started to be used in quantum applications (e.g., T center, G center, ...) including showing indistinguishable photons. We will show how a database of first principles computed data on 20,000 charged defects in silicon can be built and used to analyze the challenges and opportunities for designing quantum defects in such a small band gap material. A special focus will be on the recently discovered T center-like defects which could form attractive spin qubits. We will as well touch on how our approach can be extended to diamond, the most common host in for quantum defects proposing new defect with higher optical coherence. In these different hosts, the comparison between theory and experiment will be highlighted as well as the challenges in theoretical screening and how close work with experiments can direct the necessary development efforts in first principles methods.

### References

- 1. Komza, L., Samutpraphoot, P., Odeh, M., Tang, Y.-L., Mathew, M., Chang, J., Song, H., Kim, M.-K., Xiong, Y., Hautier, G. & Sipahigil, A., "Indistinguishable photons from an artificial atom in silicon photonics," *Nat Commun* **15**, 6920 (2024). DOI: 10.1038/s41467-024-51265-1
- 2. Xiong, Y., Mathew, M., Griffin, S. M., Sipahigil, A. & Hautier, G., "Midgap state requirements for optically active quantum defects," *Materials for Quantum Technology* **4**, 013001 (2024). DOI: 10.1088/2633-4356/ad1d38
- 3. Xiong, Y., Bourgois, C., Sheremetyeva, N., Chen, W., Dahliah, D., Song, H., Griffin, S. M., Sipahigil, A. & Hautier, G., "High-throughput identification of spin-photon interfaces in silicon," *Sci Adv* **9**, (2023). DOI: 10.1126/sciadv.adh8617

- 4. Xiong, Y., Zheng, J., McBride, S., Zhang, X., Griffin, S. M. & Hautier, G., "Computationally Driven Discovery of T Center-like Quantum Defects in Silicon," *J Am Chem Soc* **146**, 30046–30056 (2024). DOI: 10.1021/jacs.4c06613
- 5. Xiong, Y., Zhu, Y., McBride, S., Griffin, S. M. & Hautier, G., "Identifying high performance spectrally-stable quantum defects in diamond," (2025). DOI: https://doi.org/10.48550/arXiv.2504.11598

# **Topological Superconducting Heterostructures for Quantum Sensing DE-SC0022245**

## **Tunable Josephson Diode Effect for Qubit Noise Shielding**

## Enrico Rossi<sup>1</sup>, Wei Pan<sup>2</sup>, Javad Shabani<sup>3</sup>

<sup>1</sup>Physics Dept., William & Mary; <sup>2</sup>Materials Physics Dept., Sandia National Laboratories; <sup>3</sup>Center for Quantum Information Physics, Physics Dept., New York University

#### **Abstract**

We present our recent work aimed at enhancing the quality of planar Josephson junctions based on SC-SM heterostructures<sup>1,2</sup>, and designing and fabricating SQUIDs exhibiting a field-free JDE<sup>3,4,5</sup>. The enhancement of the quality of planar Josephson junctions based on SC-SM heterostructures is essential for the broader goal of the project to fabricate quantum sensors, and fault-tolerant qubits, based on the unique properties of the topological superconducting states that can be realized in such junctions. The JDE allows the realization of ideal, dissipationless, diodes and is therefore key toward the project's goal to realize noise-free, compact, quantum devices to shield qubits and quantum sensors from the noise inevitably introduced by the read-out electronics.

We have made progress toward the epitaxial growth of Al on antimonide heterostructures<sup>1</sup>, an important step toward the realization of novel SC-SM heterostructures that should allow the realization of topological superconducting states without the need of external magnetic fields. We have fabricated Josephson junctions with periodic hole structures on the superconducting contact leads (Fig. 1(a)) on InAs heterostructures with epitaxial superconducting Al. By depleting the chemical potential inside the holes' region with a top gate (Fig. 1(b)), we observed an enhancement of the junction' supercurrent, (Fig. 1(c)). We have developed the theory for the a.c. JDE in asymmetric SQUIDs<sup>3</sup> formed by Josephson junctions with different current-phase relations. We find that in such SQUIDs a strong a c. IDE can be realized with

with different current-phase relations. We find that in such SQUIDs a strong a.c. JDE can be realized, with strength, and polarity, that can be tuned also by varying the a.c. power. For SQUIDs formed by one topologically trivial junction, and one topological junction, (Fig.2

(a)) we found that the JDE is particularly strong, tunable (Fig. 2 (b)), and could be used to help detect the topological nature of planar Josephson junctions.

We have studied SQUIDs based on heterostructures formed by the Dirac semimetal Cd<sub>3</sub>As<sub>2</sub> and Al (Fig. 2(c)). A careful analysis of the

We have studied SQUIDs based on heterostructures formed by the Dirac semimetal Cd<sub>3</sub>As<sub>2</sub> and Al (Fig. 2(c)). A careful analysis of the a.c. response of such SQUIDs<sup>4</sup> revealed the presence of anomalous collective modes, Leggett modes, that strongly suggests the establishment of an uncommon superconducting state that spontaneously breaks time reversal symmetry. Such state should lead to a JDE even in the absence of any external magnetic field. We have observed such JDE<sup>5</sup> (Fig. 2(d)). This result is potentially transformative for the shielding from read-out noise of qubits and quantum sensors because it allows the realization of ideal circulators

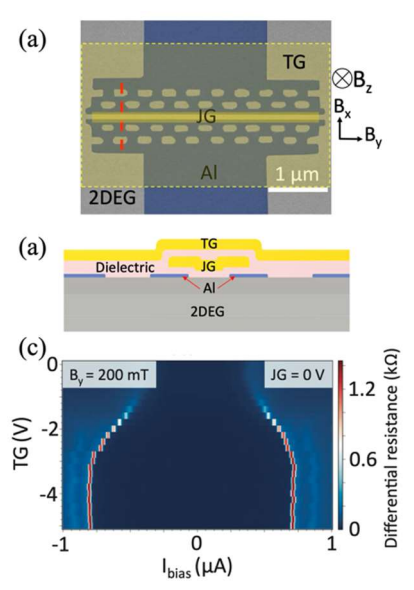


Figure 1. Planar Josephson junction based on SC-SM

and isolators without the need of magnetic fields, a fact that greatly reduces their size making them extremely compact and potentially viable for on-chip integration.

## References

1. W. Pan, K. R. Sapkota, P. Lu, A. J. Muhowski, W. M. Martinez, C. L. H. Sovinec, R. Reyna, J. P. Mendez, D. Mamaluy, S. D. Hawkins, J. F. Klem, L. S. L. Smith, D. A. Temple, Z. Enderson, Z. Jiang, E. Rossi, *Epitaxial aluminum layer on antimonide heterostructures for exploring Josephson junction effects*, Mat. Sc. and Eng.: B, **8**, 118285 (2025), DOI: 10.1016/j.mseb.2025.118285.

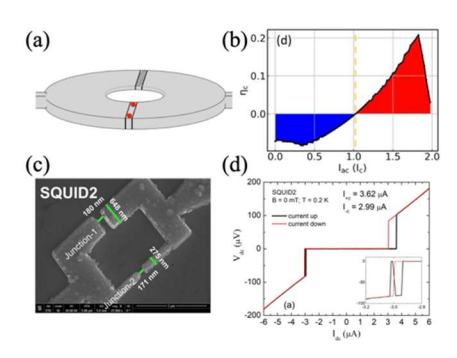


Figure 2. Results for JDE

- 2.P. Yu, H. Fu, W. F. Schiela, W. Strickland, B. H. Elfeky, S. M. Farzaneh, J. Issokson, E. Rossi, J. Shabani, *Gate tunable enhancement of supercurrent in hybrid planar Josephson junctions*, [arXiv:2404.09901] (2024), DOI: 10.48550/arXiv.2404.09901
- 3.J. J. Cuozzo, W. Pan, J. Shabani, E. Rossi, *Microwave-Tunable Diode Effect in Asymmetric SQUIDs with Topological Josephson Junctions*, Phys. Rev. Res., **6**, 023011 (2024), DOI: 10.1103/PhysRevResearch.6.023011.
- 4.J.J. Cuozzo, W. Yu, P. Davids, T.M. Nenoff, D.B. Soh, W. Pan, E. Rossi, *Leggett Modes in Dirac Semimetals*, Nature Physics **20**, 1118 (2024), DOI: 10.1038/s41567-024-02412-4.
- 5. W. Yu, J.J. Cuozzo; K. Sapkota, E. Rossi, D.X. Rademacher, T.M. Nenoff, W. Pan, *Time reversal symmetry breaking and zero magnetic field Josephson diode effect in Dirac semimetal Cd3As2-mediated asymmetric SQUIDs*, Phys. Rev. B,110, 104510 (2024), DOI: 10.1103/PhysRevB.110.104510.

## **Topological Superconducting Heterostructures for Quantum Sensing**

#### **DE-SC0022245**

# PI: Enrico Rossi<sup>1</sup>; Co-PIs: Wei Pan<sup>2</sup> and Javad Shabani<sup>3</sup>

<sup>1</sup>Physics Dept., William & Mary; <sup>2</sup>Materials Physics Dept., Sandia National Laboratories; <sup>3</sup>Center for Quantum Information Physics, Physics Dept., New York University

## Robust Superconducting Diode Effect in MBE Grown Dirac Semimetal Cd<sub>3</sub>As<sub>2</sub>

H.C. Travaglini a, J.J. Cuozzo a, K.R. Sapkota b, I.A. Leahy c, A.D. Rice c, K. Alberi c, and W. Pan a

#### **Abstract**

We present our results of robust and symmetric-inmagnetic-field SDE in asymmetric superconducting quantum interference devices (SQUIDs) [1] on Dirac semimetal Cd<sub>3</sub>As<sub>2</sub> thin films [2]. Molecular-beam epitaxy (MBE) is utilized to grow our high mobility Cd<sub>3</sub>As<sub>2</sub> thin film of 240 nm thickness. Details about growth can be found in Ref. [2]. Electron beam lithography is used to define SQUID structures. The bottom inset of Figure 1a shows an SEM image of this SQUID. The dimension of the SQUID is  $\sim 1.3 \times 1.0 \, \mu \text{m}^2$ . Electron beam evaporation is used to deposit 5 nm of titanium (to promote metal adhesion to the substrate), 230 nm of aluminum (Al), and 10 nm of gold (to mitigate oxide formation on the Al). Fig. 1a shows the quasi-four-terminal sample resistance  $R_{xx}$  as a function of temperature (T). The resistance is nearly constant and reaches  $R_{xx}\sim 6~\Omega$  at high temperatures. It drops to zero at T<sub>c</sub> ~ 1.2 K signaling a superconducting transition in the device. The top inset of Fig. 1a shows  $R_{xx}$ as a function of magnetic (B) field measured at 0.3 K. In

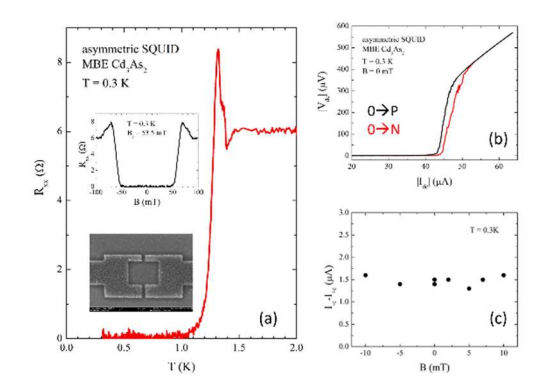


**Figure 1:** Superconducting diode effect in MBE grown  $Cd_3As_2$ . (a)  $R_{xx}$  vs T trace shows a superconducting transition at T  $\sim$  1.2K. (b) Current-voltage (I-V) for two current sweep directions. (c) The difference of critical currents as a function of B field.

the low field regime |B| < 50 mT, the device is in the supercurrent regime and  $R_{xx} = 0 \Omega$ . Beyond a critical B field of  $\sim 53.5$  mT, the supercurrent state is destroyed, and the device enters the normal state regime. Figure 1b shows the I-V characteristics in two current sweep directions (0  $\rightarrow$  P and 0  $\rightarrow$  N), measured at zero B field. A magnetic-field-free SDE is clearly observed. Furthermore, as shown in Figure 1c, the difference between the switching currents  $I_{\pm c}$  is independent of the strength and polarity of the out-plane magnetic fields in the range of -10 mT and 10 mT.

The observation of a zero-field SDE is consistent with our previous work on mechanically exfoliated Cd<sub>3</sub>As<sub>2</sub> thin flake [3], in which we show that the coupling between the surface and bulk superconducting channels in a Dirac semimetal can provide an intrinsic TRS breaking mechanism and, consequently, give rise to a field-free SDE. The same mechanism is applied here for the observed field-free SDE in the MBE grown Cd<sub>3</sub>As<sub>2</sub> thin films. To understand the origin of field resilience in our devices, we refer to recent work on SDE in multiferroic Josephson junctions [4] and speculate that an antiferromagnetic spin-spiral order (helimagnetism) might be responsible for this resilient symmetric-in-field SDE behavior. Indeed, an antiferromagnetic phase has been predicted in Dirac semimetals like Cd<sub>3</sub>As<sub>2</sub> in the presence of interactions [5]. This could serve as a possible explanation for the observed robust SDE.

<sup>&</sup>lt;sup>a</sup> Sandia National Laboratories, California; <sup>b</sup> Sandia National Laboratories, New Mexico;

<sup>&</sup>lt;sup>c</sup> National Renewable Energy Laboratory

We point out that a robust and symmetric SDE in SQUIDs using MBE grown Cd<sub>3</sub>As<sub>2</sub> thin films should allow future superconducting diode applications to take advantage of state-of-the-art semiconductor synthesis and processing.

#### References

- H.C. Travaglini, J.J. Cuozzo, K.R. Sapkota, I.A. Leahy, A.D. Rice, K. Alberi, and W. Pan, Robust and Symmetric Magnetic Field Dependency of Superconducting Diode Effect in Asymmetric Dirac Semimetal SQUIDs, accepted to APL Quantum, [arXiv:2505.21861] (2025), DOI: 10.48550/arXiv.2505.21861.
- 7. A.D. Rice, C.H. Lee, B. Fluegel, A.G. Norman, J.N. Nelson, C.S. Jiang, M. Steger, D.L. McGott, P. Walker, and K. Alberi, *Epitaxial Dirac Semimetal Vertical Heterostructures for Advanced Device Architectures*, Adv. Funct. Mater. 32, 2111470 (2022), DOI: 10.1002/adfm.202111470.
- 8. W. Yu, J.J. Cuozzo; K. Sapkota, E. Rossi, D.X. Rademacher, T.M. Nenoff, W. Pan, *Time reversal symmetry breaking and zero magnetic field Josephson diode effect in Dirac semimetal Cd3As2-mediated asymmetric SQUIDs*, Phys. Rev. B, **110**, 104510 (2024), DOI: 10.1103/PhysRevB.110.104510.
- 9. H.-Y. Yang, J.J. Cuozzo, A.J. Bokka, G. Qiu, C. Eckberg, Y. Lyu, S. Huyan, C.-W. Chu, K. Watanabe, T. Taniguchi, K.L. Wang, Field-Resilient Supercurrent Diode in a Multiferroic Josephson Junction, [arXiv: 2412.12344] (2025), DOI: 10.48550/arXiv.2412.12344.
- 10. X.-Q. Sun, S.-C. Zhang, and Z. Wang, *Helical spin order from topological Dirac and Weyl semimetals*, Phys. Rev. Lett. 115, 076802 (2015), DOI: 10.1103/PhysRevLett.115.076802.

## Quantum entanglement between a semiconductor donor and a trapped ion

**DE-SC0020378** 

Names of PI, coPI(s): Kai-Mei Fu and Boris Blinov

UW Grad Students: Vasileios Niouris, Xingyi Wang, Ethan Hansen, Carl Thomas, Rebecca Munk,

Aaron Hoyt

**UW Undergrad students:** Sam D'Ambrosia (undergrad) **UW postdocs**: Christian Zimmermann, Roman Kolodka

Collaborators: Lasse Vines (U. Oslo), Michael Titze (Sandia), Ed Bielejec (Sandia), Bethan Matthews

(PNNL), Steven Spurgeon (PNNL)

### **University of Washington**

**Abstract:** The central goal is to connect trapped ion qubits to single defects in semiconductors through a photonic link. This will be the first demonstration of entangling disparate matter qubit systems (aside from neutral atoms/ions of the same species) and mark progress toward scalable hybrid quantum systems. The immediate focus on the project is to generate indistinguishable single photons from the two different quantum emitters, a ytterbium trapped ion and a donor qubit in ZnO (either indium or tin-lithium). The two systems emit at nearly identical frequencies which can be bridged via Stark tuning and/or detuned Raman emission. The latter also enables temporal matching of the emitted photons [1].

On the trapped ion side, the Blinov group has performed theoretical analysis and numerical simulations of single photon pulse shaping to achieve >99% overlap of the emitted photons with the desired pulse shape, using both traditional computational techniques, such as genetic learning algorithms, and machine learning techniques for fast feedback. We have predicted that reversing the phase of the driving field will allow for photon shapes shorter than the limit set by the natural lifetime of the ion excited state, which could be useful given the shorter ZnO donor-bound-exciton lifetime.

On the ZnO donor side, the Fu group has realized indium donor formation via implantation and annealing [2] as well as isolation of single donors [3]. Most recently, in a related project, we have realized the synthesis of a new donor, a Sn-Li complex, which is even closer in wavelength to the Yb transition. In the Sn-Li complex we have resolved the hyperfine interaction to the longer-lived nuclear spin memory. Moving forward we may utilize the Sn-Li for this project in place of the donor.

The next step on the trapped ion side is to verify pulse shaping experimentally using a single trapped Yb<sup>+</sup> ion quantum emitter, quantified by Hong-Ou-Mandel interference with an attenuated coherent source. Trapping has been a struggle over the past year in the Blinov lab. In recent weeks, we completely rebuilt the parabolic mirror trap. It is currently back on the optical table, being set up for operation. We also constructed a backup linear trap which should be more robust, albeit with a lower photon collection efficiency (about 2% vs. 40% for the parabolic mirror trap), to mitigate risk.

In parallel, on the donor side, we are focusing our effort on ZnO photonic device fabrication for enhanced photon collection efficiency. Device fabrication in ZnO is a relatively immature area. Process development is near completion. While prior results have included ZnO donor formation via implantation and also single donor isolation, both have not been achieved simultaneously. Device integration will enable deterministically created single donors as well as the photon collection efficiency needed for hybrid entanglement schemes. The Raman excitation scheme used to match the donor photon with the ion will be informed by our recent fundamental work on the optical properties of donors [4].

### **References:**

- 1. Lilieholm JF, Niaouris V, Kato A, Fu K-MC, Blinov BB (2020) Photon-mediated entanglement scheme between a ZnO semiconductor defect and a trapped Yb ion. *Applied physics letters*, 117(15):154002. https://doi.org/10.1063/5.0019892 **Primarily supported by this award.**
- 2. Wang X, Zimmermann C, Titze M, Niaouris V, Hansen ER, D'Ambrosia SH, Vines L, Bielejec ES, Fu K-MC (2023) Properties of Donor Qubits in ZnO Formed by Indium-Ion Implantation. *Physical Review Applied*, 19(5):054090. https://doi.org/10.1103/PhysRevApplied.19.054090 **Primarily supported by this award.**
- 3. Hansen ER, Niaouris V, Matthews BE, Zimmermann C, Wang X, Kolodka R, Vines L, Spurgeon SR, Fu K-MC (2024) Isolation of single donors in ZnO. *Physical Review Letters*, 133(14):146902. https://doi.org/10.1103/PhysRevLett.133.146902 **Primarily supported by this award.**
- 4. Niaouris V, D'Ambrosia SH, Zimmermann C, Wang X, Hansen ER, Titze M, Bielejec ES, Fu K-MC (2024) Contributions to the optical linewidth of shallow donor-bound excitonic transition in ZnO. *Optica Quantum*, 2(1):7. https://doi.org/10.1364/opticaq.501568 **Primarily supported by this award.**

# **Integrated Materials Platforms for Topological Quantum Computing Devices** DE-SC0019274

# Abstract Title: Synthesis of improved mobility InAs and InGaAs-quantum wells and of PbSe SAG nanowires

Vlad Pribiag <sup>1</sup>, <u>Chris Palmstrøm</u> <sup>2</sup>, <u>Sergey Frolov</u> <sup>3</sup>, <u>Noa Marom</u> <sup>4</sup>, <u>Kunal Mukherjee</u> <sup>5</sup>, Yilmaz Gul <sup>6</sup>, Stuart N. Holmes <sup>6</sup>, and Michael Pepper <sup>6</sup>

1. U. Minnesota, 2. U. C. Santa Barbara, 3. U. Pittsburgh, 4. Carnegie Mellon University, 5. Stanford University, 6. London Centre for Nanotechnology - University College London

Abstract: A significant challenge towards developing robust quantum computing systems with large numbers of logical qubits is rapid decoherence. A promising approach to addressing this challenge is based on the concept of fault-tolerant quantum computing architectures that leverage topological quantum states such as Majorana zero-modes (MZM). Substantial progress toward realizing and detecting topological states has been enabled by quantum devices which combine semiconductors with superconductors due to the combination of processing-friendly materials that offer high spin-orbit coupling, large g-factors, ballistic transport, and the ability to create transparent interfaces with various superconductors. However, further breakthroughs leading to topological quantum computation require next-generation quantum nanostructures that offer substantial improvement in the electronic purity together with optimal coupling across the superconductor-semiconductor interface. *Here we discuss our recent results under this project, focusing on the synthesis of higher purity III-V and IV-VI materials platforms*. This work is a subset of our larger effort supported by this grant, which combines quantum device fabrication and characterization with materials synthesis and data interpretation informed by ab initio simulations and machine learning to develop robust, tunable and scalable platforms for the manipulation of quantum states

# (i) Enhancing mobility in InGaAs and InAs quantum wells on InP(001) substrates:

Critical to the superconductor/semiconductor multiterminal Josephson junction device effort is to increase the carrier mean free path (mfp) in the semiconductor. Although very high mobility InAs quantum wells can be grown on nearly lattice matched GaSb utilizing AlGaSb barriers, parallel and side wall conduction and the processing challenges of Sb-based semiconductors, makes semi-insulating InP substrates a highly desirable choice. High In content (≥75%) InGaAs quantum wells grown on InP substrates rely on InGaAs cladding layers

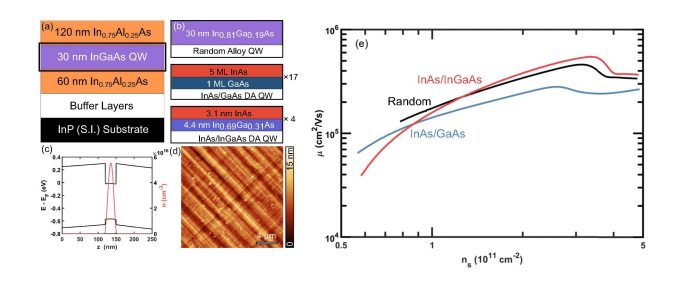


**Fig. 1:** (a) Sample structure schematic. (b) Different samples in the study. (c) Self-consistent Schrödinger-Poisson simulation of the sample structure. (d) Representative AFM micrograph of InAlAs top barrier; crosshatching typical of metamorphic growth is observed. (e) Gated Hall bar measurements of mobility vs gated carrier density.

and InAlAs barrier layers to confine electrons within a thin well. The highest mobility QWs are limited by interfacial roughness scattering and alloy disorder scattering in the quantum well, cladding and buffer layers. Efforts at UCSB have focused on increasing the electron mobility and thus the mfp in MBE-grown quantum wells (Fig. 1). The approaches taken involved investigating the use of i) digital alloys (superlattices of monolayer thicknesses of InAs and InGaAs) to reduce the alloy disorder scattering within the quantum well while achieving the same average composition as a high In ( $\geq$ 75%) concentration random InGaAs alloy and ii) strain compensation techniques during the cladding and barrier layer growth. The mobility of 545,000 cm<sup>2</sup>/Vs achieved for the digital alloy InGaAs quantum well is higher than that highest

previously reported for the equivalent random alloy ~430,000 cm<sup>2</sup>/Vs [1]. By utilizing strain compensation during the cladding and barrier layer growth, the critical thickness of the InAs can be increased before relaxation occurs and a substantially wider quantum well with increased mobility can be grown [2]. Quantum point contact devices showed 1D conductance quantization (2e<sup>2</sup>/h) up to 17 plateaus [3].

(ii) Synthesis of PbSe semiconductor-superconductor materials platforms: We are also developing procedures for PbSe nanowire networks via selective area growth (SAG) using molecular beam epitaxy (MBE) (Fig. 2), which leverage our prior work [4]. We are particularly sensitive to growth conditions that yield continuous and smooth films, with minimal non-selective growth. At the outset, we have identified a growth window of 360-375 °C for PbSe to grow selectively on exposed crystalline GaAs. Here, the sticking

of PbSe on adjacent dielectric regions is reduced to zero. This has allowed us to make smooth nanowires. The tendency for PbSe to congruently sublimate makes the use of compound sources convenient for MBE. However, we are learning that the source stoichiometry is crucial in obtaining good SAG synthesis. We show results with two batches of source material, Pb-rich PbSe and stoichiometric PbSe. We find that stoichiometric PbSe yields continuous nanowires. Pb-rich PbSe requires the addition of Se flux to improve morphology. The background carrier concentration is another important synthesis target, in addition to the surface morphology. We have discovered that PbSe is sensitive to atmospheric oxygen, and exposure at room temperature converts the films to p-type in the range of  $10^{18}$ /cm<sup>3</sup>. We are showing that insitu capping of the samples with wider bandgap GeSe (~1.1 eV bandgap) can sufficiently prevent oxygen diffusion into the PbSe to preserve the unintentional (n-type) doping of the as-grown PbSe.

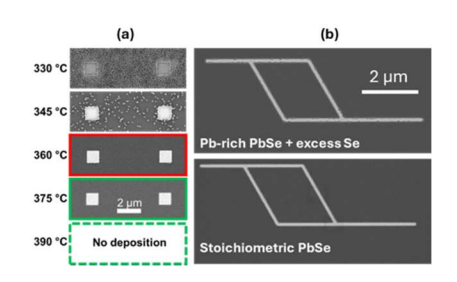


**Fig. 2:** Synthesis of PbSe SAG nanowires. (a) Growth selectivity of PbSe is enhanced at 360-375 °C, just at the limit of sticking. Polycrystalline nuclei are seen at temperatures of 330-345 °C. (b) A stoichiometric PbSe source results in more continuous nanowires.

#### **References:**

- [1]J. T. Dong et al., *Enhanced mobility of ternary InGaAs quantum wells through digital alloying*, Phys. Rev. Mater. **8**, 1 (2024) DOI: 10.1103/PhysRevMaterials.8.064601.
- [2]C. P. Dempsey et al., Effects of Strain Compensation on Electron Mobilities in InAs Quantum Wells Grown on InP(001), ArXiv:2406.19469 (2024) DOI: 10.48550/arXiv.2406.19469.
- [3]I. V. Rodriguez et al., Non-magnetic Fractional Conductance in High Mobility InAs Quantum Point Contacts, ArXiv:2503.08476 (2025) DOI: 10.48550/arXiv.2503.08476.
- [4]B. B. Haidet et al., Versatile strain relief pathways in epitaxial films of (001)-oriented PbSe on III-V substrates, Phys. Rev. Mater. 7, 024602 (2023) DOI: 10.1103/PhysRevMaterials.7.024602.

### Abstract Title Parametric interactions in superconducting multi-qubit+cavity architectures

Names of PI, coPI(s), and unpaid collaborators: <u>Raymond W. Simmonds</u><sup>1</sup>, Jose Aumentado<sup>1</sup>, Archana Kamal<sup>2,3</sup>, Zhihao Xiao<sup>2</sup>, Emery Doucet<sup>2</sup>, Taewan Noh<sup>2</sup>, Sudhir Sahu<sup>2</sup>, Leonardo Ranzani<sup>4</sup>, and Luke Govia<sup>4</sup>

NIST Boulder<sup>1</sup>, University of Massachusetts Lowell<sup>2</sup>, Northwestern University<sup>3</sup>, RTX BBN Technologies<sup>4</sup>

#### **Abstract:**

In the PIQUE (Parametrically-Induced QUantum Engineering) Program, we are developing a multielement architecture that can cancel static couplings between multiple circuit-QED elements, like qubits and cavities, but still allow strong and tunable parametric interactions. As a demonstration, we have utilized a galvanic SQUID inductive coupler that is shared by two qubits and a cavity (see Fig. 1). Here, the inductive coupling cancels the static capacitive coupling between any pair of elements at a static operation flux. Cancellation minimizes both qubit cross-talk, unintended interactions, shot-noise qubit dephasing, and energy decay of the qubits. If we modulate the flux in the SQUID coupler, we can parametrically produce all-to-all interactions between all three elements. In our experimental investigation of this system [1], we verified minimal coupling between the qubits and cavity at the cancellation flux. With applied parametric drives to the coupler, we developed a new tunable dispersive readout technique [2].

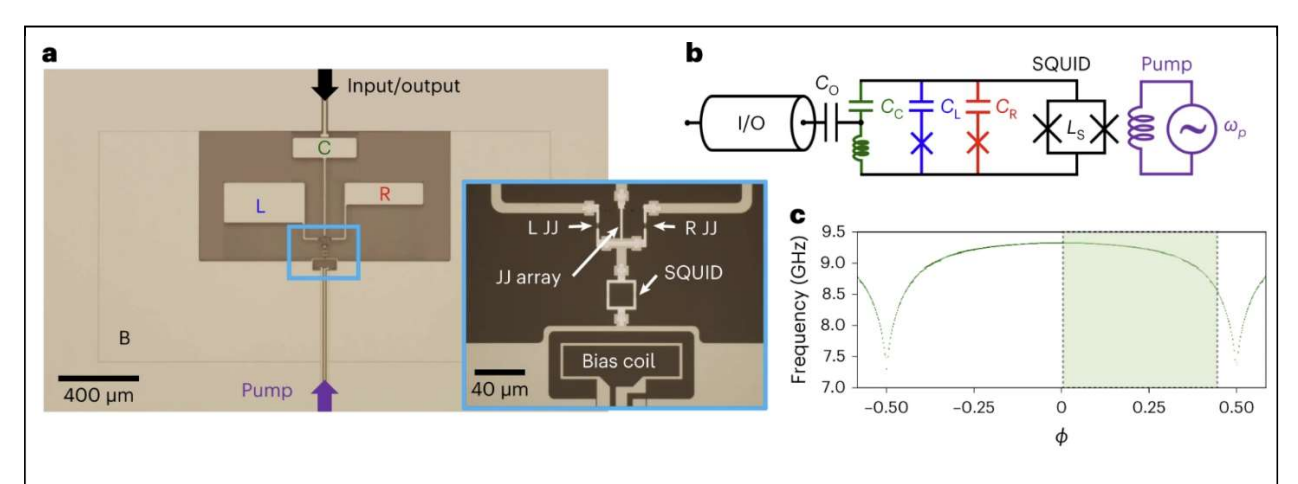


**Fig. 1: a**, Optical micrograph of a tunable circuit—QED system, where JJ stands for Josephson junction.**b**, Schematic of the system including three elements: cavity mode (C), left transmon (L) and right transmon (R). The parametric flux drive is applied through a shared SQUID coupler. **c**, Periodic cavity spectrum, where green shading denotes flux operation region.

We have shown experimentally that we can create tunable dispersive shifts between either or both qubits and the cavity and this dispersive interaction grows with the size of the parametric drive strength. In addition, we can also access both positive and negative dispersive shifts depending on the pump frequency (See Fig. 2). This demonstration of tunable qubit readout is versatile. It is possible to cancel residual dispersive interactions and tune joint two-qubit readout to distinguish all four readout states or to

make odd or even parity states indistinguishable, which is useful for generating two-qubit entanglement or error correction.

In next-generation PIQUE program, we have extended this architecture to develop a two-cavity + qubit system where the long-lived "readout cavity" is isolated and the "buffer cavity" provides photon access into and out of the system. With this device we are developing a sequentially pulsed parametric dispersive readout with integrated *in-situ* amplification. This extends our previous work by providing a phase gate on the readout cavity to capture qubit state information which can be amplified and accessed through the buffer cavity. The pulsed nature of the readout protocol protects the qubit and readout cavity throughout the measurement process.

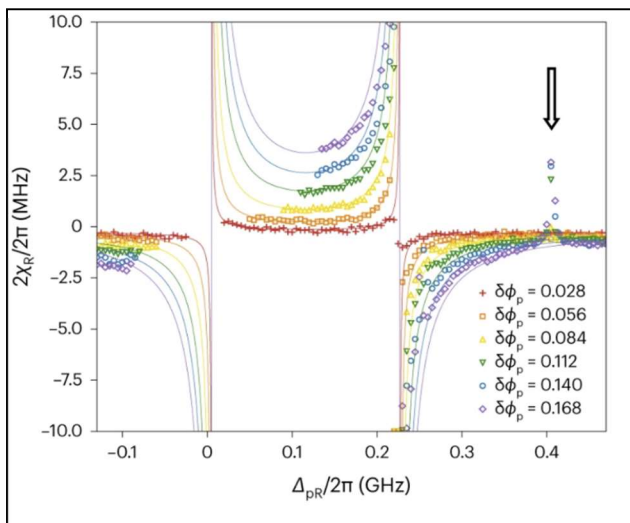


**Fig. 2:** Total dispersive shift  $2\chi_R/2\pi$  as a function of  $\Delta_{DR}/2\pi$ .

The techniques we have developed for these architectures can be scaled to larger numbers of qubits and cavities. For instance, in next-generation PIQUE program, we have developed a 3-qubit + cavity system with no static interactions, but all-to-all parametric interactions mediated via a single coupler. This general increase in connectivity is not "hardwired" and so that various Hamiltonians become software programmable via frequency-selective

pumping. In an attempt to scale to larger numbers of elements we have developed compact, high quality capacitors that can be used in coherent superconducting qubits [3].

[1] T. Noh, Z. Xiao, K. Cicak, X. Y. Jin, E. Doucet, J. Teufel, J. Aumentado, L. C. G. Govia, L. Ranzani, A. Kamal, R. W. Simmonds. *Strong parametric dispersive shifts in a statically decoupled multi-qubit cavity OED system*, **Nature Physics**, s41567-023-02107-2 (2023)

[2] Z. Xiao, E. Doucet, T. Noh, L. Ranzani, R. W. Simmonds, L. C. G. Govia, A. Kamal. *Perturbative diagonalization for time-dependent strong interactions*, **Phys. Rev. Applied** 18, 024009 (2022)

[3] Anthony P. McFadden, Aranya Goswami, Tongyu Zhao, Teun van Schijndel, Trevyn F. Q. Larson, Sudhir Sahu, Stephen Gill, Florent Lecocq, Raymond Simmonds, Chris Palmstrøm. *Fabrication and characterization of low-loss Al/Si/Al parallel plate capacitors for superconducting quantum information applications*, **npj Quantum Information** 11, 11 (2025)

Understanding the relationship between surface lattice and single photon emission dynamics in strongly confined cesium lead bromide perovskite quantum dots DE-SC0024441

### Towards non-blinking and photostable perovskite quantum dots

Chenjia Mi<sup>1</sup>, Gavin C. Gee<sup>1</sup>, Chance W. Lander<sup>1</sup>, Donghoon Shin<sup>2</sup>, Matthew L. Atteberry<sup>1</sup>, Novruz G. Akhmedov<sup>1</sup>, Lamia Hidayatova<sup>1</sup>, Sohom Chandra<sup>1</sup>, Jesse D. DiCenso<sup>1</sup>, Michael P. LaSala<sup>1</sup>, Wai Tak Yip<sup>1</sup>, Bin Chen<sup>2</sup>, Yihan Shao<sup>1</sup>, Yitong Dong<sup>1,3</sup>

Abstract: Lead halide perovskite quantum dots (QDs) have emerged as promising single-photon-emitting materials due to their uniquely bright triplet excitonic emissions. However, their insufficient single-photon emission performance and stability, often broadly attributed to fragile crystal lattices, remain poorly understood. Our QIS project aims to explore the effect of surface lattice rigidity on the single-photon emission dynamics in individual perovskite QDs. To reduce selection bias in single QD spectroscopic studies, we first sought to precisely control the size and surface morphology of perovskite QDs during synthesis by unraveling their growth mechanisms. To understand the impact of surface lattice on the stability of single-photon emission, we then embedded single QDs into a molecular crystal matrix (Figure 1a). The attractive intermolecular interactions between low-steric ligand tails in the crystallized matrix, such as  $\pi$ - $\pi$  stacking, can promote the formation of a nearly epitaxial ligand layer, significantly reducing the QD's surface energy. Here, we demonstrate that single CsPbBr<sub>3</sub> QDs covered by stacked phenethylammonium (PEA) ligands exhibit nearly non-blinking single-photon emission with high purity (~ 98%) and extraordinary photostability (12 hours of continuous operation and saturated excitations), allowing for the determination of size-dependent exciton radiative rates and emission linewidths of CsPbBr<sub>3</sub> QDs at the single-particle level (Figure 1b-1g). Additionally, benefiting from the material design, we have investigated the impact of various surface defects on the purity of single-photon emission from CsPbBr<sub>3</sub> QDs.

<sup>&</sup>lt;sup>1</sup>Department of Chemistry and Biochemistry, University of Oklahoma, Norman, OK 73019, USA

<sup>&</sup>lt;sup>2</sup>Department of Chemistry, Northwestern University, Evanston, IL 60208, USA

<sup>&</sup>lt;sup>3</sup>Center for Quantum Research and Technology, University of Oklahoma, Norman, OK 73019, USA

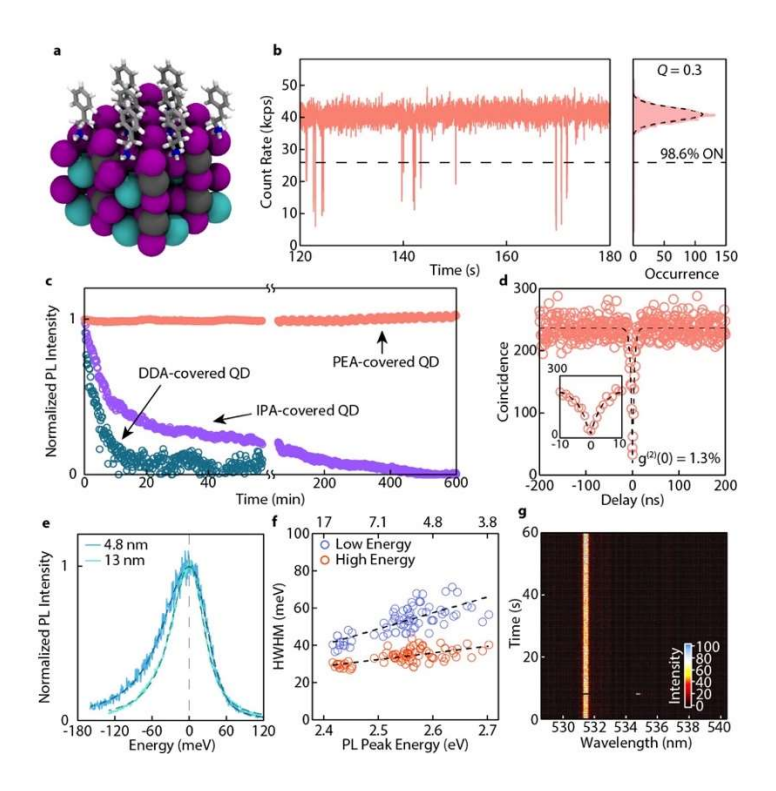


**Figure 1.** (a) A model showing molecules (PEA) epitaxially aligned on the surface of perovskite QDs. (b) PL blinking traces and intensity distribution histograms of a 4.5 nm CsPbBr<sub>3</sub> QD embedded in PEA matrix. (c) Normalized PL intensity of a collection of single PEA-covered CsPbBr<sub>3</sub> QDs (red) under 10 h of continuous laser excitation. In contrast, traditional ligand-covered QDs experienced severe photodarkening after a few minutes. (d) Second-order correlation (g<sup>(2)</sup>) function of the QD in (b). (e) PL spectra of two single CsPbBr<sub>3</sub> QDs. Dashed curves are fits, each using two Voigt functions with a common peak position for the asymmetric spectra. (f) PL linewidths (half-width half-maximum, HWHM) extracted from the high and low energy sides of PL spectra for 81 QDs. (g) PL spectra-time trace of a single CsPbBr<sub>3</sub> QD monitored at 3 K exhibiting undetectable spectral jumps/diffusions. ((b-f), adapted from Reference 2, under a Creative Commons Attribution-NonCommercial-NoDerivatives 4.0 International License)

# **References:**

- 1 M. L. Atteberry et al. Chem Mater. 2024, 36, 4521, DOI: 10.1021/acs.chemmater.4c00160
- 2 C. Mi et al. Nat. Commun. 2025, 16, 204, DOI: 10.1038/s41467-024-55619-7
- 3 G. C. Gee et al. MRS Commun. 2025, (In Press), DOI: 10.1557/s43579-025-00740-x

## Project title: Color centers in noise-free hosts for quantum sensing and communication applications

Award Number: DE-SC0025486

**Authors:** Kusal Abeywickrama<sup>1</sup>, Pralay Paul<sup>1</sup>, Melissa Artola<sup>1</sup>, Sreehari Purayil<sup>1</sup>, Sumit Gaswami<sup>1</sup>, Dhiman Biswas<sup>1</sup>, Casey Kerr<sup>1</sup>, Mritunjaya Parashar, Mohin Sharma<sup>3</sup>, Darshpreet Kaur Saini<sup>3</sup>, Bibhudutta Rout<sup>3</sup>, Thirumalai Venkatesan<sup>1</sup>, and <u>Alisa Javadi</u><sup>1,2</sup>

**Affiliation:** <sup>1</sup>Department of Physics and Astronomy, The University of Oklahoma, <sup>2</sup>School of Electrical and Computer Engineering, The University of Oklahoma, <sup>3</sup> Department of Physics, The University of North Texas

**Abstract:** The spin state of an electron in quantum emitters is pivotal in quantum technologies such as quantum communication and quantum sensing. For both types of quantum emitters, color centers, and rareearth dopants, and for the materials with the highest quality, the hyperfine interaction between the nuclei of the host crystal and the spin of the electron gives rise to fluctuating electron energy levels, which in turn cause decoherence of the spin state. Suppressing this noise calls for isotopically purified samples, which is an expensive process and poses a problem for scaling technologies based on these materials.

Interestingly, a limited number of elements (oxygen, calcium, and cerium) are free of magnetic nuclei in their naturally abundant isotopes. Given the sparsity of magnetic nuclei, color centers in naturally occurring CeO<sub>2</sub> are projected to have remarkable coherence times as long as 47ms [1]. This characteristic significantly enhances the material's potential for quantum sensing and communication applications.

CeO<sub>2</sub> benefits from several other advantages as a host material. Its relatively large bandgap (3.5 eV) allows it to accommodate color centers ranging from visible frequencies to the mid-IR range. CeO<sub>2</sub> is compatible with silicon [2] and, as a lanthanide-based host, it is adept at supporting lanthanide emitters, which are significant due to the long coherence of 4f energy levels and the long coherence of their nuclei. In addition

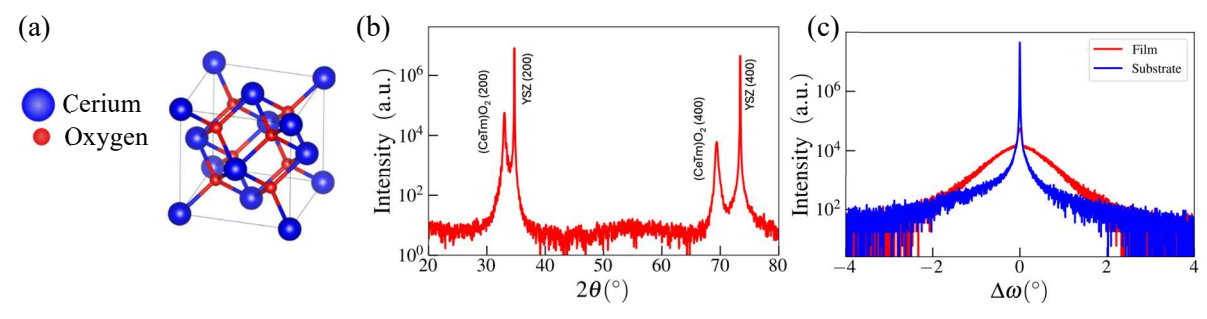


**Figure 1** (a) The crystal structure of CeO<sub>2</sub>. (b) XRD measurements on a thin film of CeO<sub>2</sub> grown on YSZ substrate indicating single crystal films aligned with the YSZ axis. (c) Rocking curve of the film showing a sharp peak on top of a broader Gaussian background.

to its technological strengths, CeO<sub>2</sub>'s biocompatibility simplifies lab handling, broadening its applications.

One of the goals of this project is to investigate the potential of rare-earth dopants (specifically, thulium dopants) in CeO<sub>2</sub> for quantum information applications, including sensing and quantum memories. Figure 1a shows the crystal structure of CeO<sub>2</sub>. In this project, we are using Pulsed Laser Deposition to grow thin films of CeO<sub>2</sub>. The main advantage of PLD is its rapid turnaround time, which allows us to fabricate films with different thicknesses and doping concentrations in a short period of time.

We have managed to grow high-quality CeO<sub>2</sub> thin films doped with trivalent thulium ions (Tm3+) at concentrations of 0.1% on single-crystalline yttria-stabilized zirconia (YSZ) substrates. We have

characterized these samples using various techniques, XRD, XRR, and AFM measurements. To achieve the desired doping concentration, we employed two distinct targets, a pure CeO2 target and a 10% Tm-doped CeO2 target and varying the laser pulses directed at each target. Figures 1b and 1c show some of these characterizations.

The XRD pattern of the thin film 1% Tm-doped CeO<sub>2</sub>, as shown in Fig. 1b, exhibits well-defined (200) and (400) diffraction peaks, confirming the epitaxial nature of the film. The presence of interference fringes around the (200) diffraction peak indicates a high degree of crystalline order and smooth interface quality. The measurements of the rocking curve performed on the (200) peak of the YSZ substrate show a sharp peak with a full-width-at-half-maximum (FWHM) of 0.01°, whereas the corresponding measurement for the CeO<sub>2</sub> film doped with Tm reveals a combination of a sharp peak (FWHM 0.05°) and a broader peak (FWHM 0.5°). This suggests that the film remains strained in the initial growth stages near the substrate interface but progressively relaxes as the thickness increases while maintaining oriented growth. As evident from the XRD curves and Rocking curves, we have been able to grow highly crystalline films that are well-aligned with the crystallographic axes of the substrate. Furthermore, our atomic force microscope measurements show very smooth films with roughness below 0.5nm.

We characterized the optical properties of CeO<sub>2</sub>:Tm<sup>3+</sup> using photoluminescence (PL) and photoluminescence excitation (PLE) [3]. The Tm<sup>3+</sup> ions in the sample were excited by a continuous wave UV laser at 355nm, plotted in in Fig. 2. The spectrum consists of strong emission peaks in red and NIR regimes with main four peaks at 654, 690, 793, and 808 nm which correspond to <sup>1</sup>G<sub>4</sub>-<sup>3</sup>F<sub>4</sub>, <sup>3</sup>F<sub>3</sub>, <sup>2,3</sup>H<sub>6</sub>, <sup>1</sup>G<sub>4</sub>-<sup>3</sup>H<sub>5</sub> and <sup>3</sup>H<sub>4</sub>-<sup>3</sup>H<sub>6</sub> transitions, respectively.

These measurements are exciting first steps in our goal of using these dopants for quantum communication and sensing applications. As the next step, we are currently working on characterizing these transitions' quantum efficiency and coherence in

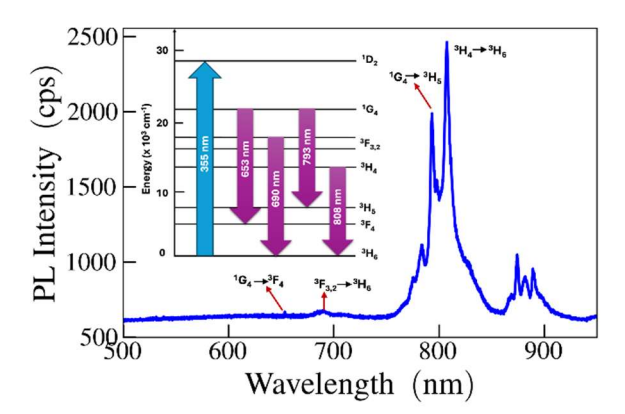


**Figure 2** Fig. 2. PL spectrum of 550 nm thick 1% Tm3+ doped film.

pump-probe measurements. Another goal is to embed these films in photonic structures to enhance their collection efficacy. We have developed a novel growth method to directly deposit nanostructures of complex oxides into pre-patterned substrates and are in the final steps of refining this technique [4].

#### References

- [1] Kanai, Heremans, Seo, Wolfowicz, Anderson, Sullivan, Onizhuk, Galli, Awschalom, Ohno, "Generalized scaling of spin qubit coherence in over 12;000 host materials," PNAS, **19**, e2121808119 (2022).
- [2] Nishikawa, Yamaguchi, Yoshiki, Satake, Fukushima, "Interfacial properties of single-crystalline CeO2 high-k gate dielectrics directly grown on Si(111)," Appl. Phys. Lett., **81**, 4386 (2002).
- [3] Abeywickrama, Paul, Artola, Purayil, Gaswami, Biswas, Kerr, Venkatesan, Javadi, "Optics of rare-earth ions in cerium oxide for application in quantum technologies", American Physical Society (APS) Global Summit (March Meeting), Anaheim, USA (2025).

[4] Biswas, Artola, Goswami, Paul, Kerr, Purayil, Summers, Hahn, Javadi, Weng, Fomra, Lezec, Venkatesan, "Growth of Self-Aligned Oxide Photonic Devices on Silicon", Materials Research Society (MRS) Fall Meeting & Exhibit, Boston, USA (2024)

Project Title: Interactions of QDs' Fast Light in Rb Vapors for Hybrid Quantum Information

**Science and Technology Award Number:** (unknown)

Abstract Title: Towards Hybrid Quantum Repeaters with Quantum Dots and alkali vapors

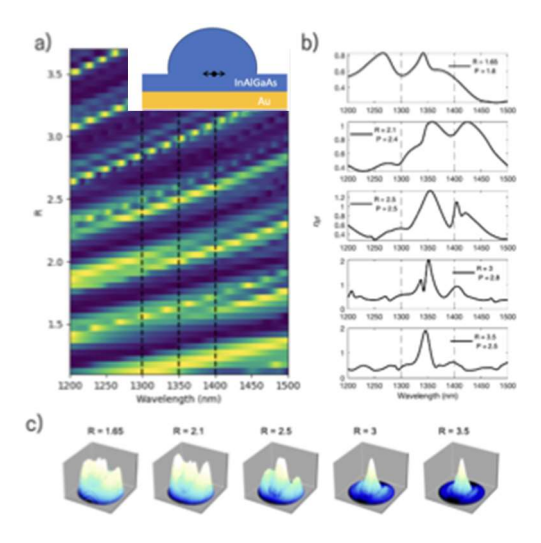
Names of PI: Joanna M Zajac (PI)<sup>1</sup>

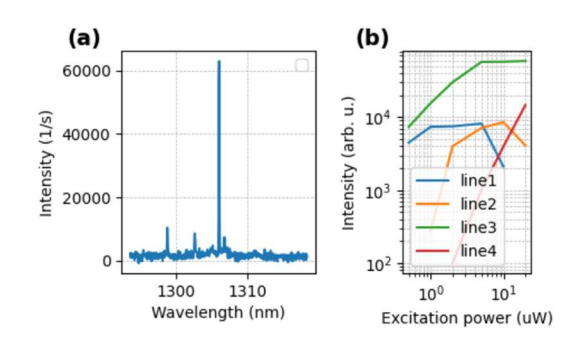
Collaborators and contributors: Tobias Huber<sup>2</sup>, Sven Höfling<sup>2</sup>, Monika Dziubelski<sup>1</sup>, and Sofia Pereira<sup>1</sup>

**Affiliation(s)** <sup>1</sup>Brookhaven National Laboratory, <sup>2</sup>Technische Physik, University of Würzburg, Am Hubland, 97074 Würzburg, Germany

**Abstract**: III-V epitaxial QDs working at near-infrared (NIR) wavelengths had been a gold standard for quantum emitters and promising candidates for memories. They exhibit high brightness, indistinguishability, and work on demand. Future long distance quantum communication networks will utilize existing optical fiber infrastructure working between 1.3 and 1.5 μm. Shifting QDs operational wavelengths into telecommunication O- and C-bands is thus important for these applications<sup>1</sup>. There are two III-V semiconductor material systems that have been considered, namely, InAs/InP and InAs/GaAs QDs.

In this work, we discuss our novel sample design with QDs based on quaternary alloy InAlGaAs, lattice matched to InP substrates, however, maintaining shorter emission wavelengths using advanced growth techniques. To increase extraction efficiency from these emitters, we embed them into specially designed and optimized microcavity strucutres<sup>2</sup>. We use these QDs to develop hybrid repeater platforms working with alkali memories. We work with diamond configuration in Rb for four-wave mixing process to convert 1.3 µm signal photons to 795 nm idler. This conversion mechanism, unlike ladder configuration such as ORCA, exhibit noise due to spontaneous emission and four-wave mixing process; however, it also has superior storage properties under EIT. I will discuss our latest progress on this topic discussing growth, material characterization and device development under my Carrier Award Project in Quantum Information.





a) transmission maps vs radius (R) and wavelength (nm) for the cavity shown in the inset, b) Transmission cross-sections for fixed radius as a function of wavelength and in c) far-field emission patterns for indicated R.

a) Low temperature  $\mu$ -photoluminescence ( $\mu$ -PL) from QDs growth for this project showing high S/N at 60 kHz. b) Excitation power sweep for several QDs within the same wafer.

- 1. Quantum dots for quantum repeaters, <u>Joanna M Zajac</u>, Tobias Huber, Sven Höfling, Arxiv (2025) (to appear in Review Modern Physics)
- 2. Dziubelski, M., and J. M. Zajac (2024), Arxiv <a href="https://doi.org/10.48550/arXiv.2412.18472">https://doi.org/10.48550/arXiv.2412.18472</a> (submitted Optics letters)
- 3. S Mandal, K Hernandez, JM Zajac, IEEE International Midwest Symposium on Circuits and Systems (MWSCAS) (2025) (Related work)

## Multiparticle Quantum Information Processing in Robust Plasmonic Lattices

#### **DE-SC0021069**

Mingyuan Hong<sup>1</sup>, Fatemeh Mostafavi<sup>1</sup>, Jannatul Ferdous<sup>1</sup>, Riley B. Dawkins<sup>1</sup>, Roberto Leon-Montiel<sup>2</sup>, Rui-Bo Jin<sup>3</sup>, Benjamin Bertoni<sup>1</sup>, Ian Baum<sup>1</sup>, Chenglong You<sup>1</sup>, and **Omar S. Magana-Loaiza**<sup>1</sup>

<sup>1</sup>Quantum Photonics Laboratory, Department of Physics & Astronomy, Louisiana State University, Baton Rouge, LA 70803, USA; <sup>2</sup>Instituto de Ciencias Nucleares, Universidad Nacional Autonoma de Mexico, Ciudad de Mexico 70543, Mexico; <sup>3</sup>School of Electrical and Information Engineering, Wuhan Institute of Technology, Wuhan 430205, China

#### **Abstract**

One of the most significant achievements of the second quantum revolution is the ability to perform tasks that are infeasible for classical computers. However, the stringent requirements for quantum resources, along with the presence of noise and loss, impose important limitations on technologies for quantum information processing. The aim of this research program is to develop robust protocols for quantum information processing by exploiting the additional interference pathways enabled by optical near fields to control complex multiparticle interactions within plasmonic platforms. Our ability to resolve specific dynamics in multiparticle plasmonic systems will be leveraged to advance quantum information processing in plasmonic lattices that are intrinsically loss-tolerant and operate without error correction. Unlike other quantum architectures, our plasmonic platform supports both bosonic and fermionic interactions, offering a robust foundation for quantum simulation and information processing.

I will describe our work on the nonclassical near-field dynamics of surface plasmons [1]. As shown in Figure 1, we isolated the constituent multiparticle subsystems of classical plasmonic waves and showed that their quantum dynamics are governed by bosonic or fermionic coherence processes [1]. Interestingly, the article *Multiphoton Quantum Statistics from Scattered Classical Light* highlights the implications of extracting quantum multiparticle systems from classical plasmonic platforms in the presence of losses [2]. Our work was selected as the Best of Optics in 2024 by *Optica's Optics & Photonics News* [3]. Remarkably, these findings enabled my team to develop robust multiphoton quantum technologies [4].

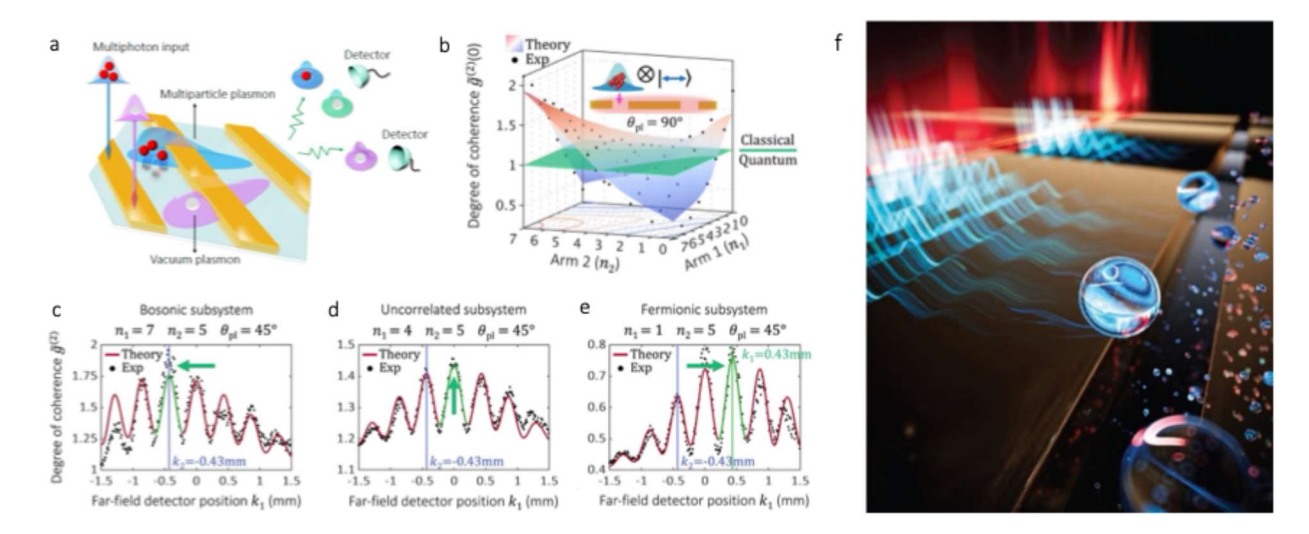


Figure 1. We investigated the nonclassical dynamics of plasmonic multiparticle systems illustrated in  $\bf a$ . As reported in  $\bf b$ , the constituent multiparticle subsystems that form classical plasmonic waves exhibit classical and quantum properties of coherence. For example, subsystems with a degree of coherence greater than one, such as the twelve-particle system ( $n_1 = 7$ ,  $n_2 = 5$ ) in  $\bf c$ , exhibit bosonic correlations. Furthermore, systems with coherence degrees close to one are uncorrelated, as shown in  $\bf d$ . Interestingly, quantum multiparticle systems with a degree of coherence below one show fermionic anticorrelations. This is shown in  $\bf e$  for a six-particle system ( $n_1 = 1$ ,  $n_2 = 5$ ) [1]. The illustration in  $\bf f$  depicts a metallic nanostructure hosting plasmonic waves produced by vacuum fluctuations of the electromagnetic field. It also shows the scattering of surface plasmons, which produces multiparticle systems with either bosonic or fermionic coherence properties [3].

We exploited these capabilities to design the plasmonic metacrystal shown in Figure 2. This structure creates a synthetic plasmonic lattice in the Fock basis, which is used to engineer multiparticle quantum systems with up to forty particles. The plasmonic lattice supports a large number of interactions that induce the formation of forbidden thermalization gaps. This novel quantum effect prevents the propagation of multiparticle states with certain statistical fluctuations.

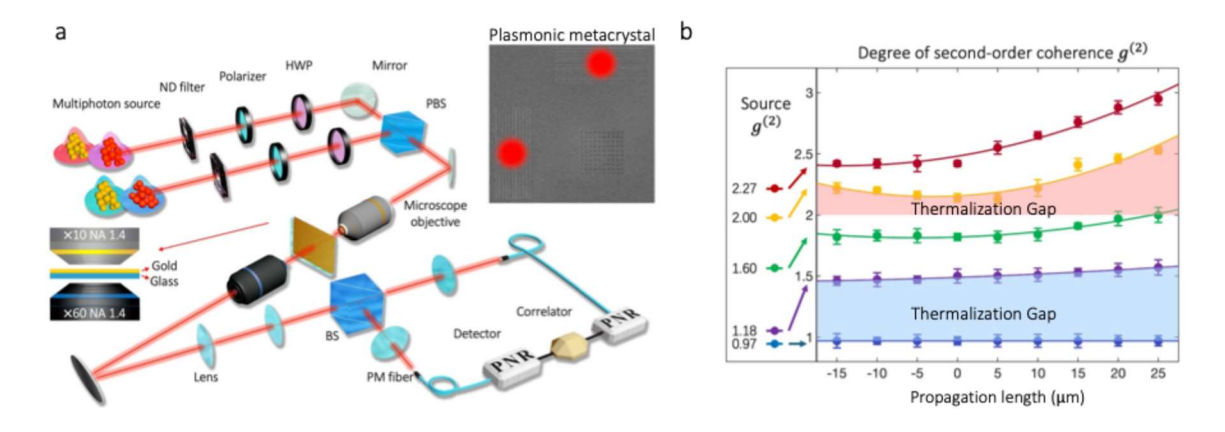


Figure 2. The experimental setup used to investigate thermalization gaps in quantum plasmonic metacrystals is illustrated in panel **a**. Two multiphoton sources are prepared in distinct polarization states using a polarizer and a half-wave plate (HWP). These sources are then combined via a polarizing beam splitter (PBS) and focused onto the two input ports of the plasmonic metacrystal, as shown in the inset of panel **a**. The transmitted multiphoton system is collected by a microscope objective and subsequently imaged using a tunable telescope, which allows measurements at different propagation planes of the plasmonic sample. The selected plane is directed through a beam splitter and analyzed using two photon-number-resolving (PNR) detectors. The metacrystal consists of one hundred plasmonic nanoantennas with varying orientations. Our experimental results are presented in panel **b**. The second-order degree of coherence of our multiphoton sources is shown in the left panel of **b**. Interestingly, the quantum statistical properties of the sources, which are not characterized by the eigenstatistics of the crystal, are modified by the crystal. These results demonstrate the first quantum statistical plasmonic metacrystal.

## **Future Plans**

We are preparing a manuscript on quantum statistical plasmonic metacrystals. This is the first platform that enables the engineering of multiphoton states across all known statistical regimes. Moreover, it represents the first demonstration of plasmonic lattices employed to implement photonic crystals sensitive to the quantum statistical properties of the light field.

#### References

- 1. M. Hong, R. B. Dawkins, C. You, and O. S. Magana-Loaiza, *Nonclassical near-field dynamics of plasmons*, Nature Physics **20**, 830-835 (2014). https://doi.org/10.1038/s41567-024-02426-y
- 2. M. Wubs, *Multiphoton quantum statistics from scattered classical light*, Nature Physics **20**, 689-690 (2024). <a href="https://doi.org/10.1038/s41567-024-02447-7">https://doi.org/10.1038/s41567-024-02447-7</a>
- 3. M. Hong, R. B. Dawkins, B. Bertoni, C. You, and O. S. Magana-Loaiza, *Isolating Bosonic, Fermionic, and Vacuum Dynamics of Plasmonic Waves*, Optics & Photonics News **35**, 27 (2024).
- 4. F. Mostafavi, M. Hong, R. B. Dawkins, J. Ferdous, R. Jin, C. You, and O. S. Magana-Loaiza, *Multiphoton quantum imaging using natural light*, Applied Physics Reviews **12**, 011424 (2025). <a href="https://doi.org/10.1063/5.0234062">https://doi.org/10.1063/5.0234062</a>

# Advanced in-situ analysis and ex-situ studies of 2D Hexagonal Boron Nitride and 2D Ferromegnets via Aberration-Corrected Scanning Transmission Electron Microscopy

#### **DE-SC0023224**

**PI:** Marija Drndic<sup>1</sup>, **Graduate student:** Rachael Keneipp<sup>1</sup>, **Unpaid collaborators:** Pia Bhatia<sup>1</sup>, Jordan Gusdorff<sup>2,3</sup>, and Lee Bassett<sup>3</sup>

The discovery of room-temperature single photon emission (SPE) in hexagonal boron nitride (hBN) launched it to the forefront of research as a promising platform for room-temperature quantum optics and

photonics. Room-temperature quantum emission centers in hBN exhibit single-photon emission and optically addressable spin states, as desired for many quantum technologies. Here we present our published<sup>1-3</sup> results and ongoing work funded by this DOE project. We created and characterized nanopores in hexagonal boron nitride (hBN) via aberration corrected scanning transmission electron microscopy (AC-STEM) drilling and photoluminescent (PL) spectroscopy. Defects on the sub-nanometer to nanometer scale are induced in hBN through electron irradiation and AC-STEM drilling<sup>1</sup>. Confocal PL spectroscopy is subsequently employed to characterize the optical activity of the defects created through electron irradiation and drilling.

The presented work is focused directly on the two-prong approach (*Thrust A* and *Thrust B*) funded by our BES QIS project (PI: Drndic) for advancing *in situ* and *operando* AC-TEM while investigating new phenomena in 2D hexagonal boron nitride (BN) and 2D ferromagnetic materials. These emerging 2D materials are interesting for the investigation of new fundamental phenomena including single-photo emission (hBN), studies and engineering of single-atom defects, room temperature ferromagnetism and nanostructure applications in quantum nanoelectronics, single-photon emission phenomena,

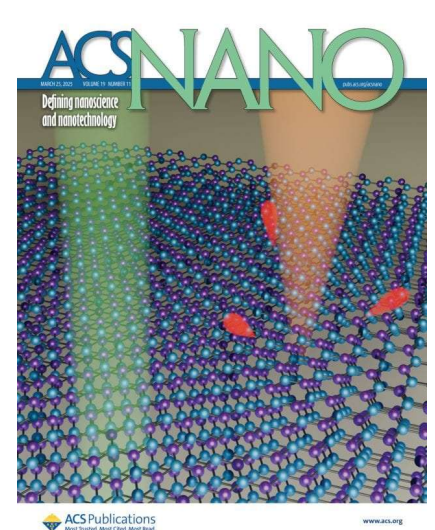


FIGURE 1. Cover art of ACS Nano illustrating optical probing of hBN films exposed to electron beams, as well as thermal annealing and oxygen plasma treatments.<sup>3</sup>

spintronics and quantum information processing. We prepared hBN samples compatible with confocal photoluminescence (PL) microscopy, transmission electron microscopy (TEM), and atomic-force microscopy (AFM), and we used those techniques to quantitatively investigate correlations between fluorescent emission, flake morphology, and surface residue. We find that the microscopy techniques themselves induce changes in hBN's optical activity and residue morphology: PL measurements induce photobleaching, whereas TEM measurements alter surface residue and emission characteristics. We also studied the effects of annealing and oxygen plasma cleaning on the structure and optical activity of hBN.

<sup>&</sup>lt;sup>1</sup>Department of Physics and Astronomy, University of Pennsylvania, Philadelphia, PA, USA

<sup>&</sup>lt;sup>2</sup>Department of Material Science and Engineering, University of Pennsylvania, Philadelphia, PA, USA

<sup>&</sup>lt;sup>3</sup> Department of Electrical and Systems Engineering, University of Pennsylvania, Philadelphia, PA, USA

We investigated two conventional methods for the transfer of 2D materials: viscoelastic stamping with polydimethylsiloxane (PDMS) and a heated transfer with poly bis-A carbonate (PC).<sup>2</sup> We characterized the resulting transfers using atomic force microscopy (AFM), aberration-corrected scanning transmission electron microscopy (AC-STEM) and electron energy loss spectroscopy (EELS). Both transfer methods yield flakes with significant and comparable residue.

We also present results on Iron Germanium Telluride (FGT), a magnetic van der Waals (vdW) material that has attracted significant interest due to its strong out-of-plane uniaxial magnetic anisotropy and high Curie temperature ( $T_c \sim 230 K$ ) relative to other vdW magnets. These properties make FGT an exciting candidate for spintronics applications. We probed the effects of geometric confinement on magnetic spin texture in FGT using low-temperature Lorentz transmission electron microscopy (LTEM), a powerful technique which enables direct observation of magnetic domains down to the nanometer scale. Our ongoing work elucidates the micromagnetic properties of geometrically confined FGT – a key step towards scalable spintronics technology.

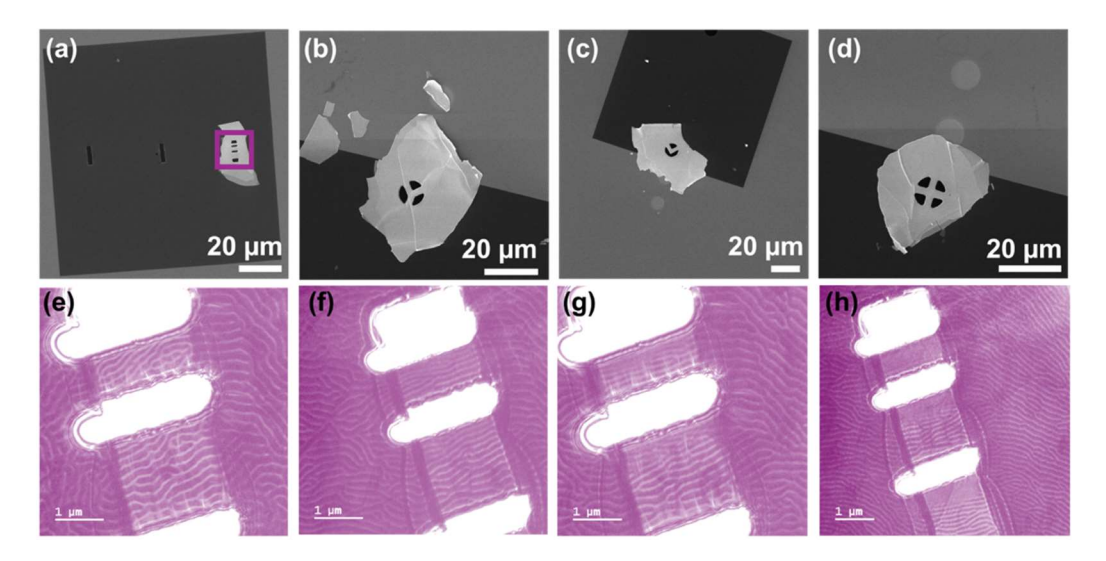


**FIGURE 2. Sculpted Fe<sub>3</sub>GeTe<sub>2</sub> flakes and corresponding LTEM data.** (a-d) Scanning electron microscope images of four devices that have been patterned using focused ion beam milling. (e-h) LTEM temperature series. All images were obtained with a 0.1043T field, 2 mm defocus, and -30° tilt. Panels e, f, g, and h were obtained at 95 K, 133 K, 149 K, and 193 K, respectively.

## **References:**

- (1) Keneipp, R. N.; Gusdorff, J. A.; Bhatia, P.; Shin, T. T.; Bassett, L. C.; Drndić, M. Nanoscale Sculpting of Hexagonal Boron Nitride with an Electron Beam. *J. Phys. Chem. C* **2024**, *128* (21), 8741–8749. https://doi.org/10.1021/acs.jpcc.4c02038.
- (2) Bhatia, P.; Shin, T. T.; Kavetsky, K.; Sailors, B. N.; Siokos, G.; Uy-Tioco, A. S.; Keneipp, R. N.; Gusdorff, J. A.; Bassett, L. C.; Drndić, M. A Tale of Two Transfers: Characterizing Polydimethylsiloxane Viscoelastic Stamping and Heated Poly Bis-A Carbonate Transfer of Hexagonal Boron Nitride. *Micron* **2025**, *189* (103747). https://doi.org/10.1016/j.micron.2024.103747.
- (3) Gusdorff, J. A.; Bhatia, P.; Shin, T. T.; Uy-Tioco, A. S.; Sailors, B. N.; Keneipp, R. N.; Drndić, M.; Bassett, L. C. Correlated Structural and Optical Characterization of Hexagonal Boron Nitride. *ACS Nano* **2025**, *19* (11), 11100–11110. https://doi.org/10.1021/acsnano.4c17676.

## Multiscale Quantum and Classical Microscopy for Superconducting Quantum Systems

**Award Number: ERKCK51** 

<u>Benjamin Lawrie</u>, Gábor Halász, Chengyun Hua, Petro Maksymovych, Matt Brahlek, Josh Damron, Sang Yong Song (pd), Yueh-Chun Wu (pd), and Nirjhar Sarkar (pd)

Oak Ridge National Laboratory

Abstract: The overarching goal of this project is to discover how charge and spin fluctuations and controlled disorder impact classical and quantum order parameters in magnetic and superconducting materials. In pursuit of this goal, two objectives are defined: (1) understand how local spin fluctuations become correlated across all length scales in magnetic systems under both equilibrium and out-of-equilibrium conditions and (2) unravel the interplay between superconductivity, magnetism, and disorder in unconventional (e.g., Fe-based) superconductors from atomic to millimeter length scales. We will address these objectives with a unique combination of spin-based quantum sensing, variable temperature quantum optical microscopies, nanoscale tunable Josephson junction and Andreev spectroscopies, and operando characterization of superconducting quantum devices. The demonstrated quantum advantage offered by our quantum microscopies will result in an unprecedented understanding of microscopic interactions in functional devices patterned from emerging quantum materials.

Over the past three years, we have made substantial advances in our understanding of the interactions between quantum sensors and magnetic and superconducting materials across a wide range of length scales. As shown in Fig. 1(a), we provided the first experimental demonstration of atomic-scale tunneling Andreev reflection (TAR) spectroscopy, and in doing so, we provided direct evidence of the sign-changing superconducting order parameter in FeSe and of the suppression of superconductivity along the nematic twin boundary<sup>1</sup>. We showed that incommensurate potentials can be used to manipulate vortex interactions and tune vortex lattice parameters in FeSe<sup>2</sup> as part of a first step toward the control of vortex

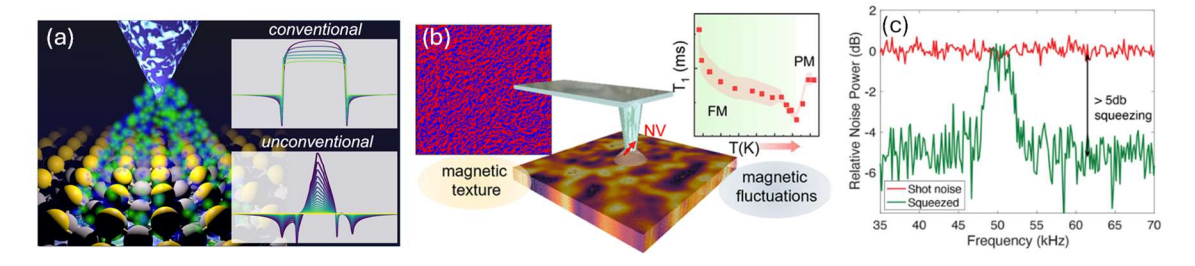


Fig. 1 (a) Schematic illustration of TAR spectroscopy on FeSe illustrating TAR spectra from conventional and unconventional superconducting order parameters<sup>1</sup>. (b) Illustration of nanoscale dc magnetic ordering (left) and temperature dependent NV relaxometry (right) as probes of spin interactions in magnetic thin films<sup>2</sup>. (c) First demonstration of squeezed magnetic circular dichroism measurements with quantum noise reduction 5 dB below the photon shot noise limit<sup>3</sup>.

interactions in superconducting quantum devices. As shown in Fig. 1(b), we used spin-based quantum sensors to unveil the universality class of a Sr<sub>2</sub>FeReO<sub>6</sub> thin film with a combination of temperature-dependent relaxometric probes of spin fluctuations and nanoscale dc magnetometry measurements<sup>3</sup>. And as shown in Fig. 1(c), we provided the first demonstration of magnetic circular dichroism measurements with a squeezed optical readout field<sup>4</sup>, a critical step toward non-perturbative quantum-enhanced squeezed vacuum measurements of Kerr rotation in materials that exhibit spontaneous time reversal symmetry breaking. Finally, we established a theoretical framework for understanding the effects of disorder on spin-triplet superconducting devices<sup>5</sup>, and we have recently shown that we can use nanoscale

helium-ion patterning to write quantum devices with controlled disorder in iron-based superconducting films.

Each of these quantum sensing modalities addresses a complementary length scale, but until now, each approach has been used in very different temperatures and magnetic fields on very different material systems. We have now established spin-based quantum sensing capabilities that function at temperatures of 50 mK-350K, we have recently shown that we can perform relaxometric probes of spin-defects in hBN in fields of up to 7T with no loss of contrast, and a new MSE-supported 1.4 K STM will allow for TAR spectroscopies to be performed on patterned devices in fields of up to 5 T. By integrating all of these approaches into a comprehensive suite of quantum sensors, we are now able to probe the interplay between superconductivity, magnetism, and disorder in unconventional (e.g., Fe-based) superconductor materials and to understand and control the effects of atomic-to-mesoscale disorder on the behavior of quantum devices patterned from these materials.

- 1. Ko, W., Song, S. Y., Yan, J., Lado, J. L. & Maksymovych, P. Atomic-Scale Andreev Probe of Unconventional Superconductivity. *Nano Lett.* **23**, 8310–8318 (2023). doi:10.1021/acs.nanolett.3c02658
- 2. Song, S. Y. *et al.* Nematically Templated Vortex Lattices in Superconducting FeSe. *Nano Lett.* **23**, 2822–2830 (2023). doi: 10.1021/acs.nanolett.3
- 3. Wu, Y.-C. *et al.* Nanoscale Magnetic Ordering Dynamics in a High Curie Temperature Ferromagnet. *Nano Lett.* **25**, 1473–1479 (2025). doi:10.1021/acs.nanolett.4c05401
- 4. Hua, C. *et al.* Quantum Enhanced Probes of Magnetic Circular Dichroism. *Adv. Quantum Technol.* **8**, 2300126 (2025). doi:10.1002/qute.202300126
- 5. Halász, G. B. Fractional magnetoresistance oscillations in spin-triplet superconducting rings. *Commun. Phys.* **6**, 1–8 (2023). doi:10.1038/s42005-023-01246-5

Modeling, probing, and controlling quantum coherence in materials FWP: SCW1674, DE-SC0020313

Diagnostics to deduce effects of impurities and electron correlations on quantum material systems

<u>Victor Brar</u><sup>1</sup>, Jennifer Choy<sup>1</sup>, Susan Coppersmith<sup>2</sup>, Mark Eriksson<sup>1</sup>, Mark Friesen<sup>1</sup>, Emily Joseph<sup>1</sup>, Shimon Kolkowitz<sup>3</sup>, Zach Krebs<sup>1</sup>, Roman Kuzmin<sup>1</sup>, Alex Levchenko<sup>1</sup>, Vincenzo Lordi<sup>4</sup>, Robert McDermott<sup>1</sup>, Keith Ray<sup>4</sup>, Leah Tom<sup>1</sup>, and Joel Varley<sup>4</sup>

<sup>1</sup>University of Wisconsin — Madison, <sup>2</sup>University of New South Whales, <sup>3</sup>University of California, Berkeley, <sup>4</sup>Lawrence Livermore National Laboratory

Abstract: In this collaborative QIS project our central aim is to gain a detailed understanding of the fundamental material origins of decoherence in superconducting and semiconducting quantum systems. These material limits originate from defects that are intrinsic to the materials used in fabrication, and also from particle interactions that drive new electronic phases that compete with superconductivity and can affect thermal transport. By combining theoretical efforts with advanced experimental methods, we aim to achieve the following goals: (i) Develop precise theoretical models that link microscopically observed defects to decoherence in quantum devices, (ii) Develop new types of probes that act as powerful diagnostic tools to identify sources of decoherence and eliminate them, (iii) Develop new quantum material and device platforms that exhibit advantages in fabrication and noise reduction, and also create new functional capabilities. Through systematic improvements in quantum materials, this effort will enable new qubit platforms to be created that exhibit much longer coherence times, higher gate fidelities, and improved thermal management.

A main thrust of our efforts has been in developing new scanned probe techniques that can visualize impurities in dielectrics and probe carrier dynamics in materials. We have shown how electrostatic force microscopy (EFM) can be coupled with density functional theory calculations to chemically identify individual near-surface impurities in dielectrics, identifying, for example, those caused by vacancies as well as from surface carbons. We have also advanced scanning tunneling potentiometry (STP) as a tool that can be utilized to directly image carrier flow in materials to quantify impurity scattering and el-el interactions.[1-3] In a third effort, a scanned Josephson junction technique was advanced that has the potential to perform quantum limited microwave absorption measurements at the nanoscale.[4] These measurements utilize high capacitance superconducting SPM tips to probe superconducting surfaces, creating a scannable Josephson junction spectrometer that can probe GHz-THz absorption with extremely high spectral sensitivity an spatial resolution.

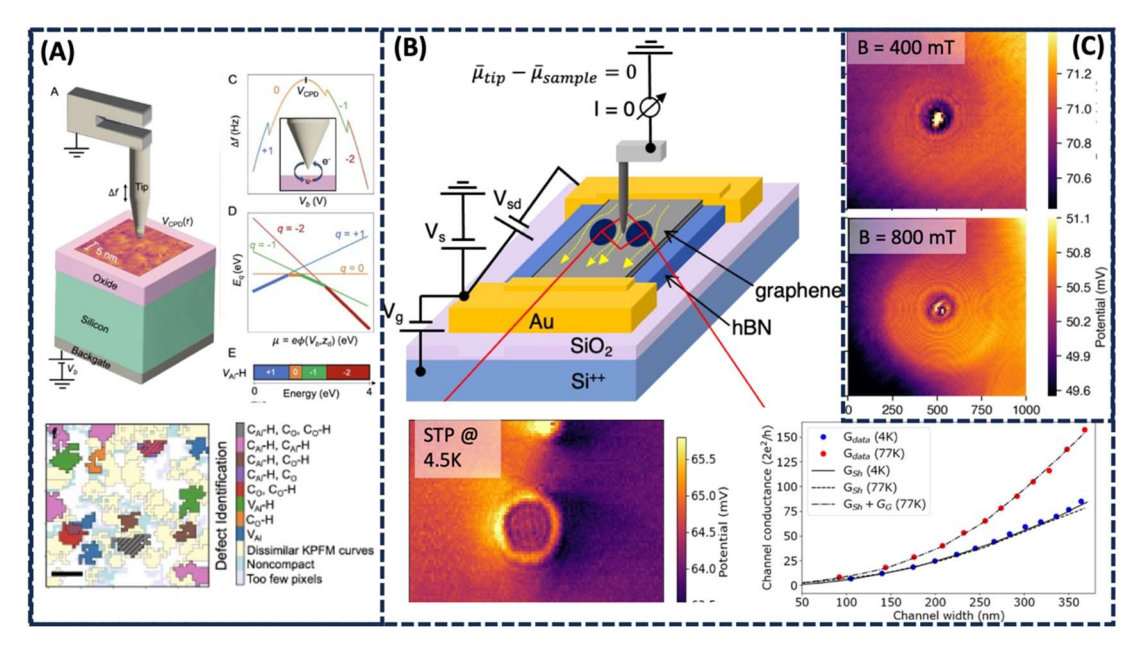


Figure 1: (A) Combined electrostatic force microscopy and DFT study localizing and chemically identifying impurities in Al<sub>2</sub>O<sub>3</sub>. (B) Scanning tunneling potentiometry (STP) study of carrier transport around electrostatic barriers in graphene. This work demonstrates how the carrier flow profile evolves as electron-electron interactions increase, driving phase transitions. Figure adapted from Ref. [2]. (C) STP study of magnetotransport in graphene near a circular barrier, revealing a transition from Ohmic behavior to quantum Hall transport. Figure adapted from Ref. [3].

A second aspect of this effort is to explore superconducting circuit architectures that allow for direct investigation of defects that drive dechoerence. These experiments include both flux tunable transmons, as well as multi-mode resonators composed of ~20,000 Josephson junctions that act as time domain spectrometers of two-level system dynamics. This latter technique works over a large bandwidth, including the operation frequencies of fluxonium qubits. Combined, these techniques have allowed us to quantify the effect of the junction oxide and deduce the role that liftoff residues play in qubit decoherence. These experiments are being performed in tandem with theoretical efforts that explore the effects of fluctuation-driven noise in superconductors, which can occur in thin superconducting films and narrow constrictions due to heating. [5]

[1] Li, S.; Levchenko, A.; Andreev, A. Hydrodynamic thermoelectric transport in Corbino geometry. *Physical Review B* **2022**, *105*, 125302. DOI: 10.1103/PhysRevB.105.125302

[2] Krebs, Z. J.; Behn, W. A.; Li, S.; Smith, K. J.; Watanabe, K.; Taniguchi, T.; Levchenko, A.; Brar, V. W. Imaging the breaking of electrostatic dams in graphene for ballistic and viscous fluids. *Science* 2023, 379, 671–676. DOI: 10.1126/science.abm6073

[3] Krebs, Z. J.; Behn, W. A.; Smith, K. J.; Fortman, M. A.; Watanabe, K.; Taniguchi, T.; Parashar, P. S.; Fogler, M. M.; Brar, V. W. Imaging the diffusive-to-ballistic crossover of magnetotransport in graphene. *arXiv*:2409.19468 **2024**. DOI: 10.48550/arXiv.2409.19468

[4] Fortman, M. A.; Harrison, D. C.; Rodriguez, R. H.; Krebs, Z. J.; Han, S.; Jang, M. S.; McDermott, R.; Girit, C. O.; Brar, V. W. Implementing Josephson Junction spectroscopy in a scanning tunneling microscope. *arXiv*:2410.03009 **2024**. DOI: 10.48550/arXiv.2410.03009

[5] Kwak, J.; Pellett, E.; König, E. J.; Levchenko, A. Fluctuation-driven excess noise near superconducting phase transition. *Annals of Physics* **2023**, *456*, 169307. DOI: 10.1016/j.aop.2023.169307

Prepared by LLNL under Contract DE-AC52-07NA27344

## DNA-Controlled Dye Aggregation – A Path to Create Quantum Entanglement DE-SC0020089

Molecular Devices to Create Entangled Exciton States and Molecular Dye Polymers for Quantum Entanglement and Quantum Circuits

<u>W. B. Knowlton</u>, a,b B. Yurke, a,b A. Supc, R. Elliota, J. Lee, a,d L. Li,a M. Ketteridge, a K. Duncan, a G. Barcenas, a O. A. Mass, D. Watt, a T. Azaz, K. Shaw, a T. Payne, G. Pascual, a S. Roy, a L. Patten, a D. B. Turner, a and R. D. Pensack

<sup>a</sup>Micron School of Materials Science and Engineering, <sup>b</sup>Department of Electrical and Computer Engineering, <sup>c</sup>Department of Physics, and <sup>d</sup>Department of Chemistry and Biochemistry, Boise State University, Boise, ID 83725; <sup>c</sup>CEM Corporation, Matthews, NC 28104

**Abstract**: Our group's <u>high-level goal</u> is to build molecular (dye) aggregate devices that create entangled exciton states at room temperature towards quantum gates and circuits. Our <u>near-term goal</u> is to synthesize oblique dimer dye aggregates and dye aggregate polymers (3-6 dyes in length). The former will be used to establish that electronic quantum beats can be observed in molecular aggregates. The latter will be used as excitonic transmission lines to build excitonic devices that create and control entangled exciton states at room temperature. DNA templates (nanobreadboards) will be used to route the polymer

dye aggregate transmission lines to form entanglement devices. Currently, we are on the verge of two groundbreaking achievements: demonstrating electronic coherence (decoherence time,  $\tau_d$ , beat frequency,  $\omega_h$ ) in dye aggregates and synthesizing dye polymer aggregates.

We limit our description of studies to those performed by 3 of the 5 highly integrated teams in our research group over the past 2 years. We identified dyes that have large dipole-dipole coupling energy, J, based on the transition dipole moment ( $\mu$ ) of each dye, resulting in dye aggregates exhibiting strong exciton delocalization. Theoretical work has been performed on two other understudied parameters fundamentally crucial for creating many-particle entangled states: (1) K (exciton-exciton interaction energy), to identify dyes capable of

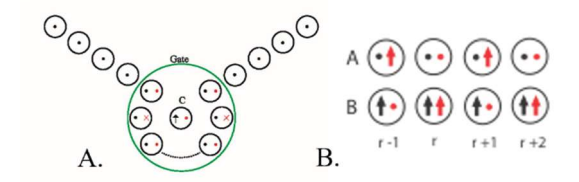


**Fig. 1**: Excitonic devices comprised of dye aggregate transmission lines that create exciton Bell states. **A.** An exciton transistor. **B.** Controlled phase shifter, a segment of a CNOT gate. Due to the arrangement of  $\mu$ 's and  $\Delta d$ 's, excitons cannot hop between transmission lines A and B but can only influence each other through the inter-row two-exciton coupling energy K. Note: Black circles represent dyes. Black dots represent  $\mu$ 's orthogonal to the plane of the figure. Black arrows represent  $\mu$ 's lying in the plane of the figure. Red dots represent  $\Delta d$ 's pointing out of the plane of page. Red x's are  $\Delta d$ 's pointing into the plane of the figure.

exhibiting large Ks (induced by the difference static dipole,  $\Delta d$ ) upon aggregation and (2) tuning the angle ( $\zeta$ ) between  $\mu$  and  $\Delta d$  within an individual dye to modify J and K in dye aggregates.

Two theoretically explored dye aggregate schemes to produce entangled exciton states were identified capable of producing maximally entangled states (Bell states). The first (**Fig. 1A**) consists of an exciton transistor-like configuration in which the absence or presence (0 or 1) of an exciton on the gate molecule C becomes entangled with whether n excitons (on the source-drain dye aggregate transmission line) remain at the source or are transferred to the drain. The second consists of a CNOT gate consisting of a circuit employing a controlled phase shifter (**Fig. 1B**) and two Haddamard gates which successfully converts a two-exciton product state into a Bell State. In both schemes, J enables excitons to propagate and K gives rise to the entanglement. Both schemes employ two types of dyes: one for which  $\mu$  and  $\Delta d$  are parallel and one for which they are orthogonal demonstrating the utility of having dyes with differing  $\zeta$ ,  $\mu$ , and  $\Delta d$ .

To construct the entanglement devices (Fig. 1), required are dyes with  $J_{m,n} \sim k_b T$ , low electronic-vibrational coupling (Huang-Rhys factor [RH]), and tunable  $\zeta$ ,  $\mu$ , and  $\Delta d$  that can be arranged linearly to form transmission. One such group of dyes are bacteriochlorins (Bchl - found in green and purple bacteria) and chlorins (Chl – found in green plants), of which chlorophyll is a subset. We synthesized synthetic Bchl and Chl monomers with the lowest RH of all dyes we have studied and synthesized) and some tunability of  $\zeta$ ,  $\mu$ , and  $\Delta d$ .<sup>3, 4</sup> Towards transmission lines, our group is using two approaches – one involves using DNA-templates to form dye aggregates and the other involves using rigid nonconjugating bridges. Here, we focus on the nonconjugating bridge approach. Nonconjugating bridging enables tuning of distance and orientation, thus J, between monomers and imparts greater rigidity to the dye aggregate effectively suppressing detrimental vibrational modes. We have demonstrated a simple clickchemistry approach for nonconjugating bridging of three different synthetic Bchl monomers used to form two different oblique (90° between dye's  $\mu$ 's) heterodimer dye transmission lines.<sup>5</sup> Oblique dimers are quite rare as compared to J- ( $\mu$ 's end-to-end) and H-dimers ( $\mu$ 's cofacial). Dipole-dipole coupling between the two dyes in the oblique dimer results in Davydov splitting of the monomer absorption

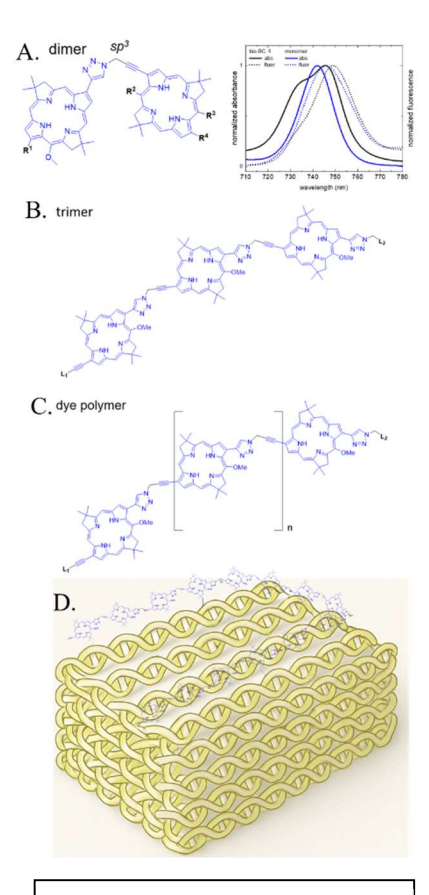


Fig. 2: A. Oblique Bchl homodimer and absorbance (& fluorescence) showing Davydov splitting as compared to the monomer. B. Trimer Bchl currently being synthesized. C. polymer dye aggregate. D. routing of a polymer dye aggregate using a DNA brick "nanobreadboard" - 3D routing possible (DNA AI created).

peak into two new excited states with equal electronic oscillator strengths; thus, they are ideal candidates for the direct measurement of  $\tau_d$  and  $\omega_h$ . Our latest effort has resulted in two additional oblique dimers – a third Bchl heterodimer and a Bchl homodimer (**Fig. 2A**), both of which show Davydov splitting with near equivalent and 99% electronic oscillator strengths and  $J_{m,n} \sim k_b T$ . We are in the process of synthesizing a trimer transmission line (**Fig. 2B**) with near future work focused on synthesizing long polymer aggregates (**Fig. 2C**) and their routing via DNA templated (**Fig. 2D**) nanobreadboards enabling quantum entanglement devices (**Fig. 1**) as well as quantum gate devices and light harvesting systems.

References: <sup>1</sup>A. Sup *et al.*, *Phy. Rev. A* **110** 022616 (2024). doi: 10.1103/PhysRevA.110.022616; <sup>2</sup>B. Yurke *et al.*, *Phy. Rev. A* **107**, 012603 (2023). doi: 10.1103/PhysRevA.107.012603; <sup>3</sup>M. Ketteridge *et al.*, *J Phys.* 

*Chem. A* 128, 7581 (2024). doi: 10.1021/acs.jpca.4c03821; <sup>4</sup>O. Mass, *Phys. Chem. Chem. Phys.* 25, 28437 (2023). doi: 10.1039/D3CP01634J; <sup>5</sup>T. Azaz *et al.*, in review *Organic Letters* (May 24, 2025). doi: N/A

## Direct Observation of Fractional Quantum Hall Quasiparticle Braiding Statistics via Interferometry

## DOE QIS DE-SC0020138

#### PI Michael J. Manfra

Affiliation: Dept. of Physics and Astronomy, Purdue University, West Lafayette, Indiana

Utilizing recent advances in materials design and anyon interferometry generated under DOE BES QIS funding DE-SC0020138, we report on new set of interferometric and controlled anyon manipulation experiments. Our ultimate goal is to demonstrate the operation of a topologically protected qubit constructed from the non-Abelian fractional quantum Hall state at n=5/2. Our project aims to realize a fundamentally new qubit platform with "built-in" protection from decoherence and provide unambiguous experimental confirmation of a long-sought phase of matter supporting non-Abelian anyons. Here we report on a series of novel experiments in which we first demonstrate the existence and controlled manipulation of Abelian anyons in the fractional quantum Hall regime.

Our most recent results have demonstrated the successful extension of Fabry-Perot interferometry to measure effective charge and braiding statistics at n=2/5, a complex higher order FQHE state with multiple circulating edge modes, effective charge  $e^*=1/5e$ , and anyonic statistical angle  $J_a=4p/5$  [1]. This result provides a necessary steppingstone to investigate interferometry at the non-Abelian n=5/2 state, where the presence of multiple edge modes, small bulk excitation gap, and small effective charge  $e^*=1/4e$  will make studies more difficult than at the primary Laughlin state at n=1/3. Fig. 1 shown below displays interference data for the inner mode with charge  $e^*=1/5e$  at n=2/5 [1]. We have also recently exploited our device design to demonstrate that the fractionalized edge modes behave as chiral Luttinger liquids as originally predicted by X. G. Wen nearly 40 years ago. Our new data is the first to show a robust tunneling exponent g and proper scaling behavior for the *tunneling of anyons* across a narrow constriction form by a quantum point contact within our interferometer design [2]. Along with our measurements of effective charge and anyonic statistics at n=1/3, measurement of the tunneling exponent g=1/3 completely parameterizes the topological order at n=1/3 and identifies the universality class of the ground state wavefunction (see Fig. 2 below).

Most recently we have designed and implemented a fundamentally new screening quantum heterostructure to interferometric measurements at the fragile non-Abelian n=5/2 state. These new heterostructures place *screening electrons in AlAs quantum wells* to provide the necessary screening while maintaining high mobility and high 2DEG density in the primary quantum well necessary to support the n=5/2. We are optimistic that incisive experiments are now feasible given our recent advances in understanding and control of quantum Hall interferometry, new advances in heterostructure design and device fabrication, and recently added measurement capabilities.

- [1] Fabry-Perot Interferometry at the n=2/5 Fractional Quantum Hall State PRX 13, 041012 (2023)
- [2] Universal Anyon Tunneling in a Chiral Luttinger Liquid, arXiv: 2502.20551, under review Nat. Phys.)

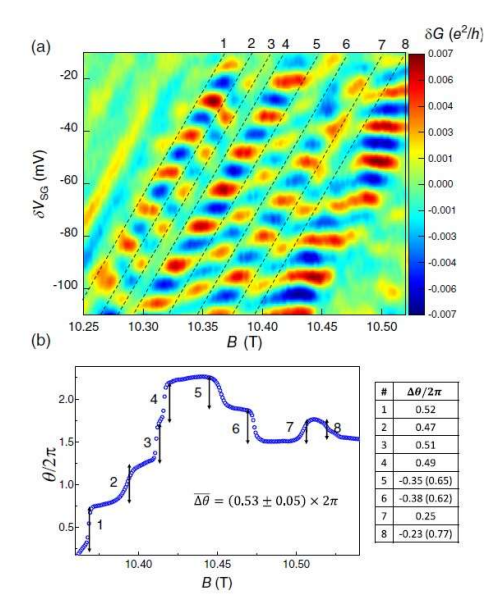


Fig. 1: (a) Conductance versus side gate voltage and magnetic field for the inner mode at v=2/5 with dashed lines indicating the positions of discrete jumps in phase. (b) Phase extracted via Fourier transform vs. magnetic field. These data indicate an anyonic phase of  $4\pi/5$ .

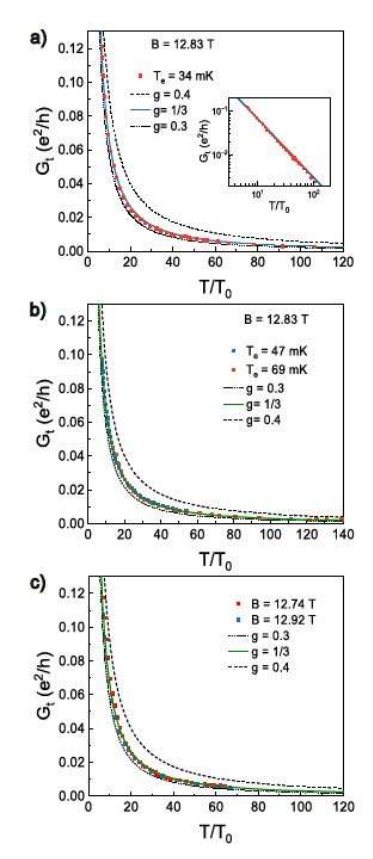


Fig. 2: (a) Scaling of zero bias tunneling conductance at T=34mK and B=12.83 T, at the center of the v=1/3 plateau. (b) Scaling of zero bias tunneling conductance at T=47mK and T=69mK, at the center of v=1/3. (c) Scaling of zero bias tunneling conductance at B=12.92T and B=12.74T, +/- 90mT away from the center of the plateau.

## Mapping the genome of coherent quantum defects for Quantum Information Science DE-SC0022289

## Stark shift effects from first principles in quantum defects

S. Griffin<sup>1</sup>, L. Alaerts<sup>2</sup>, Y. Xiong<sup>2</sup>, G. Hautier<sup>2,3</sup>

<sup>1</sup>LBNL, <sup>2</sup>Dartmouth College, <sup>3</sup>Rice University,

**Abstract:** The operation of spin qubits in quantum networks requires long spin but also optical coherence. Optical coherence is limited by the interaction of color centers with electrical fields. Electrical fields around the quantum defects from surfaces or other impurities can shift the emission wavelength (the zero-phonon-line, ZPL) through a Stark shift leading to spectral diffusion. Characterizing the Stark shift of quantum defects is of importance for designing spectrally-stable defects or to understand how to mitigate the spectral diffusion through active control.

While first principles computations have been used to understand and compute many defect properties (e.g., emission wavelength, Debye-Waller, ...), the Stark shift of color centers has not been commonly computed and diverging values are available in the literature. We report on a study of the Stark shift effect of the NV center in diamond through a slab technique as well as Modern Theory of Polarization. We show that the two techniques agree, outline a methodology to obtain these values and provide computed values of Stark shift that we estimate as a change in dipole moment between excited and ground state of 2.68 to 2.23 Debye (depending on the level of theory).

Building on our benchmark on the NV center in diamond, we also present some recent results on the T center in silicon. The T center is a doublet color center made of carbon and hydrogen and has emerged as the main spin qubit defect in silicon.<sup>2-4</sup> The defect-bound exciton nature of the excited state of the T center brings interesting question on the physical nature of the Stark shift as well as technical challenges. We have computed this Stark shift for the T center and estimate a change in dipole of around 0.79 Debye and oriented along the C-H direction. We highlight the importance of second order (polarizability) effects in bound excitons and compare our results to recent experimental data.<sup>5</sup>

- 1. Alaerts, L., Xiong, Y., Griffin, S. & Hautier, G., "First-principles study of the Stark shift effect on the zero-phonon line of the NV center in diamond," *Phys Rev Mater* **8**, 106201 (2024). DOI: 10.1103/PhysRevMaterials.8.106201
- 2. Bergeron, L., Chartrand, C., Kurkjian, A. T. K., Morse, K. J., Riemann, H., Abrosimov, N. V, Becker, P., Pohl, H.-J., Thewalt, M. L. W. & Simmons, S., "Silicon-Integrated Telecommunications Photon-Spin Interface," *PRX Quantum* 1, 20301 (2020). DOI: 10.1103/PRXQuantum.1.020301
- 3. Higginbottom, D. B., Kurkjian, A. T. K., Chartrand, C., Kazemi, M., Brunelle, N. A., MacQuarrie, E. R., Klein, J. R., Lee-Hone, N. R., Stacho, J., Ruether, M., Bowness, C., Bergeron, L., DeAbreu, A., Harrigan, S. R., Kanaganayagam, J., Marsden, D. W., Richards, T. S., Stott, L. A., Roorda, S., Morse, K. J., Thewalt, M. L. W. & Simmons, S., "Optical observation of single spins in silicon," *Nature* **607**, 266–270 (2022). DOI: 10.1038/s41586-022-04821-y
- 4. Dhaliah, D., Xiong, Y., Sipahigil, A., Griffin, S. M. & Hautier, G., "First-principles study of the T center in silicon," *Phys Rev Mater* **6**, L053201 (2022). DOI: 10.1103/PhysRevMaterials.6.L053201
- 5. Clear, C., Hosseini, S., AlizadehKhaledi, A., Brunelle, N., Woolverton, A., Kanaganayagam, J., Kazemi, M., Chartrand, C., Keshavarz, M., Xiong, Y., Soykal, O. O., Hautier, G., Karassiouk, V., Thewalt,

M., Higginbottom, D. & Simmons, S., "Optical transition parameters of the silicon T centre," (2024). DOI: 10.1103/PhysRevApplied.22.064014

## **Next-Generation Parametrically-Induced Quantum Engineering (PIQUE 2.0)**

Award Number: DE-SC0019461

Names of PI, coPI(s), and unpaid collaborators: <u>Archana Kamal</u><sup>1,2</sup>, Leonardo Ranzani<sup>3</sup>, Guilhem Ribeill<sup>3</sup>, Luke Govia<sup>3</sup>, Raymond Simmonds<sup>4</sup>, Jose Aumentado<sup>4</sup>, Zhihao Xiao<sup>1</sup>, Taewan Noh<sup>1,4</sup>, Emery Doucet<sup>1</sup>, Tristan Brown<sup>1,3</sup>, and Tarush Tiwari<sup>1,3</sup>

University of Massachusetts Lowell<sup>1</sup>, Northwestern University<sup>2</sup>, RTX BBN Technologies<sup>3</sup>, NIST Boulder<sup>4</sup>

#### Abstract:

This program aims to develop and demonstrate novel functionalities for **creation**, **control and characterization** of quantum states under a unified framework, which we refer to as PIQUE (Parametrically-Induced QUantum Engineering). Building and extending the results and unique insights generated in first-generation PIQUE (Parametrically-Induced QUantum Engineering) program, in the next-generation PIQUE program, we employed strong and tunable parametric interactions for fast, scalable and robust state preparation and control of open quantum systems. We committed to a co-design approach by developing theoretical framework and protocol design closely informed by near-term experimental modalities: specifically, use of linear dissipation and tunable couplings via parametrically-activated sideband interactions between transmons and a lossy oscillator, demonstrated in the first generation of PIQUE program. Beyond PIQUE, the new quantum control functionalities and techniques enabled by this program have already spurred several theoretical and experimental follow-up works by the superconducting circuits community.

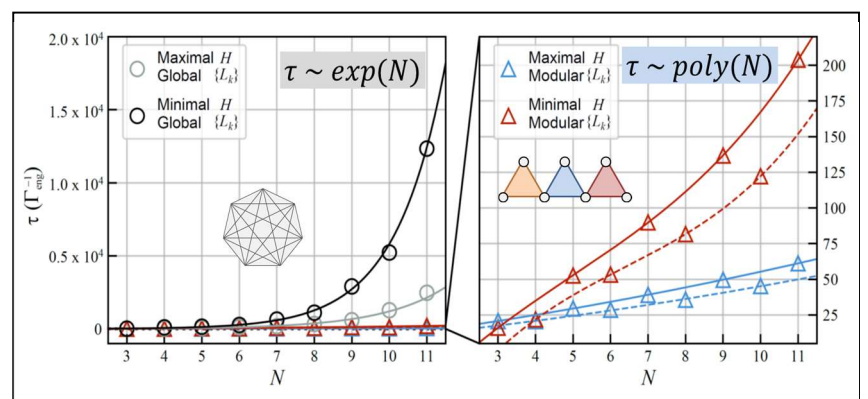


Figure 1: Stabilization time vs system size (*N*) for global (left) vs modular (right) dissipation-engineered protocols for N-qubit W-state entanglement generation. The insets shows the all-to-all vs modular dissipative coupling graph for *N*=7 protocol

In this program, we developed the first reservoir-engineered entanglement stabilization protocols that exhibit a concurrent scaling of steadystate fidelity and speed allowing a simultaneous reduction of preparation error and time [1]. Crucially, we found that using several overlapping modular dissipators (instead of a single global dissipator) can allow an exponential improvement in stabilization performance, with the stabilization time growing according to some low-degree

polynomial in the system size system size (N) for fixed amplitude drives [4] (Figure 1). Remarkably, such modular architectures allow use of bounded-depth interactions and only O(N) resources [i.e. number of dissipative and unitary drives] for stabilizing an N-qubit entangled state making such protocols both "modular" and "scalable". Further, straightforward extensions to high-dimensional entanglement is possible by using parametric drives on successive qudit levels for the stabilization of AME (2, m) state (with 1 < m < N).

We have also introduced the paradigm of "parametric circuit-QED" where similar architectures, but now pumped with off-resonant parametric drives can realize large dispersive shifts, which are *in-situ* tunable in sign and magnitude, support exact decoupling or "blind spots" [2], and frequency-selective multi-qubit

readout [3]. We developed an ab-initio theoretical framework based on sequential time-dependent Schrieffer-Wolff transformations that enables analytical calculation of dispersive shifts for strong parametric interactions (Figure 2).

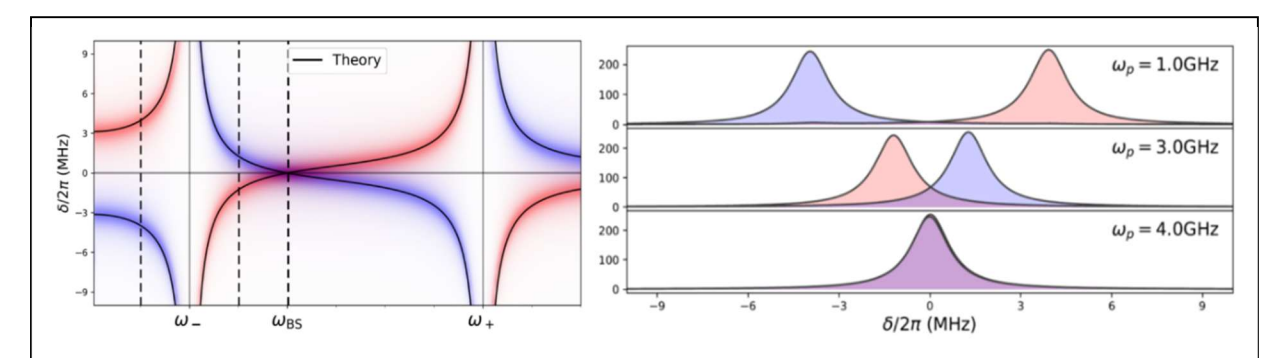


Figure 2: Comparison of analytical results for dispersive shift on resonator obtained using time-dependent Schrieffer-Wolff technique (black curves), with the resonator spectrum obtained from exact numerical simulations of the time-dependent Rabi model (color). Blue (red) correspond to profiles obtained for qubit in ground (excited) state. The line cuts show, negative and zero dispersive shifts tunable via choice of interaction frequency set by the pump  $\omega_p$ 

#### **References:**

[1] T. Brown, E. Doucet, D. Riste, G. Ribeill, K. Cicak, J. Aumentado, R. W. Simmonds, L. C. G. Govia, A. Kamal, L. Ranzani. *Trade off-free entanglement stabilization in a superconducting qutrit-qubit system*, **Nature Communications** 13, 3994 (2022)

[2] Z. Xiao, E. Doucet, T. Noh, L. Ranzani, R. W. Simmonds, L. C. G. Govia, A. Kamal. *Perturbative diagonalization for time-dependent strong interactions*, **Phys. Rev. Applied** 18, 024009 (2022)

[3] T. Noh, Z. Xiao, K. Cicak, X. Y. Jin, E. Doucet, J. Teufel, J. Aumentado, L. C. G. Govia, L. Ranzani, A. Kamal, R. W. Simmonds. *Strong parametric dispersive shifts in a statically decoupled multi-qubit cavity QED system*, **Nature Physics**, s41567-023-02107-2 (2023)

[4] E. Doucet, L. C. G. Govia, A. Kamal. *Scalable entanglement stabilization with modular reservoir engineering*, arXiv:2301.05725, doi.org/10.48550/arXiv.2301.05725 (2023)

## **Planar Systems for Quantum Information**

#### DE-SC0019481

Kaifei Kang<sup>1</sup>, Bowen Shen<sup>1</sup>, Yichen Qiu<sup>2</sup>, Yihang Zeng<sup>2</sup>, Zhengchao Xia<sup>1</sup>, Kenji Watanabe<sup>3</sup>, Takashi Taniguchi<sup>3</sup>, **Allan H. MacDonald**<sup>4</sup>, **Jie Shan**<sup>1,2,5</sup>, and **Kin Fai Mak**<sup>1,2,5</sup>

**Abstract:** The scope of this research program is to develop 2D moiré materials as a quantum simulator to implement model Hamiltonians and their phase diagrams and dynamics. Specifically, we aim to (i) develop homogeneous moiré materials with controllable superlattice potential for quantum simulation; (ii) develop methods for continuous tuning of moiré parameters, including length and energy scales, and charge density; (iii) experimentally map the equilibrium quantum phase diagram of model many-body Hamiltonians such as the Hubbard models and compare with theory; and (iv) develop methods to dynamically control the many-body Hamiltonians and investigate non-equilibrium quantum dynamics.

The emergence of 2D moiré materials has opened a new platform to explore quantum phases of matter that arise from electronic topology and correlations. In particular, twisted transition metal dichalcogenides (TMDs) in the AA-stacking structure form a honeycomb moiré lattice with two sublattice sites residing in separate TMD layers. The topmost moiré valence bands, originated from the K- and K'-valley states of the monolayer TMDs, are spin-split and spin-valley locked by a large Ising (out-of-plane) spin-orbit field, which defines the spin quantization axis. It was first predicted by our team member from the continuum model band structure calculations that flat Chern bands with spin/valley-contrasting Chern numbers emerge in small-angle tTMDs as a result of skyrmion-like interlayer hopping<sup>1</sup>. Recent experiments<sup>2</sup>, including one from our team, have demonstrated both an integer Chern insulator at moiré band filling factor  $\nu = 1$  and fractional Chern insulators at  $\nu = 3/5$  and 2/3 in tMoTe2 under zero magnetic field.

In this work, we report transport evidence of a fractional quantum spin Hall (QSH) insulating state in 2.1-degree-twisted bilayer MoTe<sub>2</sub>, which supports spin-S<sub>z</sub> conservation and a series of Landau-level-like flat Chern bands<sup>3</sup>. QSH insulators are 2D electronic materials that have a bulk band gap like an ordinary insulator but have topologically protected pairs of edge modes of opposite chiralities. Previous experiments have found only integer QSH insulators with counter-propagating up-spins and down-spins at each edge leading to a quantized conductance  $G_0 = e^2/h$  (with e and h denoting the electron charge and Planck's constant, respectively). We perform both local and local transport measurements (Fig. 1). At filling factor v = 3 of the moiré valence bands, each edge contributes a conductance 3/2  $G_0$  with zero anomalous Hall conductivity. Further, at v = 2, 4, and 6, we observe a single, double and triple QSH insulator with each edge contributing a conductance  $G_0$ ,  $G_0$  and  $G_0$ , respectively. Our results open the possibility of realizing time reversal symmetric non-abelian anyons and other unexpected topological phases in highly tunable moiré materials.

<sup>&</sup>lt;sup>1</sup> School of Applied and Engineering Physics, Cornell University, Ithaca, NY, USA; <sup>2</sup> Department of Physics, Cornell University, Ithaca, NY, USA; <sup>3</sup> National Institute for Materials Science, Tsukuba, Japan; <sup>4</sup> Department of Physics, University of Texas at Austin, TX, USA; <sup>5</sup> Kavli Institute at Cornell for Nanoscale Science, Ithaca, NY, USA

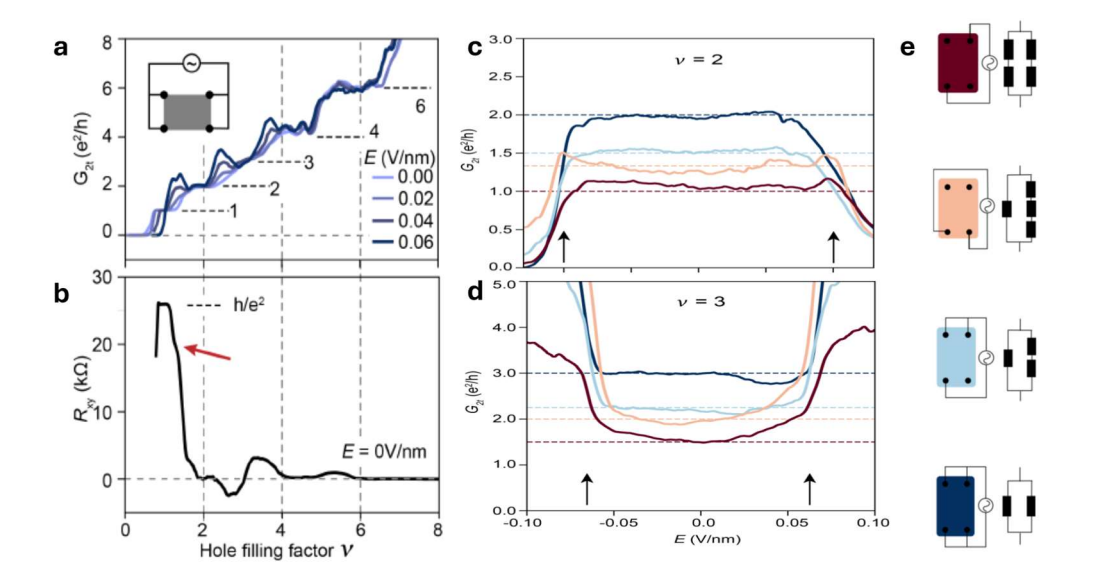


Figure 1. Integer and fractional quantum spin Hall effect in 2.1-degree twisted bilayer MoTe<sub>2</sub>. **a,b**, Hole filling factor dependence of two-terminal conductance (**a**) and Hall resistance (**b**) at 20 mK for representative electric fields in the layer-hybridized regime. The two-point conductance is quantized at  $\nu G_0$  while the Hall resistance is nearly zero for  $\nu = 2, 3, 4$  and 6. **c,d**, Out-of-plane electric-field dependence of two-terminal conductance for different measurement configurations around  $\nu = 2$  (**c**) and  $\nu = 3$  (**d**). Dashed lines denote the predicted values from the Landauer-Büttiker analysis. **e**, Two-terminal nonlocal measurement configurations (left) and equivalent circuits (right) for helical edge mode transport. The shaded rectangles represent twisted bilayer MoTe<sub>2</sub> with four contacts (black dots). Unconnected dots are floated contacts. The shade color matches the line color in **c,d**.

## **References:**

- 1. F. Wu, T. Lovorn, E. Tutuc, I. Martin and A.H. MacDonald, "Topological insulators in twisted transition metal dichalcogenide homobilayers," *Phys. Rev. Lett.* **122**, 086402 (2019).
- 2. L. Ju, A.H. MacDonald, K.F. Mak, J. Shan and X. Xu, "The fractional quantum anomalous Hall effect," *Nat. Rev. Mater.* **9**, 455-459 (2024).
- 3. K. Kang, B. Shen, Y. Qiu, Y, Zeng, Z. Xia, K. Watanabe, T. Taniguchi, J. Shan and K.F. Mak, "Observation of the fractional quantum spin Hall effect in moiré MoTe<sub>2</sub>," *Nature* **628**, 522–526 (2024).

## Multiscale Quantum and Classical Microscopy for Superconducting Quantum Systems Award Number: ERKCK51

## Disorder-enabled control of superconducting devices

## Gábor Halász, Nirjhar Sarkar (pd), Chengyun Hua, and Benjamin Lawrie

## Oak Ridge National Laboratory

**Abstract:** The primary goal of this thrust is to understand and control the interplay between disorder and superconductivity on the device scale. The key phenomenon that we aim to control through disorder is vortex tunneling across a narrow superconducting strip in a mesoscopic loop (i.e., Little-Parks) geometry. Theoretically, we study the relevant vortex-tunneling processes via Ginzburg-Landau equations in the one-dimensional limit or the London limit. Experimentally, we fabricate mesoscale superconducting rings of Little-Parks geometry using conventional electron-beam lithography patterning techniques to show integer / fractional magnetoresistance oscillations in Nb and  $Pd_3Bi_2Se_2$ . An unconventional direct ion-writing fabrication technique has also been developed to obtain cleaner devices.

Over the past three years, we theoretically established universal signatures of unconventional spin-triplet superconductors that are observable on the device scale. Spin-triplet superconductors are interesting from the fundamental perspective and because they host half-quantum vortices that are predicted to bind Majorana zero modes. The signatures we proposed directly reflect the tunneling of such half-quantum vortices, thereby revealing not only the unconventional superconducting state but also the Majorana zero modes that may allow topological quantum computing.

We primarily focused on the Little-Parks effect – a key hallmark of superconductivity that results from the macroscopic quantum coherence of Cooper pairs. Due to fluxoid quantization, the resistance of a mesoscale superconducting ring oscillates as a function of the magnetic flux going through the ring. For a conventional

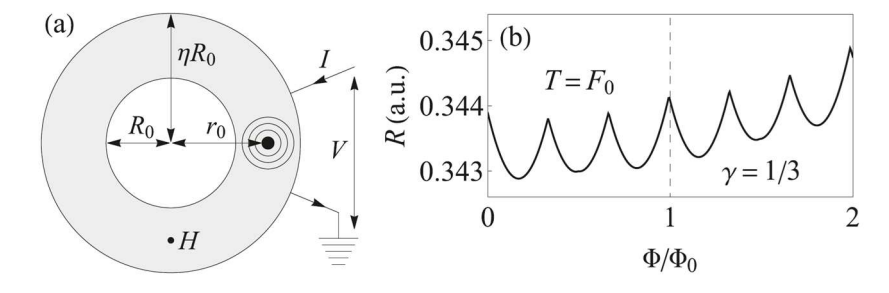


Figure 1: (a) Schematic illustration of the mesoscopic Little-Parks setup with a vortex (bullseye) tunneling across the superconducting ring<sup>1</sup>; the voltage V resulting from a bias current I is measured. (b) Disorder-induced Little-Parks oscillations with fractional periodicity  $\Delta \Phi = \Phi_0 / 3$  in the resistance R = V / I against the flux  $\Phi$  through the loop.

(spin-singlet, s-wave) superconductor, the Little-Parks oscillation periodicity is given by the flux quantum  $\Phi_0 = h / 2e$ , and the minima of the resistance correspond to integer multiples of  $\Phi_0$ . Unconventional superconductors may exhibit different kinds of Little-Parks oscillations. For example, in gapless superconductors with d-wave pairing, the Little-Parks oscillations acquire an enlarged periodicity  $2\Phi_0$ , while polycrystalline spin-triplet superconductors feature shifted Little-Parks oscillations with the resistance minima corresponding to half-integer multiples of  $\Phi_0$ .

In our theoretical work<sup>1</sup>, we showed that, for a range of temperatures in the presence of disorder, spin-triplet superconductors exhibit unconventional Little-Parks oscillations with an emergent fractional periodicity  $\Phi_0$  / n, where the integer  $n \ge 3$  is entirely determined by the ratio of the spin and charge superfluid densities.

For a different temperature range studied in another theoretical work<sup>2</sup>, it was found that the Little-Parks oscillation periodicity remains  $\Phi_0$ , but each maximum is split into two distinct peaks, with the peak width and peak separation following distinctive scaling laws as a function of temperature. These novel features in the Little-Parks effect all reflect the existence of half-quantum vortices that are exclusive to spin-triplet superconductors. Current efforts<sup>3</sup> aim to understand how the same half-quantum vortices may be revealed in color-center relaxometry, which ties this thrust to other parts of the project.

Experimental challenges in Little-Parks measurements lie in fabricating superconducting nano-rings without introducing significant sidewall damage that suppresses superconductivity, broadens transitions, and introduces uncontrolled vortex leakage paths, resulting in noisy oscillations with poor signal-to-noise ratios. This effect was observed during our experimental work on  $Pd_3Bi_2Se_2$  and Nb. Therefore, we developed focused ion beam (FIB) patterning techniques using helium/xenon ions with sub-2 nm resolution. This technique selectively converts superconducting regions to normal states through controlled ion implantation rather than material removal, preserving pristine current paths while creating well-defined boundaries. FIB patterning has successfully fabricated high-quality Josephson junctions in various superconductors and could potentially enable reproducible Little-Parks devices with enhanced signal quality. This approach also enables engineering of  $0-\pi$  junctions for topological qubits and SQUIDs as well as superconducting nanowire single-photon detectors, an opportunity that we are just beginning to explore.

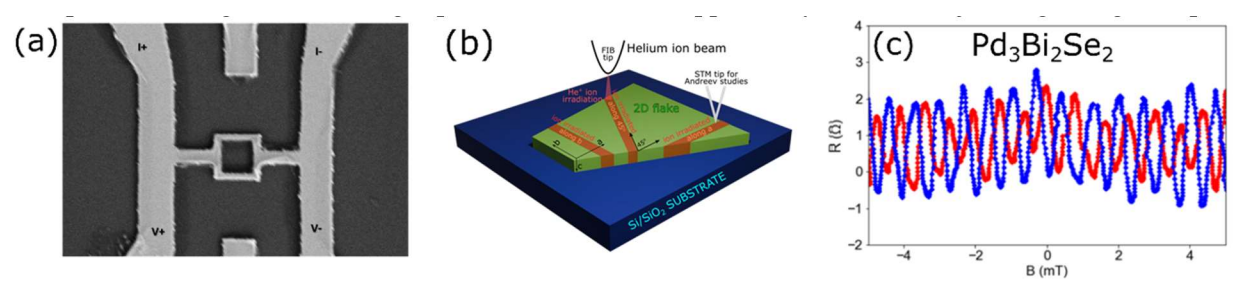


Figure 2: (a) Superconducting Nb nano-ring for Little-Parks measurements from standard electron-beam lithography and reactive ion etching. (b) Schematic sketch of FIB patterning with helium/xenon ions. (c) Little-Parks oscillations in Pd<sub>3</sub>Bi<sub>2</sub>Se<sub>2</sub>.

- 1. Halász, G. B. Fractional magnetoresistance oscillations in spin-triplet superconducting rings. *Commun. Phys.* **6**, 1–8 (2023).
- 2. Hua, C., Dumitrescu, E. & Halász, G. B. Theory of the Little-Parks effect in spin-triplet superconductors. *Phys. Rev. B* **107**, 214503 (2023).
- 3. Halász, G. B. et al. in preparation (2025).

## Project Title: Optical Information Processing Through Jointly-Optimized Diffractive Surfaces and Electronic Neural Networks

Award Number: DE-SC0023088

Name of PI and unpaid collaborators: Md Sadman Sakib Rahman, Tianyi Gan, Emir Arda Deger,

Çağatay Işıl, Mona Jarrahi, and Aydogan Ozcan

Affiliation: UCLA, Los Angeles, CA

Abstract: In this project, we are exploring the science at the intersection of AI, materials science and optics/photonics to harness the diffraction of light through structured materials composed of trainable surfaces (forming a 3D structured volume) that collectively execute a desired computational task, not achievable with standard optical design principles. These diffractive systems form optical processors that are passive (no external power), and operate at the speed of light, calculating the desired solution as the input light propagates through a thin physical diffractive system trained for a specific task. Benefiting from the scalability and parallelism of optics, diffractive processors and materials that are trained using, e.g., deep learning, create task-specific computational imagers, sensors and machine vision systems with various new capabilities. In this project, we have been investigating the information processing capacity of trainable diffractive surfaces, to inquire a deeper understanding of the limits of their computational capabilities [1-3].

Optical information processors created by trainable diffractive surfaces that are used as the frontend or back-end of electronic neural networks form hybrid information processing units. One of our
accomplishments [1] on the topic of jointly optimized collaborations between electronic neural networks
and diffractive surfaces was on learning diffractive optical communication of information around arbitrary
opaque occlusions. We demonstrated an optical architecture for directly communicating optical information
of interest around zero-transmittance occlusions using electronic encoding at the transmitter and all-optical
diffractive decoding at the receiver [1]. In our scheme, an electronic neural network, trained in unison with
an all-optical diffractive decoder, encodes the message of interest to effectively bypass the opaque occlusion
and be decoded at the receiver by an all-optical decoder, using passive diffraction through thin structured
layers. This all-optical decoding is performed on the encoded wavefront that carries the optical information
or the message of interest, after its obstruction by an arbitrarily shaped opaque occlusion. The diffractive
decoder processes the secondary waves scattered through the edges of the opaque occlusion using a passive,
smart material comprised of successive spatially engineered surfaces, and performs the reconstruction of

the hidden information at the speed of light propagation through a thin diffractive volume that axially spans < 100 wavelengths. We showed that this combination of electronic encoding and all-optical decoding is capable of direct optical communication of any arbitrary message between the transmitter and the receiver even when the opaque occlusion body entirely blocks the transmitter's field-of-view. We also reported an experimental demonstration of this scheme using a 3D-printed diffractive decoder that operates at the THz spectrum [1]. We demonstrated that this scheme could be configured to be misalignment-resilient as well as highly power efficient, reaching output diffraction efficiencies of >50%. We also showed that our encoder/decoder framework can be jointly trained to be resilient against unknown, random dynamic changes in the occlusion size/shape, without the need to retrain the encoder or the decoder. This makes the presented concept dynamic and easy to adapt to external and uncontrolled/unknown changes that might happen between the transmitter & receiver apertures.

As another exciting accomplishment [3] on the topic of collaborations between electronic neural networks and diffractive surfaces, we demonstrated a jointly optimized electronic encoder neural network and an all-optical diffractive decoder model for optical information transfer through random unknown diffusers. This electronic-optical design is composed of a CNN that encodes the input image information of interest (to be transmitted) into a 2D phase pattern, like an encrypted code, which is all-optically decoded by a jointly trained/optimized diffractive processor that reconstructs the image of the input information at its output plane, despite the presence of random unknown phase diffusers changing/evolving. constantly experimentally validated the success of this approach using terahertz radiation and a 3D-printed diffractive network [3], demonstrating the feasibility of the diffractive decoder with electronic encoding for optical

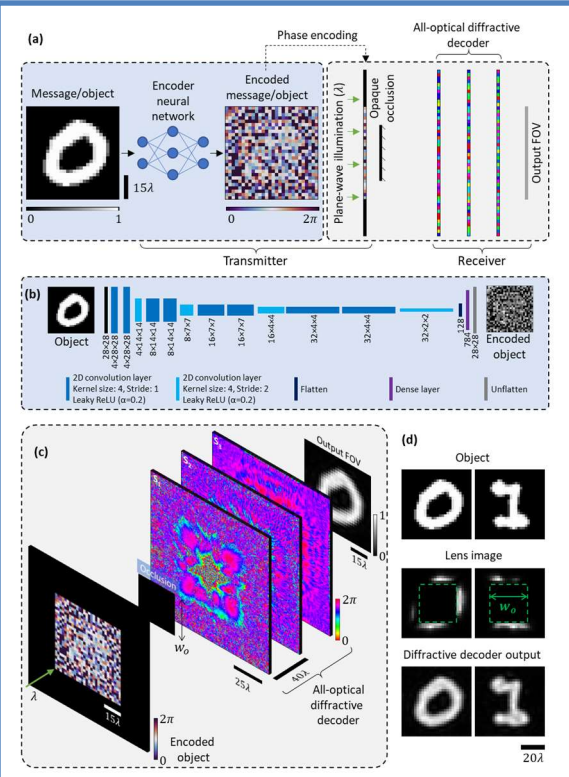


Fig. 1: Schematic of the optical communication framework around fully opaque occlusions using electronic encoding and diffractive all-optical decoding [1]. (a) An electronic neural network encoder and an all-optical diffractive decoder are trained jointly for communicating around an opaque occlusion. For a message/object to be transmitted, the electronic encoder outputs a coded 2D phase pattern, which is imparted onto a plane wave at the transmitter aperture. The phase-encoded wave, after being obstructed and scattered by the fully opaque occlusion, travels to the receiver, where the diffractive decoder all-optically processes the encoded information to reproduce the message on its output field. (b) The architecture used for the convolutional neural network (CNN) encoder throughout this work. (c) Visualization of different processes, such as the obstruction of the transmitted phaseencoded wave by the occlusion of width  $w_o$  and the subsequent all-optical decoding performed by the diffractive decoder. The diffractive decoder comprises L surfaces  $(S_1, \dots, S_L)$  with phase-only diffractive features. In this figure, L = 3 is illustrated as an example. (d) Comparison of the encoding-decoding scheme against conventional lens-based imaging.

information transmission through random unknown diffusers. The optical decoder of this hybrid model can be scaled physically (through expansion or shrinkage) to operate at different parts of the spectrum without retraining its diffractive features.

References: [1] S.S. Rahman, T. Gan, E.A. Deger, Ç. Işıl, M. Jarrahi and A. Ozcan, "Learning Diffractive Optical Communication Around Arbitrary Opaque Occlusions," *Nature Communications* DOI: 10.1038/s41467-023-42556-0 (2023) [2] C. Isıl, D. Mengu, Y. Zhao, A. Tabassum, J. Li, Y. Luo, M. Jarrahi and A. Ozcan, "Super-resolution image display using diffractive decoders," *Science Advances* (AAAS) DOI: 10.1126/sciadv.add3433 (2022) [3] Y. Li, T. Gan, B. Bai, Ç. Işıl, M. Jarrahi, and A. Ozcan, "Optical information transfer through random unknown diffusers using electronic encoding and diffractive decoding," *Advanced Photonics* DOI: 10.1117/1.AP.5.4.046009 (2023)

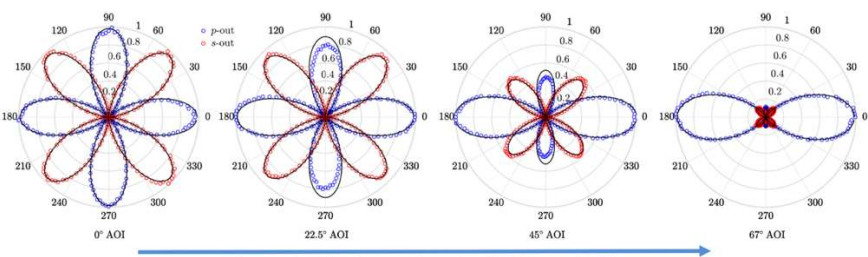
# Multimodal Quantum Material Control Monitored with Ultrafast Coherent X-Rays Award number FWP LANLE1NT (connected to DE-SC0019126)

## Enhanced and twisted nonlinear optical responses in quantum nanomaterials

**Prashant Padmanabhan**<sup>1</sup>, Tenzin Norden<sup>1</sup>, Luis M. Martinez<sup>1</sup>, Nehan Tarefder<sup>1</sup>, Kevin W. C. Kwock<sup>1,2</sup>, Luke M. McClintock<sup>1</sup>, Nicholas Olsen<sup>3</sup>, Luke N. Holtzman<sup>4</sup>, June Ho Yeo<sup>5</sup>, Liuyan Zhao<sup>5</sup>, Xiaoyang Zhu<sup>3</sup>, James C. Hone<sup>6</sup>, Jinkyoung Yoo<sup>1</sup>, Jian-Xin Zhu<sup>1</sup>, P. James Schuck<sup>6</sup>, Antoinette J. Taylor<sup>1</sup>, Rohit P. Prasankumar<sup>1,8</sup>, Wilton J. M. Kort-Kamp<sup>7</sup>, Thomas P. Darlington<sup>6</sup>, Kaiyuan Yao<sup>6</sup>, Kai Du<sup>9</sup>, Ana-Marija Nedić<sup>10</sup>, Thaís V. Trevisan<sup>10</sup>, Peter P. Orth<sup>10</sup>, and Sang-Wook Cheong<sup>10</sup>

<sup>1</sup>Center for Integrated Nanotechnologies, Los Alamos National Laboratory; Los Alamos, NM, 87545, USA, <sup>2</sup>Department of Electrical Engineering, Columbia University; New York, NY, 10027, USA, <sup>3</sup>Department of Chemistry, Columbia University; New York, NY, 10027, USA, <sup>4</sup>Department of Applied Physics and Applied Mathematics, Columbia University; New York, NY 10027, USA, <sup>5</sup>Department of Physics, University of Michigan; Ann Arbor, MI, 48109, USA, <sup>6</sup>Department of Mechanical Engineering, Columbia University; New York, NY, 10027, USA, <sup>7</sup>Theoretical Division, Los Alamos National Laboratory; Los Alamos, NM, 87545, USA, <sup>8</sup>Deep Science Fund, Intellectual Ventures; Bellevue, WA, 98005, USA, <sup>9</sup>Rutgers Center for Emergent Materials and Department of Physics and Astronomy, Rutgers University, Piscataway, NJ 08854, USA, <sup>10</sup>Department of Physics, Iowa State University; Ames, IA, 50011, USA

Abstract: In recent years, explorations of the nonlinear optical (NLO) responses of van der Waals (vdW) crystals have proven to be integral to the study of their fundamental material symmetries, while also providing a platform to revolutionize nonlinear optoelectronic and photonic devices. Here, we will discuss our recent efforts to probe the NLO properties of an emerging class of polar vdW semiconductors and extend vdW nonlinear optics to include the often-overlooked spatial degree of freedom of light. First, we will highlight our studies of bismuth telluro-halide crystals [1], where we observe giant second-order optical nonlinearity enhancements that are highly correlated with the orientation of their permanent dipole moments and domain character (Fig. 1). We will then turn our focus to nonlinear frequency-mixing processes in vdW crystals driven by twisted light [2]. Here, we demonstrate the harmonic scaling of orbital angular momentum and the free tuning of the wavelength, topological charge, and radial index of vortex light-fields, both supported by atomically thin semiconductors (Fig. 2). Our work points to new materials and structured-illumination-based methods for future vdW-based classical and quantum communication nanotechnologies.



increasing fundamental angle of incidence (AOI)

Fig. 1. p- (blue dots) and s-polarized (red dots) second harmonic generation output from BiTeBr, as a function of the linear input polarization angle with respect to the crystal's armchair direction, for increasing angles of incidence with respect to the ab-surface normal direction. The data shows significant enhancement of the nonlinear optical output and alternation of the nonlinear output's fundamental polarization dependence as the driving field's polarization becomes increasingly aligned with the c-axis oriented permanent dipole moment through the activation of the crystal's  $d_{33}$  nonlinear susceptibility tensor element.

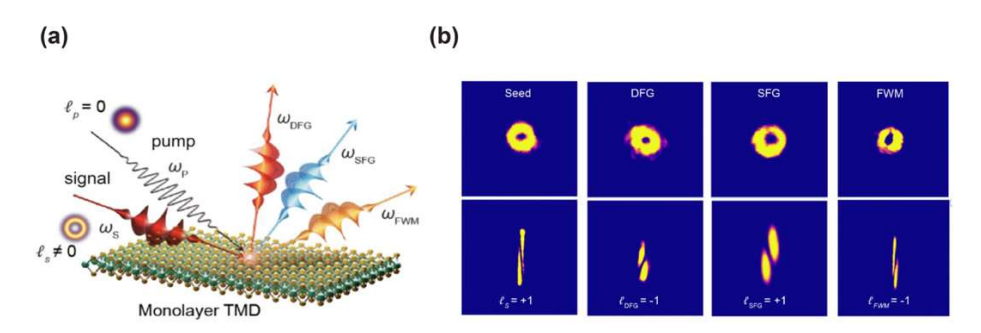
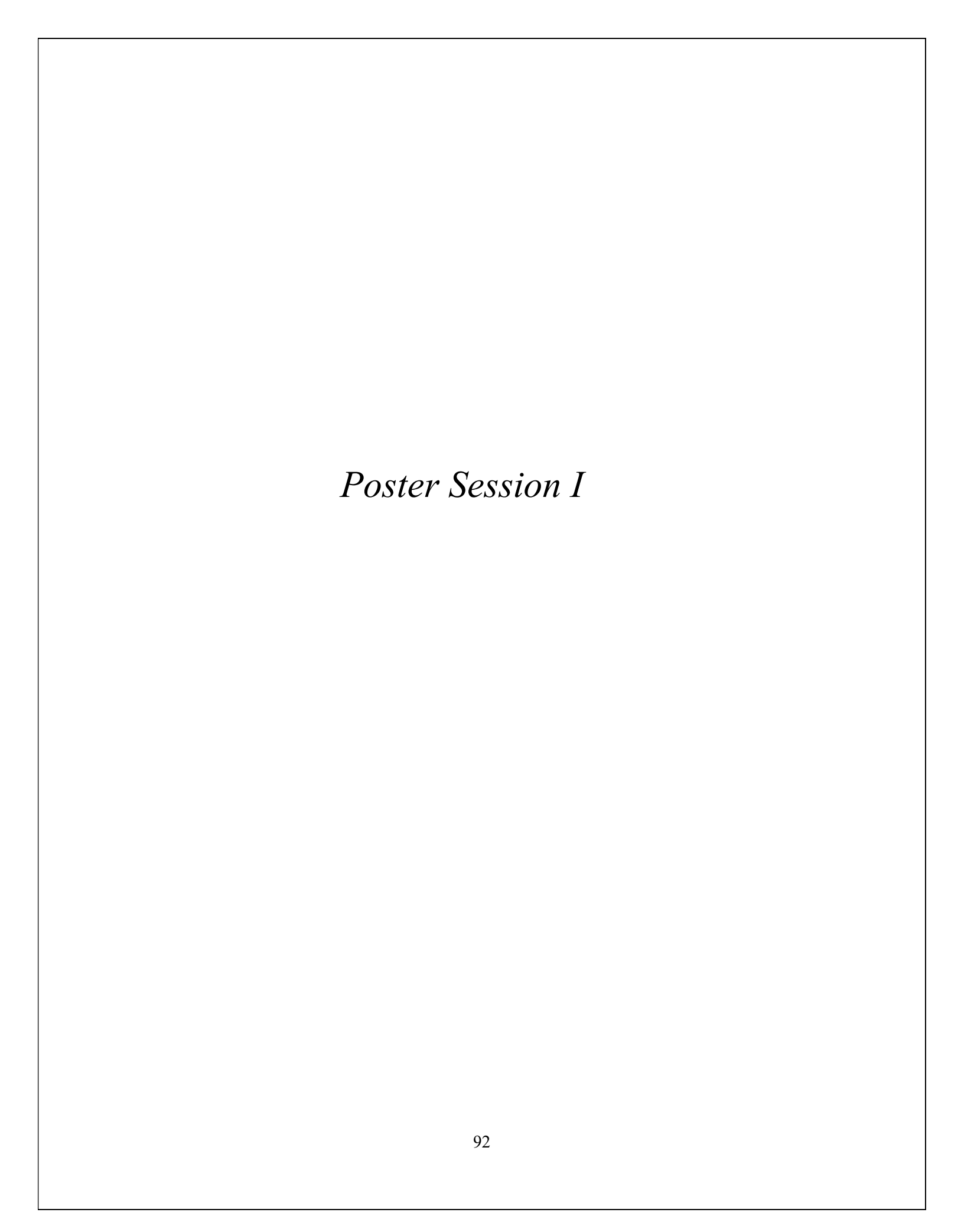


**Fig. 2.** (a) Schematic of structured difference frequency generation (DFG), sum frequency generation (SFG), and fourwave mixing (FWM) nonlinear optical responses from a monolayer transition metal dichalcogenide (TMD) driven with a Gaussian pump beam and Laguerre-Gaussian vortex seed, the latter having non-zero quantized orbital angular momentum indexed by the topological charge  $\ell$ . (b) Real-space images (top panels) of the donut shaped intensity profile of the vortex seed ( $\ell_S = +1$ ,  $\hbar\omega_S = 1.18$  eV) and resulting DFG ( $\ell_{DFG} = -1$ ,  $\hbar\omega_{DFG} = 1.92$  eV), SFG ( $\ell_{SFG} = +1$ ,  $\hbar\omega_{SFG} = 2.81$  eV) and FWM ( $\ell_{FWM} = -1$ ,  $\hbar\omega_{FWM} = 1.92$  eV) outputs. The lower panels show the corresponding momentum space maps imaged at the focal plane of a cylindrical lens. For all data, the pump beam is always Gaussian ( $\ell_P = 0$ ,  $\hbar\omega_P^{DFG} = 3.1$  eV,  $\hbar\omega_P^{SFG} = 1.63$  eV,  $\hbar\omega_P^{FWM} = 1.55$  eV).

[1] K. W. C. Kwock and T. Norden et al., manuscript in preparation – to be credited to LANLE1NT

[2] T. Norden et al., under review at ACS Nano

\_



## **Quantum Computing Approaches for Correlated Multi-Orbital Materials Simulations**

**FWP Number: A19-510-100** 

<u>Yongxin Yao</u><sup>1,2</sup>, **Thomas Iadecola**<sup>1,2</sup>, **Cai-Zhuang Wang**<sup>1,2</sup>, Anirban Mukherjee<sup>1</sup>, Joao C. Getelina<sup>1</sup>, Martin Mootz<sup>1</sup>, Feng Zhang<sup>1,2</sup>, Noah Berthusen<sup>2</sup>, Prachi Sharma<sup>3</sup>, and Peter P. Orth<sup>1,2,3</sup>

1. Ames National Laboratory 2. Iowa State University 3. Saarland University, Germany

**Abstract:** This project leverages and contributes to an expanding toolbox of quantum algorithms to carry out accurate simulations of correlated multi-orbital quantum materials. Noisy intermediate-scale quantum computers represent the first generation of quantum computing hardware that can be programmed remotely through the cloud and applied to a wide range of computational tasks. Although such devices are currently too error-prone to outperform classical computers in simulations of static and early-time dynamical properties of correlated materials, rapid progress in hardware improvements, algorithm development, and problem reformulation indicates that practical quantum advantage may soon become attainable.

The central goal of this project is to achieve practical quantum advantage by applying quantum algorithms to calculate static, dynamic, and finite-temperature properties of correlated multi-orbital quantum materials, focusing on layered transition metal oxide and rare-earth-bearing half-Heusler compounds. To realize this, the work adopts a hybrid quantum-classical Gutzwiller variational embedding (GQCE) approach that employs quantum computers as impurity solvers. It also directly applies quantum algorithms to study complex quantum spin and fermionic models, which both provide steppingstones for these algorithms' applications within the Gutzwiller approach and provide important reference points for the Gutzwiller calculations of itinerant electron systems in the strong coupling limit. Calculations will be carried out on IBM and Quantinuum quantum processing units (QPUs).

To achieve the goal of ground state simulations of multi-orbital correlated materials, we first developed and benchmarked best practices for ground-state preparation of the d-sub-shell embedded impurity models using adaptive variational quantum algorithms, a crucial step in GQCE simulations [1]. These adaptive methods enable significant circuit compression compared to standard variational quantum eigensolvers. Ground-state energies were measured on both IBM and Quantinuum quantum hardware, achieving a relative error of 0.7% using a combination of zero-noise extrapolation and symmetry-based post-selection. To further enhance circuit expressivity, trainability, and noise resilience while optimizing quantum classical resource balance, we integrated variational quantum circuits with a quantum subspace expansion [2]. We demonstrated that coordinating the number of layers in the Hamiltonian variational ansatz with the Krylov subspace expansion order significantly improves performance. Benchmark simulations of groundstate energies for one- and two-dimensional mixed-field Ising spin models were performed on noisy simulators and IBM QPUs, incorporating probabilistic error reduction techniques. Additionally, we improved the automatic ansatz generation procedure used in adaptive algorithms to reduce circuit depth and proposed the integration of tensor-network methods to reduce quantum resource requirements [3]. These combined achievements will allow us to extend simulations to full-shell d- and f-embedded impurity models, thereby enabling GOCE ground-state calculations of transition-metal and rare-earth compounds.

To advance simulations of dynamical properties of quantum systems, we integrated the adaptive variational quantum imaginary- and real-time evolution algorithms (AVQITE, AVQDS) for ground state response-function calculations, improving circuit compression by leveraging degrees of freedom in the entire ansatz [4]. Specifically, adaptive variational quantum algorithms were developed to measure real-time single-particle Green's functions and nonlinear susceptibilities. Accurate benchmark calculations are showcased for fermionic Hubbard models, molecules, and spin systems. Compared to existing methods, our adaptive algorithms yield significantly shallower quantum circuits. The next step is to combine this approach with a

real-time generalization of GQCE, enabling response function simulations of complex materials. This will support direct comparison with experimental probes, including ARPES, neutron scattering and 2D coherent spectroscopy.

To address the goal of including finite-temperature effects in correlated quantum materials simulations, we combined AVQITE with classical minimally entangled typical thermal states (METTS) sampling, resulting in the AVQMETTS algorithm [5]. The hybrid approach enables calculations of equilibrium properties at finite temperature. Using local spin models, we demonstrated approximately linear system-size scaling of quantum circuit complexity at fixed temperature. We also simulated the magnetic field dependence of the phase transition temperature in a two-dimensional transverse-field Ising model and analyzed the impact of hardware noise on AVQMETTS results. Moving forward, we will integrate this approach with the imaginary-time generalization of GQCE to enable finite-temperature simulations of correlated materials.

- 1. A. Mukherjee, et al, Commun. Phys. 6, 4 (2023). DOI: 10.1038/s42005-022-01089-6
- 2. J. C. Getelina, et al, APL Quantum 1, 036127 (2024). DOI: 10.1063/5.0217294
- 3. F. Zhang et al, *Phys. Rev. B* 111, 094310 (2025). DOI: 10.1103/PhysRevB.111.094310
- 4. M. Mootz, et al, J. Chem. Theory Comput., 20, 8689 (2024). DOI: 10.1021/acs.jctc.4c00874
- 5. J. C. Getelina, et al, SciPost Phys. 15, 102 (2023). DOI: 0.21468/SciPostPhys.15.3.102

## Scalable quantum photonic materials based on precision doped diamond nanostructures

DE-SC0025295

### Focused Ion Beam Implantation for Diamond Color Center Fabrication

Michael Titze<sup>1</sup> (Co-PI), Shei Su<sup>1</sup>, and Jelena Vuckovic<sup>2</sup> (PI)

Color centers in diamond are gaining recognition as powerful tools for quantum information science (QIS), particularly in quantum communication and sensing applications. These atomic-scale defects exhibit unique optical and spin properties, making them ideal candidates for integration into quantum devices [1]. However, a major challenge lies in the deterministic fabrication of color centers, as precise control over their spatial placement and density is essential for device functionality. Focused ion beam (FIB) technology, especially when combined with liquid metal alloy ion sources (LMAIS), offers a promising solution to overcome these challenges and enable scalable fabrication of color centers, which we have addressed as part of previous projects [2, 3]. This part of our project focuses on the fabrication of tin-vacancy (SnV) centers in diamond using FIB implantation of tin (Sn) ions generated by a AuSn alloy, as well as the development of a sodium (Na) source for creating Na-based color centers.

SnV centers in diamond have recently attracted attention due to their ability to operate at elevated temperatures compared to lighter group-IV-based color centers. Additionally, SnV centers exhibit high quantum yield and promising optical properties, including narrow linewidths and high photostability, making them suitable for QIS applications. Like other group-IV-based color centers, SnV centers benefit from their high symmetry, which reduces spectral diffusion and enhances coherence.

Sodium-based color centers are theoretically predicted to outperform group-IV-based color centers in certain aspects. For example, they are expected to exhibit a higher Debye-Waller factor, and depending on their charge state, they may possess larger spin than SnV centers. These characteristics make Na-based color centers a promising candidate for next-generation quantum devices.

The deterministic creation of color centers at specific locations remains a bottleneck for their integration into quantum devices. Typically color centers are fabricated either through broad-beam ion implantation and annealing or by incorporating impurity atoms during crystal growth, in both cases resulting in poor spatial control. In contrast, FIB technology enables the direct implantation of desired impurity atoms with nanoscale precision, typically on the order of tens of nanometers. This level of accuracy is both critical and sufficient for integrating color centers into photonic structures, such as waveguides and cavities, which are essential for fabricating quantum devices. Liquid metal alloy ion sources (LMAIS) are particularly suited for QIS applications with FIB due to their ability to emit a variety of ion species with isotopic resolution. This versatility makes LMAIS an ideal choice for creating color centers with high spatial precision.

As part of this project we have FIB implanted high-purity diamond with 117-Sn (nuclear spin-1/2 isotope) and 120-Sn (nuclear spin-0 isotope) and performed activation anneals, with the PI currently working on characterization of the implanted sample.

As part of our planned effort to study Na-based color centers in diamond, we are developing a Na FIB source. Specifically, we aim to create both sodium substitutional (Na<sub>C</sub>) and sodium-vacancy (NaV) centers through different annealing recipes. Once a FIB source is available, the ability to place Na<sub>C</sub> and NaV centers with nanoscale precision using FIB will enable experiments to explore color-center cavity interactions, a critical step for integrating Na-based color centers into quantum devices.

<sup>&</sup>lt;sup>1</sup>Sandia National Laboratories, Albuquerque, NM, 87123

<sup>&</sup>lt;sup>2</sup>Stanford University, Stanford, CA, 94305

Developing a stable Na source for FIB implantation presents unique challenges. Reports in the literature describe the use of pure-metal Na and NaLi sources, but both are prone to oxidation, making it difficult to achieve the stability required for FIB implantation. Our initial approach involved using a AuSi eutectic alloy with Na added as an impurity. While the source emitted ions from Au and Si, no Na emission was observed. Sodium is expected to be a prolific ion due to its low first ionization energy (495 kJ/mol), but mass spectra revealed no Na emission, shown in Figure 1. Sodium's high vapor pressure likely causes it to preferentially boil off during source preparation.

To address the evaporation issue, we identified  $Na_{62}Pb_{38}$  as a suitable alternative source material due to its lower melting point of 301°C and eutectic-like behavior. However, our initial attempt at creating a NaPb

source resulted in rapid boil-off of the material. Further investigation revealed that the alloy was overheated during source preparation. While the AuSi eutectic melts at 380°C, our standard fabrication procedure heats the material to 800°C to ensure full melting of the AuSi boat. This excess heat likely caused the NaPb material to boil, as the vapor pressures of Na and Pb are lower than those of Au and Si.

To prevent overheating, we developed a thermometry system to monitor and control the temperature of the NaPb crucible during source preparation. Using this system, we were able to fabricate a filament, however upon generating emission from the filament, the alloy again evaporated, ascribed to electron self-heating of the filament during emission.

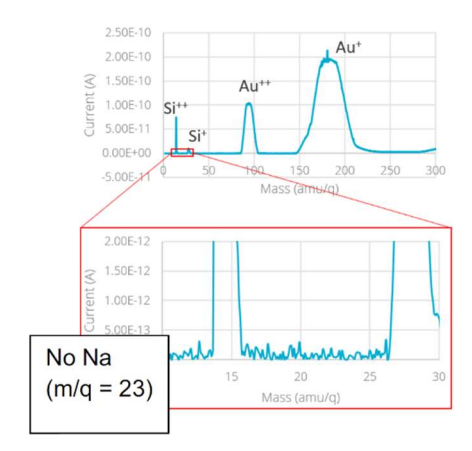


Figure 4 Mass spectrum of AuSiNa source.

FIB technology, combined with LMAIS offers a powerful solution for the deterministic fabrication of color centers. Our efforts to

develop a Na source for FIB implantation represent a critical step toward studying and integrating Nabased color centers into quantum devices. While challenges remain, we have made progress with alternative materials like NaPb.

#### **References:**

- [1] E.I. Rosenthal, et al., Physical Review X, 14, 4, 041008, https://doi.org/10.1103/PhysRevX.14.041008 (2024)
- [2] V. Chandrasekaran, *et al.*, Advanced Science, 10, 18, 2300190, https://doi.org/10.1002/advs.202300190 (2023)
- [3] M. Titze, et al., Nano Letters, 22, 8, 3212-3218, https://doi.org/10.1021/acs.nanolett.1c04646 (2022)

#### Project Title: Holographic quantum simulation of strongly correlated electron systems

Award Number: DE-SC0022102

Names of PI, coPI(s), and unpaid collaborators:

PI: Shyam Shankar, University of Texas at Austin; Co-PI: Andrew Potter, University of British Columbia; Postdoctoral associates: Joseph Sullivan, University of British Columbia; Josiah Cochran, University of Texas at Austin; Graduate students: Ameya Riswadkar, Jian Jun Liu, Aikaterini Kargioti, Theodore Shaw, University of Texas at Austin; Yuxuan Zhang, University of Texas at Austin and University of Toronto; Travis Hosack, University of British Columbia; Daoheng Niu, University of Texas at Austin; Undergraduate students: Shahin Jahabani, University of Texas at Austin; Alice Xiong, University of British Columbia; and Noah Mugan, University of Texas at Austin

**Abstract:** Quantum simulations of many-body systems in materials science and chemistry are promising application areas for quantum computers. However, the limited scale and coherence of near-term quantum processors pose a significant obstacle to realizing this potential. In this project, we have been theoretically and experimentally exploring a recently developed method for implementing quantum operations to sequentially build up a matrix product state (MPS) representation of a many-body quantum state. This approach can be used to demonstrate quantum advantage over classical simulations by efficiently using the resources of moderate-size, noisy quantum processors. We will present a theoretical and experimental study of how to employ this sequential quantum simulation algorithm to simulate the ground state energy of a highly entangled many-body spin chain.

First, we will describe how a single-mode circuit quantum electrodynamics (cQED) device, consisting of

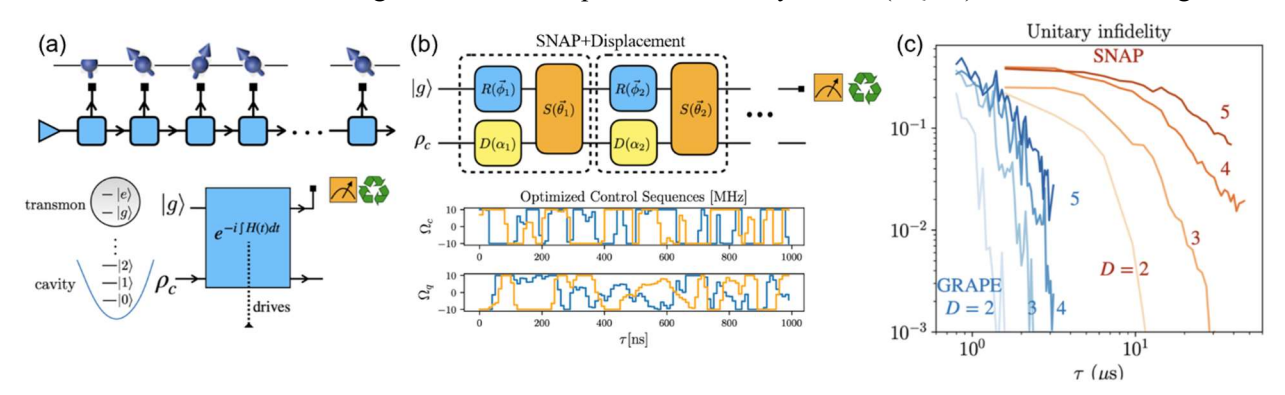


Figure 5. (a) Graphical representation of a matrix product state for a spin chain (top) and its implementation as a sequential circuit with qubit reuse (b) Synthesis of time-dependent Hamiltonian with SNAP gates or GRAPE pulse-level control. (c) Infidelity for synthesizing a unitary representing various bond-dimension D approximations of a critical Ising chain ground state.

a transmon qubit coupled to a long-lived cavity mode, can be used to implement sequential quantum simulation of a spin chain [1]. The approach, described in Figure 1, employs the transmon qubit to read out the state of each spin in the chain and exploits the large state space of the cavity as a quantum memory encoding inter-site correlations and entanglement. We numerically compared analog pulse-level control generated by Gradient Ascent Pulse Engineering (GRAPE) to digital control based on Selective

Number Arbitrary Phase (SNAP) gates. We find that analog control can accurately prepare the MPS representation of a quantum-critical spin chain in less time, thus reducing infidelity due to decoherence.

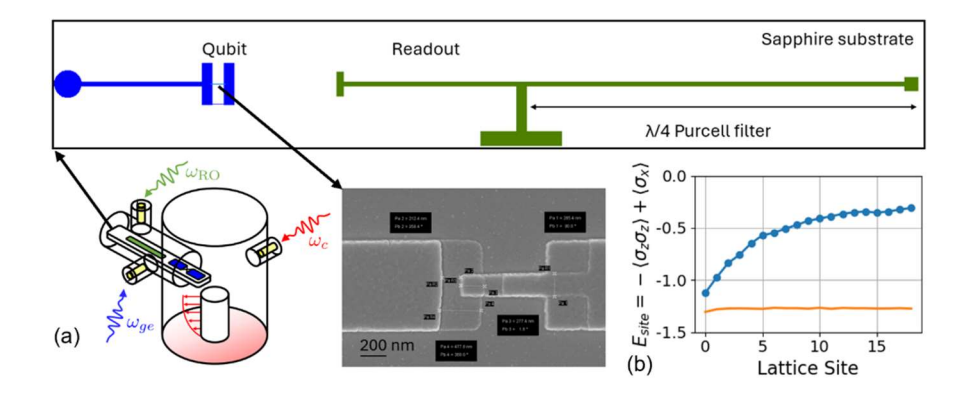


Figure 6. (a) cQED hardware consisting of a long-lived superconducting cavity (red), transmon qubit (blue) and readout (green). Qubit nonlinearity is realized with a Josephson junction. (b) Measured ground state energy (blue) compared to ideal calculation (orange).

Next, we will describe our experimental implementation of the sequential simulation protocol with superconducting quantum hardware, shown in Figure 2. We found experimentally that GRAPE based analog control is sensitive to miscalibration resulting in significant error in the measured ground state energy. To address this hurdle, we will present on progress towards realizing sequential simulation using SNAP gates.

[1] Y. Zhang et al., Phys. Rev. A 109, 022606 (2024). doi:10.1103/PhysRevA.109.022606

## **Integrated Materials Platforms for Topological Quantum Computing Devices**

#### DE-SC0019274

Abstract Title: Modeling and testing of materials and devices for topological and spin qubits

Vlad Pribiag<sup>1</sup>, <u>Sergey Frolov</u><sup>2</sup>, Chris Palmstrøm<sup>3</sup>, Noa Marom<sup>4</sup>, Kunal Mukherjee<sup>5</sup>, Shixiong Zhang<sup>6</sup>, Tomasz Story<sup>7</sup>, Moïra Hocevar<sup>8</sup>, and Vladimir Strocov<sup>9</sup>

1. University of Minnesota, 2. University of Pittsburgh, 3. University of California Santa Barbara, 4. Carnegie Mellon University, 5. Stanford University, 6. Indiana University Bloomington, 7. Institute of Physics, Polish Academy of Sciences, 8. CNRS Grenoble, 9. Swiss Light Source, Paul Scherrer Institute

Abstract: A significant challenge towards developing robust quantum computing systems with large numbers of logical qubits is rapid decoherence. A promising approach to addressing this challenge is based on the concept of fault-tolerant quantum computing architectures that leverage topological quantum states such as Majorana zero-modes (MZM). Substantial progress toward realizing and detecting topological states has been enabled by quantum devices which combine semiconductors with superconductors due to the combination of processing-friendly materials that offer high spin-orbit coupling, large g-factors, ballistic transport, and the ability to create transparent interfaces with various superconductors. However, further breakthroughs leading to topological quantum computation require next-generation quantum nanostructures that offer substantial improvement in the electronic purity together with optimal coupling across the superconductor-semiconductor interface. Here we discuss our recent results under this project, focusing on first-principles modeling of interfaces, simulation of device properties and experimental testing of IV-VI nanowire materials for spin qubits. This work is a subset of our larger effort supported by this grant, which combines quantum device fabrication and characterization with materials synthesis and data interpretation informed by ab initio simulations and machine learning to develop robust, tunable and scalable platforms for the manipulation of quantum states.

- (i) Modeling MZM materials: We have employed an array of numerical methods, including DFT-U and micromagnetic simulations, as well as tight-binding modeling, to explore the question of materials most suitable for the realization of MZMs in hybrid superconductor-semiconductor nanowire systems. Using DFT-U, we have explored the potential of two-shell nanowire architectures, where a core of a III-V semiconductor is first passivated by a shell of a larger bandgap II-VI semiconductor. This shell serves as a tunnel barrier to the outer shell of a metallic superconductor. We have explored the combinations of InSb-CdTe-Al, as well as InAs-ZnTe-Al and InAs-CdSe-Al which happen to be lattice matched [1,2]. We identified that their interlayer of group II-VI semiconductor cannot exceed the thickness of 5-10 monolayers and established the band alignment. The results for individual bulk layers were compared to ARPES.
- (ii) Modeling MZM-relevant devices: Using micromagnetic and tight-binding modeling, we have demonstrated that stray fields from proximate micromagnets can induce sufficient spin splitting in a nanowire to in principle generate MZMs. We proposed designs that are best suited for the basic 2-MZM nanowires, as well as for the more advanced fusion and braiding devices [3]. We have also established that stray fields can strongly suppress superconductivity in thin shells of Al or Sn, which can lead to false MZM positives in experiments [4].

(iii) Towards spin qubits in IV-VI quantum dots: Quantum dot spin qubits are a leading quantum computing platform, with most of the recent progress concentrated on the group IV materials family (Si and Ge or combinations thereof). This aspect of our project is exploring group IV-VI compounds which

feature strong spin-orbit interaction, large Landé g-factors, high mobilities, low resistance electrical contacts, and the possibility of isotopic purification. Some of the materials in the family are expected to be topological (SnTe) and some feature a strong dielectric response which can be leveraged e.g. for long-distance coupling of qubits. To this end, we have fabricated single and double quantum dots and explored their dot energies, spin-orbit interaction strength and anisotoropy, and the structure of their spin states. These results are in preparation for publication. We find unusual 45-degree anisotropy in both g-factor and SOI strength (Fig. 1), which hint at the crystalline origin of the phenomena. We also identify that the dots typically have quantum Coulomb energies, which allows study of an unusual regime for spin qubits. We also fabricated quantum dots on PbTe nanowires to study the fractional charge jumps that can be associated with anyon quasiparticles. We observed charge jumps that are nearly 1/3 of the quantum dot's conductance period. This was observed near zero magnetic field in a weakly interacting material, thus not in the regime where anyons are expected. We identify an explanation based on additional uncontrolled quantum dots coupled capacitively to the primary dot [5].

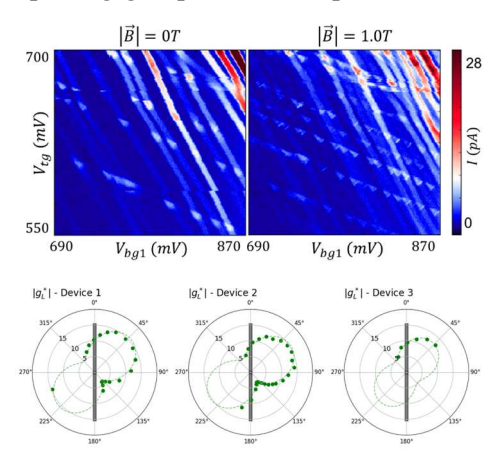


**Fig. 1:** Stability diagram (top) and g-factor anisotropy (bottom) of PbTe nanowire DQDs. These devices are useful for mapping out the properties spin-orbit coupling and Landé g-factors in this material, for topological and spin qubit applications.

#### **References:**

- [1]M. J. A. Jardine et al., *First-Principles Assessment of CdTe as a Tunnel Barrier at the α-Sn/InSb Interface*, ACS Appl. Mater. Interfaces **15**, 16288 (2023) DOI: 10.1021/acsami.3c00323.
- [2]M. J. A. Jardine et al., First-Principles Assessment of ZnTe and CdSe as Prospective Tunnel Barriers at the InAs/Al Interface, ACS Appl. Mater. Interfaces 17, 5462 (2025) DOI: 10.1021/acsami.4c17957.
- [3]M. J. A. Jardine et al., *Integrating micromagnets and hybrid nanowires for topological quantum computing*, SciPost Phys. **11**, 090 (2021) DOI: 10.21468/SciPostPhys.11.5.090.
- [4]S. M. Frolov et al., "Smoking gun" signatures of topological milestones in trivial materials by measurement fine-tuning and data postselection, ArXiv:2309.09368 (2023) DOI: 10.48550/arXiv.2309.09368.
- [5]S. Byard, M. Gomanko, and S. M. Frolov, *Apparent fractional charge signatures in PbTe quantum dots due to capacitively coupled charge trap dynamics*, ArXiv:2504.05221 (2025) DOI: 10.48550/arXiv.2504.05221.

## Multiscale Quantum and Classical Microscopy for Superconducting Quantum Systems Award Number: ERKCK51

### Light-matter interaction with quantum light

## Chengyun Hua, Benjamin Lawrie, Yueh-Chun Wu (pd)

Oak Ridge National Laboratory

**Abstract:** Magneto-optical probes of condensed matter have drawn increasing attention over the past decade because of the potential for unveiling steady-state and out-of-equilibrium spin interactions and for probing spontaneous time-reversal-symmetry breaking in unconventional superconductors. However, a major obstacle for such spectroscopies is the photoinduced heating that can perturb the material under study especially in cryogenic environments. Quantum light sources open the possibility to couple to matter without the need for strong lasers. For example, quantum sensing using squeezed light for applications

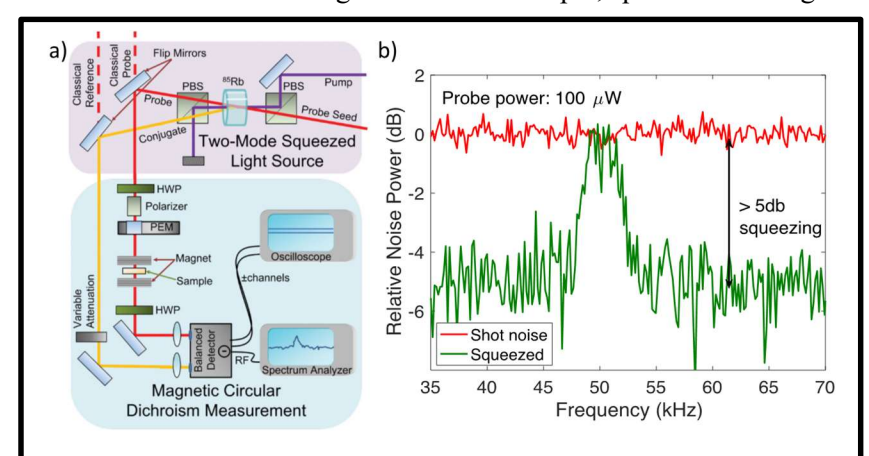


Figure 1: (a) Schematic of quantum enhanced magnetic circular dichroism experiment. (b) Demonstration of a quantum-enhanced polarization-sensitive signal (green) without a sample together with a shot noise limited trace (red) acquired with a probe power of  $100 \, \mu W$ .

ranging from gravitational wave detection to scanning probe microscopies has enabled measurements with sensitivity beyond the shot noise limit (SNL) without introducing excessive heating. Our team has substantial experience in both optical manipulation of materials in low-temperature environments and the development and application of sources. 1,2 squeezed light Recently, we have demonstrated two-mode squeezed light sources can be used to improve the minimum detectable signal in magnetic circular dichroism

(MCD) measurements by three decibels compared with state-of-the-art classical measurements, even with relatively lossy samples like terbium gallium garnet.<sup>3</sup> The two-mode squeezed light source is generated via four-wave mixing in <sup>85</sup>Rb vapor before the MCD signal is transduced onto the probe field and a balanced photodetection scheme is used to suppress noise below the SNL. By employing a two-mode squeezed light source to suppress photon shot noise, the sensitivity of the MCD measurement is enhanced, allowing detection of weaker signals with lower laser power—thereby reducing photothermal disturbances during cryogenic optical probing of quantum materials. These results establish a foundation for quantum-enhanced magneto-optical microscopies, which are especially vital for probing environmentally sensitive materials and for low-temperature measurements where increased optical power can cause unacceptable thermal disturbances.

To further minimize perturbations induced by the macroscopic photon population in bright squeezed states of light, squeezed vacuum states of light readout through dual homodyne measurement schemes (as

illustrated in Fig. 2) offer the potential for truly nonperturbative measurements of material properties in cryogenic environments. Previously, we demonstrated the first practical measurement of an microcantilever displacement using a squeezed dual homodyne readout scheme, resulting in classically inaccesible measurement sensitivity of 1.7 fm/ $\sqrt{\text{Hz}}$ . This scheme can be adapted for low-temperature magneto-optical Kerr effect measurements with the addition of a set of polarization optics. This quantumenhanced approach is predicted to achieve a sensitivity of 10 nrad/√Hz with negligible photothermal interactions compared with the cooling power of our dilution refrigerators.<sup>4</sup> Such a combination of high sensitivity and low operating temperature cannot be achieved with any classical measurement technique. This approach will enable the detection of subtle spontaneous Kerr rotation

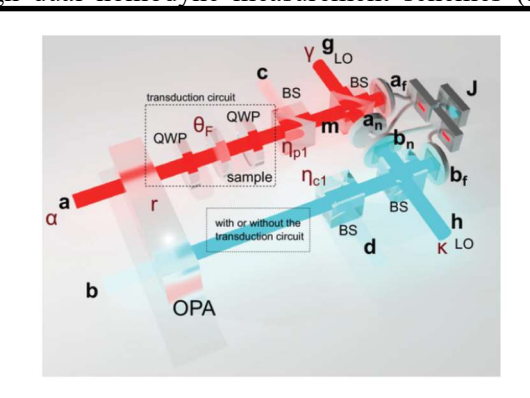


Figure 2: Optical setup for generating a two-mode squeezed light source comprising a probe and conjugate beam that exhibit intensity difference and phase-sum squeezing.

arising from time-reversal symmetry breaking in a topological superconductor, and it could also unlock new quantum enhanced probes of phonon angular momentum that have recently been explored with classical readout schemes in the core MSE program at ORNL<sup>5</sup>.

#### **Reference:**

- 1. Dowran, M. *et al.* Parallel Quantum-Enhanced Sensing. *ACS Photonics* **11**, 3037–3045 (2024). doi:10.1021/acsphotonics.4c00256
- 2. Pooser, R. C. *et al.* Truncated Nonlinear Interferometry for Quantum-Enhanced Atomic Force Microscopy. *Phys. Rev. Lett.* **124**, 230504 (2020). doi:10.1103/PhysRevLett.124.230504
- 3. Hua, C. *et al.* Quantum Enhanced Probes of Magnetic Circular Dichroism. *Adv. Quantum Technol.* 2300126 (2023) doi:10.1002/qute.202300126.
- 4. Pai, Y., Marvinney, C. E., Hua, C., Pooser, R. C. & Lawrie, B. J. Magneto-Optical Sensing Beyond the Shot Noise Limit. *Adv. Quantum Technol.* 2100107 (2021) doi:10.1002/qute.202100107.
- 5. Zhang, H. *et al.* Observation of Phonon Angular Momentum. Preprint at https://doi.org/10.48550/arXiv.2409.13462 (2024).

## Multiscale Quantum and Classical Microscopy for Superconducting Quantum Systems Award Number: ERKCK51

## **Elucidation of Quantum Spin Defect Interactions with Quantum Materials**

## Joshua T. Damron, Benjamin Lawrie, Gábor Halász, Chengyun Hua, and Yueh-Chun Wu (pd)

Oak Ridge National Laboratory

Abstract: This thrust focuses on developing and integrating advanced quantum sensing platforms using spin defects such as the boron vacancy center in hexagonal boron nitride (hBN) and nitrogen-vacancy (NV) centers in diamond to probe magnetic fluctuations and superconducting phenomena from nano to mesoscale dimensions. The use of different sensing modalities matched to the application of interest addresses critical limitations in quantum magnetometry. By using scanning NV center magnetometry and relaxometry to investigate the critical behavior of a high-Tc ferromagnetic oxide near its Curie temperature<sup>1</sup>, we addressed the technical challenges of probing the relevant length and time scales during thermally driven ferromagnetic-to-paramagnetic phase transitions, as highlighted in Figure 1. We have recently adapted this approach to capture the static and dynamic aspects of critical behavior in van der Waals ferromagnets like Fe<sub>3</sub>GaTe<sub>2</sub>, providing new insights into the universal properties governing magnetic phase transitions and demonstrating the power of NV-based techniques for studying critical phenomena across the relevant spatial and temporal scales.

Spin defects in hBN provide unique advantages for sample-sensor proximity due to their 2D and (in principle) arbitrary operational thickness as well as out of plane spin orientation allowing for close distances between the defect plane and probe system while simplifying bias field alignment. With this approach, we have recently monitored spin dynamics near a phase transition between collinear and incommensurate spiral antiferromagnetic phases using T<sub>1</sub> relaxometry of boron vacancy defects in an hBN flake transferred onto

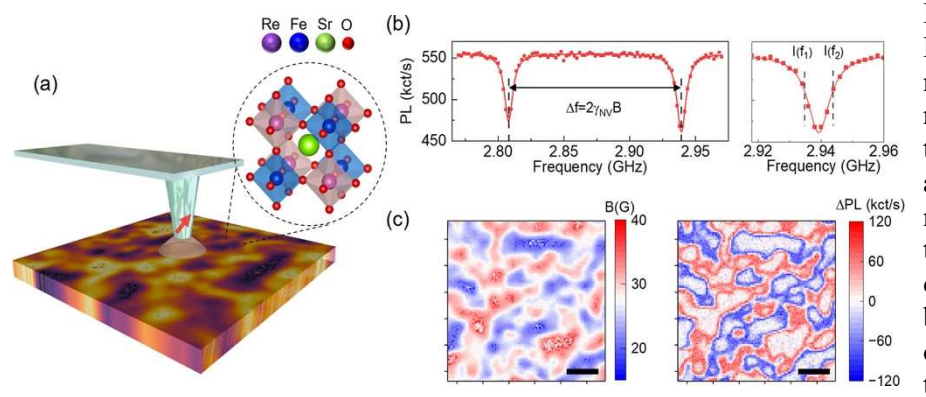


Figure 7 (a) Schematic illustration of nanoscale spin-based probe of perovskite ferromagnetic oxide Sr<sub>2</sub>FeReO<sub>6</sub>. (b) Measured ODMR spectra for imaging of local magnetic textures (scale bar 400 nm) depicted in (c).

LuMn<sub>6</sub>Sn<sub>6</sub>, as shown in Figure 2. We are currently mapping the spin dynamics near different phase transitions in LuMn<sub>6</sub>Sn<sub>6</sub> with optical relaxometry measurements in a low temperature high-field environment in order to better understand complex phase diagram of this Kagome magnet. In addition to these efforts, we have probed the energetics and dynamics of silicon

vacancy (SiV) centers in diamond under arbitrary magnetic field orientations in a dilution refrigerator.<sup>2,3</sup> These experimental approaches will be adopted for NV centers and boron vacancy spin defects to advance mK spin-based quantum sensing protocols over the next few years. Finally, in collaboration with the ORNL BES-MSE core program<sup>4</sup> we are developing new e-beam-induced etching techniques to optimize the

brightness and directionality of emission from spin defects while controlling surface chemistry to optimize spin-based sensing functionality.

- 1. Wu, Y.-C. *et al.* Nanoscale Magnetic Ordering Dynamics in a High Curie Temperature Ferromagnet. *Nano Lett.* **25**, 1473–1479 (2025). doi:10.1021/acs.nanolett.4c05401
- 2. Wu, S., Li, X., Gallagher, I., Lawrie, B. & Wang, H. Coherent population trapping and spin relaxation of a silicon vacancy center in diamond at millikelvin temperatures. *Phys. Rev. B* **111**, 035421 (2025). doi:10.1103/PhysRevB.111.035421
- 3. Wu, S.-H. et al. Experimental determination of energy-level structures of diamond silicon-vacancy

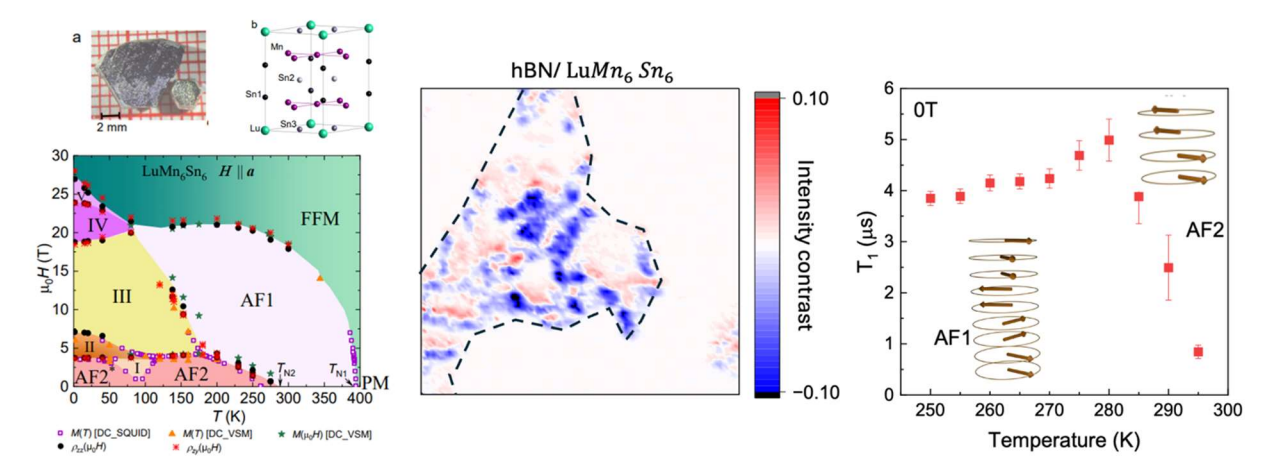


Figure 8. Antiferromagnetic kagome compound LuMn<sub>6</sub>Sn<sub>6</sub> with a rich phase diagram prepared with hBN flake on top of polished surface (left). Map of magnetic domains in LuMn<sub>6</sub>Sn<sub>6</sub> measured with boron vacancy spin defects (middle) and associated zero-field temperature dependent  $T_1$  relaxation times spanning the AF2-AF1 transition (right).

centers in off-axis magnetic fields. Phys. Rev. B 111, 155426 (2025). doi: 10.1103/PhysRevB.111.155426

4. Almutlaq, J. *et al.* Closed-loop electron-beam-induced spectroscopy and nanofabrication around individual quantum emitters. *Nanophotonics* **13**, 2251–2258 (2024). doi:10.1515/nanoph-2023-0877

Project Title: Understanding the Many-body Properties of Rare Earth-Based Materials Relevant to

**Next Generation QIS Applications** 

**Award Number: PM-062** 

Abstract Title: Neutron Scattering Studies of Quantum Coherence in Yb Spin Chains

Names of PI, (co-PI): <u>Igor A. Zaliznyak</u>¹(co-PI), Andreas Weichselbaum¹ (co-PI), Robert Konik¹ (PI), Lazar Kish¹ (Postdoc), Daniel M. Pajerowski², Andrei T. Savici², Andrey Podlesnyak², Leonid Vasylechko³, Alexei Tsvelik¹ (unfunded collaborators)

**Affiliation(s):** <sup>1</sup>CMPMSD, BNL, Upton, NY 11973, USA, <sup>2</sup>Neutron Scattering Division, ORNL, Oak Ridge, TN 37831, USA. <sup>3</sup>Lviv Polytechnic National University, Lviv, Ukraine

**Abstract:** The goal of this research program is to use neutron scattering to investigate the coherence properties of Yb and other rare earth (RE) based solid state qubit candidate systems and how these properties can be modified and manipulated using time-structured external stimuli such as laser excitation tuned to the RE specific optical transitions.

In the past and current funding periods, this program has developed an optical fiber-based setup for in-situ laser pumping of optically active samples during neutron experiments, implementing laser pump neutron probe capability for scattering experiments on QIS-relevant materials. The setup has been used for a set of initial experiments on HYSPEC and SEQUOIA spectrometers at the SNS and at WAND2 diffractometer at HFIR. The laser setup allows time-resolved stroboscopic measurements of relaxation processes in quantum systems following interaction with coherent laser photons with time resolution of about 20 to 40 microseconds. The initial experiments yielded promising results and allowed developing experimental protocols and data processing workflows for time-resolved laser pump neutron probe measurements.

One key question for potential applications of RE-based solid-state qubits in QIS is that of thermal decoherence. Thermal effects can be important for optical coupling to quantum states in crystals where interaction with energetic photons can lead to substantial heating effects resulting in a loss of quantum coherence. Indeed, conventional wisdom dictates that quantum effects become unimportant at high temperatures. In magnets, it has been expected that when thermal energy exceeds interactions between atomic magnetic moments, the moments become uncorrelated, and classical paramagnetic behavior is restored. This thermal decoherence of quantum spin behaviors is a major hindrance to quantum information applications of spin systems. Remarkably, our neutron scattering experiments on Yb chains in YbAlO<sub>3</sub>, an insulating perovskite crystal, defy these conventional

expectations [1]. We observe a sharply defined spectrum of spinons, fractional quantum excitations of spin-1/2 chains, to persist to temperatures much higher than the scale of the interactions between Yb magnetic moments. The observed sharpness of the spinon continuum's dispersive upper boundary indicates a spinon mean free path exceeding approximately 35 inter-atomic spacings at temperatures more than an order of magnitude above the interaction energy scale (Figure 1A). While the coherence of quantum excitations persists, the lower bound on quantum entanglement as quantified by quantum Fisher information, demonstrates universal power-law decline with temperature (Figure 1B).

[1] (funded by this project) "High-temperature quantum coherence of spinons in Yb spin chains", Lazar Kish, Andreas Weichselbaum, Daniel M. Pajerowski, Andrei T. Savici, Andrey Podlesnyak, Leonid Vasylechko, Alexei Tsvelik, Robert Konik, Igor A. Zaliznyak. Nature Communications (acceptance offered, 2025), https://doi.org/10.48550/arXiv.2406.16753.

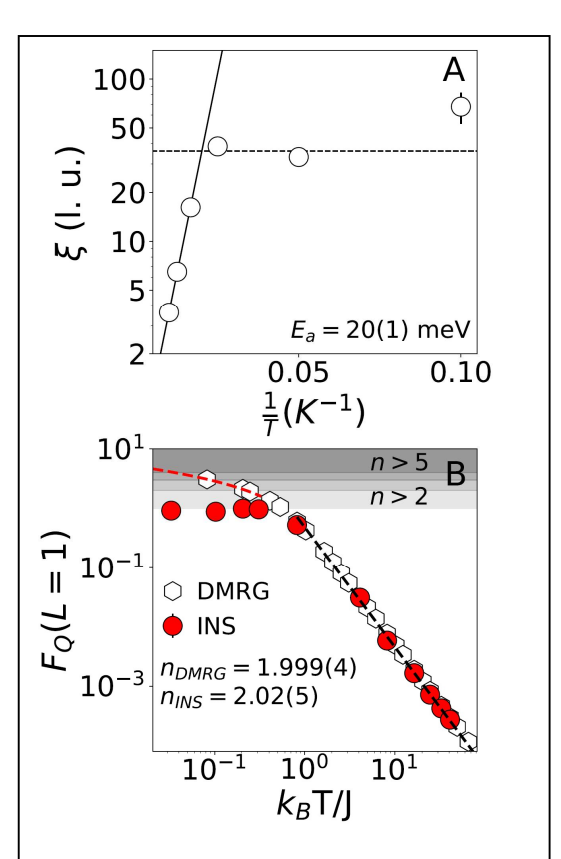


Figure 1. (A) Quantum spinon coherence length in YbAlO<sub>3</sub> obtained using the measured spinon dispersion and lifetime extracted from the spectral broadening. (B) Temperature dependence of maximal quantum Fisher information,  $F_0(L = 1)$ . Dashed black line is a power-law fit to the data in  $T \ge 2$  K range capturing asymptotic high-temperature behavior, FQ  $\sim$  (J/T)<sup>n</sup>, with n = 2. Dashed red curve, shown in the region below  $T_N = 0.8 \text{ K}$  (shaded), is a fit of DMRG data below 4 K to a logarithmic dependence, illustrating the asymptotic behavior.

Project Title: Understanding the Many-body Properties of Rare Earth-Based Materials Relevant to

**Next Generation QIS Applications** 

**Award Number: PM-062** 

Abstract Title: Witnessing Quantum Entanglement Using Resonant Inelastic X-ray Scattering

Names of PI, coPI: Mark P. M. Dean¹(co-PI), Jonathan Pelliciari¹(co-PI), Robert M. Konik¹ (PI), Igor Zaliznyak¹(co-PI), Wei He¹ (Postdoc), Lazar Kish¹ (Postdoc), Yao Shen¹, Sophia TenHuisen⁴, Mary H. Upton², Diego Casa², Petra Becker³, Matteo Mitrano⁴, Jennifer Sears¹ (unfunded collaborators)

**Affiliations:** <sup>1</sup>Brookhaven National Laboratory, <sup>2</sup>Argonne National Laboratory, <sup>3</sup>University of Cologne, <sup>4</sup>Harvard University

**Abstract:** Quantum entanglement is a fundamental property underpinning quantum many-body physics and emerging quantum technologies, such as quantum metrology, communication, and sensing. Although there are many approaches for quantifying entanglement in synthetic quantum systems, most of these are impractical for solid-state quantum materials, due to either the large number of atoms in such materials or the lack of fine-scale control. The creation and control of coherence in solid-state quantum systems requires improved methodology to detect entanglement.

Recent years has seen impressive progress in the use of neutron spectroscopy to detect entanglement in solids [1]. This has been proven to be a sensitive means to quantify spin entanglement. Resonant inelastic x-ray scattering (RIXS) is an advanced experimental method capable of detecting the spin, lattice, orbital, and charge degrees of freedom in quantum materials, with capabilities for measuring under device like conditions such as under electrical current or after illumination with a laser [2]. The RIXS process, show in the left panel of Figure 1, involves the resonant absorption of an x-ray photon, creating an intermediate state with a core hole and a valence excitation, before the hole is filled via the emission of another x-ray photon. By measuring the energy and momentum change of the x rays, one can infer the properties of the excitations created in the material.

At Brookhaven we have developed methods to use RIXS to quantify orbital entanglement of spin states in solids [3] as illustrated in Fig. 1. Our approach builds on the so-called quantum Fisher information (QFI) metric, which is connected to the probability distribution of measurements and the corresponding parameter estimation in a multiparticle quantum system. If the precision of a parameter estimation exceeds the classical limit, then it can be deduced that the system must have multipartite entanglement. Since the quantum operator associated with neutron scattering operator is Hermitian, it can be directly applied to obtain the QFI. For RIXS, the operator is non-Hermitian, and we needed to develop a new approach.

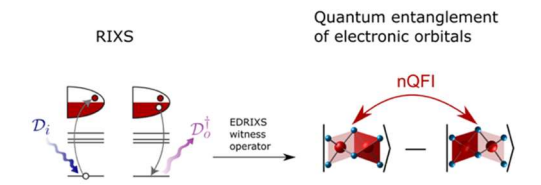


Figure 9: Witnessing orbital entanglement using RIXS. In this work, we develop a joint experimental-theoretical method to obtain an orbital entanglement witness from the RIXS intensity. We have developed a method to use RIXS to obtain the normalized quantum Fisher information (nQFI) for detection of the quantum entanglement.

The first step in the process is to measure the RIXS spectrum of the material of interest. We are currently working on transition metal and rare earth systems such as Ba<sub>3</sub>CeIr<sub>2</sub>O<sub>9</sub>, Yb:YAG, Yb:YAP. We first obtain the RIXS operator as a function of incident energy and incoming and outgoing x-ray polarization for the orbital system in question using the numerical codebase EDRIXS [4] by fitting the observed empirical spectrum to a simulation as shown in Fig. 2. We then compute the nQFI from the RIXS operator and determine the optimum conditions to detect entanglement. For example, the right panel of Figure 2 shows show the RIXS-determined nQFI for Ba<sub>3</sub>CeIr<sub>2</sub>O<sub>9</sub> varies with x-ray momentum. Choosing specific angles corresponding to constructive interference between dimer sites allows the detection of multipartite entanglement based on the values exceeding the dotted red line.

We are currently completing our studies of Yb spin systems Yb:YAG and Yb:YAP under laser illumination corresponding to the J=7/2 to 5/2 transition that is widely used in laser and communication technologies. We are also extending our work to Yb implanted van der Waals materials.

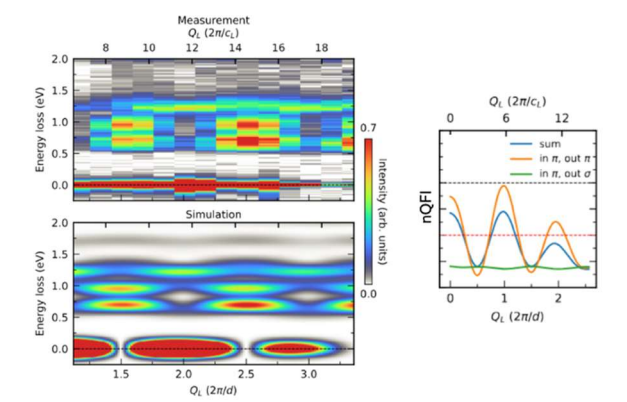


Figure 10: Top left: Ir L<sub>3</sub>-edge RIXS spectrum of Ba<sub>3</sub>CeIr<sub>2</sub>O<sub>9</sub> as a function of energy loss and momentum. Bottom left: EDRIXS simulation of the spectrum above made using the EDRIXS software based on a model for the active Ir 5d<sup>5</sup> orbitals. Right: nQFI as function of momentum for different outgoing x-ray polarizations.

- [1] A. Scheie, P. Laurell, A. M. Samarakoon, B. Lake, S. E. Nagler, G. E. Granroth, S. Okamoto, G. Alvarez, and D. A. Tennant, Witnessing entanglement in quantum magnets using neutron scattering, Phys. Rev. B 103, 224434 (2021)
- [2] Exploring Quantum Materials with Resonant Inelastic X-Ray Scattering, M. Mitrano, S. Johnston, Young-June Kim, and M. P. M. Dean, Phys. Rev. X 14, 040501 (2024)
- [3] (funded by this project) Witnessing Quantum Entanglement Using Resonant Inelastic X-ray Scattering, Tianhao Ren, Yao Shen, Sophia F. R. TenHuisen, Jennifer Sears, Wei He, Mary H. Upton, Diego Casa, Petra Becker, Matteo Mitrano, Mark P. M. Dean, and Robert M. Konik, arXiv: 2504.16653 (2024), https://doi.org/10.48550/arXiv.2404.05850.
- [4] EDRIXS: An open-source toolkit for simulating spectra of resonant inelastic x-ray scattering, Y.L. Wang, G. Fabbris, M.P.M. Dean, and G. Kotliar, Com. Phys. Comm. 243, 151–165 (2019)

#### DNA-Controlled Dye Aggregation – A Path to Create Quantum Entanglement

#### DE-SC0020089

Toward Measuring an Exciton-Exciton Coherence in a DNA-Assembled Molecular Aggregate

P. H. Davis, a,b J. E. Anthony, G. C. Dean, R. J. Stanley, Lee, Li,a,b O. A. Mass, B. Yurke, A,G W. B. Knowlton, E. W. Martin, P. C. Arpin, D. B. Turner, and R. D. Pensack

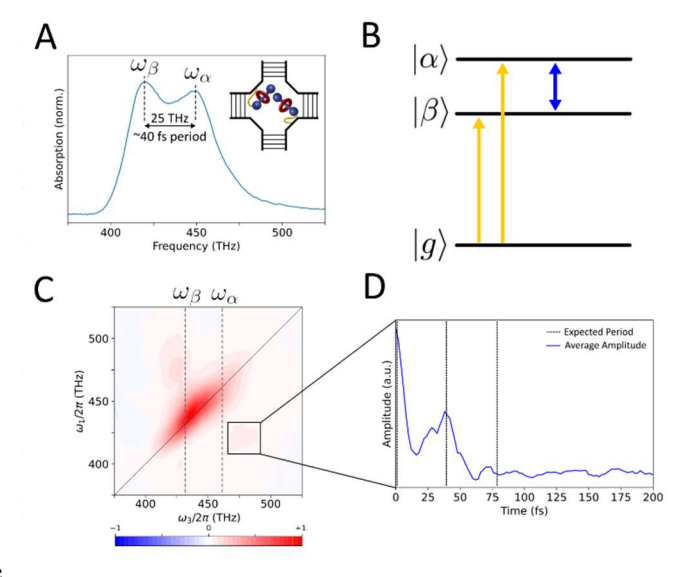
<sup>a</sup>Micron School of Materials Science and Engineering, <sup>f</sup>Department of Chemistry and Biochemistry, and <sup>g</sup>Department of Electrical and Computer Engineering, Boise State University, Boise, ID 83725. <sup>b</sup>Center for Advanced Energy Studies, Idaho Falls, ID 83401. <sup>c</sup>Department of Chemistry, University of Kentucky, Lexington, KY 40506. <sup>d</sup>Department of Chemistry and Physics, Southern Utah University, Cedar City, UT 84720. <sup>c</sup>Department of Chemistry, Temple University, Philadelphia, PA 19122. <sup>b</sup>MONSTR Sense Technologies, Ann Arbor, MI 48108. <sup>c</sup>Department of Physics, California State University–Chico, Chico, CA 95929.

Abstract: Our emphasis has been on engineering and assembling materials and building tools and analysis techniques to directly measure an exciton-exciton coherence, a key ingredient in quantum entanglement, in DNA-assembled molecular aggregates. A key significant prior development, which refined our scope, includes the discovery of squaraine:rotaxane dimers that have an oblique orientation and as such optical properties making them ideally suited to produce exciton-exciton coherence ( $\omega_h$  and  $\tau_d$ ) and entanglement. In addition, we are working to characterize the difference dipole moment ( $\Delta d$ ) of chromophores, which governs the amplitude of exciton-exciton interactions (K), also important in creating entanglement in molecular aggregates.

In pursuit of our goal to measure an exciton-exciton coherence, we refined a noncollinear optical parameter amplifier (NOPA) for producing very stable, spectrally flat, excellent spatial mode quality, and transform-limited ultrabroadband laser pulses, designed and constructed a phase-stable interferometer enabling 2D spectroscopy in the pump-probe geometry, which has higher stability and is more compatible with cryostats, and applied analysis techniques (previously only theorized) to determine if measured quantum beats are purely electronic (*i.e.*, exciton-exciton coherence), mixed electronic-vibronic, or purely vibrational.

We recently incorporated a 77 K cryostat into our optical setup, which should extend the quantum beats and improve our ability to resolve them. The figure at right shows the preliminary measurements that seemingly indicate excitonexciton coherence, however we are conducting numerous control measurements to confirm this conclusion. Our future plans include incorporating a 4 K cryostat into our optical setup, which will dramatically improve our ability to resolve and analyze the exciton-exciton After directly measuring and coherence. confirming the presence of exciton-exciton we will perform polarization coherence. determine whether measurements to coherence is indicative of entanglement, a longstanding goal in studies of molecular aggregates for the past two decades.

In parallel with the efforts above, we identified mechanisms in molecular materials that act to drastically reduce the singlet excited-state lifetime ( $\tau_p$ ), which can, under certain conditions, be detrimental to  $\tau_d$ . While in-house synthesized bacteriochlorins (BCs) featuring both dimethylamino and nitro groups appear to increase  $\Delta d$ ,<sup>3</sup> the latter substituents have a detrimental influence on  $\tau_p$  in polar solvents.<sup>4</sup> We



A) Schematic and steady-state absorption of the oblique SeTau670 dimer tethered to a DNA Holliday junction. B) Energy level diagram, with exciton-exciton coherence between states  $|\alpha\rangle$  and  $|\beta\rangle$  shown in blue. C) Normalized 2D spectrum with states  $|\alpha\rangle$  and  $|\beta\rangle$  (dashed lines). D) The average amplitude of the cross peak between  $|\alpha\rangle$  and  $|\beta\rangle$  as a function of time, with expected period of the coherence (dashed lines). One period of the exciton-exciton coherence appears to have been detected.

also identified a material system that is able to overcome aggregation-induced quenching (AIQ), a phenomenon we ascribe to the introduction of new internal conversion pathways that drastically reduce  $\tau_p$  upon aggregation (manuscript in revision). Our results suggest that it may be possible to overcome AIQ by tailoring the environment of the aggregate, that is, tailoring the local sterics and electrostatics.

Additionally, in pursuit of our goal to characterize  $\Delta d$  of chromophores, we constructed an electroabsorption spectrometer.<sup>5</sup> We used the spectrometer to characterize  $\Delta d$  of field standards, common dyes, and organic semiconductors with biocompatible tags (manuscript in preparation).

References: ¹Carbery et al. Rev. Sci. Instrum. **95**, 033002 (2024). doi: 10.1063/5.0187338 ²Barclay et al. Opt. Lett. **49**, 2065 (2024). doi: 10.1364/OL.519387 ³Ketteridge et al. J. Phys. Chem. A **128**, 7581-7592 (2024). doi: 10.1021/acs.jpca.4c03821 ⁴Duncan et al. J. Phys. Chem. C In press (2025). doi: 10.1021/acs.jpcc.5c01649 ⁵Huff et al. Rev. Sci. Instrum. **94**, 094103 (2023). doi: 10.1063/5.0153428

#### **Robust Quantum Computing for Condensed Matter Physics**

#### DE-SC0023231

**Alexander Kemper (PI)**, Department of Physics, North Carolina State University; and **James Freericks** (co-PI), Department of Physics, Georgetown University

#### **Abstract:**

In this talk, I will discuss advances we have made in bringing the power of quantum computers to bear on solving problems in condensed matter systems, in particular focusing on predicting or simulating spectroscopic experiments of systems in and out of equilibrium, which is the primary goal of this QIS project.

First, I will a **linear response framework** for quantum simulation, which establishes a direct bridge between what we can measure experimentally and the fundamental **quantum many-body state** of a material. The core of this method is its ability to compute crucial **bosonic and fermionic correlation functions** directly on a quantum computer. Unlike previous techniques, it allows for a wide range of operators within a single quantum circuit, which means you can acquire multiple

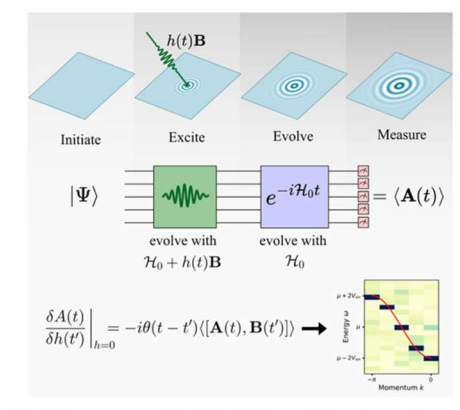
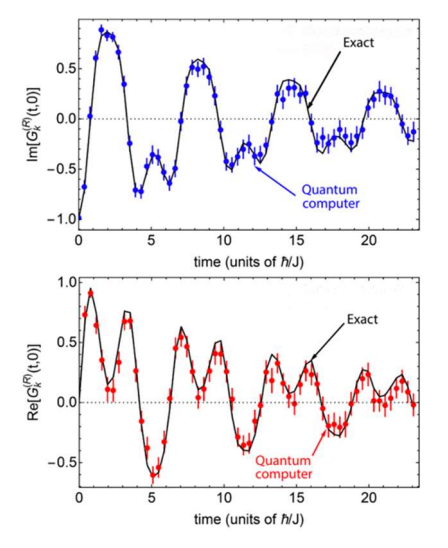


Fig. 1 | Linear response method. We establish an equivalence between the experimental measurement of a response function and an ancilla-free quantum simulation under a time dependent Hamiltonian that includes the perturbative excitation h(t)B. Following excitation, the system is evolved under  $\mathcal{H}_0$ , and A is measured. The functional derivative of  $\mathcal{A}(t) = (A(t))$  with respect to h(t) yields the retarded response function shown in the flagure. The data shown is taken from Fig. 3.

types of correlation functions—both frequency- and momentum-selective—simultaneously. This is a significant advantage because it avoids compounding errors and eliminates the need for extra "ancilla" qubits, making the process more efficient and reliable. We demonstrate this framework by applying it to a **charge-density-wave material** using IBM's quantum hardware (specifically, the ibm\_auckland superconducting quantum computer). Even in a noisy quantum computing environment, the method successfully extracted meaningful data, highlighting its robustness. This research significantly advances the possibility of using **quantum computers** to accelerate the discovery and design of new **quantum materials**. By providing a streamlined way to calculate these complex response functions, it not only enhances the capabilities of current and near-term quantum devices but also suggests potential improvements for classical simulations by offering a path to bypass computationally intensive vertex corrections. NatComm 2024, 10.1038/s41467-024-47729-z.

As an interlude, I will briefly introduce a new property of Green's functions and other observables, which allows for a form of error correction of experimental spectra (including quantum simulated spectra). PRL 2024, 10.1103/PhysRevLett.132.160403

Finally, I will pivot to the problem of open quantum system dynamics. Our work explores the simulation of **open quantum systems** on near-term quantum hardware, addressing the critical challenge of how quantum systems interact with their environment, and highlighting the potential of current quantum computers to tackle problems traditionally difficult for classical methods, particularly in the context of driven and dissipative phenomena.



Our work, completed under this project, shows that algorithms for open quantum systems outperform similarly complex nondissipative algorithms on noisy hardware. The first paper, "Simulating open quantum systems on quantum hardware with robustness to hardware errors," focuses on the remarkable robustness of open quantum system simulations to hardware errors, even with deep circuits involving up to two thousand entangling gates. This capability raises the need to be able to probe these systems spectroscopically, so int a second paper, "Measuring n-point correlation functions in open quantum systems on a quantum computer," we propose a unified hierarchical method for measuring n-point correlation functions in open or nonequilibrium quantum systems. This method involves repeatedly interrupting the system's time evolution with an ancilla qubit interaction and immediate measurement. We emphasize the robustness of this technique compared to other ancilla-based

interferometric methods like the Hadamard test, making it well-suited for noisy, near-term quantum computers. The paper demonstrates its efficacy by measuring single-particle Green's functions of a driven-dissipative fermionic system on a quantum computer, proving that dynamical correlation functions for such systems can be reliably obtained. NPJQI 2025, 10.1038/s41534-025-00964-8, and PRL 2024 0.1103/PhysRevLett.132.100601.

Both papers contribute to the growing field of quantum simulation of open systems. Together, they offer compelling evidence for the feasibility and promise of using near-term quantum computers to explore complex, environmentally coupled quantum phenomena.

## Trade off-free entanglement stabilization in superconducting circuits

Award Number: DE-SC0019461

Names of PI, coPI(s), and unpaid collaborators: <u>Leonardo Ranzani</u> (RTX-BBN Technologies), Archana Kamal<sup>2,3</sup>, Guilhem Ribeill<sup>1</sup>, Luke Govia<sup>1</sup>, Raymond Simmonds<sup>4</sup>, Jose Aumentado<sup>4</sup>, Daniel Campbell<sup>5</sup>, Tristan Brown<sup>1,2</sup>, Zhihao Xiao<sup>2</sup>, Emery Doucet<sup>2</sup>, Tarush Tiwari<sup>1,2</sup>

RTX BBN Technologies<sup>1</sup>, University of Massachusetts Lowell<sup>2</sup>, Northwestern University<sup>3</sup>, NIST Boulder<sup>4</sup>, Air Force Research Laboratory, Rome<sup>5</sup>

#### Abstract:

In the PIQUE project we aim to demonstrate novel techniques and devices to control and measure quantum systems using parametric interactions and engineered dissipation [1]. In this abstract we focus on the demonstration of autonomous state stabilization of a maximally entangled state of two transmons [2]. Unlike traditional protocols, PIQUE minimizes coherent leakage out of the target state, thus avoiding any inherent trade off between target state preparation fidelity and convergence time. We accomplish this by creating a purely dissipative channel for population transfer into the target state (Figure 1(a)), mediated by strong parametric interactions coupling the second-excited state of a superconducting transmon and the engineered bath resonator. Our scheme achieves a state preparation fidelity of 84% with a stabilization time

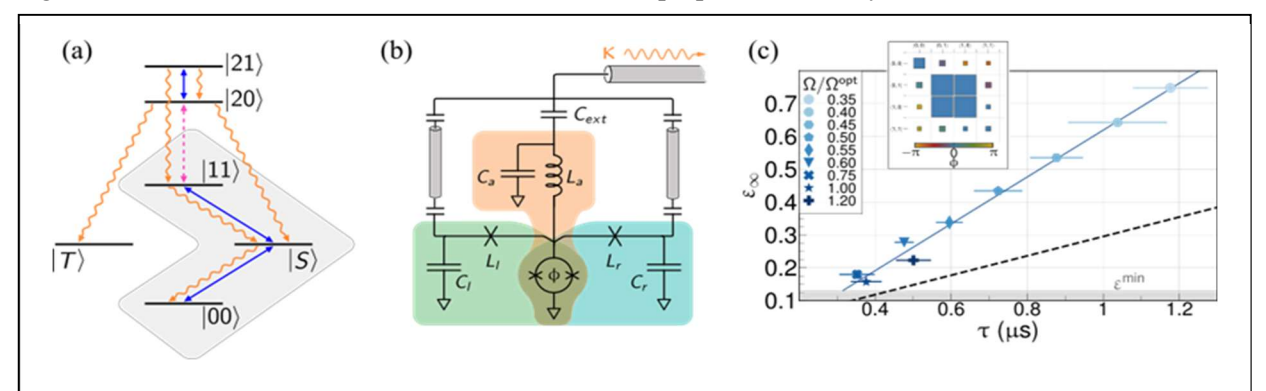


Figure 1 – (a) Energy level diagram showing dissipative preparation of Bell state. (b) Circuit schematic of the device, consisting of two transmons and a resonator connected by a joint SQUID. The resonator provides a controlled bath with finite linewidth. (c) As we increase the drive strength, preparation error and time decrease monotonically, achieving state fidelity limited only by qubit intrinsic decoherence (quantum state tomography in the inset).

constant of 339 ns, leading to a state-of-the-art 54 ns error-time product in a solid-state quantum information platform (Figure 1(c)).

In order to scale our technique to multi qubit systems, we developed a new modular tunable coupler that minimizes spurious crosstalk and maximizes linearity. The coupler (Figure 2(a)) consists of two ancilla qubits connected by a small Josephson junction. The qubits hybridize and mediate a strong interaction with an intrinsic cancellation point (Figure 2(b)), which is first order insensitive to the data qubit frequencies and results in low ZZ interaction. Moreover, at the cancellation point the effective coupling rate is approximately linear in flux, enabling fast parametric coupling and suppressed nonlinear frequency shifts.

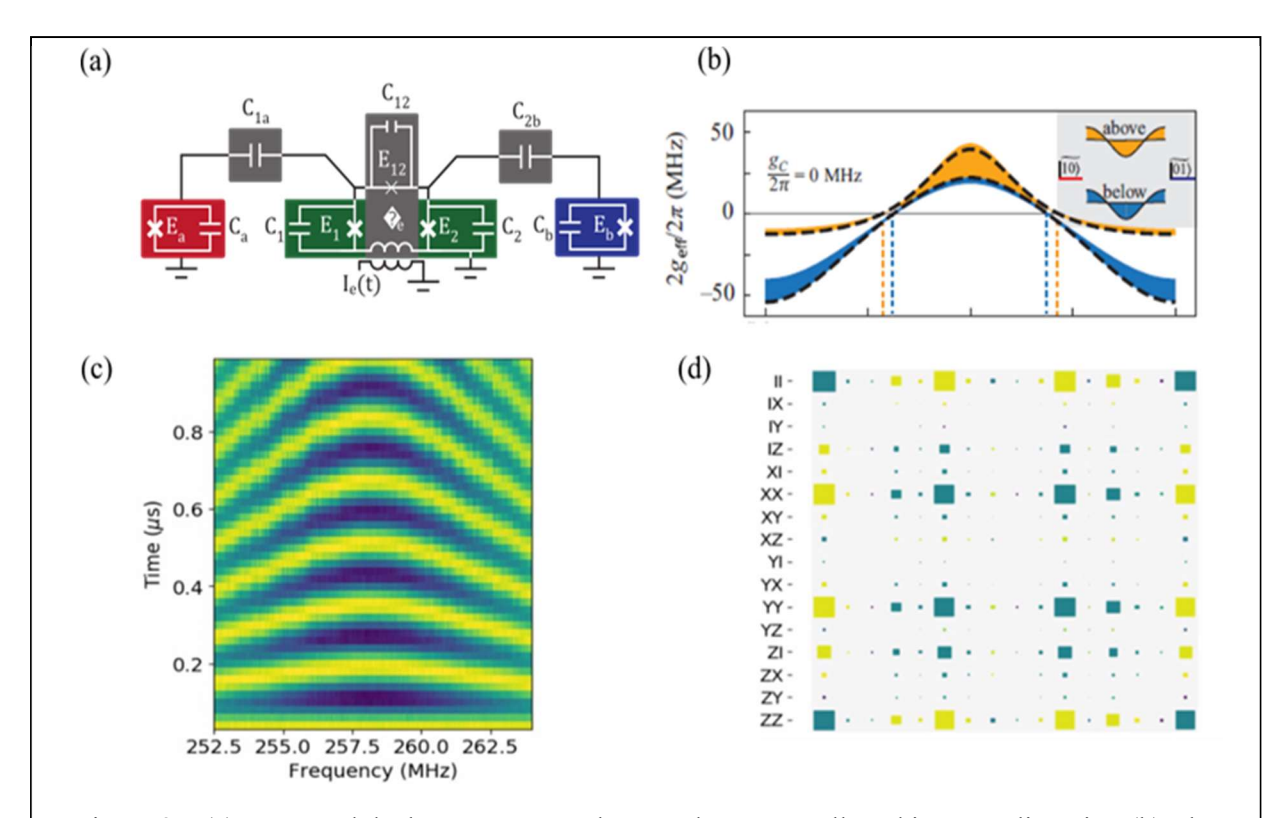


Figure 2 – (a) Improved dual transmon coupler to reduce crosstalk and improve linearity. (b) The coupler has an intrinsic zero coupling flux point near 0.25. (c) Measured parametric iSWAP between the data qubits and (d) quantum process tomography with 97% gate fidelity.

- [1] Doucet E, Reiter F, Ranzani L, Kamal A. *High fidelity dissipation engineering using parametric interactions*, **Physical Review Research**, 2, no. 2, (2020):023370.
- [2] Brown, T., E. Doucet, D. Ristè, G. Ribeill, K. Cicak, J. Aumentado, R. Simmonds, L. Govia, A. Kamal, and L. Ranzani. *Trade off-free entanglement stabilization in a superconducting qutrit-qubit system*, **Nature communications** 13, no. 1 (2022): 3994.
- [3] Campbell, D.L., Kamal, A., Ranzani, L., Senatore, M. and LaHaye, M.D., *Modular tunable coupler for superconducting circuits*, **Physical Review Applied**, 19, no. 6 (2023): 064043.

### **Quantum Sensing of Magnons Using a Qubit**

<u>Wolfgang Pfaff<sup>1,2</sup></u>, Sonia Rani<sup>1</sup>, Xi Cao<sup>1</sup>, Alejandro E. Baptista<sup>1</sup>, Philip Kim<sup>1</sup>, Pratap Kumar Pal<sup>3</sup>, Yi Li<sup>3</sup>, Valentine Novosad<sup>3</sup>, and Axel Hoffmann<sup>1,2,4</sup>

- 1. Department of Physics, University of Illinois Urbana-Champaign, Urbana, IL 61801, USA.
- 2. Materials Research Laboratory, University of Illinois Urbana-Champaign, Urbana, IL 61801, USA.
- 3. Materials Science Division, Argonne National Laboratory, Lemont, IL 60439, USA.
- 4. Department of Materials Science and Engineering, University of Illinois Urbana-Champaign, Urbana, IL 61801, USA.

#### **Abstract**

We are investigating coherent dynamics of propagating magnons in hybrid magnetic devices down to the single quantum regime and implement these effects in quantum coherent operations with circuit quantum electrodynamics (cQED) systems. Towards this end, our ultimate goal is to develop magnetic field-tolerant superconducting quantum devices and use them to engineer interactions between qubits and magnons. As a first step, we realized an integrated, hybrid cQED-magnon system integrating a superconducting transmon qubit with a YIG sample biased locally by permanent magnets [1]. Using this hybrid system, we performed high-sensitivity/high-dynamic range sensing of magnons and their dynamics (see Fig. 1): Using qubit spectroscopy we sensitively measured the occupation number of the Kittel mode of YIG with a sensitivity of a few magnon/ $\sqrt{\rm Hz}$  over a dynamic range of about 2000 magnons. Using quantum control of the qubit dynamics we also measured the decay dynamics of the Kittel mode with a sensitivity of a few ns/ $\sqrt{\rm Hz}$ , and we demonstrated a technique for resolving fast decay dynamics using a parametric pumping technique.

Since standard transmons are highly susceptible to magnetic fields we have begun to investigate field-compatible superconducting thin films as platforms for field-resilient quantum circuits. We fabricated and characterized thin-film co-planar waveguide and lumped-element resonators made from disordered superconductors (TiN and NbTiN) that have high critical fields in intrinsic nonlinear kinetic inductance (NLKI). We found high quality factors in such devices and characterized their nonlinearity. We observed strong pump-induced Stark shifts of the resonator frequency and obtained initial evidence that this nonlinearity is sufficient to dynamically control the hybridization between statically coupled resonators.

For future quantum circuit development, we will work towards the development of a field compatible quantum circuit platform with tunable interactions. Towards this end, we will work with magnetic-field-compatible eNe qubits and single-crystal YIG. The goal is to achieve strong coupling between the magnon state of a YIG sphere and the qubit state of an eNe qubit, mediated by microwave photons in a coplanar

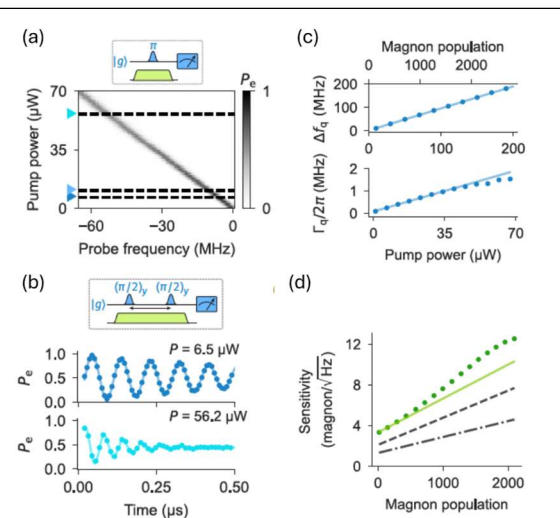


Fig. 1: (a) Qubit frequency shift as a function of pump power applied to magnon mode. (b) Ramsey decay of qubit for different pump powers. (c) Stark-shifts and dephasing rates as a function of pump power and magnon population. (d) Magnon sensitivity as a function of population.

superconducting resonator. We will explore the magnetic field tolerance of the eNe qubit and study the

evolution of coherence under strong magnetic fields in order to explore the frequency limitation of this architecture.

We also plan to study the integration of eNe qubit with YIG thin-film samples and explore quantum sensing of a single propagating magnon. For this planned work, we will continue working on magnon-photon coupling with a coplanar superconducting resonator fabricated on YIG thin films and explore time-domain coherent control of propagating magnons, similar to our recent Nature Communications publication about time-domain coherent magnon control in YIG spheres. Furthermore, we plan to explore the operation of an eNe qubit which is fabricated on YIG thin film instead on a Si substrate and study the compatibility of eNe qubit on magnetic thin film.

With respect to using superconducting qubits, we will pursue two complementary strategies. First, we will investigate the interplay of non-linear kinetic inductance (NLKI) and intrinsic quality factor, Q. If high NLKI and high Q can coexist, we will be able to develop nonlinear high-Q resonators that are field-compatible, and that can be coupled on-demand to magnon-polariton modes through a microwave pump. Second, we will use thin-film NbTiN as base layer to realize field-compatible superconducting "SNAIL-mon" qubits that combine high coherence with 3-wave mixing capability. If these qubits can be made with high-coherence in an external magnetic field, they will allow for strong tunable interactions between quantum circuit and magnon-polariton modes.

#### References

4. S. Rani, X. Cao, A. E. Baptista, A. Hoffmann, and W. Pfaff, *High dynamic-range quantum sensing of magnons and their dynamics using a superconducting qubit*, Phys. Rev. Appl., in press (2025), arXiv:2412.11859; doi:10.48550/arXiv.2412.11859.

## Modeling, probing, and controlling quantum coherence in materials FWP: SCW1674, DE-SC0020313

Modeling, probing, and controlling defects in materials for superconducting qubits and spin qubits

Alex Abelson<sup>1</sup>, Loren D Alegria<sup>1</sup>, **Victor Brar**<sup>2</sup>, Kevin R Chaves<sup>1</sup>, Yujin Cho<sup>1</sup>, **Jennifer Choy**<sup>2</sup>, Soohyun Im<sup>3</sup>, **Shimon Kolkowitz**<sup>4</sup>, **Alex Levchenko**<sup>2</sup>, **Vincenzo Lordi**<sup>1</sup>, Sean R O'Kelley<sup>1</sup>, Eunjeong Kim<sup>1</sup>, Luis A Martinez<sup>1</sup>, **Robert McDermott**<sup>2</sup>, <u>Keith G. Ray</u><sup>1</sup>, **Yaniv Rosen**<sup>1</sup>, **Paul M Voyles**<sup>2</sup>, and Christopher D Wilen<sup>2</sup>

<sup>1</sup>Lawrence Livermore National Laboratory, <sup>2</sup>University of Wisconsin — Madison, <sup>3</sup>University at Buffalo, <sup>4</sup>University of California, Berkeley

Different superconducting qubits on the same chip, or the same qubit at different times, can exhibit different relaxation times. This may be caused by different distributions of TLSs in frequency, electric dipole, and location in the qubit device. To explore the effect of TLS distribution in frequency and space, we developed a model of the interactions between the qubit and over 300 different baths consisting of 200 TLSs each. We found that TLSs in regions of high electric field in the resonator can significantly reduce the qubit coherence time, with the strongest electric fields contained in the Josephson junction (JJ). However, TLSs away from the JJ can also reduce qubit lifetime. We find that in some cases a single TLS reduces the qubit lifetime and in other cases a collection of more weakly coupled TLSs also reduce qubit lifetime [1].

To understand the nature of the TLS landscape under different conditions, we have performed TLS spectroscopy on a superconducting resonator by applying an electric bias that shifts the TLS asymmetry energy, thus bringing TLSs into and out of resonance. TLSs can then be seen as avoided crossings in the resonator transmission spectra that are hyperbolic. We also applied a large alternating electric bias while at low temperature and found that TLS hyperbolae are no longer visible, indicating a profound change in the TLS landscape. Engineering the TLS landscape could allow for qubits with dramatically longer coherence times. In another study, we analyzed TLS density and loss in tantalum superconducting resonators, finding that the grain structure and growth conditions affect loss [2]. We also used scanning electron microscopy, x-ray diffraction, low-T transport, secondary ion mass spectrometry, and transmission electron microscopy to reveal the dependence of residual impurities and screw dislocation density on Ta growth conditions [3]

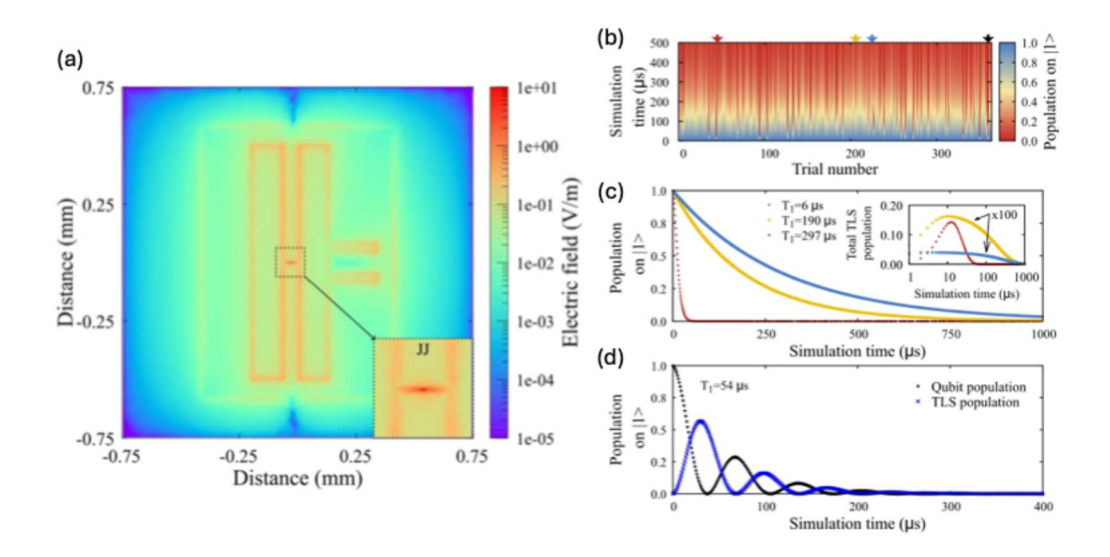


Figure 1: (a) Electric field distribution of the superconducting qubit, Josephson junction indicated. (b) Time-dependent qubit population for 364 simulated TLS baths, blue (red) indicates the excited (ground) state. (c) Linecuts for the three cases indicated by the colored arrows in panel (b), showing qubit relaxation curves when the qubit  $T_1$  is shortest (6.33  $\mu$ s, red), average (189.96  $\mu$ s, yellow), and longest (296.81  $\mu$ s, blue). Inset: corresponding total population of TLS excited states as a function of time. (d) When  $\Delta_0$  of the strongly coupled TLS is small and  $\mathbf{p} \cdot \mathbf{E}$  is large, corresponding to the trial indicated by the black arrow in panel (b), we observe an exchange of population between the qubit excited state and the collective TLS excited state. Figure adapted from Ref. [1]

We have investigated charge noise in a tantalum transmon qubit and found the charge-offset dynamics are dominated by rare, discrete jumps between a finite number of quasistationary charge configurations, a novel behavior [4]. In another study related to charge noise, calculations on defects in a  $Si_{1-x}Ge_x$  spin qubit revealed that Ge dangling bonds are more problematic charge-trapping centers than Si dangling bonds [5]. Similar computational studies on defect levels in  $Al_2O_3$  have informed upcoming work on identifying defects in that material using KPFM.

- [1] Yujin Cho, Dipti Jasrasaria, Keith G Ray, Daniel M Tennant, Vincenzo Lordi, Jonathan L DuBois, and Yaniv J Rosen. Simulating noise on a quantum processor: interactions between a qubit and resonant two-level system bath. *Quantum Science and Technology*, 8(4):045023, 2023. doi:10.1088/20589565/acf685.
- [2] Loren D Alegria, Daniel M Tennant, Kevin R Chaves, Jonathan RI Lee, Sean R O'Kelley, Yaniv J Rosen, and Jonathan L DuBois. Two-level systems in nucleated and non-nucleated epitaxial alphatantalum films. *Applied Physics Letters*, 123(6), 2023. doi:10.1063/5.0157654.
- [3] Loren D Alegria, Alex Abelson, Eunjeong Kim, Soohyun Im, Paul M Voyles, Vincenzo Lordi, Jonathan L DuBois, and Yaniv J Rosen. Growth and structure of alpha-ta films for quantum circuit integration. *Journal of Applied Physics*, 137(4), 2025. doi:10.1063/5.0245710.
- [4] Daniel M Tennant, Luis A Martinez, Kristin M Beck, Sean R O'Kelley, Christopher D Wilen, R McDermott, Jonathan L DuBois, and Yaniv J Rosen. Low-frequency correlated charge-noise measurements across multiple energy transitions in a tantalum transmon. *PRX Quantum*, 3(3):030307, 2022. doi:10.1103/PRXQuantum.3.030307.
- [5] Joel B Varley, Keith G Ray, and Vincenzo Lordi. Dangling bonds as possible contributors to charge noise in silicon and silicon–germanium quantum dot qubits. *ACS Applied Materials & Interfaces*, 15 (36):43111–43123, 2023. doi:10.1021/acsami.3c06725.

Prepared by LLNL under Contract DE-AC52-07NA27344

## Carbon-Based Quantum Information Science with Symmetry Protected Topological States DE-SC0023105

### Abstract Title: Engineering low energy modes in 1D and 2D quantum materials

Felix R. Fischer, 1,2,3,4 Michael F. Crommie, 5,2,3 and Steven G. Louie 5,2

<sup>1</sup>Department of Chemistry, University of California Berkeley. <sup>2</sup>Materials Sciences Division, Lawrence Berkeley National Laboratory. <sup>3</sup>Kavli Energy NanoSciences Institute at the University of California Berkeley and the Lawrence Berkeley National Laboratory. <sup>4</sup>Bakar Institute of Digital Materials for the Planet, Division of Computing, Data Science, and Society, University of California Berkeley. <sup>5</sup>Department of Physics, University of California Berkeley.

**Abstract:** The unmatched quality and atomically precise control over quantum electronic states in low-dimensional materials provided by a synthetic bottom-up approach represents a fertile ground for the discovery and engineering of new phases of matter with potential to advance quantum information transport, storage, and processing (I-I2). In these materials emergent phenomena arising from unique interactions of energy and disparate states of matter at atomic and molecular length-scales can be rationally designed and shaped by theory, molecular design, and quantum physics. Research efforts throughout this grant period have been organized into two themes.

Progress in 1D systems: Bottom-up synthesized graphene nanoribbons (GNRs) have emerged as testbeds for realizing simple quantum systems due to extensive opportunities to engineer their electronic structure and the ease of creating localized symmetry protected topological (SPT) states within a bulk energy gap. We successfully implemented topological zero modes (ZMs) as the basis states for the engineering of effective low-energy designer Hamiltonians in the strongly hybridized regime. In the symmetric case, realized in the topological junction interface of a 9/7/9-double quantum dot, the strong hybridization between adjacent ZMs gives rise to an exceptionally small quasiparticle gap of 0.16 eV, corresponding to a carbon-based small molecule long-wavelength infrared (LWIR) absorber (6). The case of staggered basis state energies is realized in the dilute nitrogen core-doped armchair GNRs. Here the interaction of topological boundary states at the interface between doped and undoped segments can be captured by an effective Hamiltonian where the hybridization interaction strength is tuned by the distance between topological ZMs (8). To explore the weakly hybridized regime we successfully stabilized SPT end states lining the zigzag edges of armchair GNRs by lateral fusion with 5-membered rings (3). As a function of GNR length we observe a gradual decrease of the magnetic exchange coupling 136 meV > J > 9 meV between off-zero mode end states reflected in an evolution from a closed-shell to an open-shell singlet ground state. Critical advancements to molecular on-surface synthesis protocols have enabled the realization of inversion symmetry breaking in the structure of [3]triangulene-GNRs (7). WE developed the head-to-tail fusion of [3] triangulene cores featuring a S = 1 ground state to ensure and effective mixing of the majority and minority sublattices between molecular building blocks. The resulting electronic structure is characterized by a strongly hybridized gapped bulk phase featuring magnetic SPT end states.

Progress in 2D systems: Building on our initial success in assembling metal-organic Kagome lattices from N-heterocyclic carbenes (5) we expanded the concept of ZM engineering to access hopping frustrated flat bands in nanographene frameworks. We reported the design and synthesis of a strongly hybridized  $\pi$ -conjugated COF featuring high-spin ( $S = \frac{3}{2}$ )  $D_{3h}$ symmetric aza-[3]triangulene (A[3]T) cores linked by ethynylene groups (−C≡C−) fused normal to their zigzag edges (Fig. 1). The electronic structure of this edge-sharing 2D A[3]T crystal can be modeled as a diatomic Kagome lattice. Each A[3]T unit cell hosts a set of symmetry-related sixfold degenerate Wannier basis states giving rise to a pair of valence band (VB) and conduction band (CB) complexes, each featuring a non-trivial Kagome flat band, bracketing the Fermi energy  $(E_{\rm F})$  (11). In a related effort we demonstrated the covalent assembly of a honeycomb lattice of corner linked high-spin ( $S = \frac{3}{2}$ )  $D_{3h}$  symmetric [4]triangulene cores. While electronic theory had predicted a nonmagnetic ground state reminiscent of a ying-yang diatomic Kagome lattice we were able to show that weak hybridization between corner sharing [4]triangulene cores favor a magnetically ordered ground state best described by a Néel antiferromagnet.

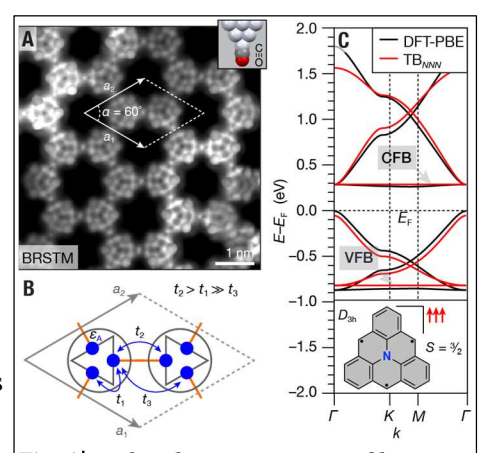


Fig. 1 | Molecular engineering of hopping frustrated flat bands in A[3]TCOFs. (A) Constant-height BRSTM image of a representative segment of the *p6mm* lattice of A[3]TCOF. (B) Intra- and interunit cell electron hopping parameters (t, t;) and onsite energy ( $\varepsilon$ A) for a diatomic Kagome lattice. (C) DFT-PBE band structure for a freestanding A[3]TCOF Kagome lattice (11).

Future directions: Engineering geometric frustration in 1D and 2D spin lattices with bottom-up synthesized nanographenes (e.g. triangular/Kagome lattice, diamond Heisenberg chain).

**Publications:** (9 published, 1 accepted, 2 under review)

- 1. McCurdy, R. D.; Delgado, A.; Jiang, J.; Zhu, J.; Wen, E. C. H.; Blackwell, R. E.; Veber, G. C.; Wang, S.; Louie, S. G.; Fischer, F. R. Robust Metallic Zero-Mode States in Olympicene Graphene Nanoribbons *J. Am. Chem. Soc.* **2023**, *145*, 15162–15170. DOI: 10.1021/jacs.3c01576
- 2. Wen, E. C. H.; Jacobse, P.; Jiang, J.; Wang, Z.; Louie, S. G.; Crommie, M. F.; <u>Fischer, F. R.</u> Fermi Level Engineering in Nitrogen Core Doped Armchair Graphene Nanoribbons. *J. Am. Chem. Soc.* **2023**, *145*, 19338–19346. DOI: 10.1021/jacs.3c05755
- 3. Jacobse, P. H.; Daugherty, M. C.; Čerņevičs, C.; Wang, Z.; McCurdy, R. D.; Yazyev, O. V.; <u>Fischer, F. R.</u>; Crommie, M. F. Five-membered Rings Create Off-zero Modes in Nanographene *ACS Nano* **2023**, *17*, 24901–24909. DOI: 10.1021/acsnano.3c06006
- 4. Pun, S. H.; Delgado, A.; Dadich, C.; Cronin, A.; <u>Fischer, F. R.</u> Controlled Catalyst Transfer Polymerization in Graphene Nanoribbon Synthesis *CHEM* **2024**, *10*, 675–685. DOI: 10.1016/j.chempr.2023.11.002
- 5. Qie, B.; Wang, Z.; Jiang, J.; Zhang, Z.; Jacobse, P. H.; Lu, J.; Li, X.; Alexandrova, A. N.; Louie, S. G.; Crommie, M. F.; Fischer, F. R. Synthesis and Characterization of Low Dimensional N-Heterocyclic Carbene Lattices *Science* **2024**, *384*, 895–901. DOI: 10.1126/science.adm9814
- Slicker, K.; Delgado, A.; Jiang, J.; Cronin, A.; Tang, W.; Louie, S. G.; <u>Fischer, F. R.</u> Engineering Small HOMO–LUMO Gaps in Polycyclic Aromatic Hydrocarbons with Topologically Protected States *Nano Lett.* 2024, 24, 5387–5392. DOI: 10.1021/acs.nanolett.4c01476
- 7. Daugherty, M. C.; Jacobse, P. H.; Jiang, J.; Jornet-Somoza, J.; Dorit, R.; Wang, Z.; Lu, J.; McCurdy, R.; Rubio, A.; Louie, S. G.; Crommie, M. F.; <u>Fischer, F. R.</u> Regioselective On-Surface Synthesis of

- [3]triangulene Graphene Nanoribbons *J. Am. Chem. Soc.* **2024**, *146*, 15879–15886. DOI: 10.1021/jacs.4c02386
- 8. Jacobse, P. H.; Pizzochero, M.; Wen, E. C. H.; Borin Barin, G.; Li, X.; Mutlu, Z.; Müllen, K.; Kaxiras, E.; Crommie, M. F.; <u>Fischer, F. R.</u> Coupling of Nondegenerate Topological Modes in Nitrogen Core-Doped Graphene Nanoribbons *ACS Nano* **2025**, *19*, 13029–13036. DOI: 10.1021/acsnano.4c17602
- 9. Liu, F.; Yan, Y.; Tang, W.; Qie, B.; Chen, J.; Wang, Z.; Louie, S. G.; <u>Fischer F. R.</u> Orbital Engineering Band Degeneracy in a Dual-Square Carbon-Oxide Framework *ACS Nano* **2025**, *19*, 15139–15147. DOI: 10.1021/acsnano.5c03671
- 10. Delgado, A.; Daugherty, M. C.; Dadich, C. M.; Ochs, W.; Björk, J.; <u>Fischer, F. R.</u> Kinetic Isotope Effect in the Radical Chain-Growth Termination of On-Surface Synthesized Graphene Nanoribbons *Nano Lett.* **2025**, *accepted*.
- 11. Yan, Y.; Liu, F.; Tang, F.; Qie, B.; Louie, S. G.; <u>Fischer, F. R.</u> Engineering Phase-Frustration Induced Flat Bands in an Aza-Triangulene Covalent Organic Kagome Lattice **2025**, *under review*.
- 12. Delgado, A.; Dusold, C.; Wu, J.; Jing, J.; Dadich, C. M.; Cronin, A.; Louie, S. G.; <u>Fischer, F. R.</u> Two-Dimensional Antiferromagnetic Spin Lattice in a Covalent Organic Framework **2025**, *under review*.

#### Van der Waals Reprogrammable Quantum Simulator

#### **DE-SC0022277**

<u>Benjamin Hunt</u><sup>1</sup>, Dengyu Yang<sup>1</sup>, Qingrui Cao<sup>1</sup>, Junwon Choi<sup>1</sup>, Erin Akyuz<sup>1</sup>, Jeremy Levy<sup>2</sup>, Patrick Irvin<sup>2</sup>, Ranjani Ramachandran<sup>2</sup>, Muqing Yu<sup>2</sup>, Jon-Paul Maria<sup>3</sup>, John Hayden<sup>3</sup>, Josh Nordlander<sup>3</sup>, Ian Mercer<sup>3</sup>, Di Xiao<sup>4</sup>, Nishchay Suri<sup>1</sup>, and Chong Wang<sup>4</sup>

1-Carnegie Mellon University, 2-University of Pittsburgh, 3-Pennsylvania State University, 4-University of Washington

Abstract: The primary motivation of this DOE-QIS project is to realize a condensed-matter (c-m) quantum simulator with an unprecedented degree of configurability. Quantum simulators have been realized in ultracold atoms, trapped ions, and superconducting qubits. However, it remains an open challenge to engineer Hamiltonians with access to emergent long-range-ordered phases at low temperatures. Consequently, efforts have focused on clean c-m quantum simulators; one prominent effort has been in moiré or artificial superlattices (SLs) in 2D van der Waals (vdW) heterostructures. However, moiré SLs are limited as a (practical) quantum simulator because the symmetry and functional form of the SL potential are entirely determined by the interlayer interactions and strain present in the twisted structure. For artificial SLs in vdW materials, such as etched holes in a gate dielectric, limits are generally set by nanofabrication techniques. The central aim of this DOE-QIS project is to combine two elements – two-dimensional (2D) vdW heterostructures and electron-beam-programmable substrates – to create a versatile new materials platform ("VR-QuSim") with primary application to quantum simulation, but also in quantum sensing, quantum information science, and materials research in strongly correlated and topological systems. The basic idea is shown in Fig. 1a. A vdW heterostructure is placed on top of a substrate that can be "programmed": an electron beam can be used to write nanostructures in the substrate

through the vdW
heterostructure, so that the
vdW + substrate can be
assembled first and
programmed as a last step.
Several candidate
programmable substrates
are possible; this abstract
will specifically discuss
our experiments on one type -insulating ferroelectric thin

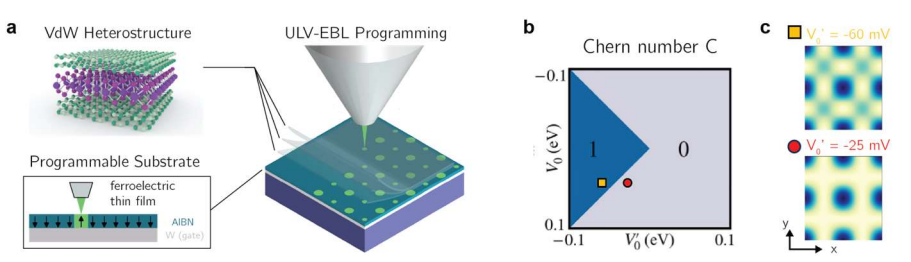


Figure 11. (a) Principle of VR-QuSIM. (b) Topological transition in bipartite superlattice by varying relative strength of sublattice potentials  $V_0$  and  $V_0$ '

films of boron-substituted aluminum nitride (AlBN) -- in which the electron beam creates nanoscale domains of electric polarization. The nanostructures in the substrate couple electrostatically to the active vdW layer and modify its electronic properties. As a key example of an advantage of our technique, we can in principle directly program superlattices with a *basis*, such as the Lieb or dice lattice, by writing the multiple sublattices with different electron beam doses (Fig. 2a,b; ref. [1]). A major motivation for this is our recent theoretical work that shows certain superlattice designs for massive Dirac fermions can induce topological transitions from a trivial insulator to C=1 and even C=2 Chern insulators (Fig. 1b, c; ref. [2]) for  $C_3$  and  $C_4$ -symmetric SL potentials.

Here we present our initial experiments on reversing the polarization of a ferroelectric thin film (boron-substituted aluminum nitride,  $Al_{1-x}B_xN$ , x=0.1) using an electron beam, characterizing the resolution of our technique using piezoforce microscopy (PFM). In a graphene/hBN Hall bar on AlBN substrate, we write half the device with a uniform pattern. This shifts the Dirac point of the patterned half relative to the unpatterned half, and we observe a p-n junction across the interface.

In graphene/hBN devices on unprogrammed AlBN films, we discovered that graphene exhibits magnetoconductance at charge neutrality that is reminiscent of the "quantum Hall topological insulator (QHTI)" phase [3]. We show evidence for quantized helical edge modes, using non-local transport measurements (Fig. 2b). We show that the usual insulating behavior of graphene at charge neutrality in the quantum Hall regime can be restored by heating the sample to 130°C. This does not alter the mobility

of the device nor the visibility of brokensymmetry Landau levels. We interpret this as suggesting the important role of the hBN-AlBN interface via interfacial water molecules and ions that screen the Coulomb interaction.

We studied four graphene devices with triangular patterns of lattice constants between 10-25 nm programmed into the FE thin film. These devices show preliminary evidence of superlattice effects: Landau levels emerging from replica Dirac points (Fig. 1c).

The most pressing current and future challenges of this work include expanding experiments to other vdW materials such as monolayer transition-metal dichalcogenides (TMDs), in which realization of certain Hamiltonians may be more easily achieved;

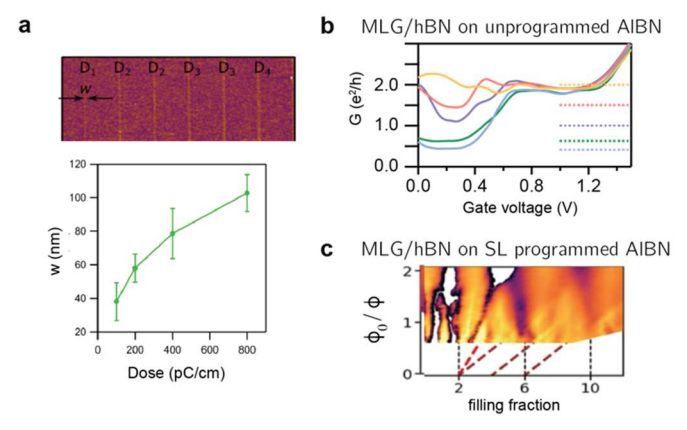
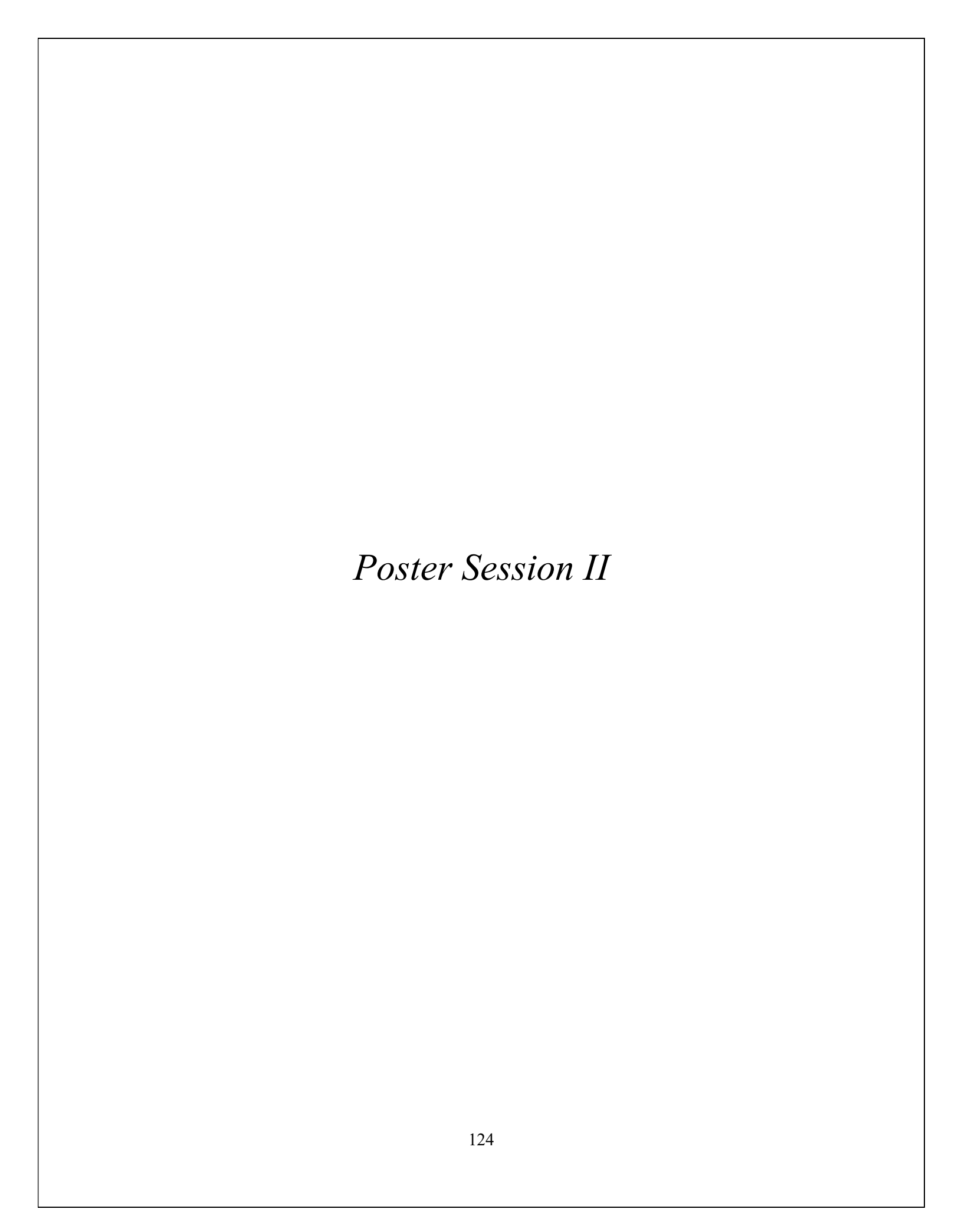


Figure 12. (a) Resolution of e-beam programming of AlBN. (b) Two-terminal (2T) transport of Graphene/hBN on unprogrammed AlBN at 4 Tesla. Dashed lines show expected conductance for different 2T configurations. (c) graphene/hBN on FE programmed with 20 nm superlattice. Color scale proportional to conductance.

verification of the ability to program superlattices with a basis or with controlled disorder; and experiments beyond magnetotransport, such as optical or scanned probe measurements.

- 1. Yang D, Cao Q, Akyuz E, Hayden J, Nordlander J, Mercer I, Yu M, Ramachandran R, Irvin P, Maria J-P, Hunt BM, Levy J (2024) Nanoscale Ferroelectric Programming of van der Waals Heterostructures. *Nano Letters*, 24(51):16231–16238. https://doi.org/10.1021/acs.nanolett.4c03574
- 2. Suri N, Wang C, Hunt BM, Xiao D (2023) Superlattice engineering of topology in massive Dirac fermions. *Physical Review B*, 108(15):155409. https://doi.org/10.1103/PhysRevB.108.155409
- 3. Kharitonov M, Juergens S, Trauzettel B (2016) Interplay of topology and interactions in quantum Hall topological insulators: U(1) symmetry, tunable Luttinger liquid, and interaction-induced phase transitions. *Physical Review B*, 94(3):035146. https://doi.org/10.1103/PhysRevB.94.035146



## Mapping the genome of coherent quantum defects for Quantum Information Science DE-SC0022289

Atomic Engineering and Characterization of Targeted Quantum Emitters in 2D Transition Metal Dichalcogenides through Scanning Tunneling Microscopy and First Principles computations

<u>A. Weber Bargioni</u><sup>1</sup>, S. Griffin<sup>1</sup>, A. Raja<sup>1</sup>, G. Hautier<sup>2,3</sup> M.M. Noack<sup>1</sup>, E. Rotenberg<sup>1</sup>, DF. Ogletree<sup>1</sup>, D. Strubbe<sup>4</sup>, G.M. Rignanese<sup>5</sup>, A. Schwartzberg<sup>1</sup>, M. Terrones<sup>6</sup>, J. Robinson<sup>6</sup>, S. Kumari<sup>6</sup>, D. Zhou<sup>6</sup>, Z. Yu<sup>6</sup>, N. Kelly<sup>4</sup>, W. Chen<sup>2</sup>, J. Zhou<sup>1</sup>, B. Barker<sup>4</sup>, Y. Xiong<sup>2</sup>, W. Chen<sup>5</sup>, J.C. Thomas<sup>1</sup>, P. Jacobse<sup>1</sup>, B. Iliyas<sup>1</sup>, and F. Wang<sup>7</sup>.

<sup>1</sup>Lawrence Berkeley National Laboratory, <sup>2</sup>Dartmouth College, <sup>3</sup>Rice University, <sup>4</sup>UC Merced, <sup>5</sup>UCLouvain, <sup>6</sup>Penn State, <sup>7</sup>UCBerkeley

**Abstract:** Quantum emitters are a foundational component of quantum information science (QIS) technologies, serving critical roles in quantum networks, quantum sensing, and photon-based quantum computing. Key technical requirements for quantum emitters include the ability to emit identical photons, sufficient brightness, and deterministic emission (ideally emitting one photon per excitation). A central challenge across all quantum emitter platforms is the precise, atomistic control of defect creation, ensuring emitters meet these stringent requirements and enabling the production of identical photons capable of entanglement.

To address the challenge of creating identical color centers, we explore two-dimensional (2D) semiconducting host materials—specifically, monolayer WS<sub>2</sub> and MoS<sub>2</sub>—which allow atomically precise defect engineering. These materials also provide direct access to defect structures and their electronic and optical properties with atomic resolution, achieved using state-of-the-art photo scanning tunneling microscopy (STM) and spectroscopy techniques. We have developed three distinct methods to create sulfur vacancies: thermal annealing <sup>1</sup>, helium ion bombardment <sup>2</sup>, and argon ion bombardment <sup>3</sup>. In the course of exploring these vacancy-creation pathways, we identified sulfur divacancy complex formation and discovered a method to engineer atomically defined one-dimensional defect lines, which host a correlated electron system known as a Tomonaga–Luttinger liquid <sup>3</sup>.

To determine optimal substitutional defects to incorporate into these vacancies, we employed theoretical high-throughput modeling to narrow down potential candidate elements <sup>4</sup>. Guided by these theoretical predictions, we have experimentally studied cobalt (Co)<sup>4</sup> substitutions, confirming with STM the theoretical prediction that the cobalt on sulfur substitution is a paramagnetic defect with two levels in the band gap. Such a candidate spin qubit had never been identified experimentally in WS<sub>2</sub>. We are currently investigating other defects in WS<sub>2</sub> ytterbium (Yb), silicon (Si), and titanium (Ti). Additionally, we are working on creating ensembles of identical Co defects in WS<sub>2</sub> to measure critical QIS-relevant properties, such as optical emission and coherence times.

Finally, we will present a novel experimental technique—gate-assisted scanning tunneling luminescence—that enables, for the first time, electrically driven exciton creation with atomic-scale precision. This breakthrough allows us to excite individual defects and measure their optical responses directly and precisely at the atomic scale. This capability not only provides an unprecedented direct correlation among structural, electronic, and optical properties of defects in 2D materials, but also significantly accelerates our progress in atomically precise color-center engineering for next-generation quantum emitters.

- Thomas, J.C., Rossi, A., Smalley, D. et al. "Autonomous scanning probe microscopy investigations over WS<sub>2</sub> and Au{111}." npj Comput Mater 8, 99 (2022). https://doi.org/10.1038/s41524-022-00777-9
- 2. Mitterreiter, E., Schuler, B., Micevic, A. *et al.* The role of chalcogen vacancies for atomic defect emission in MoS<sub>2</sub>. *Nat Commun* **12**, 3822 (2021). https://doi.org/10.1038/s41467-021-24102-y
- 3. Rossi, A., Thomas, J.C., *et al.* "Graphene-Driven Correlated Electronic States in One Dimensional Defects within WS2" accepted in *Nat Comm* (2025)
- 4. Thomas, J.C., Chen, W., Xiong, Y. *et al.* "A substitutional quantum defect in WS<sub>2</sub> discovered by high-throughput computational screening and fabricated by site-selective STM manipulation." *Nat Commun* **15**, 3556 (2024). https://doi.org/10.1038/s41467-024-47876-3

## Mapping the genome of coherent quantum defects for Quantum Information Science DE-SC0022289

## Long-lived entanglement of a spin-qubit register in silicon photonics

Hanbin Song<sup>1,2</sup>, Xueyue Zhang<sup>1,2</sup>, Lukasz Komza<sup>1,2</sup>, Niccolo Fiaschi<sup>1,2</sup>, Yihuang Xiong<sup>3</sup>, Yiyang Zhi<sup>1,2</sup>, Scott Dhuey<sup>2</sup>, Adam Schwartzberg<sup>2</sup>, Thomas Schenkel<sup>2</sup>, Geoffroy Hautier<sup>3,4</sup>, Zi-Huai Zhang<sup>1,2</sup>, and <u>Alp</u> Sipahigil<sup>1,2</sup>

**Abstract:** Spin-photon interfaces based on color centers in solids are well-suited as optically interconnected multi-qubit registers for quantum information processing. A series of well-established quantum defects in diamond have shown promise in demonstrating entanglement at long distance. However, scaling diamond-based qubit platforms for quantum applications remains a significant challenge due to fabrication difficulties. The goal of our project is to advance our understanding and quantum control of color centers in silicon, a mature host material for scalable fabrication of qubits.

Among the silicon color centers studied so far, the T center is the only system combining a telecom O-band emission (desirable for quantum communication) with a coherent electron spin qubit in the ground state (desirable as quantum memory). In our project, we focus on advancing our understanding of optical and spin coherence of this defect in nanoscale structures with guidance from first-principles hyperfine interaction calculations. After a brief introduction to earlier work funded by this program on indistinguishable photon generation from a single color center in silicon [1] and nanoscale sensing with Tcenters [2], we will present recent progress on demonstrating a multi-qubit register based on T-centers in silicon [3]. We demonstrate the initialization, coherent control, and state readout of a three-qubit register based on the electron spin of a T center coupled to a hydrogen and a silicon nuclear spin. The spin register exhibits long spin echo coherence times of 0.41(2) ms for the electron spin, 112(12) ms for the hydrogen nuclear spin, and 67(7) ms for the silicon nuclear spin. We use nuclear-nuclear two-qubit gates to generate entanglement between the two nuclear spins with a fidelity of F=0.77(3) and a coherence time of T<sup>2\*</sup>=2.60(8) ms. Our results show that T centers can realize a long-lived multi-qubit register with an optical interface in silicon photonics. We conclude by discussing ongoing work on improving qubit readout fidelities for T-centers in nanoscale devices, understanding electronic excited state dynamics under electric fields and modeling through first principles spin bath interactions and coherence times in silicon.

- [1] Komza, L., Samutpraphoot, P., Odeh, M., Tang, Y.-L., Mathew, M., Chang, J., Song, H., Kim, M.-K., Xiong, Y., Hautier, G. & Sipahigil, A., "Indistinguishable photons from an artificial atom in silicon photonics," Nat Commun 15, 6920 (2024). DOI: 10.1038/s41467-024-51265-1
- [2] A. M. Day, C. Zhang, C. Jin, H. Song, M. Sutula, A. Sipahigil, M. K. Bhaskar, E. L. Hu, "Probing negative differential resistance in silicon with a P-I-N diode-integrated T center ensemble", arXiv:2501.11888 (2025)
- [3] H. Song, X. Zhang, L. Komza, N. Fiaschi, Y. Xiong, Y. Zhi, S. Dhuey, A. Schwartzberg, T. Schenkel, G. Hautier, Z.H. Zhang, A. Sipahigil, "Long-lived entanglement of a spin-qubit register in silicon photonics", arXiv:2504.15467 (2025)

<sup>&</sup>lt;sup>1</sup>University of California, Berkeley, <sup>2</sup>Lawrence Berkeley National Laboratory,

<sup>&</sup>lt;sup>3</sup> Dartmouth College, <sup>4</sup> Rice University

## Mapping the genome of coherent quantum defects for Quantum Information Science DE-SC0022289

Sharp emission and fine structure splitting from localized excitons in Vanadium-doped monolayer WSe<sub>2</sub>

<u>A. Raja<sup>1</sup></u>, G. Hautier<sup>2,3</sup>, E. Barré<sup>1</sup>, W. Chen<sup>2</sup>, D. Blach<sup>1</sup>, G. Gupta<sup>1</sup>, Y. Xiong<sup>2</sup>, L. Leyi<sup>4</sup>, C. Yuan<sup>4</sup>, G. Eda<sup>4</sup>, S. Y. Quek<sup>4</sup>, K. Watanabe<sup>5</sup>, and T. Taniguchi<sup>5</sup>

<sup>1</sup>Lawrence Berkeley National Laboratory, <sup>2</sup> Rice University, <sup>3</sup> National University of Singapore, <sup>4</sup> National Institute for Materials Science

**Abstract:** Two-dimensional transition metal dichalcogenide (TMDC) semiconductors have attracted attention for light-matter interaction due to their strongly bound excitons arising from reduced dielectric screening and quantum confinement. Point-like defects in 2D materials hold promises as individually accessible sources of single photon emission and as a spin qubits in the same material. Our previous study has demonstrated that neutral Cobalt substitution on the sulphur site  $(Co_8^0)$  in WS<sub>2</sub> is a promising spin-photon interface for quantum communication<sup>1</sup>.

The more established and easier to synthesis Vanadium substitutional defect in WSe<sub>2</sub> (V:WSe<sub>2</sub>) has shown a broad below-gap emission associated with this defect in addition to evidence of long-range magnetism. In this work, we encapsulate high quality V:WSe<sub>2</sub> in hBN which allows us to see multiple PL emission peaks (linewidths < 1 meV) that have so far been hidden under a single broad emission. We attribute these peaks to recombination of dark excitons bound to Vw<sup>-1</sup> site. By examining the magnetic field dependent photoluminescence, we observe a Zeeman splitting yielding g-factors between 8.4 to 9.7, as well as a zero-field, fine structure splitting of about 0.9 meV in one of the peaks. We calculate the electronic structure associated with the observed defect states using Density Functional Theory and time-dependent density functional theory. These calculations help us identify the nature of the observed transition, describe the electronic structure of the defect and rationalize the magnetic field interaction. The computations and transmission electron microscopy suggests that complex defects that could be attractive emitters in the telecom might be as well present in the sample. We also discuss the potential for Fermi level tuning to prepare the defect in a neutral charge, triplet state, that would offer a spin degree of freedom and current experimental efforts in that direction.

1. Thomas, J. C. *et al.* A substitutional quantum defect in WS2 discovered by high-throughput computational screening and fabricated by site-selective STM manipulation. *Nat Commun* **15**, 3556 (2024).

# Project Title: Seeking quasiparticles in perturbed matter from low-energy spin dynamics Award Number: DE-SC0022986

Names of PI, coPI(s), unpaid collaborators: <u>Arnab Banerjee</u>, Catherine Pappas, and Roger Pynn Affiliation(s): <u>Department of Physics and Astronomy, Purdue University, West Lafayette IN.</u> Department of Physics, Technische Universitaet (TU) Delft, Netherlands. Department of Physics, IU Bloomington, Indiana.

**Abstract:** In this project we set up a platform and workflow that allows us to directly probe exotic states, including those predicted by the near-term analog quantum simulators and quantum computers, their statistics and effects of spin quantization in the low energy spectrum using state-of-the-art neutron sample environments and novel bulk approaches. The project builds upon a successful set of developments in the past three years spanning several frustrated spin systems as well as development of neutron in-situ probes. We have continues exploring the enigmatic states of Kitaev candidate a-RuCl<sub>3</sub> while introducing new thallium-based delafossites TlYb(S,Se)<sub>2</sub> and 1-6-6 Kagome metal RCr<sub>6</sub>Ge<sub>6</sub> (R=Tb, Yb). In TlYbSe<sub>2</sub> we discover a quantum disordered ground state to very low temperatures, where a possible spin liquid state is punctuated by a spin glass state from free Yb spins[1]. A likely breakdown of the Wiederman-Franz law in YbCr<sub>6</sub>Ge<sub>6</sub> due to interactions between fluctuating spins and itinerant electrons that can pave the path to understand the effects of metallic gating of frustrated spin systems. In Shastry-Sutherland magnet HoB<sub>4</sub>, we discover new phases and transitions, highlighting the importance of defects in an Ising model[2]. Finally, in RuCl<sub>3</sub>, a careful neutron measurement of the 8-9 T spin gap reveals a 9 T discontinuity and an overall gap evolution amenable support a distinct topological phase.

In the ensuing research, we develop ferromagnetic neutron spin echo spectrometry, and high field quenched magnets, as well as predictions based on quantum computers by our team, to perform a set of experiments that can help with identification of exotic magnetic states of matter with no classical analog. We desire to confirm the predictions of emergent magnetic quasiparticles, which can potentially replace

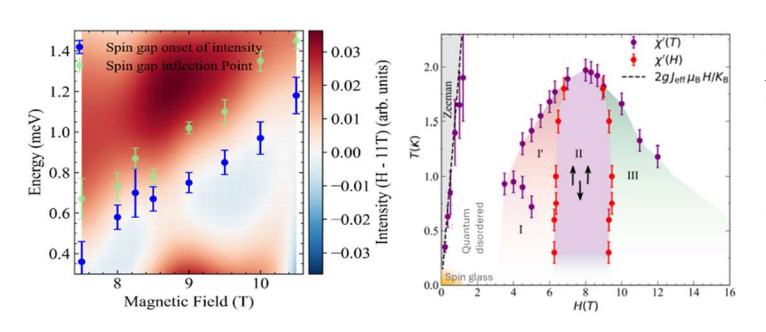


Fig. (Left) The evolution of the low energy spectral intensity in RuCl<sub>3</sub> shows a discontinuity at 9 T in both the scattering and the spin gap. (Right) The in-field phase diagram of TlYbSe<sub>2</sub> with a spin-glass below 35 mK and a quantum disordered state [1].

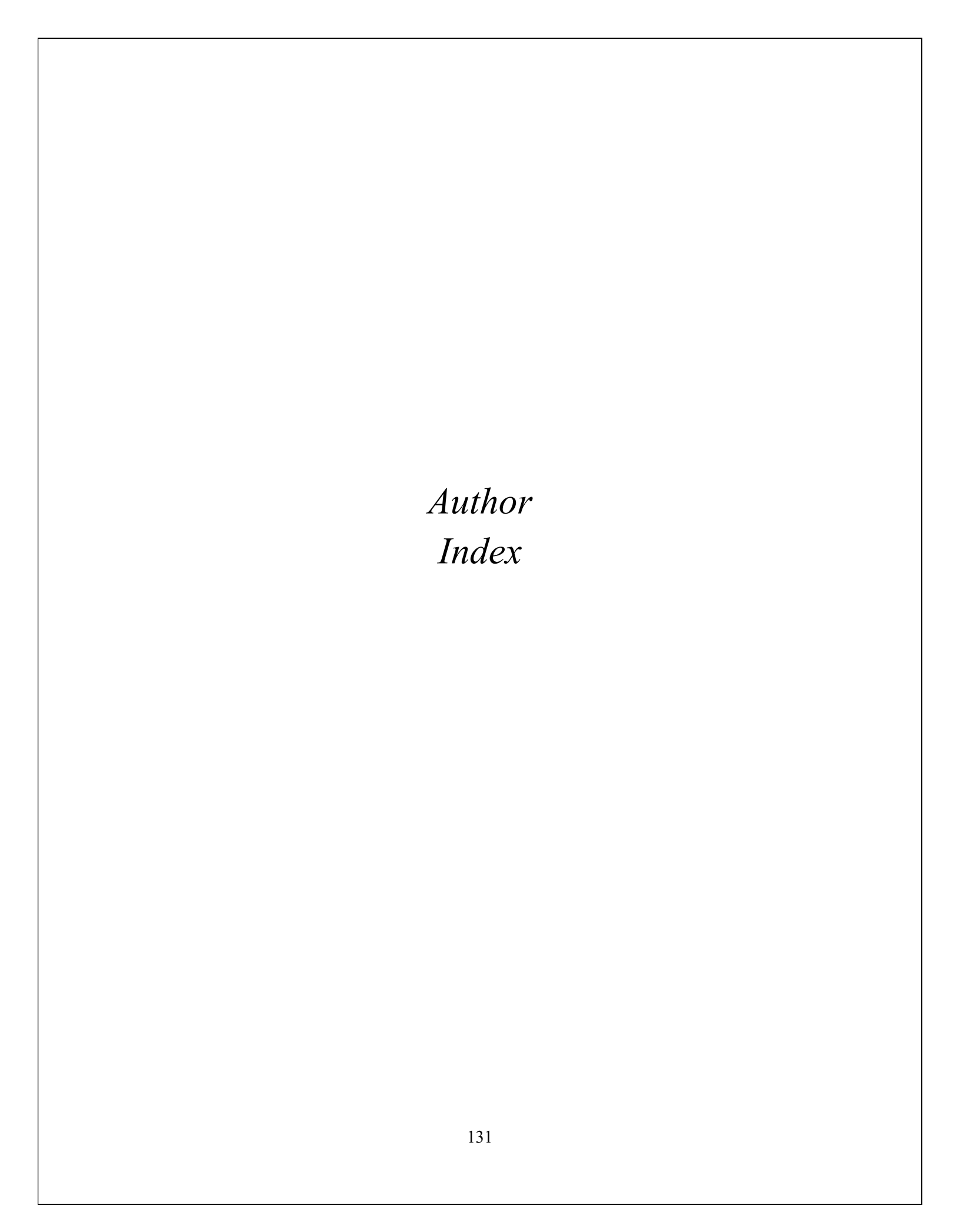
electrons as the building blocks for decoherence-resistant quantum electronics. Neutron scattering, magnetic susceptibility and thermal transport, mated to in-situ and in-operando techniques for currents and magnetic fields, in both bulk and mesoscale systems, offers unique advantages for the discovery and study of magnetic quasiparticles. Here we use a three-pronged approach: (1) We use of low energy spectroscopy techniques, including ferromagnetic neutron spin echo[3], backscattering and other Larmor techniques to measure low energy excitations to directly probe exotic spin

statistics in quantum magnets and spin liquid candidates such as TlYbSe<sub>2</sub> and RuCl<sub>3</sub> to validate quasiparticle levels; (2) We leverage the perturbation of the ground and excited states fast quenched magnetic fields to understand emergence of new quantum ordering phenomena in transverse field Ising magnets (such as TmB<sub>4</sub>), leveraging the progress and validating our predictions obtained from quantum

computers such as D-Wave[4], QuEra and Google for prediction of new quasiparticle states; (3) We clarify the interaction between itinerant electrons and frustrated magnetic states in RCr<sub>6</sub>Ge<sub>6</sub> (R=Rare Earth) which could be critical to understand gating of magnetic devices, in select materials where both co-exist. We expect to probe the neutron spectrum of these magnets as a function of changing in-operando and in-situ conditions – with changing magnetic flux and drive voltages. Our framework to cross-understand and cross-validate magnetic excitations both using quantum computation and real experiments allows us to prepare towards a future where exotic magnetic materials could be tuned towards a desired functionality based on inputs from quantum computer simulations.

#### **References:**

- [1] Belbase, B. P; Unnikrishnan, A.; Choi, E. S.; Banerjee, A. Field-tunable spin disordered phase in the triangular-lattice delafossite TlYbSe<sub>2</sub>. *arXiv.org*. https://doi.org/10.48550/arXiv.2504.05436.
- [2] Khundzakishvili, G.; Belbase, B. P.; Mahendran, P.; Zhang, K.; Xu, H.; Stoyanoff, E.; Checkelsky, J. G.; Liu, Y.; Ye, L.; Banerjee, A. Criticality and Magnetic Phases of Ising Shastry—Sutherland Candidate Holmium Tetraboride. *Materials* **2025**, *18* (11), 2504. https://doi.org/10.3390/ma18112504.
- [3] Banerjee, A.; Ehlers, G.; Gardner, J.; Kuhn, S.; Leiner, J.; Nickels, J.; Pynn, R.; Sokolov, A.; Stingaciu, L.; Zolnierczuk, P., Report on The Workshop on Scientific Benefits And Applications of Resonant Spin Echo". OSTI OAI (U.S.-D.O.E.) 2024. https://doi.org/10.2172/2448160.
- [4] Ali, A.; Xu, H.; Bernoudy, W.; Nocera, A.; King, A. D.; Banerjee, A. Quantum Quench Dynamics of Geometrically Frustrated Ising Models. *Nature Communications* **2024**, *15* (1). https://doi.org/10.1038/s41467-024-54701-4.



Abelson, Alex	117, 118	Brar, Victor	14, 28, 71, 117
Abeywickrama, Kusal		Brown, Tristan	
Adhikari, Tibendra		Buss, Max	,
Akhmedov, Novruz G		Cambria, Matthew	
Akyuz, Erin		Campbell, Daniel	
Alaerts, L		Candalori, Luca	
Alberi, K.		Cao, Qingrui	
Alegria, Loren D.		Cao, Shixun	
Aloni, Shaul	*	Cao, Xi	
Alvarado, Stephen J. G	*	Casa, Diego	
Anthony, J. E		Cavalleri, Andrea	,
Arpin, P. C		Cecil, Thomas W	
Artola, Melissa		Chand, Saroj	
Atteberry, Matthew L		Chandra, Sohom	
Aumentado, Jose		Chaves, Kevin R	
Awschalom, David		Chen, Bin	,
Azaz, T		Chen, W	
Badarneh, Mohammad		Cheong, Sang-Wook	
Bakkers, Erik		Chernyak, Vladimir	
Balaji, Yashwanth		Chien, Yu-Che	
Balcazar, Mario D	•	Cho, Yujin	
Baldini, Edoardo		Choi, Junwon	,
Balents, Leon		Choy, Jennifer	
Banerjee, Arnab		Cochran, Josiah	
Baptista, Alejandro E		Comin, Riccardo	
Barcenas, G		Coppersmith, Susan	
Bargioni, A. W		Crommie, Michael F	
Barker, B.		Cui, Eric	
Barré, É.		Cuozzo, J.J	
Bassett, Lee	66	Curtis, Jonathan B	
Basso, Luca	10	D'Ambrosia, Sam	50
Baum, Ian	63	Dahal, Sajal	36
Becker, Petra	107, 108	Damron, Joshua T	69, 103
Bedow, Jasmin	42	Darlington, Thomas P	90
Berndt, Nadia		David, Christian	
Berthusen, Noah	93	Davis, Emily	
Bertoni, Benjamin		Davis, P. H	109
Besson, Claire	18	Dawkins, Riley B	
Bhatia, Pia	66	Dean, J. C	109
Bielejec, Ed	50	Dean, Mark P. M	36, 107, 108
Biswas, Dhiman		Deger, Emir A	87
Blach, D	128	Dhuey, Scott	
Blinov, Boris	50	DiCenso, Jesse D	
Bozhko, Dmytro A		Disa, Ankit S	36
Brahlek, Matt	69	Divan, Ralu	32

Dong, Yitong56	Hautier, Geoffroy 44, 79, 125, 127, 128
Doucet, Emery 54, 81, 113	Hayden, John
Drndic, Marija	He, Wei 107, 108
Du, Kai	Hersam, Mark6
Duncan, K	Hidayatova, Lamia56
Duncan, Ryan A	Hocevar, Moïra
Durbin, Stephen M	Hoegen, Alexander v
Dyck, Ondrej12	Hoffmann, Axel 22, 32, 115
Dziubelski, Monika61	Hoffmann, Matthias C
Eda, G	Höfling, Sven
Elliot, R	Holmes, Stuart N
Eriksson, Mark71	Holtzman, Luke N
Esposito, Vincent	Hone, James C
Ferdous, Jannatul	Hong, Mingyuan63
Fiaschi, Niccolo	Hosack, Travis
Fischer, Felix R	Hoyt, Aaron
Flatté, Michael	Hua, Chengyun 69, 85, 101, 103
Foglia, Laura	Huang, Yijing36
Forst, Michael	Huber, Tobias
Freedman, Danna 6	Hughes, Lillian
Freericks, James 111	Hunt, Benjamin
Friesen, Mark	Iadecola, Thomas
Frolov, Sergey	Ihme, Matthias
Fu, Kai-Mei	Iliyas, B
Fuchs, Gregory	Im, Soohyun
Gali, Ádam 14	Irvin, Patrick
Gan, Tianyi	Işıl, Çağatay
Gao, Frank Y	Islam, Md
Gashi, Arian 30	Jacobse, P
Gaswami, Sumit 58	Jahabani, Shahin
Gee, Gavin C	Jarrahi, Mona
Getelina, Joao C. 93	Javadi, Alisa
Golesorkhi, Bahman	Jayich, Ania B
	•
Gontijo, Rafael	Jesse, Stephen
	Jin, Dafei
Graham, Thomas	Jin, Rui-Bo
Griffin, Sinéad	Johnson, Dane
Gul, Yilmaz 52	Johnson, Steven L
Gupta, G	Johnston-Halperin, Ezekiel
Gupta, Prashant 42	Joseph, Emily
Gusdorff, Jordan	Kamal, Archana 54, 81, 113
Halász, Gábor	Kang, Kaifei 83
Hamers, Robert J	Kargioti, Aikaterini
Hanlon, Dillon	Kats, Mikhail A
Hansen, Ethan	Kelly, N
Hastings, Jerome B	Kemelbay, Aidar30

Kemper, Alexander111	Lordi, Vincenzo 14,	28, 71, 117, 118
Keneipp, Rachael	Louie, Steven G.	
Kerr, Casey 58	Lupini, Andy	12
Ketteridge, M	Ma, Xiaoxuan	
Kim, Eunjeong 117, 118	Ma, Zhenqiang	28
Kim, Kab-Jin32	MacDonald, Allan H	
Kim, Kyuhyun10	Magana-Loaiza, Omar S	
Kim, Minjeong28	Mak, Kin F	
Kim, Philip115	Maksymovych, Petro	
Kish, Lazar	Malla, Rajesh	
Kleidermacher, Hannah 10	Manfra, Michael J.	
Klein, John	Maria, Jon-Paul	
Knowlton, W. B	Marom, Noa	
Kolkowitz, Shimon 14, 28, 71, 117	Martin, E. W.	
Kolodka, Roman	Martinez, Luis A	
Komza, Lukasz	Martinez, Luis M.	•
Konik, Robert M. 40, 41, 105, 106, 107, 108	Mass, O. A	
Kort-Kamp, Wilton J. M90	Matthews, Bethan	•
Kramer, P	Maze, Jeronimo	
Krapivin, Viktor	Maznev, Alexei A	
Krebs, Zach	McBride, S.	
Kumari, S	McClintock, Luke M	
Kurihara, Takayuki	McDermott, Robert	
Kuzmin, Roman	Melin, Régis	
Kwock, Kevin W. C	Mendelson, Noah	
Kwok, Wai-Kwong 32	Méndez, José	
Lander, Chance W	Mercer, Ian	
LaSala, Michael P	Meynell, Simon	
Lawrie, Benjamin	Mi, Chenjia	
Leahy, I.A	Miedaner, Peter R	
Lee, Hope	Mitrano, Matteo	
· •	Mootz, Martin	, ,
Lee, J	Morr, Dirk K	
· · · · · · · · · · · · · · · · · · ·	•	
Levchenko, Alex	Musan Nach	
Levy, Jeremy	Mugan, Noah	
Leyi, L	Mukamel, Shaul	
Li, Haoyuan	Mukherjee, Anirban	
Li, L	Mukherjee, Kunal	
Li, Yi	Munk, Rebecca	
Lim, Jinho	Munoz, Gilberto d. l. P	
Lim, Mijin	Murphy, Ryan	
Lin, Zhong	Narang, Prineha	
Liu, J	Nedić, Ana-Marija	
Liu, Jian J	Nelson, Chris	
Liu, Zi-Jie	Nelson, Keith A.	
Long, Jeffrey6	Ng, May-Ling	36

Nguyen, Quynh	36	Prasankumar, Rohit P	90
Ni, Haoyang		Pribiag, Vlad	26, 52, 99
Niklas, Jens	6, 25	Purayil, Sreehari	58
Niouris, Vasileios	50	Pynn, Roger	129
Niu, Daoheng	97	Qiu, Yichen	83
Noack, M.M.	125	Quek, S. Y	
Noh, Taewan	54, 81	Rahman, Md S. S	87
Norden, Tenzin	90	Raja, A	
Nordlander, Josh	122	Ramachandran, Ranjani	
Novosad, Valentine	22, 32, 115	Rama-Eiroa, Ricardo	
O'Kelley, Sean R		Rani, Sonia	
Ogletree, DF	•	Ranzani, Leonardo	
Oh, Hyunseok		Rappe, Andrew M	
Olsen, Nicholas		Rashidi, Arman	
Orenstein, Gal		Ray, Keith G	
Ornelas-Skarin, Chance C		Reis, David A	
Orth, Peter P		Reiter, Caitlin	
Ozcan, Aydogan	,	Ren, Wei	
Padmanabhan, Prashant		Ribeill, Guilhem	
Pajerowski, Daniel M		Rice, A.D	
Pal, Pratap K	-	Rignanese, G.M.	·
Palmstrøm, Chris	-	Riswadkar, Ameya	
Pan, Wei		Robinson, J	
Pappas, Catherine		Rohrbach, David	
Parashar, Mritunjaya		Rondinelli, James	
Park, Mike		Rosen, Yaniv	
Park, Taka		Rossi, Enrico	
Parthasarathy, Shreyas		Rotenberg, E	
Pascual, G.		Rout, Bibhudutta	
Patel, Priya		Roy, S	
Patten, L.		Rury, Aaron	
Paul, Pralay		Sahu, Sudhir	
Pearson, John		Saini, Darshpreet K	
Pelliciari, Jonathan		Santos, Elton	
Pensack, R. D		Sapkota, K.R.	
Pepper, Michael	-	Sarkar, Nirjhar	
Pereira, Sofia		Sato, Takahiro	
Pereyra, Alessandro		Savici, Andrei T	
Pfaff, Wolfgang		Schenkel, Thomas	· · · · · · · · · · · · · · · · · · ·
Podlesnyak, Andrey		Schleife, André	
Pokharel, Ganesh		Schuck, P. J.	
Polakovic, Tomas		Schwartzberg, Adam	
Poluektov, Oleg		Sears, Jennifer	
Postelnicu, Eveline		Shabani, Javad	
Potter, Andrew		Shan, Jie	
Powers, Liam T		Shankar, Shyam	
1 Owers, Liain 1		Silalikai, Silyalii	

Shao, Yihan	56	Tong, Yuhan	28
Sharma, Mohin		Travaglini, H.C	
Sharma, Prachi		Trevisan, Thaís V	
Shaw, K		Trigo, Mariano	
Shaw, Theodore		Tsvelik, Alexei	
She, Selene		Turner, D. B	•
Shen, Bowen		Upton, Mary H	
Shen, Yao		Varley, Joel	
Shin, Donghoon		Vasylechko, Leonid	
Simmonds, Raymond W 54,		Venkatesan, Thirumalai.	
Sinitsyn, Nikolai		Vidrio, Ricardo	
Sipahigil, Alp		Vila-Comamala, Joan	
Smith, Grant		Vines, Lasse	
Song, Hanbin		Voyles, Paul M	
Song, Moojune		Vuckovic, Jelena	
Song, Sang Y.		Wang, Cai-Zhuang	
Song, Sanghoon		Wang, Chong	
Spurgeon, Steven		Wang, F	
Stanley, R. J.		Wang, Jiashu	
Stanton, Jade		Wang, Nan	
Stein, Abigail		Wang, Xingyi	
Stemmer, Susanne		Wang, Xingzhi	
Story, Tomasz		Wang, Yu-Xuan	
Strocov, Vladimir		Wasielewski, Michael	
Strubbe, D.		Watanabe, Kenji	
Su, Shei		Watt, D	
Suemoto, Tohru		Wei, T.C	
Sullivan, Joseph		Weichselbaum, Andreas	
Sun, Yanwen		Weiss, Leah	
Sung, Eric		Weld, David	
<u>o</u> .		Welp, Ulrich	
Sup, A		<b>1</b> ·	
Surendran, Mythili Suri, Nishchay		Wilen, Christopher D Wilson, Stephen	
•			
Taniguchi, Takashi		Wong, Man T	
Tarefder, Nehan		Wu, Weijie	
Taylor, Antoinette J.		Wu, Wenxin	
Teitelbaum, Samuel		Wu, Yueh-Chun	
TenHuisen, Sophia		Xia, Zhengchao	
Terrones, M		Xiao, Di Xiao, Zhihao	
Thomas Corl		<i>'</i>	* *
Thomas, Carl		Xiong, Alice	
Thomas, J.C.		Xiong, Wei	
Titze, Michael		Xiong, Y4	
Tiwari, Ganesh		Xiong, Yihuang	
Tiwari, Tarush		Yang, Dengyu	
Tom, Leah	/1	Yao, Kaiyuan	90

Yao, Norman 4	Zhang, Wei	32
Yao, Yongxin93	Zhang, X	9, 19, 21, 44, 127
Yavas, Hasan36	Zhang, Xi	36
Yeo, June H90	Zhang, Xin-Yue	18
Yip, Wai T56	Zhang, Xueyue	127
Yoo, Jinkyoung90	Zhang, Yuxuan	
Yoon, Mina 12	Zhang, Zhixin	
You, Chenglong63	Zhang, Zhuquan	
Young, Andrea16	Zhang, Zi-Huai	
Yu, Kangdi8	Zhao, Liuyan	
Yu, Muqing 122	Zheng, J	44
Yu, Z 125	Zhi, Yiyang	
Yuan, C	Zhou, Brian	
Yurke, B	Zhou, D	125
Zahedian, Maryam28	Zhou, Haoxin	8
Zajac, Joanna M	Zhou, J	125
Zaliznyak, Igor A 105, 106, 107	Zhu, Diling	36
Zeng, Yihang83	Zhu, Jian-Xin	90
Zhang, Feng	Zhu, Xiaoyang	90
Zhang, Jiahao36	Zhu, Y	44
Zhang, Leon36	Zimmermann, Christian.	50
Zhang, Shixiong99	Zuo, Jian-Min	22, 32